UNIVERSITÉ DE
SHERBROOKE

Faculté de génie
Département de génie chimique

Développement des échafaudages à trois dimensions pour la formation directionnelle de réseau d'angiogénèse

Development of 3D scaffolds for directional angiogenic network formation

Thèse de doctorat en sciences appliquées
Spécialité : génie chimique et génie biotechnologique

Afra Hadjizadeh

Sherbrooke (Québec), Canada

January 2008

Canada

Résumé

L'objectif de cette étude est d'étudier la possibilité de produire des fibres polymériques modifiées en surfaces, pouvant moduler le comportement de cellules endothéliales dans certaines directions et induire une angiogénése directionnelle dans un système tridimensionnel de culture des cellules. Ceci est dans le but de développer *in vitro* un échafaudage prévascularisé et tridimensionnel sous la forme d'un réseau de fibres. Cette étude a été réalisée selon les trois étapes suivantes : 1) Modification et caractérisation des surfaces des matériaux, et plus spécifiquement, des surfaces des fibres polymériques, avec une modification de surface utilisant une stratégie de multicouche par dépôt plasmatique de polymère en greffant du dextrane et des composés bioactifs afin de produire une réponse biologique prévisible. 2) Évaluation *in vitro* des fibres de polymère modifiées en surface sur le comportement des cellules endothéliales dans un système de culture de cellules en monocouche (2D). 3) Évaluation *in vitro* des fibres de polymère modifiées en surface sur le comportement des cellules endothéliales (angiogénéese) dans des systèmes de cultures tridimensionnels (3D) de cellules.

Dans une première étape, la surface des fibres poly (terephtalate d'éthylène) (PET) de diamètre de 100 µm ou des fibres du polytétrafluoroéthylène (PTFE) (monofilaments) étaient enduites en utilisant une stratégie de modification de surface par multicouche en 3 étapes. Au début, les substrats ont été enduits avec une couche mince de dièdres polymériques, d'un polymère obtenue d'un traitment plasma de n-hepthylamine (HApp) ou d'un polymère obtenu d'un traitment plasma d'acétaldéhyde (AApp), contenant respectivement des groupes amines et des groupes aldéhydes par la technique de dépôt d'une décharge par radio-fréquence. Ainsi, le Carboxy-Méthylique-Dextrane (CMD) a été greffé de manière covalente sur les groupes

II

amines disponibles sur les surfaces des substrats qui étaient enduits avec de l'HApp ou l'AApp-PEI, en utilisant la chimie des carbodiimides hydrosolubles. Des peptides ayant la séquence Gly-Arg-Gly-Asp-Ser (GRGDS) ont été immobilisés de façon covalente sur les surfaces de fibres enduites de CMD. La caractérisation de la composition chimique de surface en utilisant la spectroscopie par photoélectrons de rayons X (XPS), la topographie par la microscopie à forces atomiques (AFM) et par la microscopie électronique à balayage (SEM) a montré la possibilité de reproduire ces étapes de multicouches lors de leurs fabrications et également la rugosité des surfaces produites par des enduits d'AApp-, d'AApp-PEI-CMD- et d'HApp-CMD. Par conséquent, ces techniques de fabrication de multicouche en surface peuvent être appliquées aux biomatériaux, en particulier des biomatériaux fibreux polymérique, avec des surfaces multifonctionnelles qui peuvent avoir une application importante en thérapie et dans le génie tissulaire, comme matériel d'échafaudage pour la régénération de tissu multicellulaire.

Dans une deuxième étape, des cellules endothéliales de veine ombilicale humaine (HUVECs) ont été ensemencées et par la suite évaluées en contact avec les fibres de polymère modifiées en surface pour étudier le comportement à moduler les cellules (par exemple, adhérence, propagation, réorganisation du cytosquelette et orientation des cellules). Le comportement de cellules était en accord avec les propriétés physico-chimiques des surfaces modifiées. L'adhérence des cellules a été réduite sur les fibres enduites de CMD-, tandis que les enduits aldéhyde, amine et GRGDS ont favorisé l'adhérence des cellules, leurs propagations, et la formation de filaments d'actine et de points focaux d'adhésion. Par contre, l'adhérence réduite des cellules sur les surfaces enduites de GRGES (controle négatif) suggère que les gains significatifs dans l'adhérence des cellules endothéliales sur les surfaces enduites

III

de GRGDS sont provoqués par des réponses biologiques spécifiques des intègrines à la surface de cellules vers les ligands de RGD disponibles sur les surfaces des subtrats. L'adhésion des cellules augmentait en fonction de la concentration (de 0.1 mg/ml à 1 mg/ml) des GRGDS. Par rapport aux substrats plats, la courbure des fibres favorisait l'orientation des cellules le long de l'axe des fibres. Par conséquent, ces fibres de polymère modifiées en surface par des enduits adhésifs aux cellules, ou non-adhésifs et particulièrement bioactifs peuvent avoir des impacts très importants dans le génie tissulaire en particulier dans les modèles tridimensionnels avec des cellules.

Dans une troisième étape, des fibres PET modifiées ont été évaluées pour leurs effets sur l'angiogénéese dans des modèles de construction de tissu 3D in vitro, en employant des trois méthodes différentes d'ensemencement des cellules. Les résultats ont montré que l'angiogénèese est produite quand les fibres étaient soit pré-enduites d'HUVECs et incorporées dans un gel de fibrine soit que les HUVECs et les fibres sans cellule ont été mis ensemble en sandwich entre deux couches de gel de fibrine. Ces résultats ont démontré que l'effet à la fois physique et chimique des surface des fibres induisait une angiogénéese et permettait d'augmenter la formation directionnelle in vitro de microvaisseaux (de structures angiogéniques) dans des modèles de gel de fibrine. En prolongeant la durée du temps d'incubation, le nombre de structures angiogéniques augmentait et un réseau se formait dans lequel des structures angiogéniques se connectaient d'une fibre à une autre, suivant un espacement optimal de 200 à 600µm entre les fibres.

Ces résultats démontrent qu'en employant un matériel fibreux polymérique qui est enduit en surface d'un composant de la matrice extracellulaire, tel que le peptide de RGD ou de la gélatine, il devient possible d'augmenter et de diriger la formation de structures

angiogéniques. Ainsi, les deux objectifs principaux de cette étude, qui étaient (i) d'établir la faisabilité de pré-vasculariser d'une reconstitution d'un tissu in vitro, et (ii) d'influencer le guidage des structures angiogéniques dans une direction prédéterminée en utilisant le phénomène dit de *'contact guidance'* et des molécules bio-actives à l'aide des fibres modifiées en surface, ont été en grande partie réalisés.

Dans cette étude, l'idée d'employer une fibre polymérique (100μm de diamètre) pour moduler la cellule endothéliale et pour induire l'angiogénéese est tout à fait originale. Par ailleurs, la modification de la surface des fibres polymérique en employant des enduits multicouches, y compris des traitements (adhésives) des polymères au plasma (HApp et AApp), la présence d'un matériel non-fouling (CMD) et de molécules bioactives (RGD), n'a jamais été rapportée par d'autres. De plus, la caractérisation physico-chimique de ces enduits sur la surface des fibres ainsi que leurs influences sur le comportement, tel que l'adhérence, l'étalement, et la modulation, des cellules endothéliales dans un système de culture en monocouche (2D) et sur l'angiogénéese dans des systèmes de culture tridimensionnel n'ont pas été rapportées auparavant.

Abstract

The objective of this study is to investigate the possibility to produce surface modified polymeric fibres with the capability of both directional endothelial cell (EC) patterning and inducing angiogenesis in a 3D cell culture system. This is the goal for developing an *in vitro*, prevascularized 3D scaffold, made of a fibre network. This study was conducted in three steps as following: 1) surface modification and characterization of materials, and more specifically, polymeric fibre surfaces, involving a multilayer, surface modification approach, using plasma polymer deposition methods, dextran and certain bioactive compounds grafting, to induce predictable biological responses. 2) *In vitro* evaluation of the surface modified polymer fibres towards EC behaviour in a 2D cell culture system. 3) *In vitro* evaluation of surface modified, polymer fibres towards EC behaviour (angiogenesis) in three 3D cell culture systems.

Initially, the surfaces of 100-μm diameter poly (ethylene terephtalate) (PET) or polytetrafluoroethylene (PTFE) fibres (as monofilaments) were coated, utilising a multilayered-surface modification strategy, performed in three steps. These substrates were initially coated, using the radiofrequency glow discharge deposition technique, with a thin, polymeric interfacial bonding layer, produced via n-hepthylamine plasma polymer (HApp) or an acetaldehyde plasma polymer (AApp), having amine and aldehyde groups, respectively. Carboxy-methyl-dextran (CMD) was then covalently immobilized, using water-soluble carbodiimide chemistry (EDC/NHS), onto the surface amine groups, present either on the HApp-coated or on AApp-PEI-coated substrate surfaces. In the last step, GRGDS peptides were covalently immobilized onto the CMD-coated fibre surfaces. The subsequent characterization of the applied, surface chemical composition, using X-ray photoelectron spectroscopy (XPS), topography examination by atomic force microscopy (AFM), and

scanning electron microscopy (SEM), showed that the multilayer fabrication steps were successful and that the surface roughness, generated by the AApp-, AApp-PEI-CMD- and HApp-CMD coatings, was present.

Therefore, these multi-step surface fabrication techniques can be applied to produce specific biomaterials, particularly fibrous biomaterials supporting multifunctional surfaces that are likely to have important applications in "tissue engineering" and as "scaffolding material", used for multicellular tissue regeneration.

The second research theme involves the *in vitro* evaluation of surface modified substrates towards EC behaviour. For this purpose, human umbilical vein ECs (HUVECs) were seeded and grown on surfaces to evaluate the cell responses such as cell adhesion, spreading, cytoskeleton reorganization and cell orientation. Some alternative substrates were also examined in order to further characterize the cell behaviour. The cell behaviour was related with the surface physicochemical properties of the test modified surfaces. On CMD-coated substrates, cell adhesion was reduced, in contrast the amine-, aldehyde- and GRGDS-coated substrates promoted cell attachment and spreading and actin filaments and focal adhesions formations. Conversely, the reduced cell adhesion on GRGES (negative control), demonstrates that the increased EC adhesion, on GRGDS-grafted surfaces were attributed to specific biological responses of cell surface integrins towards the RGD ligands present on the surfaces. Cell adhesion was enhanced as the GRGDS solution concentration was increased from 0.1 mg/ml to 1 mg/ml. In comparison with "flat" substrates, fibre curvature promoted cell orientation along the fibre axis. These observations demonstrate that these surface-modified polymer fibres, bearing cell adhesive, non-adhesive and bioactive coatings, can have very important impacts in the success of tissue engineered devices.

In the third step, surface modified PET polymer fibres were evaluated towards "angiogenesis" in *in vitro* 3D tissue construct models, using three different methods of cell seeding. The result showed that angiogenesis process occurred when either HUVEC pre-coated fibres were embedded in fibrin gel, or HUVECs and cell-free fibres were sandwiched together between two layers of fibrin gel. These results suggest that the physical effect of the fibres, in conjunction with the surface chemistry, promotes *in vitro* EC attachment, induces angiogenesis and enhances directional angiogenic structures formation in the fibrin-based models. By prolonging the incubation period, the number of angiogenic structures increased and a network was formed, in which angiogenic structures interconnected to each other, from one fibre to another, following an optimal fibre spacing ranging from 200 to 600 μm.

These results demonstrate that through the use of a fibrous polymeric material that is surface coated with cell adhesive materials, in particular with extracellular matrix components such as RGD peptide or gelatin, it becomes possible to both enhance and direct the angiogenic process. Therefore, the two main goals of this study which were (i) to establish the feasibility of pre-vascularizing an *in vitro* tissue construct, and (ii) to influence the guidance of microvessel growth in a pre-determined direction, using phenomena known as "contact guidance" by means of polymer fibers and as "signaling molecules" by means of ligand-integrin interactions were largely achieved.

In this study, the idea of using polymer fibre (100-μm diameter) for both EC patterning and inducing angiogenesis is quite original. Moreover, polymer fibre surface modifications by using multilayer surface coatings, including cell adhesive plasma polymer (i.e. HApp and AApp), non cell adhesive material (i.e. CMD) and bioactive molecules (i.e. RGD), has not

been previously reported by others. In addition, the physicochemical characterization of these fibre surface coatings as well as their influence on EC behaviors (i.e. cell adhesion, spreading and patterning) in 2D cell culture system and toward angiogenesis in 3D cell culture systems (i.e. by using hydrogel) have not been reported elsewhere.

Acknowledgments

This study has been performed at the University of Sherbrooke in Dr. Vermette's laboratory whose input is acknowledged, in respect of financial support for the materials, and the characterization required for the experimental part of this research project.

It is my considerable pleasure to express here my sincere thanks to those people who have supported me so encouragingly during these four past years.

Firstly, my very special thanks are offered to Professor Charles J Doillon for the many discussions and pertinent advice from the outset and during the completion of this thesis. I wish to express my special thanks to my two supervisors; Professor Charles J Doillon and Professor Gervais Soucy for accepting, in the final steps, the supervisory role in the research project, leading towards my thesis defence. I sincerely thank them both for their wonderfully insightful comments and suggestions, proposed during the writing of this thesis.

I would also like to thank Laurie Martineau, and all of the people at Professor Doillon's laboratory for their very kind collaborations and the training I received from them in respect of the cell culture experiments undertaken.

I also gratefully acknowledge the "contribution" of my husband, Davod Mohebbi Kalhori, who was my "teammate" and friend during these four project years, for his useful scientific discussions, suggestions and collaborations from the very beginning of this project, especially in respect of 3D tissue construc and 3D scaffold design.

Very special thanks are also expressed for the very warm collaboration of Marc G. Couture and his technical assistance, especially for his expertise in the drawing (by using SolidWork software) of my designs and making of many nice fibre holders and frames, which greatly facilitated my difficult experiments, when performed with very fine fibres. Thanks are

To my son

Sepehr

Table of Contents

XVI

XVII

List of Figures

XXIII

XXXIII

List of Tables

List of Abbreviations

AApp	Acetaldehyde plasma polymer
ANOVA	Analysis of variance
bFGF	Basic fibroblast growth factor
CMD	Carboxy-methyl-dextran
ECM	Extracellular matrix
ECs	Endothelial cells
EDC	1-ethyl-3-(3Dimethylaminopropyl)-carbodiimide
FAs	Focal adhesions
FN	Fibronectin
FEP	Perfluorinated poly (ethylene-*co*-propylene)
kDa	Kilodaltons (molecular weight)
HApp	N-hepthylamine plasma polymer
HUVECs	Human umbilical vein endothelial cells
MW	Molecular weight
NHS	N-hydroxysuccinimide
PET	Poly (ethylene terephtalate)
PHMSH	Porous hollow membrane sheet
PTFE	Polytetrafluoroethylene
RFGD	Radiofrequency glow discharge deposition
RGD	G-R-G-D-S (Gly-Arg-Gly-Asp-Ser) peptide
RGE	G-R-G-E-S (Gly-Arg-Gly-Glu-Ser) peptide
2D	Two dimensional
3D	Three dimensional
VEGF	Vascular endothelial growth factor
VN	Vitronectin
vWf	von Willebrand factor

Chapter 1

Introduction

1.1. Problem statement

Tissue engineering attempts to develop new techniques, as alternative therapies, for the repair or replacement of diseased or damaged tissues and organs. The goal of this approach is to overcome the scarcity problem in the supply of tissues and organs for transplantation therapy, by employing scientific and engineering principals to produce suitable biological tissues or organs (ATALA 2004; FUCHS, et al. 2001; MERTSCHING, et al. 2005, GOMES and REIS 2004). Though this field has been considerably advanced during past few years, the preserving of viable cells within thick and large tissue constructs both *in vitro* and *in vivo* is still a challenging issue. This is because the tissue construct needs a vascular system to at least supply oxygen for the transplanted cells before their longer term integration (i.e. vascularization) into the host tissue. However, the vascularization does not often promptly take place after implantation, resulting in cell death within the tissue construct (MERTSCHING, et al. 2005). Therefore, the *in vitro* development of a pre-vascularized tissue construct is one possibility to solve this problem. For the achievement of this aim, the development of scaffolding materials with the capability of induction angiogenesis, to enhance the vascularization, particularly *in vitro*, is the focus of attentions towards the fabrication of viable and functional tissue constructs. Therefore, in this thesis, it is proposed to use a fibrous polymeric material (as scaffolding material) and to coat them on surface with an ECM component in order to induce angiogenesis in a 3D tissue construct. In fact, this approach is

1

aimed at influencing the vascularization by means of scaffold material composition and architecture. These goals will be achieved through the use of the "contact guidance" phenomenon, to modulate 3D patterning of the EC by enhancing the ECs migration, proliferation and orientation, and the ECM components, to support the ECs attachment, and thereby to directe angiogenesis *in vitro*.

The chemistry, topography and physics of polymeric materials at the cell-biomaterial interface strongly influence the function of the different cell types (WONG, et al. 2004). It has earlier been shown that most cell types self orient themselves and often move along fibres (WEISS and GARBER 1952) both biological (DUNN and EBENDAL 1978; SCHNELL, et al. 2007; VERNON, et al. 2005) and synthetic (CURTIS and RIEHLE 2001; NEUMANN, et al. 2003; SCHNELL, et al. 2007), having diameters in the nanometer or micrometer range, this behaviour being known as "contact guidance". Moreover, many studies have reported that micropatterned substrates, having parallel microgrooves of less than 100μm in size, are able to orient different cell types (BARBUCCI, et al. 2002). However, in the transfer of these results from a 2D model study to a 3D tissue engineering scaffold lies a great challenge (BASHUR, et al. 2006; BARBUCCI, et al. 2002). Biomaterials, bearing micro-channels (YU and SHOICHET 2005) or porous (HURTADO, et al. 2006; PAPENBURG, et al. 2007) structures, are often used as 3D scaffolds for the induction and orientation of cell or tissue ingrowths. Nevertheless, synthetic or biological fibres could also be used to modulate cell patterning by performing the phenomenon of "contact guidance", when dispersed in a 3D environment. The use of polymer fibres to control and direct cell responses, either for 3D cell patterning or for directing microvessel network formation within tissue engineering scaffolds, can be an easy and very effective approach in the field of tissue engineering. Synthetic polymer fibres can be

used in various formats in tissue engineering scaffolds, such as individual dispersed fibres within a 3D composite or networked to a tissue engineering scaffold.

However, the surfaces of a synthetic biomaterial often adsorb various proteins involved in biological media, resulting in the formation of an non-uniform protein layer on the implant surface (MCLEAN, et al. 2000b), in which the types of proteins and their conformations depend on the underlying surface properties. Moreover, the adsorbed proteins can exchange over time, thus producing unpredictable biological responses on the active surfaces (JUNG, et al. 2003; KRISHNAN, et al. 2004). In order to overcome such early stage, non-specific protein adsorption onto such biomaterial surfaces, these surfaces can be pre-coated with a layer of a bioactive compound that is able to exhibit predictable biological responses (MCLEAN, et al. 2000b). This has been conducted in many studies over the recent years (HADJIZADEH, et al. 2007; HERSEL, et al. 2003; MAHESHWARI, et al. 2000; RADOMSKI, et al. 1989; UNGER, et al. 2004). However, the use of proteins in medical applications is rather less demanding than peptides. This is because a protein may exhibit proteolytic degradation which makes it difficult for it to be used in long term applications (HERSEL, et al. 2003). Moreover, their biological activity may be influenced by the properties of the underlying substrate and their immobilization methods, causing difficulties in the comparison of the results obtained between one study and another (NEFF, et al. 1999). One solution employed to overcome the above mentioned problems is that of using cell binding motifs (i.e. small peptides) which exhibit greater stability towards environmental effectors (e.g. pH-variations, storage, conformational changes and heat treatments). In addition, in contrast with the large ECM proteins which normally comprise of many cell binding domains, the small peptides, by presenting only one single motif, can thus address one

3

specific type of cell adhesion receptor, resulting in the selective cell adhesion phenomenon (HERSEL, et al. 2003). Therefore, in order to create a selective bioactive surface, the small peptides are preferable to be employed.

A bioactive substrate can be fabricated through the use of biomolecules in three ways; i.e: (i) physical binding (van der Waals or electrostatic) (ii) chemical reaction and (iii) simple mixing (HUANG 2002). Physical adsorption often occurs immediately upon contact of a surface with a protein containing solution (HORBETT 1981; HUANG 2002). However, such an adsorbtion process is often reversible; the adsorbed molecules may desorb from the surface over time (JUNG, et al. 2003; KRISHNAN, et al. 2004). In contrast, covalently attached molecules can be more stable under physiological conditions and may even be more resistant to interruption under harsh environments (HUANG 2002). However, it should be noted that covalently immobilized biomolecules on rigid surfaces may encounter a change in the conformation or orientation of the biomolecule which may disturb the bioactive center of the molecule. This will cause a reduction in the molecule's activity to occur, and therefore, in order to overcome this problem, a spacer layer, located between the target surface and biomelecule, will be needed for the immobilization of bimolecules on it (HUANG 2002). In addition, the material surface is often encountered with an absence of appropriate surface functional groups needed to support the covalent attachment. One possible solution to this obstacle is that of providing adequate surface functionalization to these materials. For this reason, chemical or physical surface modifications are needed (HERSEL, et al. 2003). Therefore, in the designing of bioactive surfaces, the use of a multilayer surface modification strategy consisting of surface functionalization, spacer molecule grafting and biomolecule

4

immobilization can be an effective approach for the provision of the desired bioactive surfaces with the capability of exhibiting predictable biological responses.

Several published studies have reported on the surface modification of 2D substrates with cell-adhesive and cell-resistant coatings (HADJIZADEH, et al. 2007; HERSEL, et al. 2003; MASSIA and STARK 2001). However, there are only a few studies reporting investigations on the feasibility of fabricating and applying bioactive surfaces for 3D tissue development, with the aim of providing the particular surface chemistry within a 3D environment, desirable for directing cell responses and tissue culture. Therefore, it is possible that bio-active poymer fibres may offer a new approach first for cell patterning and then for tissue regeneration, this being one of the objectives of this thesis.

In vitro angiogenesis, i.e. the tube-like structures formation with the presence of lumen by ECs, was first reported by Folkman and Haudenschild (1980) (VAILHE, et al. 2001). However, from a physiological viewpoint, a perfect *in vitro* angiogenesis model should be able to provide the environment desirable in order to perform all of the *in vivo* angiogenesis phases (i.e. those arising from the initial activation of ECs in the preexisting vessel, upto the final tube formation and the vascular network remodeling). Preferably, the system should also be easy to both generate and to use, as well as being both reproducible and quantifiable (VAILHE, et al. 2001). In the physiological condition, angiogenesis occurs in a 3D environment, thus an *in vitro* anogiogenesis investigation should be performed within a 3D system. To achieve thses aims, several 3D angiogenesis systems have been developed (FOURNIER and DOILLON 1992; NEHLS and DRENCKHAHN 1995b; VERNON and SAGE 1999; VAILHE, et al. 2001). Among the several EC culture systems, a most interesting model was presented by Nels in 1995, in which EC-seeded micro-carriers (beads) were

embedded in a fibrin gel. In this model, the capillaries are spread radially outwards from the beads by the invading fibrin gel in the presence of growth factors (NEHLS and DRENCKHAHN 1995a; NEHLS and DRENCKHAHN 1995b). Accordingly, I proposed, as reported in the present thesis, to develop a similar system by replacement of the micro-carriers by the above mentioned, surface modified polymer fibres to the design of a 3D *in vitro* pre-vascularised tissue construct, consisting of fibrin gel and polymer fibres. These fibres can then be "networked" to form a scaffolding material for tissue engineering; in order to produce a pre-vascularized construct with directional microvessels. Therefore, this design is expected to be able to have a major impact in the regeneration of *in vitro* pre-vascularized, tissue-engineered, constructs.

1.2. The scope of this thesis

The overall objective of this research project is that of fabricating a scaffolding material to both enhance and to guide the vascularization within a 3D environment, which, in turn, will create a desirable directional condition for the blood microvessel formation and the subsequent 3D tissue development. In order to achieve the above mentioned aims, the following three specific objectives have been considered for this study:

1. Surface modification and characterization of flat and fibrous materials, and more specifically, polymeric fibres surfaces, using a multilayer, surface modification strategy, generating the needed cell adhesive, non-adhesive and bioactive coatings, required to produce the desired biological response.

2. *In vitro* evaluation of surface modified substrates towards EC behavior in a 2D cell culture system.

6

3. *In vitro* evaluation of surface modified polymer fibres towards the EC behavior

(angiogenesis) in 3D cell culture systems.

Objective 1:   Surface modification and characterization of materials, and more specifically, the surfaces of polymeric fibres, with cell resistant and cell adhesion compounds.

It is widely believed today that surface chemistry, physics and topography are all involved in the control of the behaviours of the different cell types present on polymeric materials at the cell-biomaterial interface. In order to achieve controlled and predictable biological responses, I propose to pre-coat the surface of polymer fibres with a layer of bioactive compounds that can exhibit predictable biological responses. To achieve this aim, one of the objectives of this study has been that of developing and then characterization of bioactive polymer fibres in order to both stimulate and direct the biological responses occuring within 3D environments. For this purpose, a thin polymeric layer, having either amine or aldehyde groups, was deposited onto the prepared substrates by means of "radiofrequency, glow discharge deposition" (RFGD). Plasma polymerization of n-heptylamine or acetaldehyde was performed within a custom-built plasma reactor. It has been demonstrated that by using this method it is possible to deposit a "cross-linked" organic thin film, with appropriate functional groups on various substrates (MOROSOFF 1990). Subsequently, carboxy-methyl-dextran (CMD), covalently grafted onto the n-heptylamine plasma polymer (HApp) or the acetaldehyde plasma polymer (AApp) coated surfaces, using the water-soluble, carbodiimide chemistry (ethyl (dimethylaminopropyl)-carbodiimide/N-hydroxysuccinimide) (EDC/NHS). CMD is a polysaccharide, with carboxyl groups that can be used as a "platform" for covalently grafting of bioactive compounds, and also as a low-fouling layer to limit undesirable protein adsorption

7

or cell adhesion (MCLEAN, et al. 2000b). Finaly, specific bioactive molecules (e.g. the arginine-glycine-aspartate peptide sequence or RGD) were covalently immobilized onto previously CMD coated surfaces, by the use of the carbodiimide chemistry, as described above, for the CMD coatings. The characterization of the coatings, in each step of the multi-layer surface modification sterategy, has been performed by X-ray photoelectron spectroscopy (XPS) analyses. Additional characterization of the multi-layer fabrication steps has been also carried out, using the AFM and SEM analysis techniques.

Objective 2: *In vitro* evaluation of surface modified polymer fibres towards EC behavior in a 2D cell culture system.

The control over cell functions (e.g. cell adhesion, spreading, orientation and proliferation), using biomaterial surface properties, could have a prominent impact on the design of smart biomaterials, prepared in order to generate functional tissues and organs. The presence of micro-curvature and bio-signals on a surface may mediate cell patterning (i.e. orientation) by promoting the cell-cell and cell- matrix interactions (MAGNANI, et al. 2003). To this aim, in this phase of the study, the effect of fibre curvature in comparison to that of flat surfaces in addition to the chemical composition of the fibre surface on the ECs behaviours, were studied in terms of their adhesion, spreading, cytoskeleton reorganization and orientation, all within a 2D (monolayer) cell culture system. For this aim, human umbilical vein endothelial cells (HUVECs) were seeded and grown onto fibres and flat substrates to observe cell behaviour (i.e. cell adhesion in early culture, subsequent spreading, cytoskeleton reorganization, and cell orientation).

8

Objective 3: *In vitro* **evaluation of the surface modified polymer fibres towards EC behavior (angiogenesis) in a 3D cell culture system.**

In the tissue engineering approach formation of a viable, thick and large-scale tissue construct (e.g. muscle) *in vitro* and *in vivo* is still one of the unresolved issues (LEVENBERG, et al. 2005). Therefore the development of a pre-vascularized tissue construct *in vitro* could be one of the more promising solutions to overcome this problem. This present study proposes to develop a vascularized in *vitro* 3D tissue construct, using surface modified polymer fibres to enhance and guide the microvessel formation within a 3D scaffold. In this part of the study, the above mentioned surface modified PET monofilaments were evaluated towards angiogenesis in 3D cell culture systems. To do that, three *in vitro* cell culture systems, using different cell seeding methods, were designed and constructed, having both untreated and surface-modified polymer fibres embedded in a fibrin gel, in order to demonstrate the feasibility of directing microvessel formation within a 3D environment. In these systems, HUVECs has been either introduced onto the whole surfaces of the fibres or dispersed around the cell-free fibres.

Chapter 2

Literature review I: Biomaterials in tissue engineering

2.1. Overview

Biomaterials have been widely used in biomedical devices, and they are the subject of intensive research for their use in tissue engineering applications (e.g. in scaffolding materials). However, upon implantation, due to exposure to a multi-component biological media, various proteins may adsorb onto the surfaces of the implanted biomaterials (MCLEAN, et al. 2000b), with some exchange over time (Vroman effect) (JUNG, et al. 2003; KRISHNAN, et al. 2004), which affects the appropriate performance of the biomaterials. This problem can be solved by pre-coating a biomaterial surface with a layer of a bioactive compound which exhibits a predictable biological response (MCLEAN, et al. 2000b). For this reason, the role of biomaterials in tissue engineering is briefly reviewed in this chapter. Then, the cell-ligand interaction, surface modification and characterization, using biologically active molecules, e.g. RGD peptides, and the fabrication and characterization of cell resistant surfaces, have been studied. Next, the *in vitro* evaluation of the surface modified biomaterials has been presented. Finally, the explanations for the effect of material properties on cell behavior have been advanced.

2.2. Introduction to biomaterials used in tissue engineering

Materials, having typical chemical, physical, mechanical or electrical properties, named biomaterials that are produced by employing or mimicking biological events. These materials are frequently used in medical devices, for example dental implants, artificial hip joints, artificial blood vessels, etc. (HANKER and GIAMMARA 1988; SCHACHT 2004).

In the field of biomaterials the attentions have been focused on the production of materials with the capability of controlling cell responses at the molecular level with the aim of transforming cultured cells to form new tissues (MEDDAHI-PELLE, et al. 2004). Synthetic polymeric biomaterials, with such capability for controlling cell functions and cell-cell interactions, can be used either in cell-free implants as matrices to promote the tissue regeneration or those implants that support cells for transplantation (HUBBELL 1995). It has been demonstrated that upon contact with biological media a layer of proteins is formed at the biomaterial surface (BENMAKROHA, et al. 1995). Since in the healing process, the integration of an implant into the host tissue is required; therefore the adsorption of ECM proteins (e.g. FN or vitronectin (VN) in an active conformation) to an implant surface will be a beneficial event in this interaction (HUANG 20002). For this reason, these phenomena have been mimicked on the inert implant surfaces by incorporating extracellular matrix (ECM) components, or their functional domains (i.e small peptides such as RGD), to promote cell adhesion (HADJIZADEH, et al. 2007; KOUVROUKOGLOU, et al. 2000; OLIVIERI and TWEDEN 1999). For example, the use of the small peptides containing RGD sequence has shown to accelerate the healing process and improve the quality of the regenerated tissue (STEED, et al. 1995). Conversely, in some other applications (e.g. contact lenses, artificial blood vessels, etc.) non-spesific adsorption of proteins from the surrounding biological media is required to be controlled (Haung 2002).

11

Towards achieving this aim, many studies have been conducted, using non-fouling materials, e.g. poly (ethylene glycol) (ALCANTAR, et al. 2000; PASCHE, et al. 2005), polysaccharides (HADJIZADEH, et al. 2007; MCLEAN, et al. 2000a; MASSIA and STARK 2001) to prevent the occurrence of undesirable biological events.

Therefore, the surface-coated artificial biomaterials, developed in the biomaterials field, can be classified into two main categories, 1) biomaterials coated with a specific adhesive compound towards a typical biological entity and 2) materials coated with compounds resistant towards the biological entities present. By employing these two approaches, the creation of materials capable of exhibiting selective biological responses, is presently the subject of intense research activity. These materials may then be "patterned" in both 2D and 3D forms to generate multi-cellular tissue constructs. These approaches continue to be assayed for application in both recent and future research to produce complex cellular arrangements, as found in natural tissues and organs (HUBBELL 1995).

2.3. Basic biology of integrin stimulated cell adhesion (bioactivity)

A material is described as being bioactive if it has interaction with or effect on any living cell or tissue. The paragraph below explains the basic mechanisms of this interaction. The interaction of a cell with neihgboring cells and surrounding ECM takes place via cell membrane receptors (Fig. 2.1). Among these membrane receptors, the integrins form the most multi-purpose group. These cell surface glycoprotein receptors are made by a heterodimer of α- and β-subunits (membrane proteins) (HERSEL, et al. 2003). These proteins, bearing large extracellular parts, couple together and create adhesive heterodimers (CAI, et al. 2006), which can match with a ligand (i.e. the ECM proteins or specific peptides) (Fig. 2.2) (HODIVALA-

DILKE, et al. 2003). During cell aggregation and angiogenesis, the integrins play their role by binding to the ECM proteins (e.g. FN and VN) or to the cell surface immunoglobulin proteins, e.g. intercellular adhesion molecule-1 (ICAM-1) and vascular cellular adhesion molecule-1 (VCAM-1) (DUNEHOO, et al. 2006). According to the literature, certain integrins play more roles than others in cell biology, for example; $\alpha v \beta 3$ integrin binds many ligands, including FN, VN, von Willebrand factor (vWf), osteopontin, bone sialoprotein, tenascin, and thrombospondin (HERSEL, et al. 2003).

Studies on the cell adhesion activities of ECM proteins such as VN, fibrinogen, collagen, vWf, and laminin, have shown that the small peptide sequences, including Arg–Gly–Asp (RGD) tripeptide involved in these proteins (Fig. 2.3), are cell adhesion sites towards the cell adhesion receptor present on the cell membrane (ENGEL1991). During the last several years, many studies have reported on the use of the RGD peptides as a small immobilized cell adhesion domain to promote cell attachment on the synthetic surfaces. This is because of its ability to bind to more than one cell membrane receptor (HERSEL, et al. 2003). Since after establishing FAs, cell contractile forces are able to displace weakly adsorbed ligands, leading to weak cell adhesions, for strong cell adhesion promotion, the covalently grafting of RGD peptides to synthetic surface is required. Moreover, in the case of presence of mobile ligands, these ligands will be removed by cell internalization (HERSEL, et al. 2003).

For example, in our previously published study (HADJIZADEH, et al. 2007); it was found that covalently grafted RGD onto glass and PET, via dextran spacer layer, promoted HUVEC adhesion and spreading. Similarly, covalently linked RGD on glass (MANN, et al. 1999), PET and PTFE substrates (MASSIA and HUBBELL 1991a) or polystyrene plates (HOLLAND, et al. 1996) has been found to modulate HUVECs functions in terms of increasing cell adhesion

and spreading. Furthermore, Tyr-Ile-Gly-Ser-Arg (YIGSR) peptide (found in laminin), an integrin receptor ligand, has also been covalently linked to glass substrates that have shown an increase in the spreading and proliferation of HUVECs (MASSIA and HUBBELL 1991a). Arg-Glu-Asp-Val (REDV) peptide (found in FN), has been found to be a specific EC adhesion peptide. Covalently grafted REDV on a PET surface, initially coated with polyethylene glycol, stimulated the attachment and spreading of ECs, but not that of the fibroblasts (HOLT, et al. 1994; HUBBELL, et al. 1991), smooth muscle cells and platelets (HUBBELL, et al. 1991).
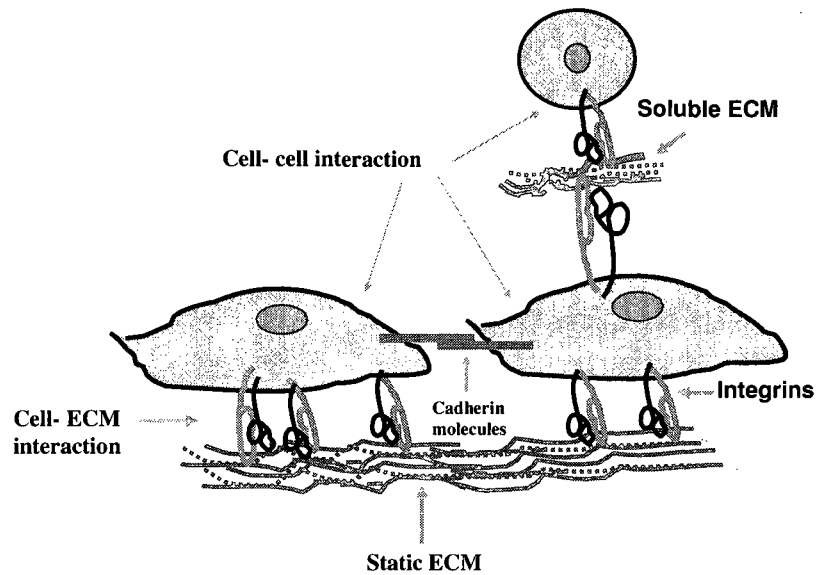
Figure 2.1: Schematic illustration showing cell-cell and cell-ligand (ECM protein) interactions (adapted from WARY 2005)
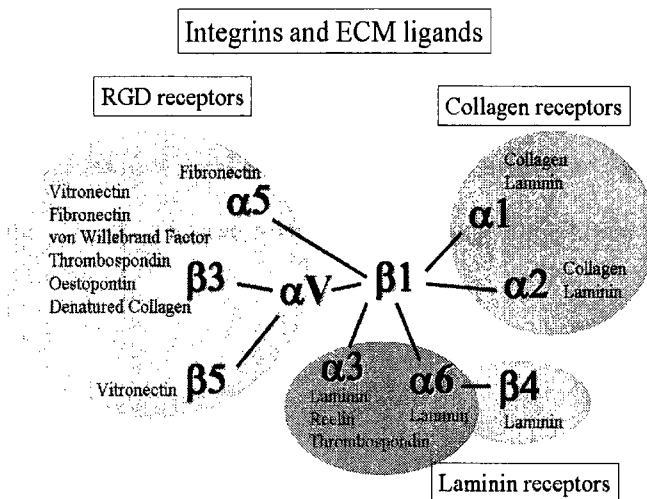
Figure 2.2: Integrins (heterodimer of α- and β-subunits) and their ECM ligands (reproduced from HODIVALA-DILKE, et al. 2003)
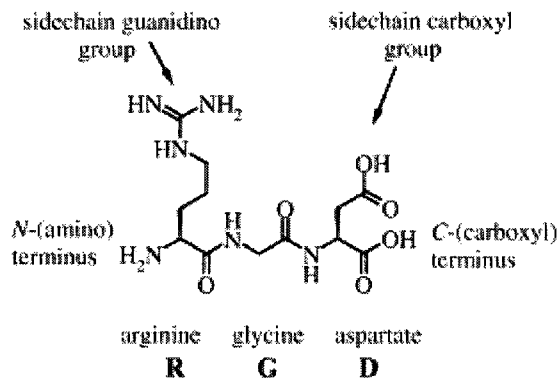
Figure 2.3: The sequence, molecular formula and nomenclature of RGD tripeptide (reproduced from HERSEL, et al. 2003)

2.3.1. Advantages of peptides to proteins (ligand selection)

As mentioned above, substrate surface functionalization to obtain desired cell surface interactions has drawn the attention of many researchers. In cell-biomaterial interface, protein containing compounds mediate cell-substrate interactions. These compounds can be introduced onto substrate surface in three ways: (i) by pre-immobilization process onto the surface of the material, (ii) by adsorption process from medium that surrounds the substrate or

(iii) through the protein secretion by the cells during earlier culture (NEFF, et al. 1999). For this purpose, over the few last decades, ECM proteins have been widely incorporated onto synthetic biomaterials and used to promote interactions of the cell with the biomaterial (NEFF, et al. 1999) in both *in vivo* (SEEGER and KLINGMAN 1985) and *in vitro* (KAEHLER, et al. 1989) applications

The use of proteins, however, may cause some problematic conditions in the medical applications. Since these materials are susceptible to break down due to proteolytic degradation, their long-time applications, without continuous refreshment, are impossible (HERSEL, et al. 2003). Moreover, the effects observed for a certain protein depend on many factors including the underlying surface properties (e.g. chemical, topographical and charge), the method of immobilization and protein adsorption from the surrounding environment. All of these factors may cause diversity in the results obtained from one study to another. The protein conformation and/or orientation may change on different surface types, depending on surface chemical composition, wettability, topography and charge (NEFF, et al. 1999). Since cells bind to specific domains within their protein ligands (i.e. ECM proteins) through cell membrane receptors (i.e. integrins), the changes in either orientation or conformation of ligand on the surface relative to its cell binding domain will strongly influence the ability of cells to attach to these surface bound proteins. Moreover, additional non-specific proteins may be adsorbed from the surrounding biological media onto the test surface. These events will make it difficult to find a precise relationship between the ligand and the resulting cell behavior (NEFF, et al. 1999). Therefore, the use of small peptides instead of the large proteins, offers many advantages, including: (1) they exhibit higher stability towards heat treatment, storage, conformational changing and pH-variation, (2) able to be packed at higher density on their

surfaces, and (3) to bind to a specific cell surface receptor due to their representing only one single motif (HERSEL, et al. 2003).

2.3.2. Bioactive molecule (ligand) immobilization

Incorporation of bioactive ligands into a polymeric substrate can be achieved in four different ways: (i) physical adsorption, through the van der Waals interactions, (ii) adsorption through hydrophobic and electrostatic forces, (iii) inclusion in the input bulk composition, or (iv) immobilization via chemical reaction (HUANG 2002). As the immobilization of bimolecules via chemical reactions is the focus of the attention of this thesis, then a brief comparison between this method and that of physical adsorption is introduced in the paragraph below.

It has been reported that, each approach may have both advantages and drawbacks. The physical adsorption of biomolecules onto surfaces is fast and generally allows for the maintenance of the biomolecule bioactivity, due to the process being performed under mild conditions (HORBETT 1981; HUANG 2002). Most proteins, adsorb on hydrophobic surfaces, via hydrophobic interactions (SCHAEFERLING, et al. 2002). However, on such protein adsorbed surfaces some exchanges may occur over time (Vroman effect) (JUNG, et al. 2003; KRISHNAN, et al. 2004). According to the explanation of this phenomenon, in the process of protein adsorption to a surface, the small proteins with low-molecular-weights first reaching a surface are displaced by the larger proteins that arrive late (VROMAN, et al. 1971).

Covalent immobilization of a biomolecule onto the surface of a polymeric substrate produces an irreversible bond which is more stable under the physiological conditions (HUANG 2002). However, it should be noted that covalent grafting of a biomolecule onto a solid

surface may change the conformation or orientation of the biomolecule and thus disturb its bioactive center. As a result, a reduction in the molecule's activity is caused (HUANG 2002). Therefore, a spacer layer will be needed to be used as a platform on which to covalently immobilize the biomolecule. In addition, the material surfaces usually encounter an absence of the appropriate surface functional groups to support the covalent attachment. One possible approach for overcoming these problems is that of providing surface functionalization to these materials. For this reason, there are currently a large number of research groups that have focused on these chemical and physical surface modification methods, and are endeavouring to produce thereby surfaces that are capable of inducing successful immobilization of the biomolecules (HERSEL, et al. 2003).

Chemical and physical treatments to introduce functional groups for covalent immobilization of ligands

Several methods, based on chemical and physical treatments, have been employed to introduce functional groups onto the polymer surface. For example, track-etching, reduction, oxidation, or plasma deposition has all been used to produce appropriate surface chemical groups on PET and Teflon surfaces. For instance, PET has been modified by track-etching to generate a mixture of carboxyl and hydroxyl groups, which may then be treated, either by using reducing against (e.g. sodium borohydride) to obtain uniform hydroxyl functionalization, or they can be oxidized by using an oxidizing agent (e.g. potassium permanganate) to obtain the carboxylic acid end groups. As another example the surfaces of Poly (tetrafluoroethylene-co-hexafluoropropylene) (FEP) can be treated, by the reduction of this polymer with appropriate reducing agents (e.g. sodium naphthalide), to thereby generate carbon-carbon double bonds. These may then be converted to carboxyl groups within a further

oxidation step (HERSEL, et al. 2003). In addition to surface functionalization by means of "wet chemical" treatments, plasma-deposited polymeric thin films also offer an alternate route to create a platform having appropriate surface functional groups, for later use in the biomolecule immobilization performed on various materials (HADJIZADEH, et al. 2007).

Surface modification by plasma polymerization

The term "plasma" is used here to refer to the very high energy content of the "fourth state of matter" which includes equal numbers of oppositely charged species. Over recent decades, "cold plasma" has been increasingly used to induce chemical reactions on the surface of various substrates by active species generated in the plasma environment, including both organic and inorganic materials. It has also been demonstrated that the surface properties of materials, including their surface roughness, surface energy and their optical and electrical properties, can all be modified via the plasma process. Thus polymer surfaces can be treated in cold gas plasma in three ways, i.e. plasma treatment, plasma induced grafting, and plasma polymerization, leading to the creation of materials with new properties for biomedical applications (MOROSOFF 1990).

Plasma treatment

Surface treatment by plasma is a plasma reaction process employed for the surface modification of materials, by creating atomic substitution or by alteration of the molecular structure of the surface at low temperatures. In this process, both high energy ultraviolet light and charged species (i.e. high energy ions and electrons) are created in the gases present, such as oxygen, nitrogen, argon, etc. This energetic event provides the input energy necessary to fracture polymer bonds and thereby initiate chemical reactions at the polymer surface, altering

the top few atomic layers without significantly affecting the bulk properties of the polymer [website ref.1].

Plasma-induced grafting

The plasma-induced grafting process takes place in two steps, the surface is initially functionalized by the use of a gas-plasma treatment, and then a desired monomeric chemical is grafted onto the functionalized substrate via polymerization treatment (GUPTA, et al. 2002).

Plasma polymerization

Plasma polymerization has now become widely accepted and used to modify the surfaces of a wide range of materials. In this process, the vapor of an organic chemical is polymerized, at low temperatures to produce a cross-linked thin film on the substrate surface. In the plasma polymerization, the plasma is initially created through the ionization of gases or vapors present in the reactor, and secondly, the fragmentation of monomeric chemicals (i.e. organic vapors) leading to the polymerization takes place. Various positive ions, e.g., $C+$, $CH+$, $CH2+$ etc.; radicals and other excited fragments are produced when high-energy electrons crash with hydrocarbon molecules, resulting in the formation of plasma polymer on the surface. The properties of these plasma deposited thin polymeric films can be influenced by the plasma polymerization parameters, such as the monomer flow rate, the system pressure and the discharge power (MOROSOFF 1990).

2.3.3. Methods for the covalent immobilization of RGD peptides to functionalized surfaces.

Generally, peptides and proteins are grafted onto those particular polymers that contain carboxylic acid groups, via a stable, covalent amide bond. This union can be achieved by the reaction of an activated surface, carboxylic acid group with the nucleophilic N-terminus of the peptide. Carboxylic acid groups may be activated through the use of a condensing agent which can accelerate the reaction between the COOH groups at the surface and the NH_2 groups of the protein or RGD peptide, e.g. 1-ethyl-3-(3Dimethylaminopropyl)-carbodiimide (EDC, water soluble carbodiimide, WSC), dicyclohexyl-carbodiimide (DCC) or carbonyl diimidazole (CDI) (GAO, et al. 2003; HERMANSON 1996; HERSEL, et al. 2003).

However, the use of this coupling method may lead to two problems being encountered, including: (i); intermolecular condensation of the RGD peptide. This event can take place due to the existence of further reactive groups within the RGD molecule (Fig. 2.3) (i.e. the two carboxyl groups, one at the C-terminus and the other in the aspartic acid side chain and also the nucleophilic guanidino group of the arginine side chain), and (ii); deactivation of carboxyl groups due to hydrolysis of the coupling reagent and activated carboxyl groups (HERSEL, et al. 2003). One possibility for overcoming these problems involves the use of protected RGD peptides (i.e. the reactive amino acid side chains are blocked with protecting groups) and to use non-aqueous solvents, such as dimethylformamide (DMF), dichloromethane or acetone. However, this immobilization strategy has to be performed under "harsh" reaction conditions in order that the protecting groups (HERSEL, et al. 2003) are satisfactorily removed.

It should be noted that, the coupling process through the use of unprotected RGD peptides in water, is also possible. This approach is conducted via a two step procedure, as an

alternative. In this two step procedure, the carboxyl group is initially activated to produce an active ester, e.g. the N-hydroxysuccinimide (NHS) ester which is less prone to hydrolysis. The peptide is then coupled with the activated carboxyl group, either in water, dichloromethane or DMF, in the presence of EDC (Fig. 2.4) or DCC to activate the carboxyl groups for subsequent reaction with NHS (HERSEL, et al. 2003). The half-life of the NHS active esters can be affected by varying the pH of the aqueous solution. At near neutral pH values, the half-life time ranges between several minutes and hours, depending on the substituents attached to the α-carbon atom. The higher pH values and salt concentrations can cause a reduction in the half-life time of the NHS active ester, bringing it down to less than 1 min. The coupling of the activated carboxyl groups with the amine groups is usually completed in a period of between 1 and 2 hrs. The product yield may be controlled by varying the coupling condition, e.g., it can be increased by lowering the pH and/or temperature values over a longer coupling time. Moreover, the use of higher peptide solution concentrations may produce higher peptide densities on the surface (HERSEL, et al. 2003).

RGD peptides can also be immobilized on polymer surfaces, via pre-activated amino or hydroxyl groups, or via some other methods. For more detailed discussions on these matters, see the following references (HERMANSON 1996) and (HERSEL, et al. 2003) respectively.
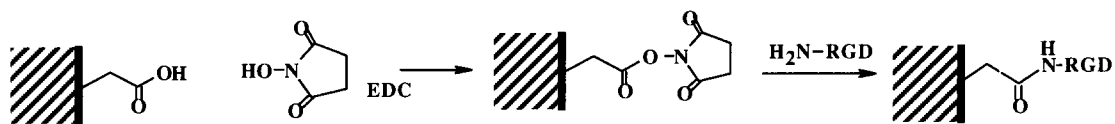
Figure 2.4: RGD peptides linked via the N-terminus to carboxyl groups, carboxyl groups (COOH) being preactivated with a carbodiimide and NHS, to generate an active ester on the polymers (adapted from HERSEL, et al. 2003).

22

2.3.4. RGD surface arrangement

A certain minimum spacing between the RGD sequence and the binding site of the integrin may sometimes be important for cell attachment, so that, in order to mimic the position of the RGD sequence in its distinct protein, the RGD peptide must project from an artificial surface in order to reach the binding site of the integrin. This can be achieved by the covalent grafting of the RGD, via a spacer molecule. However, despite the many reports that have been published about the effects of the spacer on the activity of RGD peptides, the role of the spacers on the activity of the RGD is still not fully understood. The revealed data are often in disagreement from one study to another. Therefore, more investigation is still needed to better clarify this issue (HERSEL, et al. 2003).

Taken together, the best way to produce a stable bioactive surface is the covalent immobilization of the bioactive peptide, e.g. RGD peptides, via a two step procedure conducted on an initially functionalized surface. Among the several methods presented for surface functionalization, the plasma polymer deposition with an appropriate functional group, e.g. NH_2 or CHO, can be the preferred method because the plasma deposition can be performed on a variety of substrates. In addition, in order to retain the maximal activity of a covalently immobilized biomolecule, a "spacer layer" is often introduced between the target surface and the biomolecule. To achieve this aim, those polymers with non-fouling properties and containing extra functional groups are the more demanding materials (LOFAS and JOHNSSON 1990; HERSEL, et al. 2003). Then, bioactive molecules, e.g. peptide sequences and growth factors, can be covalently attached to the surfaces containing these polymer chains so as to promote cell-surface interactions.

23

2.4. Low- fouling materials

Besides the bioactive surfaces, protein-resistant or non-fouling surfaces are also important in many fields, including biomedical devices, tissue engineering and biosensors (HUANG 2002). Protein adsorption and cell adhesion on biomaterial surfaces are known to be related to the interfacial forces present between the substrate surface and contacting biological entities. These interfacial forces (i.e. the electrostatic interactions, hydration forces, and steric-entropic effects) are generated by surface chemical groups, wettability, charge and surface structure of the biomaterial (MCLEAN et al. 2000a). To produce low-fouling surfaces, some polymers, such as poly (ethylene glycol) (PEG) (ALCANTAR, et al. 2000; ZHANG, et al. 1998; PASCHE, et al. 2005), poly (vinyl alcohol) (BARRETT, et al. 2001) and some polysaccharides, e.g. carboxymethyl dextran (CMD) (HADJIZADEH, et al. 2007; MCLEAN et al. 2002a), have been studied and have shown to possess the ability to minimize the adsorption of proteins (MCLEAN et al. 2002b) and cell adhesion (HADJIZADEH, et al. 2007; MCLEAN et al. 2002a). These polymers can be also employed as functional platforms for bimolecule immobilization, to produce specific biological responses.

2.4.1. Polyethylene glycol (PEG)

PEG is a polymer, having hydrophilic and electrically neutral properties that have been widely used for protein- and cell-resistant surface modifications. Un-modified, PEG polymer chains are linear, having only two terminal reactive groups (Fig. 2.5). Therefore, in using this polymer as a platform (spacer layer) for biomolecule grafting only one of the two reactive groups will become available for the biomolecule coupling. Subsequently, non-sufficient concentrations of covalently

attached bioactive molecules will be produced, to promote biospecific responses on their surfaces (MASSIA and STARK 2001).

PEG
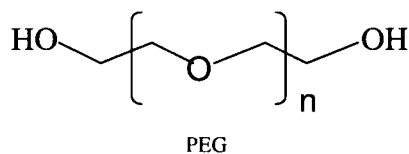
Figure 2.5: Polyethylene glycol polymer.

2.4.2. Polysaccharides

In addition to PEG, polysaccharides as low-fouling materials have also been the focus of attention in recent biomaterials research. Polysaccharide coatings can prevent the adhesion of mammal cells to synthetic biomaterials and reduce adhesion of bacteria *in vitro* and in *in vivo* applications (MORRA and CASSINELI 1999). Thus, dextrans, and their derivatives, have been used as low-fouling coatings (LOFAS and JOHNSSON 1990; MCARTHUR, et al. 2000a). The interfacial forces involved in the interactions of polysaccharide coatings with biological molecules, and cells present in biological media, arise from their chemical composition and structure. In fact, polysaccharides mainly reject proteins or cells by their hydrated, hydrogel-like structure and the steric-entropic forces generated by their mobile molecular chains (MCLEAN, et al. 2000a).

Carboxymethyl dextran (CMD) (Fig. 2.6) is a derivative, a carboxymethyl substitution of dextran, which is synthesized by the reaction of dextran with bromoacetic acid (LOFAS and JOHNSSON 1990). CMD has been of interest in this thesis study because of its low-fouling properties and the incorporated COOH groups which are able to be employed to covalently

immobilize biomolecules. A schematic of the CMD chains, grafted onto the substrate surface, having carpet-pile like structure is shown in figure 2.7.
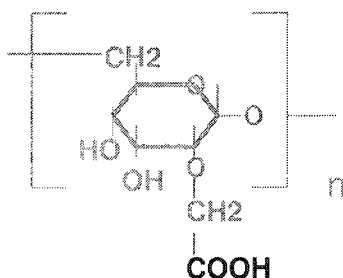
Figure 2.6: Carboxymethyl dextran (CMD) (adapted from MCARTHUR, et al. 2000)

Figure 2.7: CMD chains having COOH groups (black dots) grafted on the surface with a carpet-pile like structure

2.5. Physicochemical characterization of surface modified polymers

2.5.1. Characterization of thin film coated surfaces

The most recent physicochemical surface analysis methods that have been widely used for the analysis of thin film coated surfaces are: - XPS, AFM and SEM (See appendix for more details on the basics of these techniques). The elemental and chemical composition of surfaces can be analyzed by electron spectroscopy for chemical analysis (ESCA) or XPS (RATNER and CASTER 1997). The topography of the surfaces can also be quantitatively and qualitatively analyzed by AFM (LEGGETT 1997). SEM is still being used in morphological analysis because of having a more satisfactory depth of focus (~ 300 times greater than that of

a light microscope). Many studies have employed the XPS technique (GENGENBACH, et al. 1996) and AFM (HARTELY, et al. 2000) for the measurement of surface elemental compositions and the surface topography of plasma coated surfaces, respectively. Similarly, XPS (MASSIA and STARK 2001; MCLEAN, et al. 2000a) has been employed to characterize the above-mentioned polysaccharide grafted surfaces.

2.5.2. Characterization of RGD modified polymers

The analyses of RGD grafted surfaces should be capable of revealing the presence of RGD peptides, either directly or indirectly. According to the literature, several methods have been employed for the qualitative and quantitative analysis of RGD coated surfaces (HERSEL, et al. 2003; GODDARD et al. 2007). Among the range of available spectroscopic base methods, XPS has been most frequently used for direct dectection of covalently grafted RGD on those surfaces, displaying a coating rich in both nitrogen and in C=O carbons. Moreover, this technique is capable of detection the vertical distribution of nitrogen (by varying the take-off angle), revealing the presence of the peptide in at least 10 nm (the XPS analysis) depth (HERSEL, et al. 2003). By incorporating an elemental tag (e.g. fluorine or iodine) into the RGD peptide, the quantification of covalently grafted RGD will also be possible (BILTRESSE, et al. 2005; HERSEL, et al. 2003). Evaluation of the biological activity of the RGD-coated surfaces is another indirect method that has been used to determine the RGD densities on the surface, by measuring the amounts of attached cells (HERSEL, et al. 2003).

Several other spectral and non-spectral methods have also been employed to analyse RGD-coated substrates, both qualitatively and quantitatively. These methods have been explained in

detail in two excellent review articles provided by Hersel et al. (2003) and Goddard et al. (2007).

2.6. *In vitro* evaluation of surface modified biomaterials towards cell behavior

In vitro studies have been performed in order to evaluate the biological properties of the modified material surfaces for future medical applications. For the biomaterials that will be applied as matrix for anchorage-dependent cells; cell attachment, cell spreading, cytoskeletal reorganization, formation of focal adhesions, proliferation and cell motility are mainly evaluated (HERSEL, et al. 2003). The 4 first named events, which comprise the basic process of integrin-mediated cell adhesion (HERSEL, et al. 2003), have been explained in Chapter 6 (section 6.2).

Cell adhesion to artificial surfaces is important for its use in many biomedical and biotechnological applications. In the case of anchorage-dependent cells, adhesive interactions play important roles in cell functions such as cell survival, growth, and differentiation, by activating various signaling pathways (KESELOWSKY, et al. 2004). For instance, it has been shown that not only is the cell attachment but the cell morphology also is an important parameter in the EC growth, when cultured on adhesive plastic culture dishes (coated with poly (2-hydroxyethyl methacrylate)) (FOLKMAN and MOSCONA 1978) and FN coated substrates (INGBER 1990). According to the published reports, cell adhesion to RGD-coated polymers is time-dependent (HERSEL, et al. 2003). In many studies, cell adhesion is tested, usually 1-6 h, after cell seeding (BILTRESSE, et al. 2005; HADJIZADEH, et al. 2007;

HERSEL, et al. 2003; LARSEN, et al. 2006; MASSIA and STARK 2001). In order to quantify the cell adhesion, non-adherent cells can be eliminated through washing, shaking or centrifugation. The attached cells can be quantified by the use of different colorimetric methods (HERSEL, et al. 2003). Cell spreading can be qualitatively evaluated by the observation of cells under the microscope (optical microscope or SEM), and the use of specific fluorescent compounds makes it possible to visualize the actin filaments by fluorescence microscopy. By use of immunocytochemistry with specific antibodies, the components involved in focal adhesions can be detected. Cell motility can also be measured (e.g. by the use of time-lapse microscopy) and the physical processes involved in the migration of cell have been explained in the following references (LAUFFENBURGER and HORWITZ 1996; SHEETZ, et al. 1999).

To ensure if cell adhesion on RGD coated surfaces is due to the biospecific interaction between the cells and RGD, the three following controls can be employed: (i) non-coated surface, (ii) surfaces coated with inactive peptides (or negative control peptide) and (iii) competition between covalently bound and un-bound RGD peptides. The unbound peptides can be introduced to the culture system before or after cell attachment, which may prevent cell adhesion or lead to cell detachment, respectively (HERSEL, et al. 2003).

2.7. Effect of biomaterial properties on cell behavior

Material properties, such as chemical, topographical, and mechanical features, can be classified into three groups of stimuli, to which a cell will respond (CURTIS and WILKINSON 1997; TAN and SALTZMAN 2002; WONG, et al. 2004). These three different types of cues exhibit almost similar effects; e.g. the cell shape has been changed by modifying the chemistry, topography, or mechanics of the substrate (Fig. 2.8) (WONG, et al. 2004).
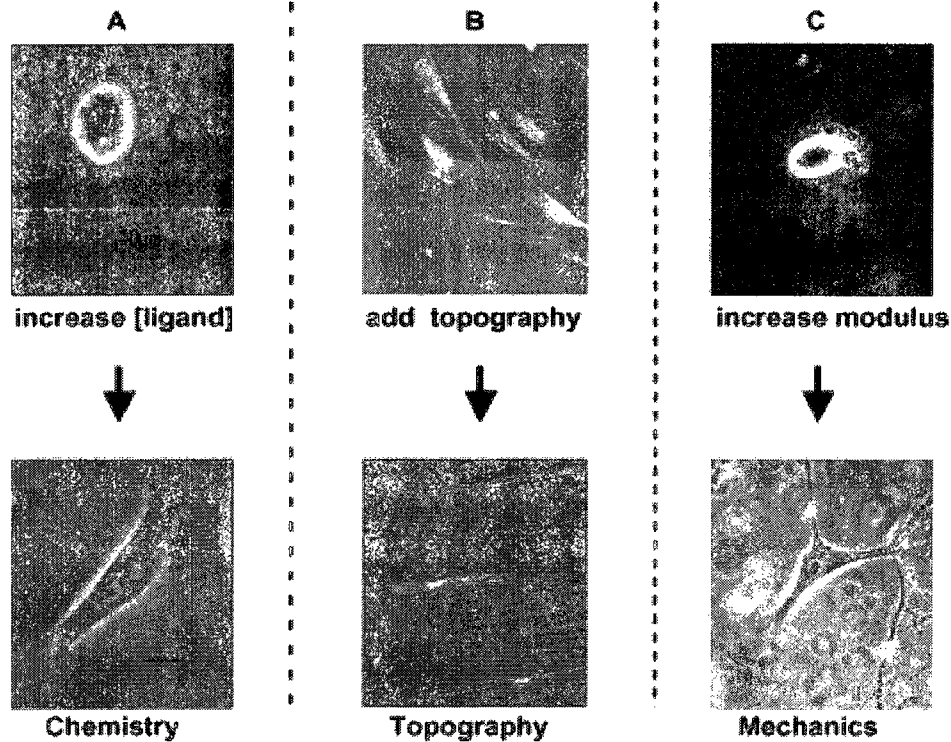
Figure 2.8: The effect of substrate surface chemistry, topography or mechanics on cell response: A) Fibroblasts on type I collagen-coated polyacrylamide substrata. Top panel has lower surface concentration than bottom panel. B) Vascular smooth muscle cells on polydimethylsiloxane (PDMS) substrata; with no topographical features (top panel), and with microgrooved topography (bottom). Both textured and nontextured PDMS were treated with FN. C) VSMCs on polyacrylamide substrata with different elastic modulus. The lower panel is stiffer than the upper panel. Substrata have been modified with collagen (reproduced fromWONG, et al. 2004).

2.7.1. Material stiffness

There are several reports advising that cells are able to respond to the substrate stiffness (LO, et al. 2000; PELHAM and WANG 1998; YEUNG, et al. 2005; YAMAMURA, et al. 2007). The stiffness of the surface, supporting cell attachment, influences cell behaviour in terms of cell morphology and protein expression. However, this effect, depending on cell membrane receptors, varies with different cell types. For example, fibroblasts and ECs spread

30

and form actin stress fibers only when grown on surfaces with an elastic modulus greater than 2,000 Pa. (YEUNG, et al. 2005). Lo et al. (2000) have demonstrated that fibroblast cells probe substrate rigidity to select their preferable direction to move. In addition, they believed that controlling the mechanical strain within a flexible substrate can be another concept to guide cell movement direction. It has been concluded that the cells may respond to substrate rigidity via their contractile forces by which they interpret the deformation in the substrate and determine a new preferable direction to move on a surface. In addition, it has been found that not only cell movement rate but also cell shape can be affected by substrate rigidity (LO, et al. 2000). They found these by culturing the cells on substrates with different rigidities, but with the same chemical properties. The mechanical properties of substrates not only affect cell behaviour in 2D (monolayer) cell culture but have also been reported to regulate the 3D network formation by the ECs. For example, Ingber et al. (1989) have shown that the softer materials increased the formation of tube-like structures in 3D. Sieminski et al. (2004) suggested that the relative magnitudes of the forces generated by the ECs and the matrix stiffness may also play a regulatory role in the microvessel formation in *vitro* and *in vivo*. Moreover, bovine pulmonary microvascular ECs formed dense, thin networks in the flexible collagen gel, whereas thicker networks were formed in the rigid gel (YAMAMURA, et al. 2007).

2.7.2. Surface topography

A range of studies have demonstrated that the surface topography directly affects cell behavior, such as its orientation, migration, cytoskeletal production and arrangements (ANDERSSON, et al. 2003; CURTIS and WILKINSON 1997; TAN and SALTZMAN 2002;

31

FLEMMING, et al. 1999). The topographical factors affecting cell behavior can be classified into two main categories, including the shape and scale factors. In the case of the shape factor, the surface topography, which can influence cellular interactions, includes the grooves, ridges, pores, steps, nodes, wells, and adsorbed protein fibres (BARBUCCI, et al. 2002; CURTIS and WILKINSON 1997; FLEMMING, et al. 1999; IBRAHIM, et al. 2007; PALMAZ, et al. 1999; LIU, et al. 2005). For the scale factor, many studies have appeared reporting on the effect of nanometer or micrometer range features on the cell responses (ANDERSSON, et al. 2003; BARBUCCI, et al. 2002; BARBUCCI, et al. 2005; PAPENBURG, et al. 2007; SCHNELL, et al. 2007; SENESI, et al. 2007). A review article describing the effect of the substrate surface topography with various shapes and scales on different cell types has been provided by Flemming et al. (1999).

According to some published reports, EC behavior, mostly involving cell migration and orientation, can be influenced by the micro-topography of the substrate. For instance, the effect of micropatterned (10, 25, 50 and 100μm stripes) materials on EC behaviour have been investigated in terms of cell attachment, migration and orientation. In decreasing the stripe dimensions, a more "fusiform" shape of the adherent ECs has been observed. At the same time, these stripes have promoted the cell migration and orientation (BARBUCCI, et al. 2002). A pattern of parallel grooves at micrometric scale increased (2x) the migration rate of the ECs over the metallic surfaces used for endovascular stent applications (PALMAZ, et al. 1999). However, it has been shown that the surface chemistry is dominant in modulating different cell responses (BARBUCCI, et al. 2003; PASQUI, et al. 2005). For example, Pasqui et al. (2005) have reported that the stripped micropatterns of hyaluronan (Hyal) and aminosilanized glass stimulated the lymphatic ECs orientation. However, they have shown that topographical

parameters in conjunction with surface chemistry become effective in controlling cell behaviour, but not solely. Barbucci et al. (2003) have also reported that the surface chemistry was dominant in modulating different cell behaviors on the grooves with 250 nm height and 100, 50, 25 or 10 μm widths, obtained by the photoimmobilization of natural polysaccharide hyaluronic acid (Hyal) and its sulfated derivative (HyalS) fixed on silanized glass. In addition, it has been reported that nano scale surface features can influence the EC function. Miller et al. (2004) have shown that nano-structured substrates (i.e. cast PLGA) promoted the EC and smooth muscle cell growth. Furthermore, increased roughness of the biomaterial surfaces, even at the 10-100nm scale, promotes the adhesion and growth of the HUVECs on polyurethane coated by PEG-RGD (CHUNG, et al. 2003b).

Contact guidance

Guided cell movement is an important fundamental process occurring in the development and regeneration of cells and tissues. The surface topography, including the fibre diameter or its curvature, is an interesting concept to promote cell behavior, including cell movement and orientation (CURTIS and RIEHLE 2001; HADJIZADEH, et al. 2007; KHANG, et al. 1999; SANTOS, et al. 2007). For instance, different cell types have shown to be able to both initially orient and then move along the available biological or synthetic fibres with fibre diameters less than100μm (CURTIS and RIEHLE 2001; KHANG, et al. 1999). This phenomenon, which is now called "contact guidance", was discovered by Paul Weiss (1945) (Figure 2.9) (CURTIS and RIEHLE 2001). Khang et al. (1999) investigated the interaction of fibroblast cells onto PET fibres with different diameters and observed that cells orient along the fibre axis (108 μm diameter). Their study suggested that the degree of cell orientation depended on

33

the fibre diameter, the maximum cell orientation occured with fibres diameter in the range of 21-108 μm. Also, carbon fibres were able to orient migrating cells and thus enhance their movment (CURTIS and RIEHLE 2001). Further investigations into the effect of fibre diameter on cell behavior would be useful towards the better understanding of the role of dimensional patterning.
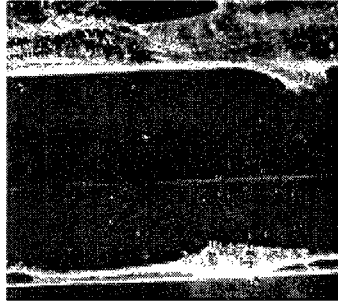
Figure 2.9: Contact guidance, a scanning electron microscopy (SEM) image of two epitenon cells highly aligned to the "steps" previously created in a grooved silica substrate (reproduced from CURTIS and RIEHLE 2001).

Therefore, the use of fibrous biomaterials can be an alternative to apply the phenomenon of "contact guidance" to modulate the cell responses. To further this aim, PET and polytetrafluoroethylene (PTFE) fibres are 2 representative biomaterials which can be the appropriate choices for studying the effect of curvature on cell behavior, or more specifically, the 3D cell patterning. Indeed, they have been utilized extensively as vascular prosthesis and also in many related studies (BILTRESSE, et al. 2005; LI, et al. 2001; LIU, et al. 2006; XIE, et al. 2002; ZHAO, et al. 2003). Most importantly, they are amenable to many of the surface modification methods to produce the more desirable surface chemistry.

2D versus 3D cell patterning

The two dimensional (2D) patterning of proteins and cells on the surface is of particular interest for use in many biotechnological and biomedical applications, including bioanalytical

devices, medical and dental implants, and in studies of cell material interactions in tissue engineering (THISSEN, et al. 2006). 2D cell patterning has been performed by means of cell adhesive and non-adhesive coatings on the surfaces, which has been provided with the aid of various techniques such as surface masking (THISSEN, et al. 2006) or lithography (MIRONOV, et al. 2003; RINGEISEN, et al. 2006). Lithographic methods have been used to provide patterns of pre-coated 2D surfaces to promote both cell adhesion and repulsion on the microscopic scale. The patterned surfaces are introduced to a concentrated cell solution by which areas with cell adhesion compounds trap cells in suspension, while areas with cell repulsive molecules are left acellular (RINGEISEN, et al. 2006). Recently, Thissen et al. (2006) have employed a similar method, called surface masking, by which means they have provided a surface with cell adhesive and a cell resistance area by means of a plasma polymer and a non-fouling material, respectively.

However, *in vivo* cells live in a 3D environment in contact with the surrounding 3D mesh-like fibres of the ECM, but not on a pure 2D surface (CUKIERMAN, et al. 2002; GEIGER, et al. 2001). The interactions of those cells with 3D ECM matrix play the main roles in regulating the cell functions, including cell growth, migration, differentiation and survival; and in mediating other physiological responses such as tissue organization and matrix remodelling (HYNES 1999). Flat and rigid 2D surfaces can influence the cell-matrix interactions, organized by integrins and the signals that they transmit. Thus, artificially rigid 2D substrates may not provide such condition to exhibit the *in vivo* reality by forcing cells to adapt to these surfaces (WOZNIAK, et al. 2004). In addition, 2D substrates also have limitations in transferring cultured cells to the tissue mass.

35

Regarding the influential role of the environment in which the cells are located, in respect of cell functions, control over this environment is needed in the scaffold design for both cell and tissue growth. To further this aim, the cells should be grown in a 3D environment, having proper and close characteristics such as chemical, topographical and mechanical to those of *in vivo* environments (CUKIERMAN, et al. 2002). However, fabrication of scaffolding material with 3D structures on the micrometric scale is still a real issue in the biomaterial field to thereby design an appropriate substrate. The majority of the current fabrication techniques are based on the related processes used in the microelectronics field. Up until now, the 4 techniques that have been mainly used are the followings: lithography (i.e. photolithography, soft lithography), direct writing, and laser ablation (LIU, et al. 2005). However, lithographic methods are not able to provide heterogeneous patterns of cells or molecules in 3D tissue scaffolds because of the reliance of these techniques on covering the surface of the patterns by cell adhesion molecules to attach the cells to the surface (RINGEISEN, et al. 2006).

3D structures can also be produced by the last two techniques, although these techniques are limited in the creation of complex patterns, due to the methodological restrictions. Readers interested in more information on the above mentioned 4 techniques are referred to the following publications (ENTCHEVA and BIEN 2005; LIU, et al. 2005).

There are also several published reports studying cell behavior towards micro-fabricated substrates including patterns of grooves, pores, spheres, nodes, and cylinders which are close to 3D patterning (FLEMMING, et al. 1999; KHADEMHOSSEINI, et al. 2006; MATSUDA and NAKAYAMA 1996). Among these, groove structures have been utilized more than others in the study of controlling cell response by surface topography. Theses investigations have

36

demonstrated that cells orient themselves along the grooves long axis by establishing their cytoskeletal elements to lie parallel to these features (FLEMMING, et al. 1999).

Cell printing, as an advanced technique in tissue engineering, has attracted much attention over the past few years. This technique has the capability of fabricating heterogeneous 3D scaffolds in a cell-by-cell printing fashion. The different methods of this technique have been described in a review article, provided by Ringeisen et al. (2006). However, although tissue engineering is optimistic to fabricate advanced tissue constructs and, as a result, to generate organ by using this technique, vascularization of these tissue constructs still remains a challenging issue (MIRONOV, et al. 2003). Electrospinning is another method for fabricating 3D scaffolds, which can be used to fabricate fibrous scaffolds with nanoscale resolution (KHADEMHOSSEINI, et al. 2006). Fibrous scaffolds have recently become the focus of interest in tissue engineering to promote the EC adhesion, then growth, and subsequently, the angiogenesis stimulation (SANTOS, et al. 2007; UNGER, et al. 2005a; UNGER, et al. 2005b).

When taken together, and in considering the cost and complexity of the fabrication and subsequent surface treatment of substrates, fabricated by means of methods explained above, the use of individual polymer fibres (monofilaments) in order to achive 3D cell patterning and 3D scaffold fabrication, can be an alternative. Polymer fibres can be easily surface modified with the desired cell adhesive or non-adhesive compounds. Then, the surface modified fibers can be either used individually, networked to form a scaffold or join together in a composite with other desired scaffolding materials, e.g., hydrogels, to produce patterned constructs in various shapes and sizes. The latter can be also used as a model substrate to study cell behavior for involvement in different aims in tissue engineering.

2.7. 3. Surface chemistry

The effect of surface biochemistry on cell function, being one of the objectives of this thesis, has been explained earlier in this chapter. Here, as a complement to that, the effect of surface functional groups, wettability and charge are briefly reviewed.

Functional groups

As mentioned earlier, the responses of different types of cells on polymeric materials depend on the surface chemistry. Usually, cells attach to biomaterial surfaces via a layer of adsorbed proteins such as VN and FN. On the other hand, the conformation and orientation of adsorbed proteins may be affected by the underlying substrate properties, e.g. surface chemistry and wettability (KESELOWSKY, et al. 2003). Subsequently, these events may influence integrin receptor binding and subsequent cell functions (KESELOWSKY, et al. 2004; KESELOWSKY, et al. 2005). For a better understanding of the underlying molecular mechanisms governing these events, some studies have been undertaken by Keselowsky and others, by creating defined functional groups (i.e. CH_3, OH, COOH, and NH_2) by using self-assembled monolayers (SAMs) of alkanethiols on gold. Then the effects of surface chemistry on FN adsorption, integrin binding, and cell adhesion have been studied by using these model surfaces. They found that all of the three following test parameters i.e., FN adsorption, $\alpha_5\beta_1$ integrin binding to the adsorbed FN and subsequent cell adhesion strength to FN-coated surface were affected by surface chemistry, following the trend: OH > COOH = NH_2 > CH_3 (KESELOWSKY, et al. 2003). However, in a similar study reported by Lee et al. (2006), the FN adsorption showed the trend: OH< COOH< NH_2< CH_3 on a model system of alkylsilane SAMs with the same functional groups (i.e. OH, COOH, NH_2 and CH_3) created. Therefore, the full understanding of the effect of surface chemical groups on protein adsorption and

subsequent events (e.g. cell adhesion) remains a challenging issue to fully understand and requires more intensive investigations.

Two other surface characteristics, arising from the surface chemistry, may have influence on cell functions, and have been classified separately as 1) wettability (hydrophilicity) and 2) charge, in the literature.

Wettability

There are some published studies reporting the relationship between surface wettability and cell behavior, by culturing different cell types on polymers of different wettabilities. Most of the studies have shown that surfaces with a moderate wettability (40-50 degree, water contact angle) exhibit the highest levels of cell attachment (ARIMA and IWATA 2007; LEE, et al. 1998; VAN WACHEM, et al. 1985; WEBB, et al. 1998). Such surfaces may adsorb proteins present in serum or secreted by cells, resulting in the creation of a favorable surface to modulate the functions of the different cell types, e.g., adult human endothelial cells (HEC) (VAN WACHEM, et al. 1985). Arima and Iwata (2007) have also demonstrated that in addition to surface wettability which plays the main role in cell adhesion, the surface functional groups, its surface density, and the cell type also influence this phenomenon.

Charge

Some studies have shown that cell behavior also depends on substrate surface charges. Amongst them, as an example, Lee et al. (1997) have published a study in which acrylic acid (AA), sodium p-styrene sulphonate (NaSS), and N, N-dimethyl aminopropyl acrylamide (DMAPAA) were copolymerized to fabricate positively and negatively charged surfaces. In these surfaces the gradient of the grafted surface functional groups were changed. The surfaces having positive charge (DMAPAA-grafted) showed higher cell attachment than the surfaces

having negative charge (AA-grafted). The authors concluded that surface functional groups, charges and wettability all influence cell responses, including adhesion, spreading, and growth (LEE, et al. 1997).

Chapter 3

Literature review II: Tissue engineering and vascularization

3.1. Overview

Recently, the development of new blood vessels around or in the interior of a tissue engineered device, in particular scaffold materials, has become a big challenge in order to repair or replace diseased or damaged tissues. To this aim, this study will focus on *in vitro* guided angiogenesis in a 3D culture system, comprising a filamentous polymeric scaffold, ECs and a hydrogel. Therefore, the present chapter is comprised successively of the description of blood vessels and microvessels in the normal situation, the mechanisms of blood vessels formation in adult that include both vasculogenesis and angiogenesis, the importance of vacularization in tissue engineering, and then an overview of the literature on the different approaches employed to induce and develop a vascular network towards an implant.

3.2. Blood vessels and capillaries

Blood vessels supply oxygen and nutrients for most tissues in the body (CARMELIET and COLLEN 2000) by carrying the blood (rich in oxygen & nutrients) from the heart to the tissues and organs and inversely carrying the blood (poor in oxygen & nutrients but rich in wastes) from them to the heart (Fig. 3.1) (RATCLIFFE 2000; [website ref.2]).

Capillaries function to distribute blood within tissues and organs permitting the diffusion of oxygen and nutrition from the blood in to the tissue and diffusion of the waste products of the metabolism (such as carbon dioxide) from the tissue in to the blood
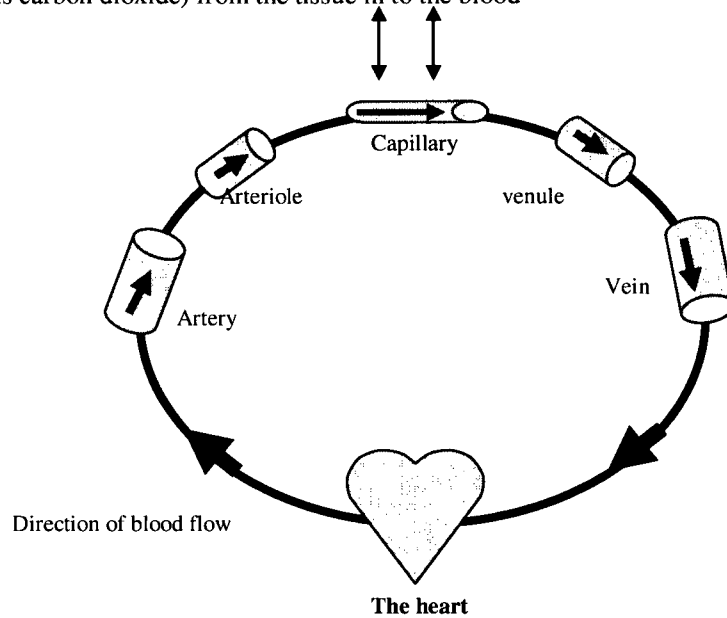
Figure 3.1: Blood is carried by arteries, arterioles, capillaries from the heart to the tissues and by capillaries, venules, and veins from tissues to the heart, (adapted from RATCLIFFE 2000; [website ref. 2])

They form a branched system of arteries, of decrementing sizes, as they enter a specific organ or tissue to form a network of microvessels or capillaries. Capillaries are the major elements that perfuse the blood and allow the diffusion/exchanges of oxygen, nutrients, and wastes, due to their state to the cells composing the tissue/organ. Capillaries are then incrementing in size as they exit from the tissue/organ to form veins that return blood to the heart and lung. Capillaries are composed of an EC monolayer, surrounded by an EC basement membrane and pericyte cells, embedded within the basement membrane (Fig. 3.2) [website ref. 4]. Capillaries of different tissues can be different in their cellular morphology and they have been classified into three categories (Fig. 3.4), including capillaries with continuous walls, capillaries with small openings in their walls and discontinuous capillaries (CLEAVER

42

and MELTON 2003). Figure 3.3 shows the structure and the wall composition of small vessels. Nascent vessels are simple tubes formed by ECs, which then mature and specialize in structure to form capillaries, arterioles and venules (JAIN 2003). Small vessels (i.e. arterioles and venules) have an advanced coverage of mural cells compared to the capilaries (CLEAVER and MELTON 2003; JAIN 2003).

a)   b)
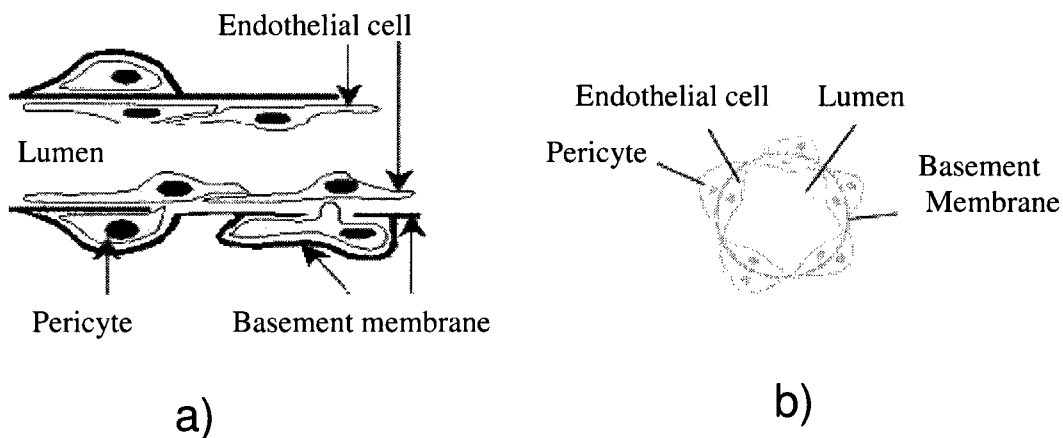
Figure 3.2: Capillary blood vessels in cross-section a) [reproduced from website ref. 4] and b) [reproduced from website ref. 3]
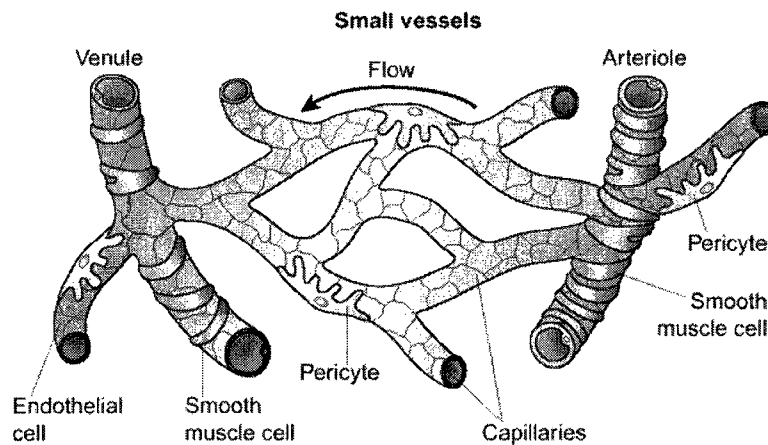
Figure 3.3: Morphology and wall composition of small vessels: arterial, venules and capillaries. Capillaries consist of ECs surrounded by a basement membrane and a sparse layer of pericytes embedded within the EC basement membrane. Arterioles and venules have an increased coverage of mural cells compared with the capillaries (reproduced from CLEAVER and MELTON 2003).

a **Continuous**

Intercellular cleft   Lumen

Basement membrane   Nucleus of endothelial cell

b **Fenestrated**

Fenestrae

c **Discontinuous**

Intercellular cleft
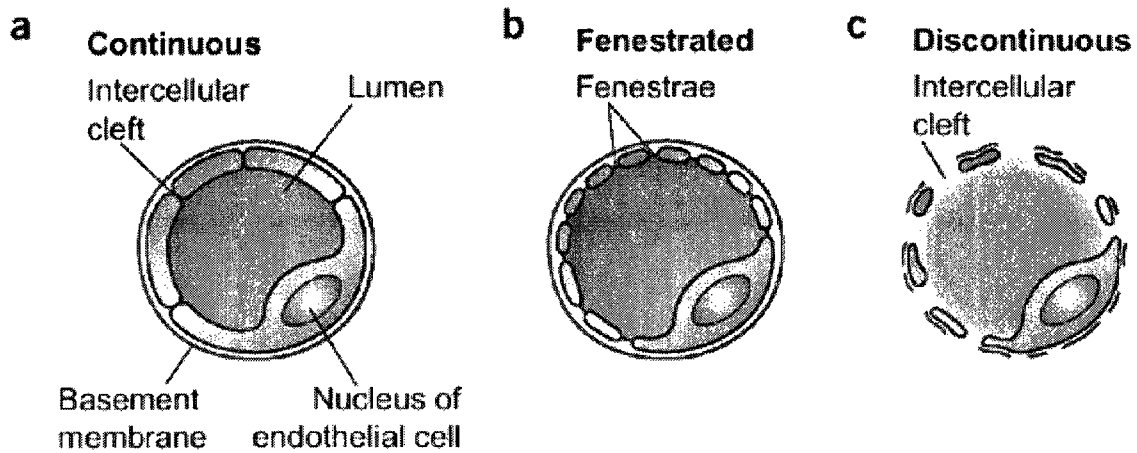
Figure 3.4: Capillaries with different cellular morphologies: (a) continuous capillaries; (b) capillaries with small openings; and (c) discontinuous capillaries (reproduced from CLEAVER and MELTON 2003).

3.2.1. Microvessel formation

According to recently published reports, in both the developmental and the adult microenvironments, neovascularization probably takes place via two different processes called angiogenesis and vasculogenesis (UCUZIAN and GREISLER 2007; SHIU, et al. 2005).

Vasculogenesis

Vasculogenesis refers to the process by which angioblasts (EC precursors) proliferate and form a primitive network of vessels which is called the primary capillary plexus (Fig. 3.5). Then, this primitive vessel network plays the role of a scaffold for the angiogenesis (SHIU, et al. 2005).

44

Angioblasts

Primitive Vascular Network
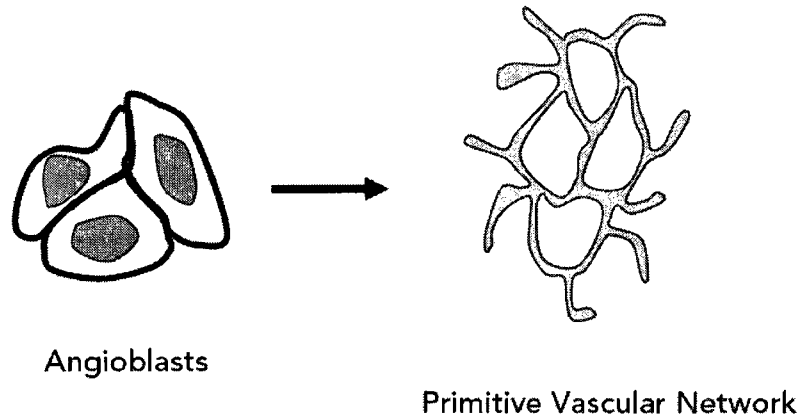
Figure 3.5: Vasculogenesis: formation of a primitive network of vessels from angioblasts (EC precursors) during the early stage of embryonic development (reproduced from SHIU, et al. 2005).

Angiogenesis

In terms of a fundamental definition, angiogenesis is the development of new vessels from pre-existing vessels that occurs through two mechanisms called vessel splitting and sprouting (SHIU, et al. 2005).

Vessel splitting (intussusception)

In this process a single capillary divides into two capillaries from within. As shown in Figure 3.6, activated ECs from the capillary wall extend out contrarily into the lumen side and fuse. This event creates a pillar-like structure across the vessel, which then elongates along the vessel axis and generates two parallel microvessels (SHIU, et al. 2005).

Vessel sprouting

Sprouting (or tubular morphogenesis or sprouting angiogenesis) refers to the phenomena by which a new vessel forms from a pre-existing vessel (capillary or venule), when activated ECs migrate, proliferate and elangate through the surrounding matrix (Fig. 3.6) (SHIU, et al. 2005).

45
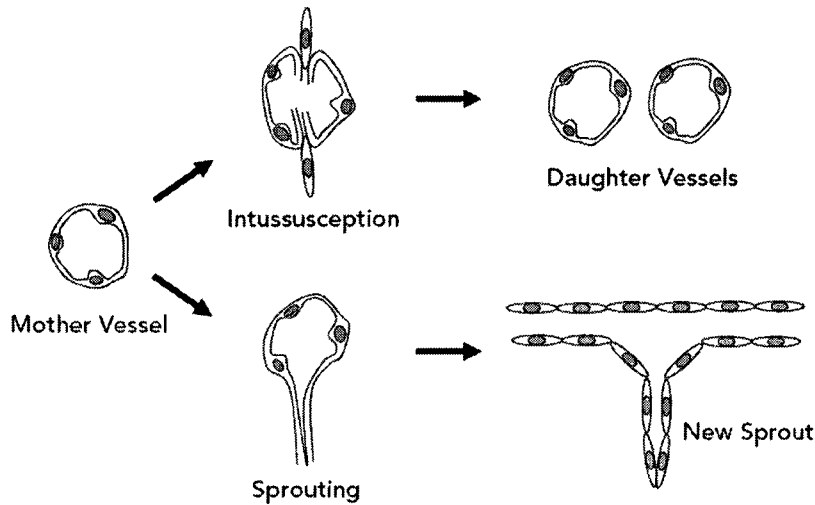
Figure 3.6:   In the angiogenesis process (both in embryo and adult), the activated ECs of the preexisting vessels form new vessels, via two different mechanisms (i.e. splitting (intussusception) and sprouting) (reproduced from SHIU, et al. 2005).

In considering the molecular mechanisms, the normal angiogenesis is a complex process that takes place through a complex interaction between vascular cells, the surrounding extracellular matrix and many angiogenic factors, including VEGF, fibroblast growth factors and, angiopoietin-1 (Ang-1). The following events occur during sprouting angiogenesis (Fig. 3.7): 1) vessel destabilization, 2) matrix remodeling, 3) EC proliferation, 4) EC migration, 5) cell-cell contact, 6) tube formation, 7) mesenchymal cell proliferation and migration 8) recruitment of pericytes, 9) formation of the basement membrane around the new vessel (vessel stabilization) (PAPETTI and HERMAN 2002). The main effectors involved in angiogenesis are soluble molecules, extracellular matrices, cell–cell interactions, and mechanical forces (PAPETTI and HERMAN 2002; SHIU, et al. 2005). Readers interested in the mechanisms of angiogenesis, and the effectors involved in this process, are referred to the following references (BACH, et al. 1998; CARMELIET 2000; CARMELIET and COLLEN,

2000; COLLINSON and DONNELLY, 2004; FOLKMAN and D'AMORE 1996; RISAU 1997; UCUZIAN and GREISLER 2007; YANCOPOULOS, et al. 2000).

I) Soluble factors

The process of angiogenesis is regulated by various soluble factors. These compounds contribute to angiogenesis; to its induction, acceleration or inhibition (PAPETTI and HERMAN 2002). An excellent review, describing the modulation of angiogenesis by soluble factors, has been provided by Papetti and Herman (2002). In paragraghs below only the definitions and functions of these factors have been briefly presented.

Vascular endothelial growth factor (VEGF)

Among many soluble factors, the most well-known angiogenic factor is VEGF. Six isoforms of VEGF have been known among whichVEGF$_{165}$ is the most commonly expressed isoform. VEGF is a glycoprotein with a molecular weight of about 34-45 kDa. Many types of tissues produce VEGF (at low levels), but when angiogenesis is required the production of VEGF is increased. VEGF is one of the main effectors of the vascular ECs that play major roles in angiogenesis. These are: 1) increases in EC permeability, 2) stimulates uPA/PAI-1 (plasminogen activators) production by EC, 3) stimulates EC proliferation, 4) inhibits EC apoptosis, 5) enhances EC migration, and 6) stimulates *in vivo* angiogenesis (LI, et al. 2003; PAPETTI and HERMAN 2002).

Fibroblast growth factors (FGFs)

Basic FGF (b-FGF, pI = 9.6) and acidic FGF (a-FGF, pI = 5) consist of polypeptides (18-25 kDa MW) that are the members of the family of angiogenic growth factors. FGFs play roles in EC proliferation, migration, EC production of collagenase and plasminogen activator. Moreover, bFGF contributes in ECs tube formation within 3D collagen matrices (PAPETTI and HERMAN 2002).

Angiopoietins and Tie receptors

Angiopoietins are known as EC specific growth factors acting as partners of the VEGF. Four types of angiopoietins have been identified (Ang-1 through Ang-4), among which Ang-1 induces *in vitro* EC sprout formation and increases the stability of endothelium. Conversely, Ang-2 opposes Ang-1 signaling, resulting in the destabilization of endothelium. Tie receptors are the receptors of the above mentioned angiopoietins (LI, et al. 2003; PAPETTI and HERMAN 2002).

Platelet derived growth factor (PDGF)

Platelet derived growth factor, or PDGF, was originally identified in platelets. PDGF may play a role in the differentiation and proliferation of pericytes and, as a result, helping the capillary wall to be more stable (PAPETTI and HERMAN 2002).

Other soluble factors

During vacularization, a growth factor called transforming growth factor (TGF-β) is produced by both ECs and pericytes which plays a role in angiogenesis in *vitro* and *in vivo* (LI, et al. 2003; PAPETTI and HERMAN 2002). In addition, some other soluble factors contribute in angiogenesis, but it is not demonstrated that they play as prominent role as the

48

above growth factors on the vasculature. For example, other growth factors, such as tumor necrosis factor-alpha (TNF-α), transforming growth factor-alpha (TGF-α), epidermal growth factor (EGF), and the colony stimulating factors (CSFs), show angiogenic properties (PAPETTI and HERMAN 2002).

II) Membrane-bound factors

Membrane-bound proteins are also important in angiogenesis. The membrane bound factors play their roles when cells are in close contact with each other and their matrix. Endothelial membrane-bound factors that regulate many functions involved in the vasculature have been classified into 3 categories, including integrins, ephrins, and cadherins. Among the members of these 3 groups, the integrin $\alpha_v\beta_3$, VE cadherin, and ephrin-2B, respectively, play prominent roles in angiogenesis (PAPETTI and HERMAN 2002).

Integrins

Since in the process of angiogenesis ECs invade the ECM to migrate through it, the integrins are required to mediate the interaction of ECs with ECM in this event. Among many cell membrane integrin receptors, $\alpha_v\beta_3$ plays an important role in angiogenesis. This integrin binds to ECM proteins such as VN, FN, vWf, and fibrin, and is produced in *vitro* on ECs in the presence of growth factors such as VEGF and bFGF (PAPETTI and HERMAN 2002).

49

Table.3.1: The effect of integrins on EC and vasculature (PAPETTI and HERMAN 2002)

Integrins	Roles
$\alpha_v\beta_3$	• Mediates *in vitro* EC attachment, spreading, and migration • Mediates angiogenesis by: -expression on angioblasts before and during vasculogenesis -binding to matrix metalloproteinase-2 -localizing the active form of the enzyme at the tips of the angiogenic blood vessels -regulating localized degradation of the ECM -mediating EC migration by adhering to the modulated matrix
$\alpha_v\beta_5$, $\alpha_1\beta_1$ and $\alpha_2\beta_1$	• Regulating angiogenesis by: -adhesion to ECM -localization of proteases to capillary sprouts -enhancing EC survival

Cell junction proteins

The two most extensively studied EC junction proteins that are produced primarily at the cell-cell junctions of the ECs and are involved in angiogenesis, are VE-cadherin (a member of Ca^{+2} binding transmembrane molecules) and platelet EC adhesion molecule-1 (PECAM-1 or CD31) (a member of immunoglobulin superfamily of cell adhesion molecules) (SHIU, et al. 2005). Studies have shown that cadherins stabilize EC junctions in the vessel wall and enhance EC survival (PAPETTI and HERMAN 2002). When ECs migrate during angiogenesis, cell-cell junctional compounds are temporarily disconnected, but then they are re-connected to form a new vessel (ILAN and MADRI 2003; SHIU, et al. 2005).

Eph-B4/Ephrin-B2

Eph receptors and ephrin ligands are a class of receptor/ligand pairs which play a prominent role in blood vessel formation. Ephrin-B2 (a member of the ephrin family) is expressed on arterial ECs in embryo, and its receptor (eph-B4) is located on venous ECs. Theses two components mediate the contact and signaling between arterial and venous which

is necessary for the remodeling of the primary capillary plexus (PAPETTI and HERMAN 2002).

III) Extracellular Matrix (ECM)

ECM plays many important roles in regulating angiogenesis, such as performing signaling activities, reserving and regulating growth factors and acting as scaffold support. It has also been reported that during the process of angiogenesis, migration of ECs and development of new capillary depends on the production and organization of the ECM components, including FN, VN, collagen, laminin, and tenascin (INGBER, et al. 1995). As mentioned earlier, ECs interact with one or more ECM molecules via their integrin receptors (e.g. $\alpha_v\beta_3$ or $\alpha_v\beta_5$) which transduce the signals between them (LI, et al. 2003; SHIU, et al. 2005).

IV) EC migration

EC migration is essential during angiogenesis. In the 3D environment of the ECM, this process is regulated by chemotactic (i.e. cell motility by chemical stimuli), haptotactic (i.e. directional motility of cells), and mechanotactic (i.e. cell motility by mechanical forces). In addition invasion of the ECM enables the cells to migrate. These events take place through cytoskeletal remodeling, resulting in cell migration in several steps through which the ECs extent, contract, and move their rears towards the front and finally advance (LAMALICE, et al. 2007).
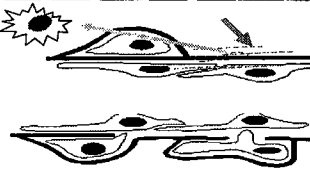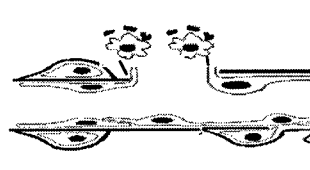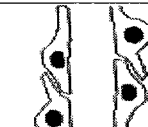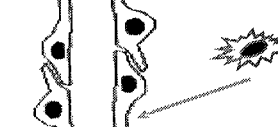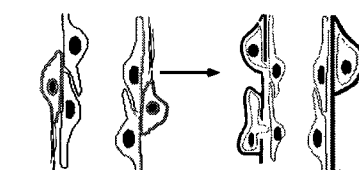
Figure 3.7: Mechanisms of angiogenesis and related activators, adapted from (PAPETTI and HERMAN 2002; [website ref. 4])

52

V) Biomechanical Forces

In addition to the above described factors, divers mechanical forces, including forces generated by cells, forces that are applied to cells via ECM, and the forces applied by external causes (e.g. blood flow and muscle activity) play prominent roles in angiogenesis (SHIU, et al. 2005). For example, laminar flow stabilizes and protects the vessel wall, by increasing stress fiber expression in ECs. Turbulent flow promotes blood vessel formation (PAPETTI and HERMAN 2002).

3.3. Importance of vascularization and angiogenesis in tissue engineering

Tissue engineering employs the principals of science and engineering to the design, construction, growth and treatment of living tissues (CURTIS and RIEHLE 2001; FUCHS, et al. 2001; GOMES and REIS 2004). Tissue engineering can be useful in plastic and reconstructive surgery for current clinical methods such as flap surgery (for the treatment of skin defects) or in production of materials for implantation (e.g. for breast reconstruction). Though engineered cartilage or thin tissue (i.e. skin) have currently been presented for clinical use (LASCHKE, et al. 2006), still many other tissue types for replacement or substitution remain under investigation, e.g. liver, bone, muscle, and nervous tissues. Interesting information about the progress, perspective and clinical applications of tissue engineering products can be found in the following references (ATALA 2004; LAVIK and LANGER 2004; MUSCHLER, et al. 2004; VATS, et al. 2003).

In tissue engineering applications, first a small part of tissue is taken from the patient, and the cells are then isolated and expanded to provide the required number of cells in culture. These cells are seeded into an appropriate 3D scaffold to form the tissue construct needed,

which will finally be implanted back into the patient's body (LASCHKE, et al. 2006; BORGES, et al. 2004). However, due to the lack of rapid vascularization of tissue construct after implantation, the seeded cells are not supplied adequately which leads to the death of the transplanted cells (BORGES, et al. 2004; KIRKPATRICK, et al. 2003; LASCHKE, et al. 2006). Since the supply of oxygen via diffusion is limited to a distance of about 150 to 200 μm from the neighboring capillaries, the rapid vascularization of such 3D construct after implantation play a prominent role in cell survival and as a result in the function of 3D tissue constructs. Particularly, this issue must be addressed to the scaffold guided tissue generation for the creation of complex, large-scale structures such as large bone defect, liver, lung and etc. (EISELT, et al. 1998). In fact, the vascularization of the engineered tissues remains as a great challenge in clinical applications of tissue engineered products. For these reasons, fabrication of vascularized constructs has become one of the attractive research subjects in tissue engineering (UCUZIAN and GREISLER 2007; LASCHKE, et al., 2006). In addition to the above explained issues, the angiogenesis is the subject of an intensive research in current years because of its importance for the use in many clinical applications including (e.g. wound healing, oncology, ophthalmology, vascular disease, and etc.). As an example, cardiovascular diseases are one of the great causes of death worldwide. Therefore, the study of angiogenesis, particularly enhancing angiogenic capabilities of tissue engineered constructs *in vitro*, could considerably affect health care (UCUZIAN and GREISLER 2007).

3.4. Enhancing the vascularization of tissue engineering constructs

As explained earlier, vascularization of the engineered tissue constructs is a challenging issue in the field of tissue engineering. This issue has been addressed since 1979 when Erol and Spira initiated the method of "arteriovenous shunt loops" *in vivo*, a method in which new blood vessel formation is promoted by the increased shear stress and wall tension, within the loops' vasculature (LASCHKE, et al. 2006). In addition to this approach which can be used to engineer vascularized tissue *in vivo* (BACH, et al. 2006; LOKMIC, et al. 2007), the research has been focused on new approaches. The most recent research tends to enhance the angiogenic properties of tissue engineered constructs by means of new approaches, such as: enhancing the ability of scaffolds to support vascularization by scaffold architecture (GAFNI, et al. 2006; YIM, et al. 2006); biomechanics (SHIU, et al. 2005; YAMAMURA, et al. 2007); and scaffolding materials, by using ECM components (BORSELLI, et al. 2007; HODDE 2006; WILLIAMS, et al. 2006; WU, et al. 2007) and angiogenic growth factors (ELCIN and ELCIN 2006; ENNETT, et al. 2006; KAIGLER, et al. 2006; KURANE, et al. 2007; LAI, et al. 2006; NILLESEN, et al. 2007). Moreover, stimulation of vasculogenesis by means of endothelial progenitor cells (EPCs) within the construct (HUMPERT, et al. 2005; MADEDDU 2005; MCCLOSKEY, et al. 2005; SUURONEN, et al. 2006b; YI, et al. 2006) and inducing of angiogenesis by external mechanical forces (BILODEAU, et al. 2005; SHIU, et al. 2005) have been reported. However, in this thesis I will focus on the role of scaffolds in the vascularization of tissue engineered constructs.

3.4.1. Enhancing the vascularization of tissue engineering scaffolds

A tissue engineering scaffold is a 3D framework made of an implantable biomaterial which should have the following three capabilities: (i) providing a space for tissue growth, (ii) containing a space-filling matrix for cell localization, and (iii) enhancing vascularization of the forming tissue (EISELT, et al. 1998). More details on this subject can be found in a review provided by Yarlagadda et al. (2005).

In order to fabricate scaffolding materials with a capability for enhancing angiogenesis, some studies have been performed to produce biomaterials that modulate EC responses (HADJIZADEH, et al. 2007; UNGER, et al. 2004; UNGER, et al. 2005b). In addition, the recent research has focused on the enhancing the vascularization of a polymeric scaffold by means of the scaffold's composition (by incorporating ECM components and GFs), architecture and biomechanics.

Enhancing the angiogenic ability of scaffolding material by ECM components

One of the more interesting concepts for developing scaffolds, used in tissue engineering, is to mimic the architecture and composition of the ECM of the tissue to be regenerated. To further this aim, specific ECM compounds with angiogenic properties have been introduced into the biomaterials to enhance microvessel formation and tissue ingrowths (BATTISTA, et al. 2005; CRONIN, et al. 2006; FOURNIER and DOILLON 1992; FOURNIER and DOILLON 1996; WU, et al. 2007). ECM molecules can be simply mixed with scaffolding material, immobilized on the surface of these materials or even to employ naturally occurring scaffolds composed of ECM proteins.

ECM molecules mixing with scaffolding material

Biomaterials, when combined with ECM molecules, have shown a potential to induce microvessel formation *in vivo* and *in vitro*. Fournier and Doillon (1992) have investigated the effect of FN and hyaluronic acid (HA) on tube formation in fibrin gel by means of an *in vitro* model. Their study has shown the formation of tube-, branch- and capillary-like structures within the fibrin. In addition, it has been currently reported that a portfolio of crosslinked chitosan-collagen blends, seeded with pre-adipocytes, could induce vascularization and form adipose tissue *in vivo* (WU, et al. 2007). Furthermore, EC differentiation and vascularization in 3D collagen constructs were strongly promoted by the introduction of FN to this system (BATTISTA, et al. 2005). Biological-based hydrogels, such as laminin-1, type I collagen, fibrin glue and HA, are resorbed and replaced by vascularized connective tissue *in vivo* (CRONIN, et al. 2006). Collagen-based matrices have effectively delivered endothelial progenitor cells (EPCs) to ischemic tissue *in vivo* in which EPCs integrated into the vascular structures (SUURONEN, et al. 2006a).

ECM molecules immobilization

Enhancing angiogenesis, by means of biological molecules (e.g. ECM compounds) coated onto the surface of synthetic polymeric materials, has rarely been reported. Fournier and Doillon (1996) have shown that composite fibrin matrices consisting of angiogenic compounds such as HA, FN and FGFs adsorbed onto Dacron meshes, enhanced the angiogenesis *in vivo*. As another example the ECM-coated ePTFE induced both angiogenesis in implant-associated tissue and the neovascularization of the pores within the ePTFE, while uncoated ePTFE did not (KIDD, et al. 2002). Porous polyethersulfone hollow fibres (having pore diameters of about 100μm) coated with gelatin or FN were investigated toward

angiogenesis using HUVECs. Cells attached onto gelatin and FN coated surfaces formed microvessel-like structures when introduced into an angiogenesis model (UNGER, et al. 2005b). Thus, the attachment of ECM proteins to the surfaces of target materials creates a desirable surface for cells, mimicking a close approximation to their natural cell environment.

Naturally occurring scaffolds composed of ECM compounds

In addition to synthetic scaffolds, biological scaffolds composed of ECM components (e.g. small intestinal submucosa (SIS)), have also been studied for potential tissue engineering applications (BADYLAK 2007; LASCHKE, et al. 2006). It has been suggested that these scaffolds show a rapid interaction with the host tissue. Since the scaffolds naturally consist of angiogenic components (i.e. growth factors and structural elements such as FN, elastin, collagen, etc.), they may thus accelerate angiogenesis (LASCHKE, et al., 2006; HODDE 2002). Readers interested in this subject are referred to the review article provided by Hodde (2002).

Gelatin

Gelatin is a biodegradable and biocompatible compound that is composed of denatured polymers derived from collagen. This "compound" has been long successful in being used for pharmaceutical and medical applications and is the focus of attentions for use in tissue engineering products (CHOONG, et al. 2006; YOUNG, et al. 2005). Gelatin hydrogels have been used for sustained release of growth factors to promote tissue regeneration and vascularization in tissue engineering (DOI, et al. 2007; YOUNG, et al. 2005). Moreover, it has been demonstrated that the gelatin-coated surfaces promote cell adhesion. But the gelatin coating, via physical adsorption, is not stable with time, it dissolves easily in the culture

medium, resulting in the cell detachment. Therefore in order to produce a stable gelatin-coating on a surface, immobilization of the gelatin by means of chemical reaction is required (CHOONG, et al. 2006). Covalently gelatin-coated materials have promoted EC adhesion and proliferation (CHOONG, et al. 2006). However, there are few instances in the literature that demonstrate the enhancement of angiogenesis through the use of this kind of substrate (UNGER, et al. 2005b).

RGD-containing peptides

There are many published reports describing the effects of tripeptide RGD on tissue regeneration, *in vivo* and *in vitro*. For example, the RGD-containing matrix has the potential to accelerate the healing reaction and improve the quality of regenerated tissue in orthopedics (KARDESTUNCER, et al. 2006), cardiovascular (TWEDEN, et al. 1995), diabetic (STEED, et al. 1995; WETHERS, et al. 1994), and brain tissue repair investigations (CUI, et al. 2006). However, there is presently little evidence showing the effect of the RGD peptide on the enhancement of the angiogenesis (CUI, et al. 2006).

By way of contrast, it has been reported that RGD peptides inhibit angiogenesis (BUERKLE, et al. 2002; HAUBNER and WESTER 2004; KIM, et al. 2006; MEEROVITCH, et al. 2003; SHEU, et al. 1997; WESTLIN 2001). For targeting of angiogenic vessels, $\alpha_v\beta_3$ integrin antibodies have been produced and are under investigation for use as antiangiogenic compounds. In addition to these compounds, small peptides such as RGD, which binds to $\alpha_v\beta_3$, can target this integrin receptor. In the testing of both linear and cyclic RGD peptides, in order to target the $\alpha_v\beta_3$ integrin, the cyclic peptides, having a ring system, have exhibited higher resistant to proteolysis and higher affinity to the target than their linear equivalents

(ZHANG, et al. 2007). In fact, the RGD sequence is a cell binding system that mediates the ECs attachment to the ECM by means of specialized cell membrane receptors i.e., $\alpha_5\beta_1$ and $\alpha_v\beta_3$ integrins. It has been demonstrated that the RGD-containing peptides are able to detach the ECs from their plastic or ECM-coated substrate, by competing with the binding of the RGD-containing ECM compounds to integrins. As mentioned earlier, during angiogenesis, the ECs interact with RGD-containing ECM compounds i.e., FN, laminin, and collagen. VWf and VN are other RGD-containing molecules that have been shown to be present in the ECM when wound healing and tumor angiogenesis occur (SHEU, et al. 1997). These interactions play prominent roles in the EC functions, i.e., adhesion and migration. Since the EC adhesion and migration are two important factors in the angiogenesis, the RGD sequence thus modulates the interactions between the sprouting ECs and the ECM molecules during microvessel development (SHEU, et al. 1997). Although RGD coated implants accelerated wound healing, there are insufficient studies showing the effect of such implants on the enhancement of the angiogenesis phenomenon.

Enhancing the angiogenic ability of scaffolding material by growth factors (GFs)

GFs are the most important effectors in the process of blood vessel formation. As explained earlier, over recent decades, many types of GFs have been identified and are now available for the use in related applications. Among them more important factors are VEGF, PDGF and FGFs. These factors may play the main role in the vascularization of the implanted tissue constructs, by accelerating the penetration of the newly formed vessels from the surrounding tissue into the implant. However, the inclusion of GFs into the scaffolding material and the subsequent sustained delivery of these compounds to an appropriate tissue

site can be an alternative (LASCHKE, et al. 2006). GFs can be incorporated into synthetic scaffolds in three different ways: (1) blending of the GFs with particles of the polymer before the polymer being processed into the scaffold. In this way, the GFs release rapidly, within days to weeks (HUANG, et al. 2005; HOSSEINKHANI, et al. 2006; LASCHKE, et al. 2006), (2) incorporating spheres, in which GFs have been initially encapsulated, into the scaffolds, resulting in growth factor release over a longer time (KEDEM, et al. 2005; ROYCE, et al. 2004; LASCHKE, et al. 2006), (3) physical or covalent immobilization of growth factors into the scaffolding materials (CHUNG, et al. 2006; KOCH, et al. 2006; STEFFENS, et al. 2004; YAO, et al. 2004).

Influence of scaffold architecture on the induction of angiogenesis

In addition to the scaffold composition, the structure of the scaffold has also been shown to influence the vascularization of a tissue construct (LASCHKE, et al. 2006). For example, higher levels of angiogenic activity have been observed in dermal equivalent tissue in 3D cultures than in monolayer cultures (LASCHKE, et al. 2006). This has been concluded to be due to the cellular content of the VEGF messenger, ribonucleic acid (mRNA), produced by fibroblasts cultured on a 3D scaffold made of PLGA, which was much higher than that of fibroblasts grown on a 2D surface (as monolayers) (PINNEY, et al. 2000). Moreover, Koike et al. (2004) reported that the HUVECs-seeded 3D construct induced a network of stable blood vessels formation *in vivo*. In addition, the pore size of the scaffolds has been shown to play some role in the microvessel formation (CHOU, et al. 2006; DZIUBLA and LOWMAN 2004; KARAGEORGIOU and KAPLAN 2005; LASCHKE, et al. 2006). According to some reports, angiogenesis occurs faster within those porous structures bearing pores with a size above 250

microns, than in those with pores below 250 microns (LASCHKE, et al. 2006). For example, pore sizes of greater than 300 microns have been recommended in bone tissue engineering for bone regeneration and the formation of capillaries (KARAGEORGIOU and KAPLAN 2005).

Moreover, fibrous scaffolds have recently been investigated in order to enhance the tissue vascularization (GAFNI, et al. 2006; IGARASHI, et al. 2007; YIM, et al. 2006). For instance, fibres composed of chitosan-alginate-heparin fabricated by means of interfacial polyelectrolyte complexation (PEC) fibre showed good cell infiltration and vascularization *in vivo* (YIM, et al. 2006). Very recently, nanofibrous materials made from bioabsorbable and biocompatible polymers mimicking the ECM structure have been investigated for use in tissue-engineered scaffolds (IGARASHI, et al. 2007).

Directional control of microvessel formation

Directional control of vascular sprout is of interest in tissue engineering in order to engineer directional tissues. Recently, directional control of microvessel formation, by means of chemical or physical stimuli, has become an attractive research subject (BORSELLI, et al. 2007; GAFNI, et al. 2006). ECs that had been cultured on a specifically designed filamentous biodegradable polymeric scaffold, and then implanted in mice, resulted in a guided angiogenesis with subsequent functional blood vessel formation. This method can also be applied for vascular engineering (GAFNI, et al. 2006). In addition, it has been recently shown that the control of directional vascular sprouting is possible by a spatial distribution of the matricellular cues. In the 3D semi-interpenetrated network of collagen-HA, the increase in the amount of HA within the matrix led to a reduction in the sprout formation, demonstrating the

possibility of being able to control vascularization by creating HA gradients within the collagen network (BORSELLI, et al. 2007).

Influence of scaffold biomechanics on the induction of angiogenesis

Various mechanical forces, such as externally applied forces (e.g. generated by blood flow and muscle contractions) (BONGRAZIO, et al. 2006; CULLEN, et al. 2002; MIYATA, et al. 1991; SHIU, et al. 2005), cell- and ECM-generated forces (SHIU, et al. 2005), all regulate the blood vessel formation.

In addition, 2D and 3D angiogenesis systems have shown that the stiffness of substrates influences the angiogenic activity of the ECs. In the 2D (monolayer) angiogenesis system, when the stiffness of the gel increased network formation on the gels surface reduced. Similarly, in 3D angiogenesis system, stiffer matrix decreased sprout formation. Therefore, capillary sprouting demands a more malleable environment (SHIU, et al. 2005). On the other hand, tube formation may not occur in very soft ECM gels, due to the contraction of the gels by the cell contractile forces, and cells may undergo apoptosis when they are not capable of developping an adequate tension that they need for their shape stability and survival. Therefore, a matrix with a moderate level of malleability will be required to be used in the study of angiogenesis phenomena (SHIU, et al. 2005).

3.5. Stimulation of vascularization by stem cells

In general, for the tissue regeneration three basic elements, i.e. scaffold, growth factors and cells are required. Recently, the use of stem cells (primal cells found in multicelluar organisms), as the EC source, is a particular interest in the development of vascularized tissue constructs. Endothelial propgenitor cells (EPCs), derived from bone marrow, have been shown in cultures, to differentiate into three important blood vessel cell types, being: ECs, pericytes, and vascular smooth muscle cells (LASCHKE, et al. 2006). A review describing the bone marrow-derived EPCs, and their capability for vascular regeneration, has been provided by Murayama et al. (2002). Bone marrow cells and EPCs have been seeded onto vascular grafts to create tissue-engineered vascular grafts, with a long-term functionallity (LASCHKE, et al. 2006; ASAHARA and ISNER 2002). In addition, the use of bone marrow cells in the investigation of angiogenesis and the tissue regeneration, has drawn the attentions of many researchers over recent years (HUANG, et al. 2005; HUMPERT, et al. 2005; MARKOWICZ, et al. 2006; SUURONEN, et al. 2006b; UENO, et al. 2006; ZHOU, et al. 2007). For example, ECs derived from EPCs, when seeded with human smooth muscle cells, have stimulated angiogenesis on porous biodegradable (i.e. PGA-PLLA) scaffolds (WU, et al. 2004). Similarly, ECs derived from stem cells, *in vitro*, once embedded in 3D collagen gel, have been shown to induce vasculogenesis (MCCLOSKEY, et al. 2005). In addition to stem and/or progenitor cells used to achieve vasculogenesis, the CD133+ progenitor cells, incorporated into injectable collagen-based matrix, promoted vascularization capability of the implanted construct *in vivo* (SUURONEN, et al. 2006b).

3.6. Engineering vascularized tissues *in vitro*

Recently, more attention has been focused on the *in vitro* vascularization methods (LEVENBERG, et al. 2005; SUURONEN, et al. 2006a; TREMBLAY, et al. 2005). This is because, the major problem for the application of an *in vitro* tissue-engineered construct, such as skin (TREMBLAY, et al. 2005) or thick and complex tissues such as muscle (LEVENBERG, et al. 2005), is the slow rate of vascularization, which may lead to tissue death after implantation (TREMBLAY, et al. 2005). Therefore, fabrication of a pre-vascularized tissue *in vitro* can be a promising way to prevent this obstacle. The idea behind this approach is that a network of newly formed microvessels may be engineered *in vitro* by the seeding of a scaffold with ECs. After implantation of the engineered tissue constructs, the ECs involved in newly formed networks within the construct should be able to connect to the vasculature system of the surrounding tissues. However, even by adopting this approach, a number of problems still remain to be solved (LASCHKE et al. 2006). The process of vascularization under *in vivo* conditions is a complex phenomenon which depends on the variety of signalling factors (e.g. VEGF and PDGF) and involves other cell types (i.e. smooth muscle cells and pericytes). Thus, the seeding of a scaffold with ECs only is not enough to enable new functional blood vessels *in vitro* to develop. Therefore, the current techniques employed for the fabrication of tissue constructs should be improved so as to produce tissue constructs having their own functional vascular system, prior to implantation (LASCHKE, et al. 2006). To address this issue a few relevant reports have recently been published. For example, a pre-vascularized reconstructed skin through the culturing of human keratinocytes, fibroblasts and ECs in a collagen sponge *in vitro* has been developed. This construct has shown successful interconnections made to host blood vessels in less than 4 days following

implantation (LASCHKE, et al. 2006). Moreover, Levenberg et al. (2005) have produced a vascularized engineered skeletal muscle tissue constructs by the co-seeding of myoblasts, embryonic fibroblasts and ECs, on biodegradable, porous polymer scaffolds. In this construct the embryonic fibroblasts has increased the VEGF expression, and also influenced the formation and stabilization of the microvessels. The vascularization, perfusion of blood and survival of the muscle tissue construct, have been achieved after the transplantation of tissue constructs *in vivo* (LEVENBERG, et al. 2005). It also has been noticed that the scaffold composition of the 3D matrix plays an important role in this approach (HELM, et al. 2007).

3.7. *In vitro* angiogenesis models

Formation of tube-like structures with the presence of lumens by ECs in vitro has been observed since 3 decades ago and called angiogenesis (FOLKMAN and HAUDENSCHILD 1980). However, from a physiological viewpoint, a perfect *in vitro* angiogenesis model should be able to perform all of the *in vivo* angiogenesis phases (i.e. initial activation of ECs in the preexisting vessel, ECs proliferation, migration, cell-cell attachment, final tube formation and vascular network reorganization). Moreover, the fabrication, application and quantification of the system should also be easy (VAILHE, et al. 2001). Under physiological conditions, angiogenesis occurs in a 3D environment, thus an *in vitro* angiogenesis investigation needs to be performed within a 3D system. To match this aim, many 3D ECs culture system (angiogenesis models) have been developed (FOURNIER and DOILLON 1992; NEHLS and DRENCKHAHN 1995b; VERNON and SAGE 1999; VAILHE, et al. 2001). Among the several EC culture systems, one interesting model was presented by Nels in 1995, in which EC-seeded micro carriers (beads) were embedded in a fibrin gel. In this model, the capillaries

spread out radially from the beads by invading the fibrin gel in the presence of growth factors (NEHLS and DRENCKHAHN 1995a; NEHLS and DRENCKHAHN 1995b). Accordingly, I propose in the present thesis study, to develop a similar system by replacing the microcarriers by polymer fibres that can also be used as scaffolding material in tissue engineering, in order to produce a pre-vascularized construct with directional microvessels. This design could therefore have a major impact in the generation of tissue engineered constructs for directional tissue regeneration.

3.8. Polymeric scaffolding materials

A polymeric tissue engineering scaffold may be either synthetic or naturally derived, that can perform various functions including: space filling, delivering bioactive molecules and cells, and providing desirable 3D environments for tissue growth (DRURY and MOONEY 2003). Thus, in respect of the requirements of each application, the materials selected for the scaffold should exhibit appropriate physical, chemical and structural properties (DRURY and MOONEY 2003). For this reason, several types of polymeric materials have been previously investigated to be used in tissue engineering applications in various formats, including polymer fibres and hydrogels.

3.8.1. Polymeric fibres

Among the biocompatible polymers, some can be used in a fibre format, as listed in Table 3.2. In this present thesis, I propose to use PET fibre because of its good amenability for surface treatment, its semi transparency which eases the *in vitro* visualization under culture conditions, and its commercially availability in a desired range of fibre diameters. Another

choice could be PTFE fibre, these two polymers being selected because they are two representative biomaterials, due to their wide range applications in vascular prosthesis, and also in many related studies (BILTRESSE, et al. 2005; LI, et al. 2001; LIU, et al. 2006; XIE, et al. 2002; ZHAO, et al. 2003). Moreover, by enhancing their ability to support controlled EC adhesion, proliferation, migration, and particularly angiogenesis, a promising route to address their drawbacks in vascular prosthesis applications can be envisaged.

Table 3.2: Some commercially available biocompatible polymers that can be used as fibres

Polymer	Typical applications	
Polyethylene terephthalate (PET)	Vascular grafts, sutures	(CHINN, et al. 1998; KHANG, et al. 1999)
Polytetraflouroethylene (Teflon®)	Vascular grafts, sutures	(CATANESE, et al. 1999; THOMSON, et al. 1991)
Polylactic / polyglycolic acid	Sutures	(MATTHEW 2002)
Polyamides (nylons)	Sutures	(SHIMAMURA, et al. 2006)
PHAs	Vascular grafts, sutures, heart valve	(SHISHATSKAVA, et al. 2004; VALAPPIL, et al. 2006; WILLIAMS, et al. 1999)
Polypropylene	Vascular grafts, sutures	(KONSTANTINOVIC, et al. 2006)
Silk	Sutures	(CALKINS, et al. 2007; UNGER, et al. 2004)
Carbon fibre	Sutures	(BROWN and POOL 1983; EVANS, et al. 1987)

3.8.2. Hydrogels

Hydrogels are network of polymers that have been crosslinked through typical chemical and physical bonds and employed as scaffold materials in tissue engineering. Theses materials are composed of either synthetic or naturally derived highly hydrated polymer chains (with a water content > 30% by wt). Attention has been focused on the utilization of hydrogels in tissue engineering applications, due to their typical characteristics, including being degradable,

being soft similar to many tissues, and having a mesh-like structure similar to that of the surrounding ECM (DRURY and MOONEY 2003). Hydrogels can be used as: space filling agents, bioactive molecule- and cell/tissue- delivery vehicles (DRURY and MOONEY 2003). Since softer materials have been shown to be a suitable matrix for angiogenic-like structure formation, hydrogels can be used as vascularizable implant materials (DZIUBLA 2003). Some synthetic hydrogels such as poly (2 hydroxyethyl methacrylate) (PHEMA) (DZIUBLA and LOWMAN 2004) and natrualy-derived including gelatin (DOI, et al. 2007), HA (CUI, et al. 2006), collagen (YAMAMURA, et al. 2007) and fibrin (FOURNIER and DOILLON 1992; NEHLS, et al. 1994) have been used to investigate angiogenesis. Among the above mentioned hydrogels, both collagen and fibrin have been widely used in tissue engineering applications to date.

Collagen is a well-known and important biomaterial, used in tissue engineering for various soft-tissue replacements. However, there is one drawback to the use of collagen gel for soft-tissue construct fabrication. The collagen gel is contracted by cultured cells over time, resulting in a major reduction in the construct size and cell death. To overcome these problems short collagen fibres have been incorporated into the collagen gels (GENTLEMAN, et al. 2007). Fibrin and collagen gels have been used mainly as cell delivery and localization agents in the applications that the initial mechanical functionality is not so important (CUMMINGS, et al. 2004; HAYEN, et al. 1999; NAKATSU, et al. 2003).

Fibrin has been widely used in investigations related to tissue engineering products, particularly in angiogenesis investigations (FOURNIER and DOILLON 1992; JOCKENHOEVEL, et al. 2001; NEHLS, et al. 1994). For instance, it has been used as a natural matrix for EC growth and has been also used as a coating for ePTFE vascular grafts to

promote EC adhesion and resistance to prevent EC loss due to shear stress (GOSSELIN, et al. 1996). The precursor of fibrin gel is fibrinogen which is purified from blood. The degradation of the fibrin gel occurs within a few days by the plasminogen present in the culture medium, thus a degradation control will be required to make the use of fibrin gel possible (JOCKENHOEVEL, et al. 2001). Moreover, the structure of fibrin gel and its long-term maintenance are influenced by the parameters involved in gel formation process. For example, low pH value and ionic strength increases the gel permeability coefficient (Ks) and creates large pore sizes. In contrast, high pH and ionic strength decrease of the gel pore sizes and Ks (BLOMBACK and OKADA 1982).

To sum up briefly, malleable substrates (e.g. hydrogels) having chemical, mechanical and structural properties similar to those of soft tissues, and the ECM, can be excellent candidates to support microvesssel formation. Fibrin gel has been widely employed in tissue engineering applications because of its ease of use and appropriate properties for blood vessel formation. Therefore, I propose to use the fibrin gel in tissue construct design as space filling material. Moreover, it is hypothesized that the PET fibre and fibrin gel by different mechanical properties to be appropriate candidates in order to orient the ECs and, as a result, to stimulate ECs tube formation.

3.9. Conclusion

Overall, in order to achieve a vascularized tissue construct, several methods are currently under investigation. These include the induction of vascularization capability of scaffolds by means of ECM components, angiogenic growth factors, the architecture and the biomechanics of scaffolds. In addition, pre-vascularized tissue substitutes can be engineered through the use

of progenitor ECs and stem cells. However, none of the above mentioned approaches can provide the prompt vascularization required for at least oxygen supply for transplanted cells at early stage implantation. Therefore, the existing techniques should be further developed to generate microvascular networks within the 3D tissue constructs *in vitro*, prior to implantation. For achieving this aim, the development of scaffolding material with an angiogenic capability to enhance vascularization, particularly *in vitro*, can be an alternative approach. Thus, this thesis proposes to use a fibrous polymeric material which will be surface coated with an ECM component such as RGD peptide or gelatin, for induction of angiogenesis. This approach aims to use the phenomena of contact guidance to modulate 3D patterning of the EC by enhancing EC migration, proliferation and orientation and ECM components to support EC attachment. This approach results in the formation *in vitro* of a directional angiogenesis which can be applied to many applications in tissue engineering such as therapeutic angiogenesis and pre-vascularised tissue construct fabrication. In addition, this strategy aims to evaluate the angiogenesis ability of ECM components, e.g. RGD *in vitro*. Moreover, as explained earlier in Chapter 2, in order to fabricate these fibres I propose to employ a multilayer surface modification strategy using plasma polymerization, non-fouling material coating and biomolecule immobilization. The fibres fabricated in this way can be used for various applications in tissue engineering, i.e. plasma coated fibres can be used as cell adhesive, non-fouling material coated fibres, as cell-resistant and bimolecular coated fibres as predictable cell adhesive fibres.

Chapter 4

Materials and methods

4.1. Overview

In this chapter, the materials and methods utilized for surface modification, characterization and evaluation of the surface modified substrates, towards the behaviour of HUVECs, in 2D and in 3D cell culture system, will be explained. The surfaces of polymer fibres, PET monofilament with a 100-μm diameter, were first coated with a thin film of plasma polymer to produce amine groups, by HApp. The procedure was followed by covallently grafting of CMD onto the surface amine groups using water-soluble carbodiimide chemistry (EDC/NHS). Then, GRGDS were covalently immobilized onto the CMD-coated fibre surfaces. In the adhesion assay, the surfaces of various other substrates such as expanded PTFE monofilaments, and flat surfaces (e.g. borosilicate glass, microscope cover slips or FEP films) were modified in the same way (i.e. using the same multilayer surface, modification sterategy) as explained above and used for some complementary studies.

Moreover, CMD and RGDS grafting has also been performed, via the AApp method, onto the surfaces of the same polymer fibres, as well as on flat surfaces. The AApp plasma-coated surfaces were then amino-functionalized, using polyethylenimine (PEI). Then, CMD and finally RGD were grafted onto amino-functionalized surfaces by the same method as previously explained.

X-ray photoelectron spectroscopy (XPS) was utilised to analyze the multi-layer surface fabrication steps. AFM and SEM were also used to provide topographical maps of the plasma- and CMD- coated surfaces.

In order to test these modified surfaces towards the HUVECs behaviour, the modified surfaces were initially evaluated in a 2D (monolayer) cell culture system, *in vitro*. HUVECs were seeded and grown on the fibres to evaluate the cell behaviour in terms of cell adhesion, spreading and orientation) as well as on flat surfaces, which were used for detailed characterization of cell behaviour (i.e. focal adhesion (FAs) and stress fibers formation). Phase contrast microscopy, epifluorescence microscopy and laser scanning confocal microscopy were used to observe the cell seeded surfaces.

For the testing of surface modified fibres towards ECs patterning, and subsquent, microvessel formation, the surface modified PET fibres were tested in a 3D environment containing fibrin gel. Three different *in vitro* systems have been used to investigate microvessel formation. In the first system, both HUVECs and the fibres were embedded in the fibrin gel simultaneously. In the second system, the HUVECs, and fibres having various coatings, were sandwiched between two layers of fibrin gel. In the third arrangement, cell adhesive fibres were pre-coated with HUVECs and then embedded in the fibrin gel. The visualization of the systems was directly performed, using phase contrast microscopy, epifluorescence microscopy, and confocal microscopy during the culture period or through the provision of histology sections and immunohistochemistry.

4.2. Multilayer surface modification and characterization of flat and fibrous substrates with cell adhesive, cell non-adhesive and bioactive compounds

4.2.1. Materials

Various substrates (Table 4.1) were employed for the surface coating, depending on the intended end-use. Commercially available, 100-μm diameter monofilament made of PET (cat. # ES305910, Good fellow, Devon, USA) were used for most of the experiments performed in this study. PET fibres were selected for this role because of; a) their commercial availability as monofilaments, b) their amenability to withstand the multi-step surface modification used in this study, c) their biocompatibility, and d) their resistance towards standard autoclave sterilization methods, and moreover, e) in being "semi transparent".

Table 4.1: Materials utilized for the multilayer surface modifications.

Substrates	Plasma polymers	Dextrans	Biomoleculs
PET fibre	N-Hepthylamine plasma polymer (HApp)	MW 70 kDa	GRGDS
ePTFE fibre		MW 500 kDa	GREDS
Borosilicate glass	Acetaldehyde plasma polymer (AApp)		Gelatin
FEP film			FN

Perfluorinated poly (ethylene-*co*-propylene) tape from Dupont (Teflon FEP Type A, Mississauga, ON, Canada) were used as additional substrate for the surface topography characterization of coatings, and borosilicate glass substrates (Assistent, Sondheim, Germany) were used for monitoring the cell behaviors in more details, that were otherwise difficult to

perform directly on the polymer fibres. These substrates were chosen mainly for their ease of use.

ePTFE (Sutures from W.L Gore & Associates (CV-7, mean dia.109 μm) (measured diameter under microscope was about 200-μm) were used as complementary substrates for the cell adhesion and spreading tests. N-heptylamine (99.5% purity, cat. # 126802, Oakville, ON, Canada) and Acetaldehyde (> 99.9% purity, cat. # 00070 Saint-Louis, MO, USA), used in plasma polymerization, were obtained from Sigma-Aldrich. Dextrans of 70 and 500 kDa molecular weights were purchased from Amersham Bioscience (cat. # 17-0280 and # 17-0320, Uppsala, Sweden). GRGDS (cat. # 44-0-23) and GRGES (cat. # 44-0-51) peptides were purchased from American Peptide Company (Sunnyvale, USA). FN (cat. # f4759 Saint-Louis, MO, USA) and gelatin (cat. # G9391 Saint-Louis, MO, USA) were obtained from Sigma-Aldrich.

4.2.2. Fibre holder designing

Manipulation of the single and thin (100-μm) polymer monofilaments was difficult during the multi-step procedures of this study, i.e., surface modification; characterization and *in vitro* evaluation. To overcome this problem, Teflon frames (Fig. 4.1), in two different sizes and shapes, were designed to be used as fibre holders during the process of fibre surface modification, characterization and biological evaluation. Non-conductive, 3-mm thick Teflon frames [~5 x 7 cm rectangular holder (Fig. 4.1A) and ~2-cm diameter circular holder (Fig. 4.1 B)] to hold the fibres in the plasma zone steady. The rectangular frame was designed and used for the purpose of facilitating the sample preparation (i.e. as either ~5- or 7-cm fibre lengths) for the XPS characterization. The circular frame was designed and used in order to hold the

75

fibres within 12-multiwell culture plates in cell culture tests. Teflon was selected as the appropriate material from which the frames were constructed because it is "workable" and non-conductive, in addition to being both chemically and biologically inert. The above mentioned work has been previously published (HADJIZADEH, et al. 2007)
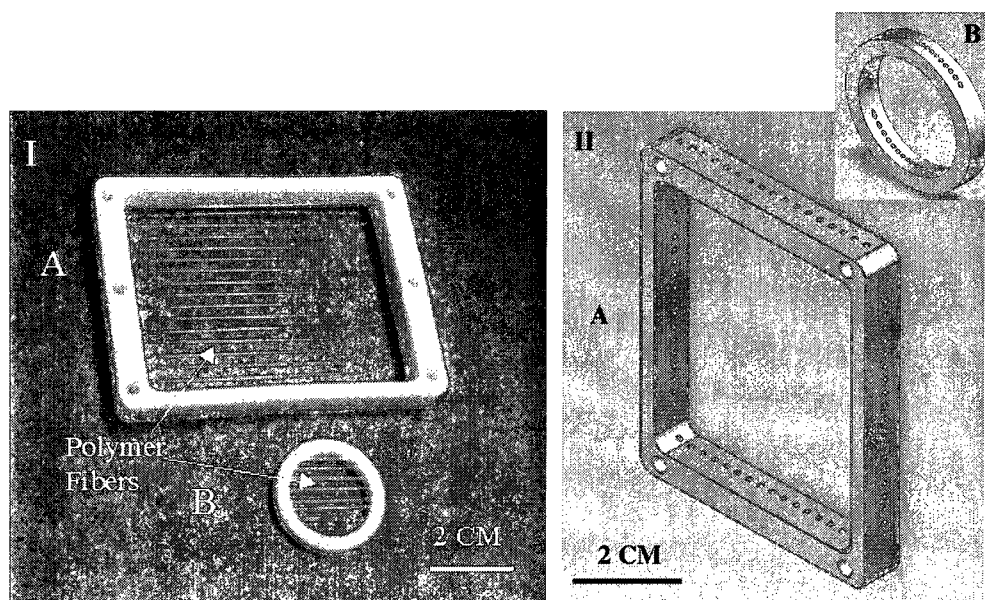
Figure 4.1: A) Picture of the "rectangular" frame used to hold polymer fibres (as single filaments) within the plasma zone, during fiber surface modification to modify the fibre surfaces and subsequently, to perform XPS analyses. B) Picture of the circular frame used to hold single filaments within the plasma zone, to modify the fibre surfaces, subsequently to use in the cell culture experiments. Picture I (photograph) shows the position of the fibres on the frames (as an example). This picture has been previously published (HADJIZADEH, et al. 2007). Picture II, showing the isometric view of the frames, was drawn with the aid of SolidWork software (drawn by Marc G. Couture).

4.2.3. Polymer fibre placement onto the holders

Fibres (PET and ePTFE monofilaments) were manually fixed onto the support holders. By means of a needle, the test fibres were passed through the holder holes and secured to the holder such that all fibres were "aligned" on the same side of the holder (Fig. 4.11B). This

made it possible that all fibres to stay at the same level, so as to rest on the base of the cell culture plate which was essential in the cell culture tests. The above mentioned work has been previously published (HADJIZADEH, et al. 2007)

4.2.4. Substrate cleansing

In the cleaning procedure, all substrates, including fibres secured onto the frames, were initially immersed in a surfactant solution (RBS® Detergent 35, Pierce Biotechnology, Rockford, IL, cat. # 27952), overnight. The substrates were then "sonicated" for 10 minutes in the RBS solution, followed by a further 10 minute "rinsing" in ethanol (ACS grade). The substrates were then properly rinsed in "Milli-Q" water (having a resistivity about 18.2 MΩcm) and in final step, blow-dried using a flow of 0.2-μm filter-sterilized, compressed air. The above mentioned work has been previously published (HADJIZADEH, et al. 2007).

4.2.5. Introduction of amine groups onto substrates by means of plasma polymer deposition

Polymer fibres (PET and ePTFE monofilaments), firmly secured into fibre holders, and the previously mentioned flat substrates, were exposed to a Radio Frequency Glow Discharge (RFGD) plasma of n-heptylamine vapour, to produce surface functional groups, which can be used as a platform for immobilization of further layers by wet chemistry. The reactor employed for the plasma polymerisation was a custom-built batch reactor (Fig. 4.2), in which the plasma was produced in vacuum via a radio frequency supply. The substrates, including the holders bearing the fibres, were placed on the lower circular electrode, having a diameter of 9.5 cm. The thin plasma polymer film was deposited by using n-heptylamine vapour. The

experimental parameters selected for the *n*-heptylamine plasma deposition were as follows: -
RF frequency, 50 kHz, RF power, 80 W and initial monomer pressure, 0.040 Torr. The thin
film deposition time was set at 70 s, and the distance between electrodes was fixed at 10 cm.
The above mentioned study has been previously published (HADJIZADEH, et al. 2007).

4.2.6. Deposition of reactive acetaldehyde groups on substrates by means of plasma polymerization

In order to produce aldehyde functional groups on the target surfaces, surface
functionalization was initially performed by acetaldehyde plasma deposition in the same
fashion as described for the HApp, with the treatment conditions being set as follows:-
frequency, 50 kHz, power load, 80 W, and initial monomer pressure, 0.300 Torr. The
deposition time was set at 70 s and the electrode distance set at 10 cm. The above mentioned
study has been previously published (HADJIZADEH and VERMETTE 2007).
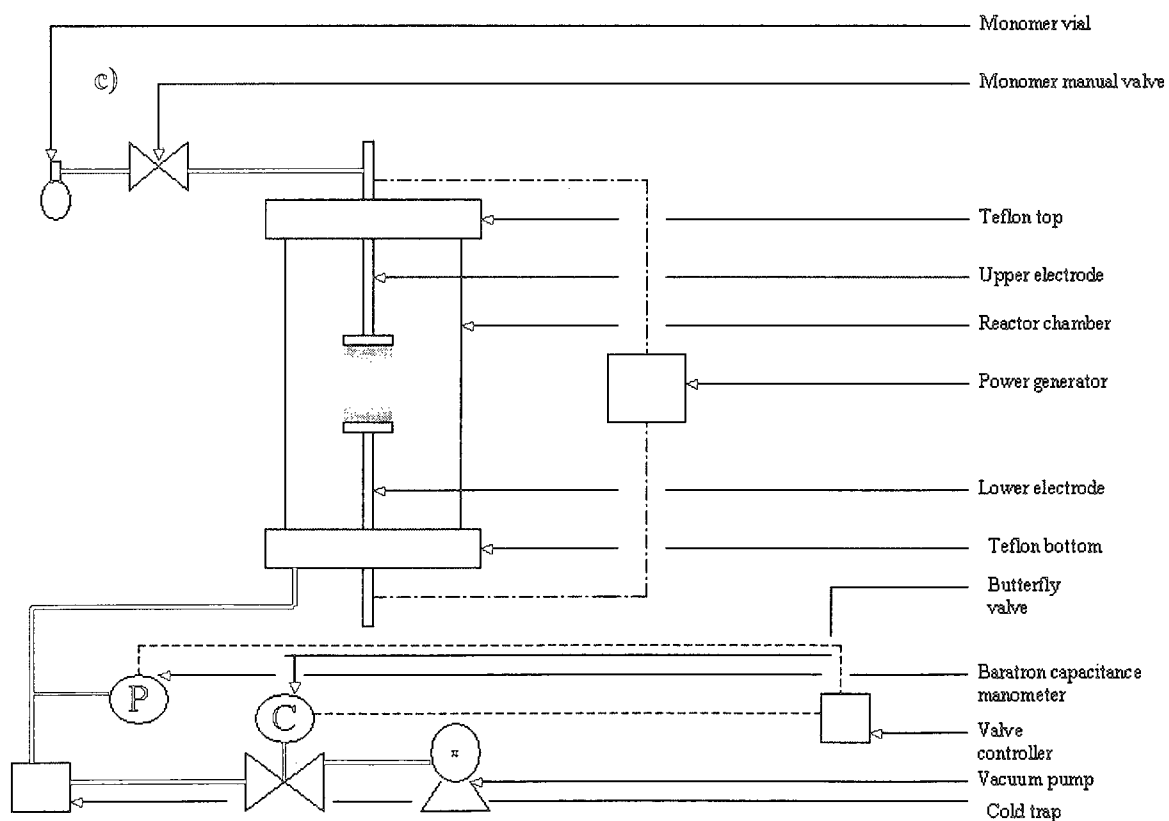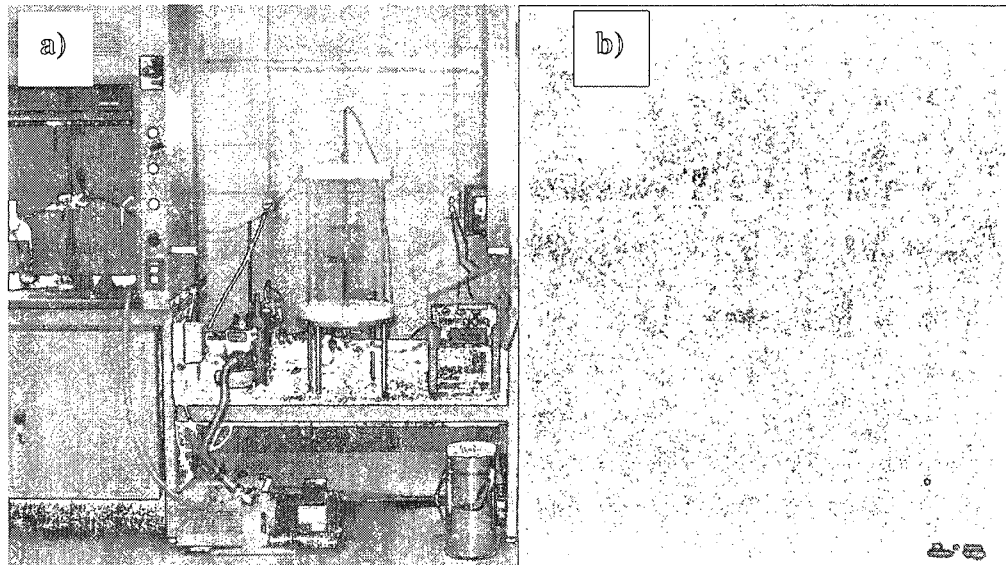
Figure 4.2: a) Picture of reactor and apparatus; b) Picture of N-heptylamine Plasma Enhanced Chemical Vapour Deposition (PECVD) process c) Schematic of PECVD experimental design (reproduced from MARTIN, et al. 2007)

4.2.7. CMD synthesis and characterization

CMD was prepared by using dextrans, of two different molecular weights (MW 70 kDa, 500 kDa), that were carboxy methylated up to a substitution level of around 50% of using bromoacetic acid (cat. # 3016, Lancaster Synthesis Inc., Pelham, NH), by the performance of previously published reaction procedures (LOFAS and JOHNSSON 1990; MCLEAN, et al. 2000a). In this process, CMDs, with about a 50% ratio of carboxyl groups per glucose ring unit, were prepared by dissolving 10 g of dextran in 50 ml of 2 N NaOH, also containing 1 N bromoacetic acid. The solution was stirred overnight, dialysed against Milli-Q water, 0.1 N HCl, and finally Milli-Q water for 24 h each. The solution was then lyophilized and stored at - 20°C until needed. The degree of carboxylation achieved was determined using 1H NMR. According to these analyses, the ratios obtained were ca.1 carboxyl group per 2 sugar units. The above mentioned study has been previously published (HADJIZADEH, et al. 2007).

4.2.8. CMD immobilization onto plasma-modified substrates

CMD was grafted directly to the HApp-coated fibres, using water soluble carbodiimide chemistry (MCLEAN, et al. 2000a), using one (1) and 2 mg/ml CMD solutions prepared with Milli-Q water. Following dissolution, of CMD in Milli-Q water, 19.2 mg/ml of 1-ethyl-3-(3Dimethylaminopropyl) carbodiimide (EDC) and 11.5 mg/ml of N-hydroxysuccinimide (NHS) were added to the CMD solutions. Holders holding the HApp-coated fibres (monofilaments) as well as HApp-coated flat substrates were then immersed in the resultant CMD solution and allowed to react overnight under gentle agitation conditions. In order to remove any non-covalently attached CMD, the substrates were immersed into an agitated 1M NaCl solution for 24 hrs, followed by immersion into Milli-Q water for 24 hrs under vigorous

agitation, and then rinsed in Milli-Q water for subsequent use. All the steps of this procedure were performed at room temperature. The above mentioned study has been previously published (HADJIZADEH, et al. 2007).

In the case of the acetaldehyde plasma coated surfaces, the CMD was immobilized via a plasma step and the PEI spacers by two solution reaction steps (MCLEAN, et al. 2000a). The aldehyde groups present on the surface were reacted (via reductive amination) directly with a solution of polyethylenimine (PEI, Polyscience Inc., PEI 3 mg/ml in Milli-Q water at pH 7.4), using sodium cyanoborohydride (3 mg/ml, reducing agent). To remove any non-covalently attached PEIs, the substrates were immersed in 1M NaCl solution for 24 hrs under vigorous agitation condition, followed by immersion in agitated Milli-Q water for 24 hrs and finally rinsed in Milli-Q water. Amine groups, provided by the PEI on the substrates surfaces, were then used for covalent attachment of CMD in the same way as described earlier for HApp-coated surfaces. This procedure was also performed at room temprature. The above mentioned study has been previously published (HADJIZADEH and VERMETTE 2007).

4.2.9. Biomolecules (e.g. RGD) grafting onto CMD-coated substrates

Peptide (i.e. GRGDS and GRGES) immobilization was performed, according to a sequential (i.e. two-step) procedure, being similar to those described elsewhere (GAO, et al. 2003; HERSEL, et al. 2003). In order to limit the possibility of any damage to the GRGDS and GRGES peptides due to substrate sterilization, the peptide immobilization was conducted under sterile conditions, using autoclaved CMD-coated substrates. CMD-coated substrates, including the fibres, were immersed in Milli-Q water and autoclaved at 121^0C for 25 minutes. The autoclave-sterilized CMD-coated fibres were then immersed in filter-sterilized (low-

binding 0.22-μm syringe filters, Millipore corporation, Bedford, MA, USA) solutions of EDC

(19.2 mg/ml) and NHS (11.5 mg/ml) in PBS (1X, pH 7.4), at room temperature for 4 hrs,

followed by further rinsing with PBS (pH 7.4; 2 x 15 minutes). The substrates were then

incubated in a filter-sterilized (0.22-μm) peptide solution of 0.1, 0.5 or 1 mg/ml GRGDS or

GRGES, made in PBS (pH 8) for 2-3 hrs at room temperature. Following rinsing with PBS

(pH 8, 3 x 15 minutes) to remove "unbound" free peptides, the substrates were allowed to dry

under a sterile hood. This two-step sequential procedure is advantageous in order to avoid the

inter-molecular condensation of the RGD peptides, because in using this procedure, the

carboxyl groups of the aspartate side chain are not activated for coupling (GAO, et al. 2003).

Furthermore, FN (100 μg /ml) and gelatin (100 μg /ml) were immobilized on the substrates in

the same way as previously described for the RGD immobilization. The above mentioned

study has been previously published (HADJIZADEH, et al. 2007).

Figures 4.3A and 4.4 show, schematically, the multi-step procedure for biomolecule

immobilization, via the HApp or the AApp and the CMD interlayers, onto a PET

monofilament, respectively.
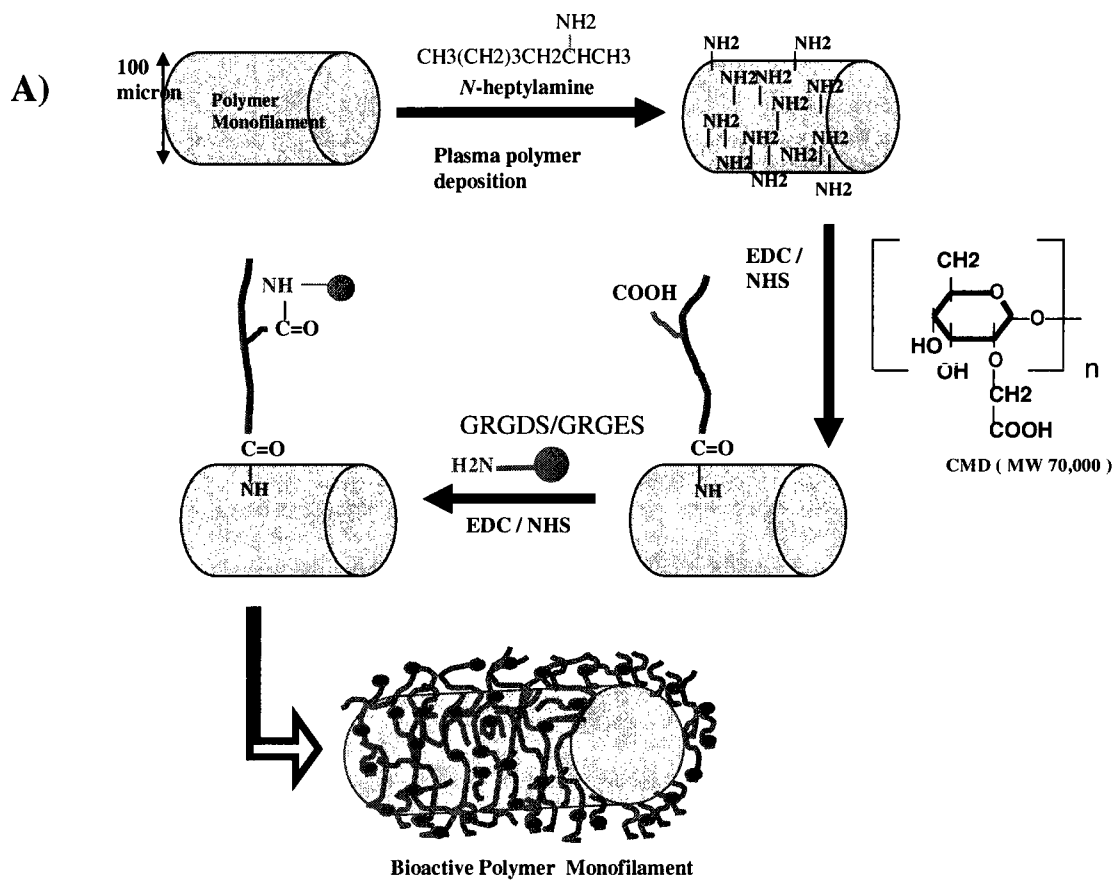
Figure 4.3: A) Schematic diagrams for the methods used for the covalent surface immobilization of GRGDS and GRGES peptides, via HApp and CMD interlayers. B) The chemical sequence of the GRGDS and GRGES peptides. These diagrams have been previously published (HADJIZADEH, et al. 2007).
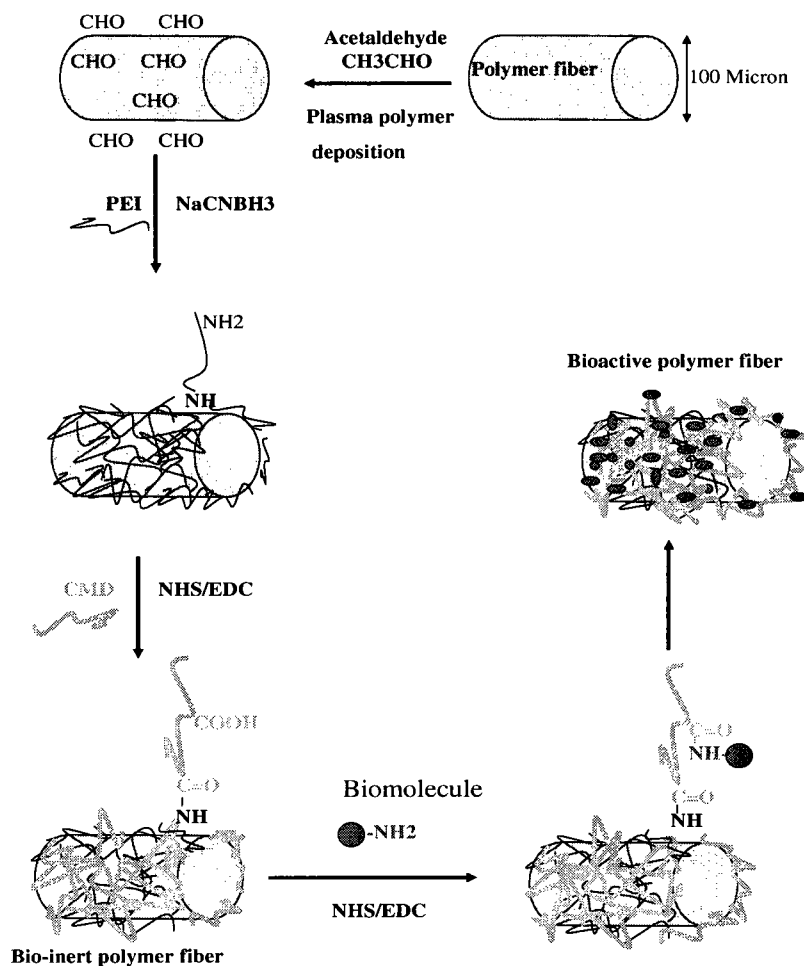
Figure 4.4: Schematic diagrams of the methods used for the covalent surface immobilization of biomolecules (proteins/peptides) via AApp-PEI and CMD interlayers

4.2.10. Surface characterization by XPS

Fibres were fixed onto a particular fibre holder made of stainless steel for the XPS analysis. XPS analyses were performed on an AXIS HS spectrometer (Kratos Analytical) with a monochromatic Al Kα (X-ray source, with operating power of 120 W). The total pressure in the main vacuum chamber was set at 2×10^{-8} mbar during the analysis. The chemical elements were detected from survey spectra. Collection of the C1s high-resolution spectra were performed at 40-eV pass energy for those individual peaks of interest. Atomic percentage for

each element was determined by calculating its integral peak area. The calculations of peak intensities were conducted by use of a Shirley-type background and the sensitivity factors provided by the instrument manufacturer. A value of 285 eV (the C1s hydrocarbon (CH_x) peak) was used as a reference to correct surface charging effects (created due to the charging of the surfaces under X-ray irradiation) for all binding energies. In elemental quantification, a random error for the instrument has been considered (a range between 1 and 2% of absolute values for atomic percentages >5%). In addition, by considering electron attenuation length of ~3 nm for a C1s photoelectron in a polymeric substrate and setting the angle of the emission normal to the surface the XPS analysis depth has been assumed to be about 10 nm. This value has been approximated from which about 95% of detected signal originates (MCLEAN, et al. 2000a). The above mentioned study has been previously published (HADJIZADEH, et al. 2007).

4.2.11. AFM analyses

In order to perform the AFM measurements, surface coated and un-coated substrates were placed on microscope slides covered with "double-sided" tape adhesive. These samples were treated with 0.2-μm filter-sterilized compressed air for the removal of free particles and dust from the surface. A Bioscope (Digital Instruments, Santa Barbara, CA), coupled to a Zeiss inverted microscope, connected to a Nanoscope IIIa controller, was employed to scan the surface of the samples in air by "contact mode", using Si_3N_4 cantilevers with a spring constant of 0.12 N/m. AFM scan controls were appropriately set (to provide sufficient contact force and high gains) to avoid tip artifact generation during scanning of the samples. The "height images" obtained were processed with n-surf (1.0 beta) software.

4.2.12. SEM analysis

A Cold Field Emission Gun Scanning Electron Microscope (FEGSEM) (HITACHI S-4700 SEM) was employed to examine the surface morphology of the coatings and to evaluate their homogeneity over the entire sample surface. As the specimens were non-conductive, their surfaces were coated with a thin layer of platinum (Pt) using a plasma sputtering apparatus, prior to SEM observation.

4.3. *In vitro* evaluation of the surface modified substrates towards EC behavior in a 2D (monolayer) cell culture system.

4.3.1. Cell culture

HUVECs were provided from Dr. C.J. Doillon (Universite Laval, Québec City), isolated from human umbilical cord veins, as previously described (JAFFE 1980). HUVECs were cultured in M199 culture medium (cat. # M5017, Sigma-Aldrich, Saint-Louis, MO, USA) containing 2.2 mg/ml sodium bicarbonate (Fisher, Fair Lawn, USA), 90 µg/ml sodium heparin (cat. # H1027, Sigma-Aldrich, Saint-Louis, MO, USA), 100 U/100 µg/ml penicillin/streptomycin (cat. # 15140-122, Invitrogen Corporation, NY, Grand Island, USA), 10% fetal bovine serum (FBS, cat. # F1051, Sigma-Aldrich, Saint-Louis, MO, USA), 2 mM L-Glutamine (cat. # 25030149, Invitrogen Corporation, NY, Grand Island, USA), and 25 µg/ml endothelial growth factor supplement (ECGS, cat. # 356006, BD Biosciences, San Jose, CA, USA). The above mentioned study has been previously published (HADJIZADEH, et al. 2007).

4.3.2. Cell seeding onto polymer fibres

Cell cultures on the polymer fibres were performed by adapting procedures, described previously (NEUMANN, et al. 2003; UNGER, et al. 2004). In order to evaluate the effect of surface-modified polymer fibres towards the HUVEC responses, fibres were positioned in parallel onto a circular Teflon holder (~2 cm in diameter, Fig. 4.1IB). In this holder, fibres were distanced from each other by approximately 0.1 to 2.0 mm. Fibres were then surface-modified, and subsequently they were sterilized directly on the holders; the non-coated PET or ePTFE fibres, HApp- and CMD-coated fibres were placed in Milli-Q water and autoclaved at $121^{0}C$ for 25 minutes. Three specimens of uncoated, cleaned PET or ePTFE monofilaments, along with PET or ePTFE monofilaments coated with 1) HApp, 2) HApp + CMD, 3) HApp + CMD + GRGDS, 4) HApp + CMD + GRGES interlayers were investigated. Holders holding the fibres were placed into wells of 12-multiwell tissue culture polystyrene (TCPS) plates, then rinsed in sterile PBS (pH 7.4), and incubated in M199 culture medium for 1-2 hrs to keep fibres hydrated until the cells were seeded. Then, 1 ml of M199 culture medium, containing ~ 1×10^{6} cells, was directly poured into the well, containing the fibre secured on the holder. Cells of passages 3 to 5 were used in all experiments. Fibres were incubated for 1 hr and shaked gently. Afterwards, the holders holding the fibres were transferred to new 12-multiwell culture plates, containing fresh M199 culture medium or they maintained in their previous conditions and incubated in a CO_2 incubator at $37^{0}C$ and 5% CO_2. Controls were carried out with HUVECs, grown directly onto the plastic surface of the 12-multiwell culture plates. The above mentioned study has been previously published (HADJIZADEH, et al. 2007).

4.3.3. Cell attachment test

Cell attachment tests were performed following the initial 4-hrs incubation period as reported previously (HERSEL, et al. 2003; MAHESHWARI, et al. 2000). The culture media were removed from wells and cells were incubated with a solution of Hoechst 33258 (cat. # H1398, Molecular Probes Inc., Burlington, ON, Canada) at a concentration of 10 μg/ml in fresh M199 culture medium for 30 minutes. Samples were then visualized under an inverted microscope (Nikon, Eclipse TE 2000-S), using fluorescence and phase contrast imaging. Images were captured using a 10X objective and a digital CCD camera (Regita 1300R, QIMAGING, Burnaby, BC, Canada), and imaging software (Simple PCI, Compix Inc., Cranberry, state, USA). The number of attached cells (stained for nuclei) per fibre length were counted, using SigmaScan5 software. Cell adhesion was studied on all samples and expressed as relative cell adhesion percentages. The relative cell adhesion was defined as the ratio of the cell number on surface coated PET fibres to that of uncoated PET fibres (as control). The number of attached cells (stained for nuclei by Hoechst) per fibre length were counted, 4 hrs after cell seeding. The comparison of groups were performed by using ANOVA (by using SigmaStat software), and a P value ≤ 0.05 was considered statically significant. The percentage of relative cell adhesion was calculated by taking ratios of average numbers of adherent cells on untreated PET, HApp-, CMD-, and peptide-grafted fibres to the average number of adherent cells found on untreated PET fibres, multiplied by 100. Similarly, the relative standard deviations (SD) were calculated by taking the ratio of SDs of adherent cells on untreated PET, HApp-, CMD-, and peptide-grafted fibres to the average number of

adherent cells found on untreated PET fibres multiplied by 100. The above mentioned study has been previously published (HADJIZADEH, et al. 2007).

4.3.4. Cell spreading test

In order to monitor cell spreading, HUVEC-seeded fibres were maintained in culture within an incubator (37^{0}C, 5% CO_2) for 4 days. The culture medium was replenished every 2 days. For the cell staining, cell-seeded fibres were gently washed with PBS (3 times) and then fixed in a formaldehyde solution (3.75 % wt/v) in PBS for 15 minutes. Following washing with PBS (x3), cells adhered on fibres were then permeabilized, using a Triton X-100 solution (0.5 % v/v in PBS) (Sigma Chemical Co.) for 5 minutes. Following two further rinses in PBS, the samples were incubated in a mixture of TRITC-phalloidin (1:100 dilution, cat. # P1951, Sigma Chemical Co.), to stain for actin filaments, and SYTOX Green Nucleic Acid Stain (1μM, cat. # S7020, Molecular Probes, OR, USA) or with Hoechst 33258 (at 1:100 dilution), to stain for nuclei, in a blocking buffer solution (a solution containing 20% bovine serum albumin(BSA) (in PBS)) for 1 hr at room temperature and in darkness. The staining solution was removed and, after 3 washes with PBS, the preparations were then visualized on an Olympus Fluoview 300 confocal microscope, and also on an epifluorescence microscope. Images were captured using a COOLSNAP-Procf camera on Image-pro plus imaging software or by means of digital CCD camera and imaging software (Simple PCI). All experiments were replicated two or more times. The above mentioned study has been previously published (HADJIZADEH, et al. 2007).

4.3.5. Dil-acetylated LDL staining

To ensure cell maintenance on GRGDS (at concentrations of 0.5 mg/ml and 1 mg/ml)-coated fibres, the live cells were initially stained with Dil-acetylated LDL (Acetylated low-density lipoproteins) (cat. # BT-902, Biomedical Technologies Inc., Stoughton, MA, USA) at day 2. Then, the samples were observed, by phase contrast or confocal microscope, every day. This experiment was performed in order to qualitative evaluate the growth and stability of HUVECs on the RGD coated surfaces in culture for a period of 10 days to verify the stability of RGD coating under cell culture conditions. The above mentioned study has been previously published (HADJIZADEH, et al. 2007).

4.3.6. Cell seeding onto surface-modified flat substrates

Observation of actin filaments and focal adhesion structures

Detailed observation of actin filaments and focal adhesion structures was very difficult to perform directly on the polymer fibres, because of the lack of full "transparency" within these fibres. Therefore, surfaces of borosilicate glass substrates were modified and sterilized, under the same experimental conditions as those used to activate polymer fibres surfaces, with the aim of gathering more information on the effects of surface coatings on the actin filament and the focal adhesion formation of cells seeded on various coatings.

Borosilicate glass substrates, with the different modified surfaces, were placed in the wells of a 12-multiwell culture plate. HUVECs were then seeded onto these samples at a density of 1×10^4 cells/cm^2 and cultured, as for the polymer fibres. Following 4 days of culture, the samples were fixed and "permeabilized" by the same procedure as described previously (section 4.3.4), and then incubated for 1 hr with a primary antibody (Monoclonal Anti-

Vinculin, Sigma, cat.# V4505), at a dilution of 1:25 within the same blocking buffer as described above (section 4.3.4). Each sample was then washed three times with the PBS for 5 minutes, and then incubated with secondary antibody (1:250 dilutions of Anti-Mouse IgG, Sigma, and cat. #A2304), within the same blocking buffer, for 1 hr. Samples were twice washed with PBS (5 min each), then mounted in mounting fluid with a coverslip. The edges of samples were sealed with "nail polish" and stored in a dark enclosure until observation by epifluorecence microscopy. The experiments were replicated two or more times.The formation of actin filaments and FAs on each substrate was observed at least in 4 microscopic fields. The above mentioned study has been previously published (HADJIZADEH, et al. 2007).

4.4. *In vitro* evaluation of surface modified PET fibres towards microvessel formation in 3D cell culture systems.

4.4.1. Cell culture

HUVECs were purchased from Cambrex (cc-2519, Walkersville, MD USA) or provided from Dr. Doillon as mentioned in section 4.3.1. HUVECs were cultured (in the same condition as explained in section 4.3.1), i.e. at 37°C and 5% CO_2 in a M199 culture medium containing 2.2 mg/ml sodium bicarbonate, 90 µg/ml sodium heparin, 100 U/100 µg/ml penicillin/streptomycin, 10% fetal bovine serum 2 mM L-glutamine, and 25 µg/ml ECGS. HUVECs between passages 2 and 4 were used in all experiments. Human fibroblasts extracted from human foreskin were cultured in M199, containing 2.2 mg/ml sodium bicarbonate, 90 µg/ml sodium heparin, 100 U/100 µg/ml penicillin/streptomycin, 5% fetal bovine serum 2 mM L-glutamine, at 37°C and 5% CO_2. Fibroblasts between passages 5 and 10 were used in

all experiments. Fibroblasts were provided from Dr. Vermette's laboratory that was obtained from Dr. C.J. Doillon (Universite Laval, Québec City).

Fibrinogen (cat. # F8630), Thrombin (cat. # T3399) and Aprotinin (cat. # A1153), used in 3D angiogenesis models, were provided from Sigma-Aldrich.

4.4.2. Construction of the three *in vitro* cell culture systems

First system: System containing polymer fibres and HUVECs dispersed in fibrin gels

In this system (Fig. 4.5), fibres were embedded in a fibrin gel mixed with HUVECs; uncoated, cleaned PET monofilaments and PET monofilaments coated with i) HApp + CMD, ii) HApp + CMD + RGD, and iii) HApp + CMD + gelatin were tested. Fibres were placed in the wells of 12-multiwell culture plates, then rinsed in sterile PBS (pH 7.4), and incubated in M199 culture medium for 1-2 hours to keep fibres hydrated until they embedded in fibrin gel. To construct the culture system containing fibrin gel, HUVECs and fibres; fibres were first transferred into the wells of 12-multiwell culture plates and then 500 µl of fibrinogen solution (containing 2.5 mg fibrinogen) in M199 medium was placed in each well of a 12-multiwell culture plate. HUVECs, at a density of 1×10^5 cells/ml suspended in serum free M199, were added (500 µl) to the wells, followed by a thrombin solution (1 unit/ml). After polymerization of fibrinogen into fibrin gel (5 min at room temperature and 20 min at 37°C and 5% CO_2), one ml of supplemented medium M199 was added to each well. Then, the assembled system was incubated at 37°C and 5% CO_2 for at least 10 days.
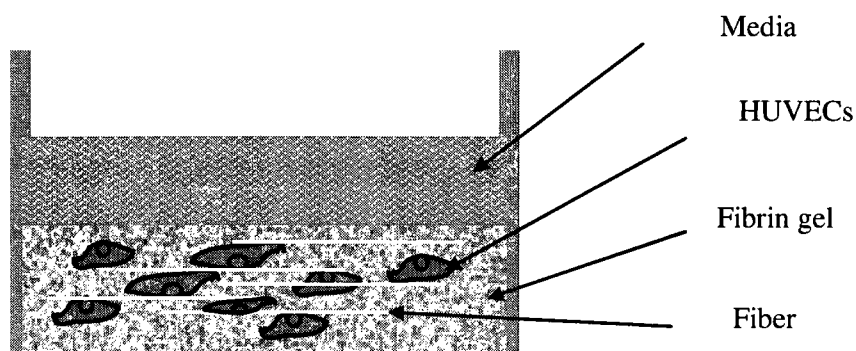
Figure 4.5:   Schematic diagram of the procedure used in the first system, fibres were combined in fibrin gel containing dispersed HUVECs.

Second system: System with HUVECs sandwiched between fibrin gels containing cell-free fibres

In this system (Fig. 4.6), uncoated cleaned PET monofilaments and PET monofilaments, coated with: - i) HApp, ii) HApp + CMD, iii) HApp + CMD + RGD, iv) HApp + CMD + gelatin and v) HApp + CMD + RGE, were investigated. Holders supporting the fibres were placed in the wells of 12-multiwell culture plates, then rinsed in sterile PBS (pH 7.4), and incubated in the M199 culture medium for 1-2 hours to keep the fibres hydrated until the cells seeded. This system was produced by an adaptation of a previously described procedure (BACH, et al. 1998). To make the underlying fibrin gel, 500 μl of fibrinogen (2.5 mg/ml) (solution) in M199 medium was placed in each well of a 12-multiwell culture plate and thrombin (1 unit/ml) was added. After polymerization of the fibrinogen into fibrin gel (5 min at room temperature and 20 min at 37°C and 5% CO_2), holders supporting the fibres were then transferred onto the top of the gel and HUVECs suspended in the serum free M199 were seeded at a density of 1×10^5 cells/well onto the underlying fibrin gel. One milliliter of medium M199 supplemented as indicated in section 4.3.1, was added to each well. Once a confluent

monolayer (~24hrs after seeding) formed, the culture medium was removed and the same

procedure was repeated to generate a second fibrin gel layer over the cell surfaces. After fibrin

gel polymerization, a 1 ml of supplemented medium M199, along with 0.15 units/ml aprotinin

was added to each well.
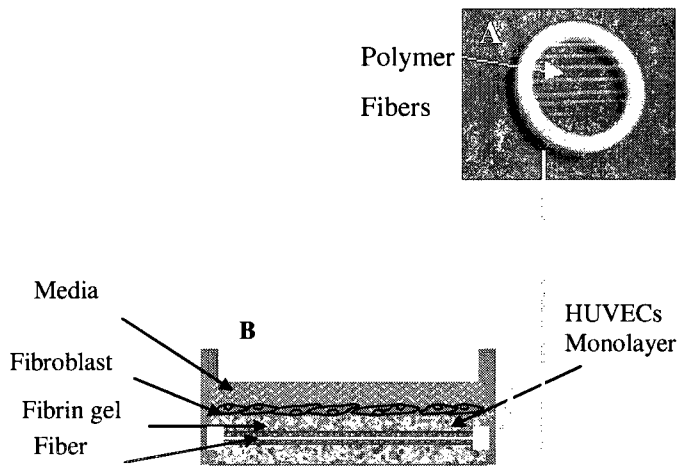
Figure 4.6: Schematic diagram of the procedure used in the study in second system in wich
fibres were maintained parallel in a Teflon holder ring (A), HUVECs and holders
supporting polymer fibres were sandwiched between two layers of fibrin gel on
which a layer of fibroblast was seeded and then culture medium added (B).

Third system: System with cell-pre-coated fibres embedded in fibrin gel

Preparation of the fibres covered by HUVECs

Cell cultures on the PET fibres with different cell-adhesive coatings, were performed by

the application of procedures previously described in section 4.3.2. Three specimens of the

cleaned, uncoated PET monofilaments (controls) and of the PET monofilaments coated with: -

i) HApp, ii) HApp + CMD + RGD and iii) HApp + CMD + gelatin were investigated. Holders

supporting the fibres were placed in the wells of 12-multiwell culture plates, then rinsed in

sterile PBS (pH 7.4), and incubated in M199 culture medium for ~ 1-2 hr to keep the fibres

hydrated until the cells were seeded. Then, 1ml of M199 culture medium, containing 1×10^6

cells (between passages 2 and 4), were directly poured into the well containing the fibre holder. The fibres were incubated in a CO_2 incubator at 37^0C and 5% CO_2, HUVECs were allowed to attach to the cell adhesive polymer fibres by incubating cells with fibres in M199 for about 4 hrs, then the medium was replaced with a fresh one, supplemented as indicated in section 4.3.1, and the samples were kept in the culture up to its confluence. When the entire surfaces of the fibres were covered with HUVECs, they were then used for the angiogenesis experiments. The procedure is summarized on Figure 4.7. It should be noted that cell confluency on both uncoated PET and surface coated PET, as mentioned earlier (i-iii), will not be achieved in the same time period, because the initial cell uptake of uncoated PET fibre, in comparison to surface coated fibre, is too low as we have previously reported (HADJIZADEH, et al. 2007).

Embedding of HUVEC -pre-coated fibres in fibrin gel

This method (Fig. 4.7) has been adapted from a previously reported method (NAKATSU, et al. 2003). In brief, the holders supporting HUVEC-precoated fibres were embedded in a fibrin matrix, prepared as follows: holders supporting HUVEC- coated fibres were placed in a 12-multiwell culture plate, then 1 ml of fibrinogen solution (2.5 mg/ml) in M199 culture medium (pH 7.4) with or without aprotinin (0.15 units/ml) was added to each well of the 12-multiwell culture plate, and then thrombin (1unit/ml) was added to each well. The fibrinogen solutions were left to polymerize for 5 min at room temperature and then incubated at 37°C and 5% CO_2 for 20 min. One (1) ml of EGM-2 (Cambrex, cc-3162) (containing 2% FBS) was added to each well and 4 x 10^4 fibroblast cells were "seeded" on the top of the gel (as

95

monolayer). The culture medium was replenished every other day and the culture system was

monitored each day for 20-30 days.
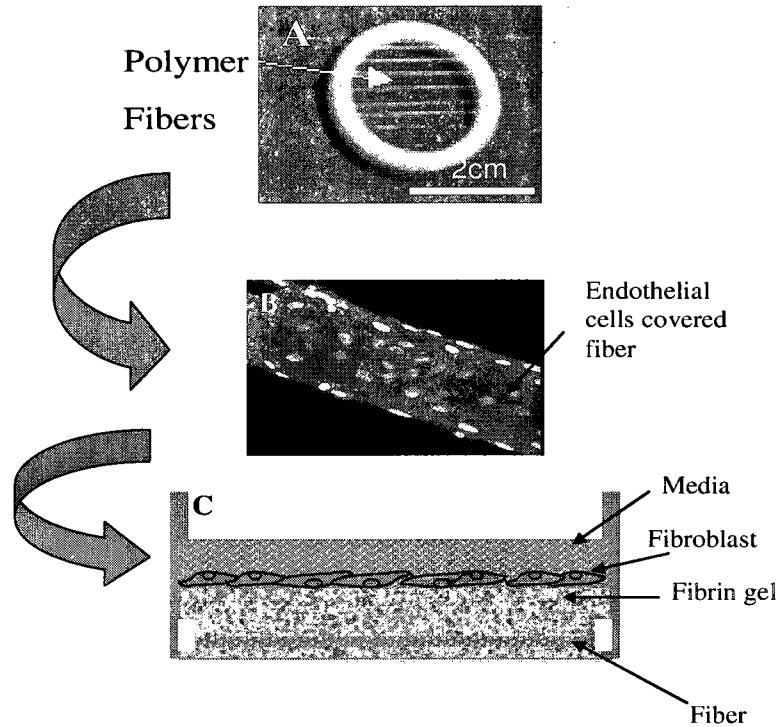
Figure 4.7: Schematic diagram of the procedure used in the third system, and observations made under the microscope. Fibres were maintained parallel within a Teflon holder ring (A); HUVECs were then seeded and grown on the fibres until confluence (in this example, cells on the fibre were stained for actin filaments, using TRITC–phalloidin, and counterstained with Sytoxgreen to highlight the position of the nuclei) (B). The holder was embedded in a fibrin gel, on which a layer of fibroblast was seeded, and the culture medium then added (C). Fibre diameter: 100μm.

4.4.3. Observations

For the observation of the EC behaviour (i.e. tube-like structure formation) during the 20-30 days cell culture period, specimens were observed daily by the use of phase contrast or confocal microscopy. In addition, cells were stained with DiI-acetylated LDL (BT-902, Biomedical Technologies Inc., and Stoughton, MA, USA) at day 2 or 3 and the formation of tube-like structures was periodically observed. Images were recorded by means of a digital

CCD camera (Regita 1300R, QIMAGING, and Burnaby, Canada) and imaging software (SimplePCI, Compix Inc., Cranberry, USA). The 3D systems were also observed through an Olympus Fluoview 300 confocal microscope, the images being captured using a COOLSNAP-Procf camera on Image-pro Plus imaging software. Test fibres were observed at different magnifications (i.e. X4, X10 and X20 objectives) and the images recorded as high-resolution files.

4.4.4. Images and processing

In the third system, fibres were photographed at low magnification (by using the X4 and X10 objectives) and recorded into the high-resolution files (*.TIFF) in order to identify and quantify the effects of fibre distance and incubation time on angiogenic-like structure formation. An image-processing software (i.e. Image J, Scion Co., Frederick, Maryland) was employed for counting the number of angiogenic-like structures. Angiogenic-like structures (regardless their lengths) that originated from the initially formed tube-like structure, situated along the fibre, were counted. The number of vessels was reported per unit length of the fibre (i.e. vessel number /mm).

4.4.5. Statistical analysis

Statistical analysis was performed using SigmaStat software (Systat Software, Inc., Point Richmond, CA). Vessel number per unit length of fibre was determined; comparison between groups was performed by using ANOVA (one-way analysis of variance) with a p value set at ≤ 0.05. The data were reported as mean values $\pm$ standard errors of the mean (SEM).

4.4.6. Histological sections

Constructs (i.e. fibrin gels, involving the fibres on the holders) were "fixed" in a 10% neutral buffered, formalin solution overnight. The constructs were gently removed from their wells, and then proceeded in order to provide the paraffin wax sections. Sections with a 6-μm thickness were cut and the immunohistochemistry was performed, using a vWf (Factor VIII) anti-body with hematoxylin as a counterstain (this test has been processed at the Department of Pathology of University of Sherbrooke).

Chapter 5

Results and discussion I: Surface modification and physicochemical characterization

5.1. Overview

In biomedical applications, surface modifications aim to improve biomaterial surface properties, for example, non cytotoxic, adhesion, and non fouling performances towards cells response. In the study of scaffolding materials for use in the tissue engineering, the chemistry and physics (e.g. surface roughness) of the implant's surface must be studied in depth as these two parameters can affect cell and tissue response. For this reason, one of the objectives of this thesis is the surface modification exploring a multilayer fabrication strategy to change the surface properties of the biomaterials on which new surface functional groups and the topography are generated for better cell adhesion or repulsion without affecting the bulk properties of the polymer. This multilayer surface modification consists of the following steps and aims:

> 1) HApp or AApp was deposited on the surfaces as a thin polymeric interfacial layer containing amine or aldehyde groups respectively, by RFGD deposition. These coatings offer two advantages i) introducing new functional groups (i.e. amine or aldehyde) to covalent grafting of a second desired layer (e.g. CMD), and ii) altering physicochemical properties of the surface to enhance cell adhesion and growth.

2) CMD was then covalently attached onto the amine groups present on the material surfaces using water-soluble carbodiimide chemistry (EDC/NHS); prior to CMD grafting, the acetaldehyde coated surfaces were amine functionalised by grafting PEI via aldehyde groups. The CMD graft layer will play two roles i) non-fouling towards proteins and cells, and ii) introducing carboxy functional groups in order to covalently immobilize bio-active molecules.

3) In a final step, RGD peptides or other biological molecules were covalently grafted onto the surface carboxylic groups available on those surfaces using water-soluble carbodiimide chemistry with the aim of inducing an integrin-mediated cell adhesion.

The performance of multi-layer fabrication steps was confirmed by XPS analyses which were performed for providing detailed quantitative results of the surface elemental composition. In addition to the XPS analysis, the existence of thin films obtained by plasma deposition, and the subsequent CMD immobilization on the surfaces were visualized by SEM and AFM which produced topographic maps of the analyzed surfaces and provided qualitative results of the different coatings. The AApp plasma-deposited and CMD coated surfaces presented the roughest surfaces among others. Therefore, these multi-step surface fabrication techniques can be applied to fabricate biomaterials with multifunctional surfaces, and thus that can have important applications in tissue engineering such as scaffolding materials for multicellular tissue regeneration.

5.2. Surface elemental composition analyses by XPS

In tissue engineering applications, the chemistry of the biomaterial surface must be studied in depth because the cell-material interactions take place at the atomic scale. XPS has been employed to quantify the elemental composition of surfaces, by introducing a surface to an X-ray beam. In this event, the core level electrons of the atoms are ejected (RATNER and CASTER 1997). Kinetic energies corresponding to these electrons are detected and employed to produce analytical results as survey spectrum, elemental percentage and high resolution C1s spectra of the surface (RATNER and CASTER 1997). Therefore, in this present thesis, XPS analyses have been performed at all stages of the multilayer surface fabrication.

5.2.1. Plasma polymer deposition

As indicated in Table 5.1, the elemental composition determined by XPS analyses revealed the successful surface modification of substrates by HApp and AApp. XPS analyses of clean untreated PET fibres show C-C, C-O and C=O components in the C1s high-resolution spectra (Fig. 5.1A), located at 285, 286.5 and 289 eV, respectively. This is in agreement with the PET polymer chemical bonds and XPS analyses of the PET polymer obtained from other studies (WEN, et al. 2006; [Website ref.5]).

HApp coating

HApp was deposited onto the surfaces as a thin, polymeric interfacial layer having amine groups by RFGD deposition, previously explained in Chapter 4 (see section 4.2.5). XPS analysis of HApp layers on PET fibres (Fig. 5.1B and Table 1.1) show a polymer comprised of hydrocarbon- and nitrogen-containing species, which is identical to the data previously

obtained by others on different substrates (MCLEAN, et al. 2000a; GRIESSER, et al. 2002). The oxygen atomic concentration reduced from 25.1% for an uncoated PET monofilament to 3.1% for a HApp-coated PET monofilament, showing the presence of a uniform and thick plasma polymer layer on HApp-coated PET monofilament.

In addition to PET fibres, HApp was deposited on various substrate surfaces, such as ePTFE fibres and PCL membrane, and characterized by XPS. The fluorine atomic concentration was reduced, from 76.54 % for an uncoated PTFE monofilament to 0 % for a HApp-coated PTFE monofilament (Table 5.1), and also the shift related to the fluorine atom in the C1s high-resolution spectra (Fig. 5.2I), located at 292eV, totally disappeared, indicating the existence of a uniform and thick plasma polymer layer on the HApp-coated PTFE fibres. Therefore, these results demonstrate that the HApp layers were thicker than the 10-nm analysis depth of the XPS instrument.

Moreover, to verify the performance of this coating on substrates with various shapes, the same HApp coating was generated on the PCL porous membrane. The elemental composition (Table 5.1) and the XPS high resolution spectra of PCL (Fig. 5.2II) all were in agreement with those obtained for the PET fibre (Table.5.1) and (Fig. 5.1).

Therefore, HApp can be deposited onto different materials, with of different geometries, such as fibrous or flat polymeric substrates, with porous or nonporous surfaces, thereby producing a uniform film and thicker than 10 nm. Plasma polymerization has been widely utilized for the surface modification of biomaterials, in the field of biomaterials. This is due to the typical characteristics of the plasma polymer films, such as: - being smooth, free of pinhole and other defects, and displaying good adhesion towards various substrates (MOROSOFF 1990; GENGENBACH, et al. 1996). However, since these plasma polymer

films rapidly oxidize in air, they should be used promptly after their preparation (GENGENBACH, et al. 1996; GENGENBACH, et al. 1994).

AApp coating

AApp was deposited onto the surfaces as a thin, polymeric interfacial layer; having aldehyde groups, by the RFGD deposition route as previously explained in Chapter 4 (see section 4.2.6). As listed in Table 5.1, the successful surface modifications, achived by use of AApp on the PET fibres, were obvious after determination of the elemental composition by XPS analyses. XPS elemental ratios (Table5.1) and C1s high-resolution spectra for the aldehyde plasma surface (Fig. 5.3B) were identical to those reported earlier (MCLEAN, et al. 2000a). The decreases in the oxygen atomic concentration, from 26.6% in PET to 16.69% on the AApp-coated surface (Table 5.1) along with the disappearance of shifts in the 286.5eV and 289eV spectral lines (Fig. 5.3B) show a thick plasma polymer coating on the AApp-coated substrates.

In addition to PET fibres, AApp was also deposited on various surfaces such as PTFE fibres and flat surface borosilicate glass (used as references), and was characterized by XPS. The reduction in the fluorine atomic concentration, from 76.54 % for an uncoated PTFE monofilament to 0% for an AApp-coated PTFE monofilament (Table 5.1), indicated the presence of a uniform and thick plasma polymer layer. In addition, the XPS C1s spectra (Fig. 5.2IV) of the PTFE fibres, coated with AApp layers, showed the disappearance of the spectral shift, related to the fluorine in 292 eV, demonstrating that the AApp layer was thicker than the 10-nm analysis depth of the XPS instrument. Similarly, the disappearance of the shift related to the silicon in AApp-coated borosilicate glass (Table 5.1 and Fig. 5.2 III), is additional proof

of the successful surface coating with Aapp, as well as the applicability of use of this coating on rigid, non-polymeric substrates. Therefore, AApp deposition can be performed on various substrates, such as: flat, fibrous, polymeric and non-polymeric surfaces, producing a uniform and thicker coating than earlier mentioned 10 nm films.

Table 5.1: Elemental compositions, determined by XPS of HApp- and AApp-coated substrates.

Samples	Atomic concentrations (%) ± Standard deviation					Atomic ratios (%)		Exposure to oxygen
	C 1s	O 1s	N 1s	F1s	SI1s	N/C	O/C	
PET fibres	74.8 ± 2	25.1 ± 2	0.0 ± 0.0	0	0	0.000	0.34	NA
PET+HApp	88.6 ± 0.4	3.1 ± 0.5	8.3 ± 0.4	0	0	0.094	0.03	>1hour
PTFE fibre	23.46	0	0	76.5	0	0	0	NA
PTFE +HApp	91.6	2	6.4	0	0	0.07	0.022	>1hour
PCL* film	78.5	21.5	0	0	0	0	0.27	NA
PCL film+HApp	85.25	8.15	6.6	0	0	0.08	0.1	>1day
PET fibre +AApp	80.5	19.5	0	0	0	0	0.24	>1 hour
PTFE fibre +AApp	81.08	18.92	0	0	0	0	0.23	>1 hour
Borosilicate glass	4.25	63.15	0	0	22	0	14.85	NA
Borosilicate +AApp	83.9	16.1	0	0	0	0	0.19	>1 hour

* PCL porous film was prepared by the immersion precipitation method, using chloroform (solvent) and water (non- solvent).
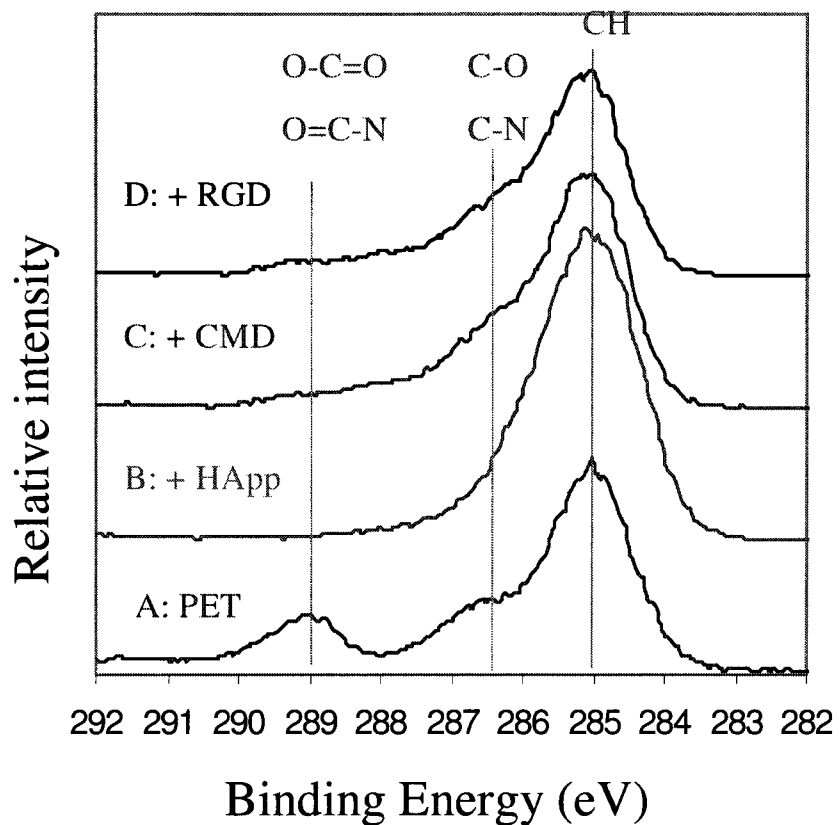
Figure 5.1: High-resolution XPS C1s spectra of: (A) clean untreated PET fibres, (B) PET fibres + HApp layer, (C) HApp + CMD (70kDa, 1:2, 2 mg/ml), and (D) HApp + CMD + GRGDS (0.5 mg/ml). The spectra have been displayed relative to each other in the Y-direction to allow for comparison of the peak positions. This figure has been previously published (HADJIZADEH, et al. 2007).
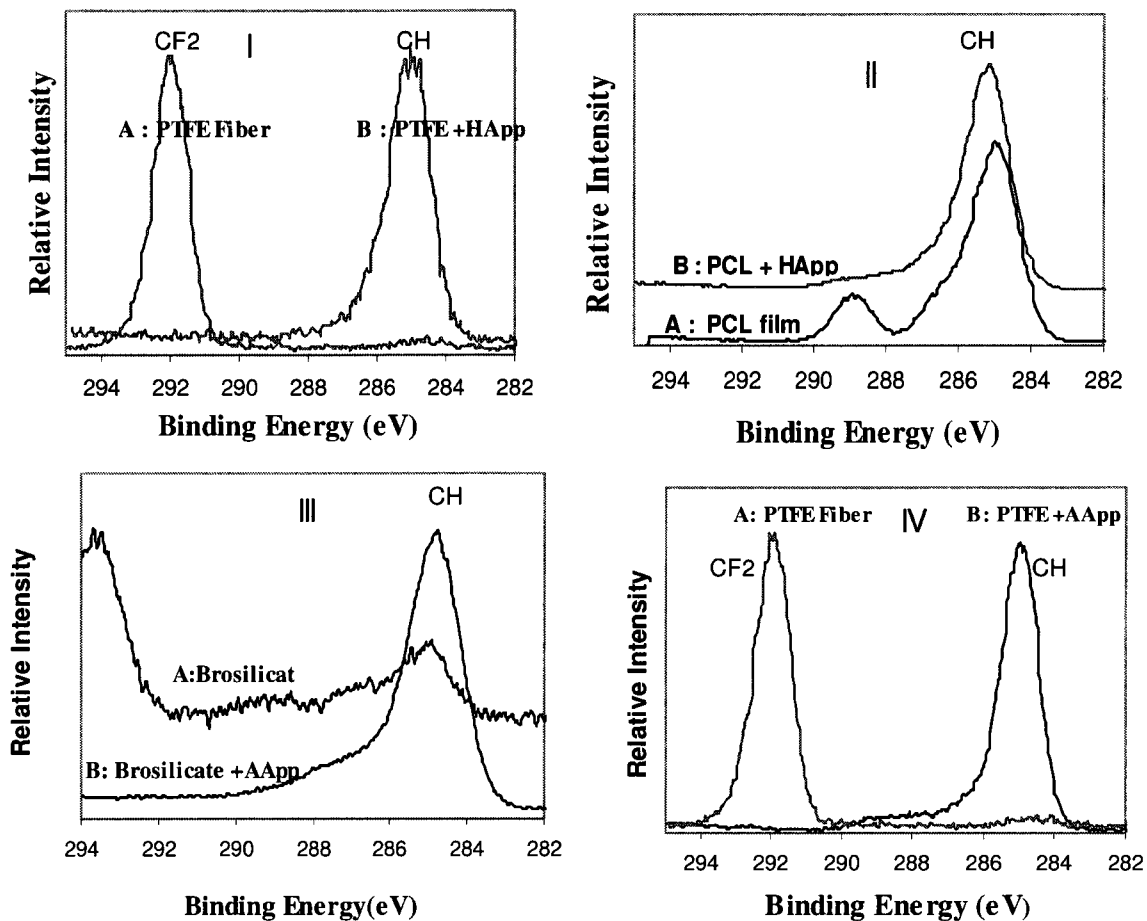
Figure 5.2: High-resolution XPS C1s spectra of HApp and AApp-coated substrates: **I)** clean, untreated PTFE fibre (A) and PTFE fibre + HApp (B) this figure has been previously published (HADJIZADEH and VERMETTE 2007). **II)** Clean, untreated PCL membrane (A) and PCL membrane + HApp (B) this figure has been previously published (HADJIZADEH and VERMETTE 2007). **III)** Clean, untreated borosilicate glass (A) and borosilicate glass + AApp (B), **IV)** clean, untreated PTFE fibre (A) and PTFE + AApp (B)
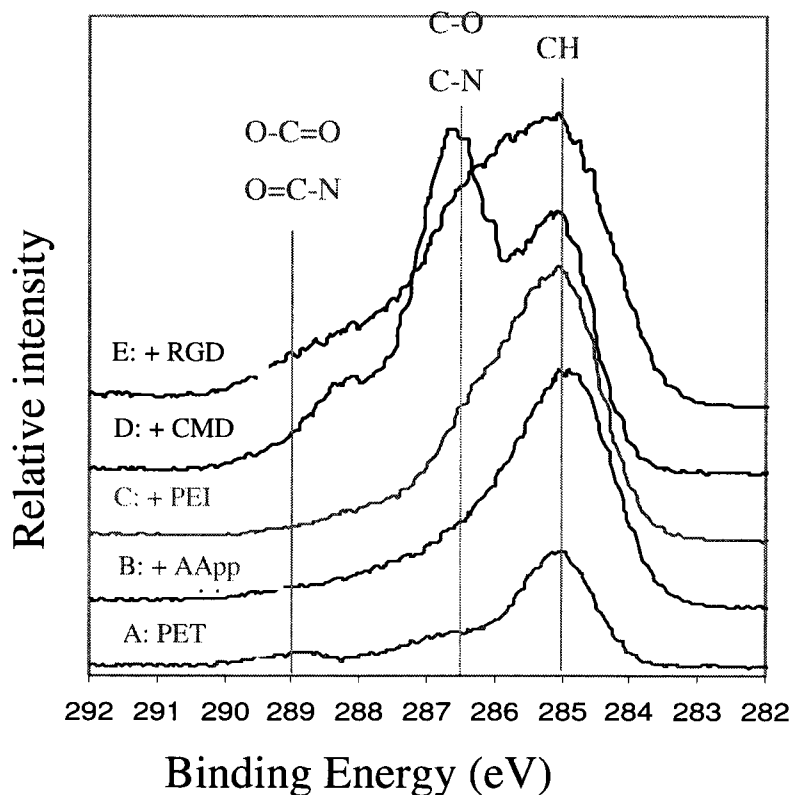
Figure 5.3:   High-resolution XPS C1s spectrum of **A)** PET monofilament, **B)** PET + AApp,
C) PET + AApp + PEI, **D)** PET + AApp + PEI + CMD, **E)**
PET+AApp+PEI+CMD+GRGDSP, the spectra have been displaced relative to
each other in the Y-direction to allow comparison of peak positions This figure
has been previously published (HADJIZADEH and VERMETTE 2007).

5.2.2. CMD immobilization

CMD immobilization via HApp interlayer

CMDs were synthesized from dextrans of two distinct molecular weights (70 and 500 kDa

MW), according to previously reported procedures (LOFAS and JOHNSSON 1990;

MCLEAN, et al. 2000a), as previously explained in Chapter 4 (see section 4.2.7), with about a

50% ratio of carboxyl groups to the sugar units. The degree of carboxylation achieved was

examined, using 1H NMR. The experimentally determined ratios were ca. 1 carboxyl group

per 2 sugar units (the results of the NMR analyses can be seen in the Appendix, section 10.3).

CMD was then covalently grafted onto the surface amine groups available on the surfaces, using water-soluble carbodiimide chemistry, as previously explained in Chapter 4 (see section 4.2.8). The increase in atomic concentration, from 3.1% for a HApp-coated PET monofilament to about 18.2 % for a CMD-coated PET monofilament, indicates an uniform CMD layer (Table 5.2). The appearance of chemical shifts related to the C-O (286.5 eV) and C=O (289 eV), observed in the high-resolution C1s spectra, also prove the successful grafting of the carboxy-methyl-dextrans onto the HApp interlayer (as shown in Fig. 5.1C). The presence of a nitrogen signal demonstrates that the CMD graft layer (in the dry state and under vacuum) was much thinner than the XPS analysis depth (i.e. 10 nm). These results are identical to those of a previous study, using the same multilayer structure (MCLEAN, et al. 2000a).

The effects of the CMD molecular weight and CMD solution concentration on the effectiveness of this coating were examined on the effectiveness of the CMD coating. To this aim, CMDs, with two different molecular weights (i.e. 70 and 500 kDa) and two CMD solution concentrations (i.e. 1 mg/ml and 2 mg/ml) were used. As shown in Figure 5.4, the XPS surface chemical compositions of the four CMD coatings were similar. As shown in Figure 5.5, only for the autoclaved CMD coating (70 kDa, 1:2, and 2 mg/ml) a significant reduction in atomic O/C ratio in comparison to the control (i.e. CMD, 70 kDa, 1:2, 2 mg/ml) at $P \leq 0.05$ was observed. However, CMD-coating of 70 kDa molecular weight and CMD solution concentration of 2 mg/ml shows a lower N1s/C1s ratio (0.062) among the other CMD coatings (Table 5.2 and Figure 5.5 B), demonstrating that the CMD coating in this condition generates a thicker CMD layer on the surface. As a result, CMD with a 70 kDa molecular

weight, a carboxylation ratio of 1:2, and a CMD solution concentration of 2 mg/ml, were selected to produce the CMD-coated PET fibres for use in biological testing of these fibres.

To permite the use of these fibres in cell and tissue culture applications, they need to be sterilized, using standard sterilization procedures. As autoclaving is the optimal and desirable method for the sterization of biomedical devices, the effect of autoclaving on the CMD coating on the fibres was evaluated by XPS. XPS analyses of autoclaved samples showed an alteration in the surface elemental composition of this coating (Table 5.2 and Fig. 5.5C). These observations suggest that some CMD molecules have detached themselves during the autoclaving conditions, though extensive rinses with 1M NaCl solution were used to remove physisorbed CMD molecules from the fibres, following CMD immobilization. Another possibility is that the CMD coatings collapsed during autoclaving. A decrease observed in the atomic O/C ratio, following autoclaving of the CMD-coated fibres, supports these two suggestions (Fig. 5.5C). The above mentioned results and discussions, about CMD, have been previously published (HADJIZADEH, et al. 2007).

Table 5.2: Elemental compositions determined by XPS of the CMD immobilized PET fibres

Samples	Atomic concentrations (%) ± Standard deviation			Atomic ratios (%)		Exposure to oxygen
	C 1s	O 1s	N 1s	N/C	O/C	
PET+HApp	88.6± 0.4	3.1 ± 0.5	8.3± 0.4	0.094	0.03	>1hour
PET+HApp+CMD(1:2, 70 kDa, 1 mg/ml)	75.8± 2	18.2± 0.5	6.0± 1.3	0.079	0.24	>3days
PET+HApp+CMD(1:2, 70 kDa, 2 mg/ml)	77.4± 0.6	17.8± 0.6	4.8± 0.7	0.062	0.23	>3days
PET+HApp+CMD(1:2, 70 kDa, 2 mg/ml) following autoclave	81.0± 1	13.5± 1.5	4.9± 0.2	0.061	0.17	>3days
PET+HApp+CMD(1:2, 500 kDa, 1 mg/ml)	77.2± 0.3	17.1± 0.6	5.7± 0.2	0.073	0.22	>3days
PET+HApp+CMD(1:2, 500 kDa, 2 mg/ml)	77.1± 1.7	18.1± 0.1	6.0± 1.7	0.078	0.24	>3days
PET +AApp	80.5	19.5	0.0	0.0	0.24	>1hour
PET +AApp +PEI	78.8 ±1.3	16.6± 4.4	4.5± 3	0.057	0.21	>5hours
PET+Aapp +PEI +CMD 1:2(70 kDa) 1 mg/ml	67.51	26.4	6.12	0.09	0.4	>1days
PET+AApp+PEI +CMD 1:2(70 kDa) 2 mg/ml	71.9±4.4	24.8±4.4	3.3±0.0	0.045	0.34	>1days

1:2 means a carboxylation degree of 1:2.
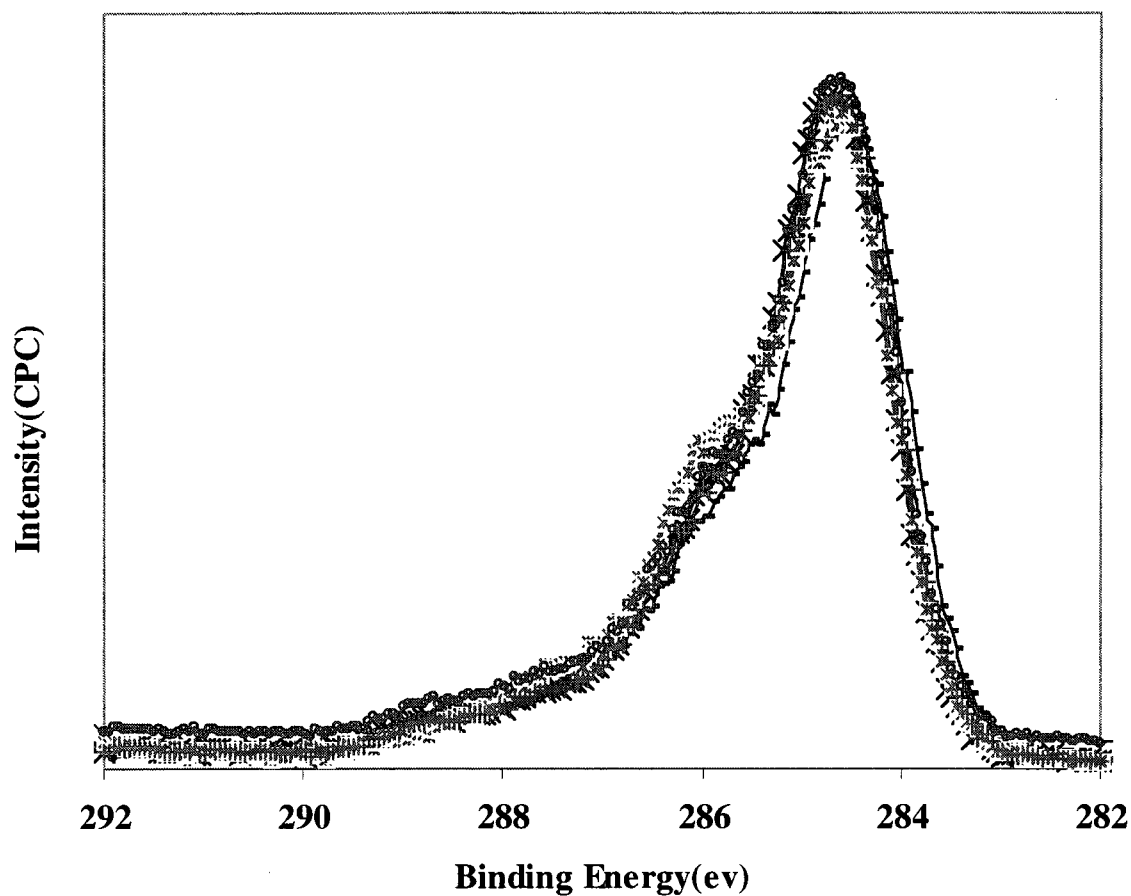
Figure 5.4: High-resolution XPS C1s spectra of (O) PET + HApp + CMD (70kDa, 1 mg/ml), (+) PET + HApp + CMD (70kDa, 2 mg/ml), (x) PET + HApp + CMD (70kDa, 2 mg/ml) (autoclaved), (-) PET + HApp + CMD (500kDa, 1 mg/ml), and (*) PET + HApp + CMD (500kDa, 2 mg/ml). CMD with a ratio of 1 carboxyl group to 2 sugar units was used. This figure has been previously published (HADJIZADEH, et al. 2007).
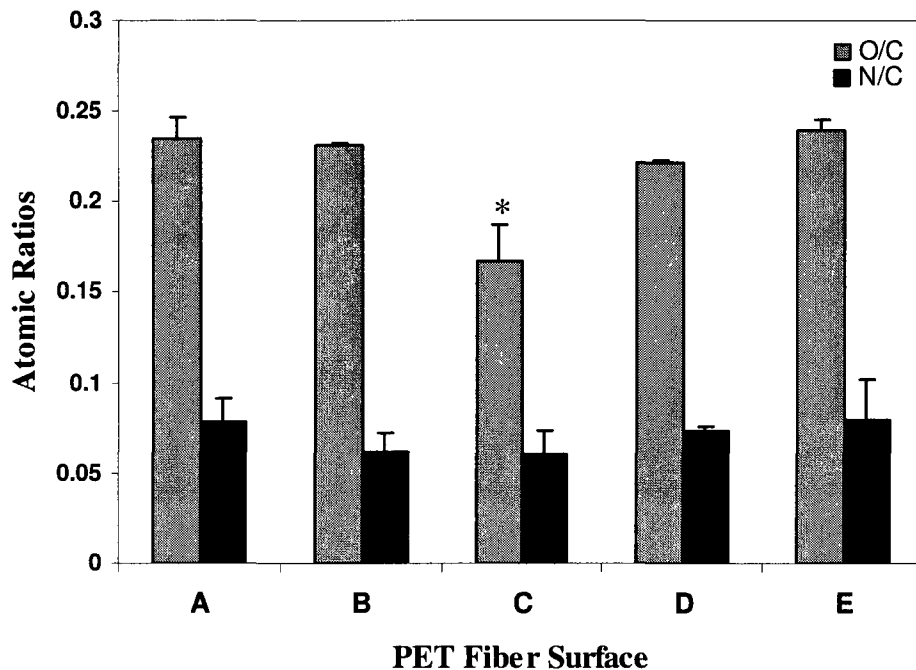
Figure 5.5: Atomic O/C and N/C ratios of CMD-coated PET fibres produced under various conditions. A) PET + HApp + CMD(70kDa, 1:2, 1 mg/ml), B) PET + HApp + CMD(70kDa, 1:2, 2 mg/ml), C) PET + HApp + CMD(70kDa, 1:2, 2 mg/ml) (autoclaved), D) PET + HApp + CMD(500kDa, 1:2, 1 mg/ml), and E) PET + HApp + CMD(500kDa, 1:2, 2 mg/ml). Error bars represent the standard deviations, * indicates those values significantly different from the control (PET + HApp + CMD (70kDa, 1:2, 2 mg/ml)) by ANOVA at p ≤ 0.05. This figure has been previously published (HADJIZADEH and VERMETTE 2007).

CMD immobilization via AApp interlayer

In this method, the CMD was grafted onto the AApp layer via the polyimine (PEI) (generates surface amine groups) spacer layer. So this method consists of immobilizing the CMD via a plasma step, and the PEI spacers, by the two solution reaction steps. Immediately after the plasma polymer deposition, the aldehyde groups (CHO), generated by AApp on the surface, were reacted (via the reductive amination reaction) with a solution of PEI and sodium cyanoborohydride ($NaBH_3$) acting as the reducing agent (MCLEAN, et al. 2000a). Then the CMD, with 70kDa MW were immobilized onto the PEI spacers, via the use of carbodiimide

chemistry in the same way as conducted for the CMD immobilization, via HApp (see section 4.2.8). Then, all the product layers (i.e.AApp, the PEI and CMD) were analyzed by XPS (Table 5.2). The XPS C1s spectrum of the PEI grafted onto the AApp is shown in Figure 5.3C. The increased in nitrogen content (but not oxygen) shown in table 5.2 suggests that the height increase of the C1s shoulder at 286.5eV can be attributed to the introduction of the C-N species of the PEI. The increase in the atomic concentration of oxygen by the CMD coating (Table 5.2), and the presence of C-O (286.5eV), C=O (289eV), observed in the high-resolution C1s spectra, revealed the presence of covalently grafted CMD on the AApp-PEI-coated surface (Fig. 5.3D). The observation of the nitrogen signal, following the CMD grafting, shows the presence of the PEI chains at the outer surface of the coating (among the CMD chains), a situation identical to that reported elsewhere (MCLEAN, et al. 2000a). This can be either because of a thin CMD coating or it may be due to an artefact, created by the rearrangement of the CMD chains caused by the vacuum prior to the XPS analysis. The XPS C1s spectrum of the CMD (Fig. 5.3D) shows that the CMD graft layer was thicker when the CMDs were immobilized by means of a PEI spacer layer grafted onto the Aapp, in comparison with the case of direct grafting onto the HApp surface (Fig. 5.1C).

As shown in Table 5.2, the CMD of 70 kDa molecular weight with a CMD solution concentration of 2 mg/ml, shows a lower N1s/C1s ratio (0.045) than that of CMD, with a CMD solution concentration of 1 mg/ml (0.09). This suggests that the CMD coating in this condition may produce a thicker CMD layers on the surface. This is identical to the result of the same experiment, performed on HApp (Table 5.2). As a result, the concentration of 2 mg/ml, CMD of 70 kDa molecular weight, with a carboxylation ratio of 1:2, can be an optimal concentration, when using this method.

5.2.3. RGD immobilization

RGD peptide immobilization via HApp and CMD interlayer

In the final step, RGD was covalently grafted onto the surface carboxylic groups, available on the surfaces using water-soluble carbodiimide chemistry which was conducted using a two step, sequential procedure. To avoid any (expected) damage to the RGD peptides during the substrate sterilization before the cell culture, peptide immobilization was performed under sterile conditions; using autoclaved CMD-coated substrates (see Chapter 4, section 4.2.9).

The XPS analyses showed the emission of C1s at 286.5eV and 289 eV (Fig. 5.1D), which correspond to the C-N and C-O-NH emission lines, respectively (PORTE-DURRIEU, et al. 1999). Moreover, the N1s/C1s ratio, determined on the GRGDS-coated samples was higher than that of CMD (Table 5.3), which confirms the presence of covalently immobilized GRGDS on the CMD-coated PET fibres. In addition, the atomic N/C ratio increased when the GRGDS concentration, from 0.1 mg/ml to 1 mg/ml (Table 5.3). The above mentioned results and discussions, about RGD, have been previously published (HADJIZADEH, et al. 2007).

114

Table 5.3: Elemental composition of RGD immobilized PET fibre

Samples	Atomic concentrations (%) ± Standard deviation			Atomic ratios (%)		Exposure to oxygen
	C 1s	O 1s	N 1s	N/C	O/C	
PET+HApp+CMD(1:2, 70 kDa, 2 mg/ml) following autoclave	81.0± 1	13.5± 1.5	4.9± 0.2	0.061	0.17	>2days
PET+HApp+CMD(1:2, 70 kDa) +GRGDS (0.1 mg/ml)	78.0± 3.5	16.8± 3.2	5. 2± 0.4	0.067	0.22	>2days
PET+HApp+CMD(1:2, 70 kDa) +GRGDS (0.5 mg/ml)	76.3± 1	18.2± 0.75	5.5± 2	0.072	0.24	>2days
PET+HApp+CMD(1:2, 70 kDa) +GRGDS (1 mg/ml)	72.0± 1.4	21.7± 0.5	6.4± 0.7	0.089	0.30	>2days
PET+Aapp +PEI +CMD 1:2(70 kDa) 1 mg/ml	67.51	26.4	6.1	0.09	0.4	>2days
PET+Aapp +PEI +CMD(1:2(70 kDa) 1 mg/ml) +GRGDSP (0.1 mg/ml)	69.6	22.5	7.9	0.11	0.32	>2days
PET+Aapp +PEI +CMD(1:2(70 kDa) 1 mg/ml) +Gelatin (0.1 mg/ml)	78.9	17.7	3.4	0.04	0.22	>2days

1:2 means a degree of carboxylation of 1:2.

RGD peptide immobilization via AApp and CMD interlayers

XPS analysis of samples containing the covalently grafted GRGDSP peptide, on the surface of immobilized CMD, is shown in Figure 5.3E. A decrease in the height of the C1s shoulder at 286.5eV (Fig. 5.3E) is related to the presence of RGD. In addition, an increase in the N/C ratio, from 0.09 in CMD-coated to 0.11 in RGD-coated surface, was observed (Table 5.3). It should be noted that these experiments were performed, using GRGDS peptides in a manner similar to the GRGDS immobilization, via HApp. However, due to some practical errors with GRGDS, only the data related to the GRGDSP peptide are reported hereinafter.

The GRGDSP peptide has one additional amino acid [i.e., proline (P)]. The result demonstrates the existence of covalently grafted RGD, via AApp and CMD, on the surface. In addition to the RGD peptides, gelatin was also grafted onto the CMD-coated PET fibres, the coating being analyzed by XPS (Table 5.3). When layered together (i.e. HApp, PEI, CMD, gelatin or RGD), it is difficult to characterize precisely the biological molecules, such as the gelatin or RGD because of the similarity in the chemical composition between the two neighbouring layers. To overcome this problem, several other methods are able to be employed (HERSEL, et al. 2003) amongst them one is the evaluation of cell attachment capability of RGD-coated surfaces, in which the number of attached cells indicates the density of the RGD on the surface. I have selected this technique to study cell attachment to the fibers (see Chapter 6). However, as a perspective, tagged molecules, such as the fluorine-labeled RGD, could provide better characterization of the RGD immobilization by XPS.

5.3. Surface topographical analyses by SEM and AFM

Topographical analyses were essential to provide (i) additional proof of existence of the distinct coatings on the material (fibre) surface, and (ii) providing a topographical map of the modified surfaces that may affect cell-biomaterial interactions. As discussed earlier in Chapter 2, substrate surface topography, at micrometric and nanometric scales, is an important parameter that affects cell behavior (SENESI, et al. 2007; BARBUCCI, et al. 2003). Therefore, in addition to the chemical properties of the surface, the topographical properties are also important in cell-biomaterial interactions and these should be investigated in formulating the designs of new biomaterials.

Surface topographical characterization offers the following parameters:

1) qualitative determination of micrometric and nanometric scale features, created by the manufacturing techniques, on PET fibres that may affect cell behavior;

2) the effect of plasma polymer deposition on the alteration of these features on fibre surfaces;

3) providing additional proof of successful surface coating by means of plasma polymerization, produced by RFGD fed with N-hepthylamine or acetaldehyde vapors and the subsequent CMD grafting;

4) observing the nanometeric scale topography generated by mutilayer surface fabrication via two different plasma polymers, HApp and AApp that may affect the cell function in contact with these surfaces.

To further this aim, SEM and AFM were used to evaluate the morphological features of the untreated PET fibre and FEP film and the same substrates coated by HApp, Happ-CMD, AApp and AApp-CMD. FEP film used for providing an additional source of data to prove that the surface features observed on the PET fibres were due to the surface coatings and that the SEM and AFM techniques were applicable to detect the surface texture of surface coated and uncoated PET fibres also. Yet, RGD-coated surfaces were not topographically analyzed because of their low molecular weights and low concentration, as used in this study. Therefore, I believe that RGD should not considerably alter the topography of the surface.

5.3.1. CMD immobilization via AApp

Both SEM and AFM analysis of the uncoated PET fibres showed relatively clean surfaces, as shown in Figures 5.6A and 5.7A and 5.8A. These analyses showed that uncoated clean PET fibres have some random groove-like defects at the micrometric or nanometric scale, generated by the manufacturing techniques (Fig. 5.7A and 5.8A). The AApp coating was found to exhibit a rough surface on both the PET fibre (Fig. 5.7 and Fig. 5.8) and the FEP film (Fig. 5.9), in comparison with the uncoated surfaces. The presence of some AApp-generated features at nanometric scale can be seen on the PET fibre in Figures 5.7B and 5.8B, and on the FEP film in Figure 5.9B, which may result from the plasma process. These features appear to be distributed on the surface. However, it was also observed that, in some areas, peaks of AApp accumulate on the surface (Fig. 5.7IIB), generating randomly distributed features. Since the XPS results showed the formation of a uniform thick AApp layer on the substrate in the AApp deposition, this suggests that accumulation of AApp on the surface occurred after generating a saturated uniform AApp film on the surface. As observed in Figure 5.8C, the PEI coated surface shows a similar topography as the AApp coated surface. The CMD coated sample also exhibits a rough surface (Fig. 5.7C and 5.8D), similar to the AApp and PEI surfaces. Therefore, AApp deposition generates nanometric scale features (i.e. roughness) on the surface, as demonstrated by both SEM and AFM analyses on two different substrates (i.e. PET fibre and FEP film). Moreover, subsequent CMD coatings applied on the AApp-coated surface increases the surface roughness through either creating new features or in following features previously created by the Aapp, and which are detectable by both SEM and AFM techniques.

A) PET Fiber
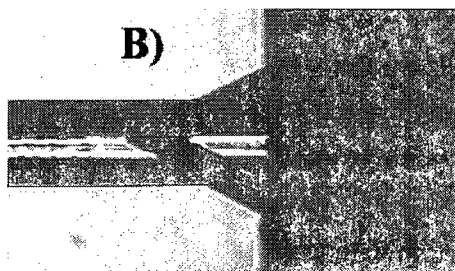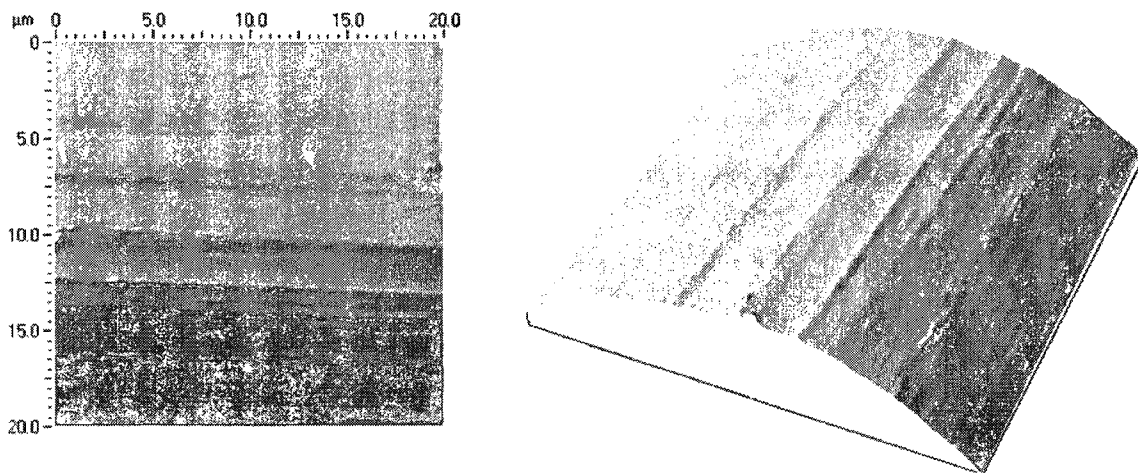
Figure 5.6: A) Surface topography of a clean PET fibre (Scan size area = $20x20\,\mu m^2$), B) position of AFM tip on the PET fibre during surface imaging of the PET fibre using AFM.
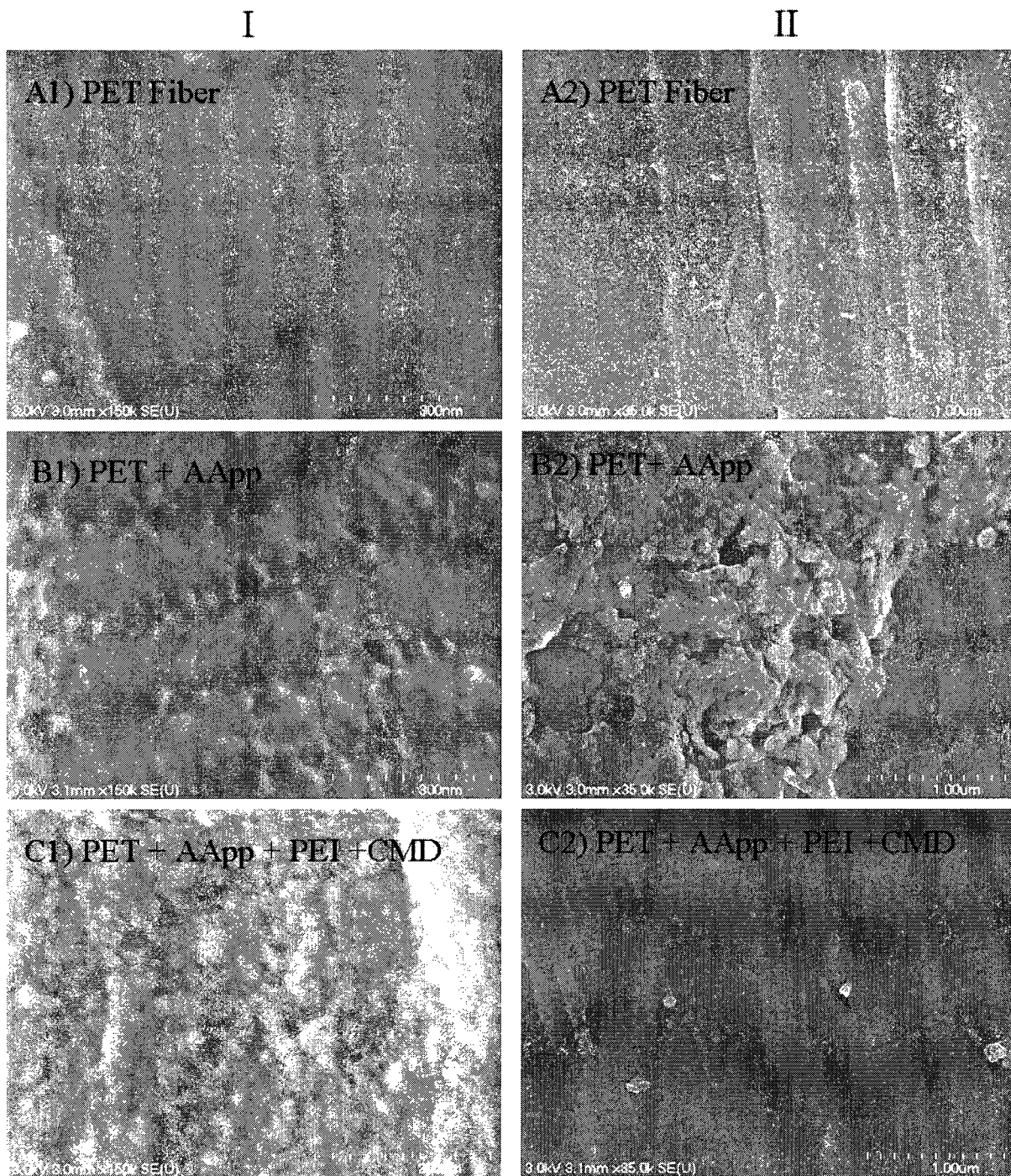
Figure 5.7: SEM images of CMD coated PET fibres via AApp: **I)** Magnification: x150 k, **II)** Magnification: x35k. These analyses were performed for samples from two experiments at different magnifications and over at least two areas of the sample.
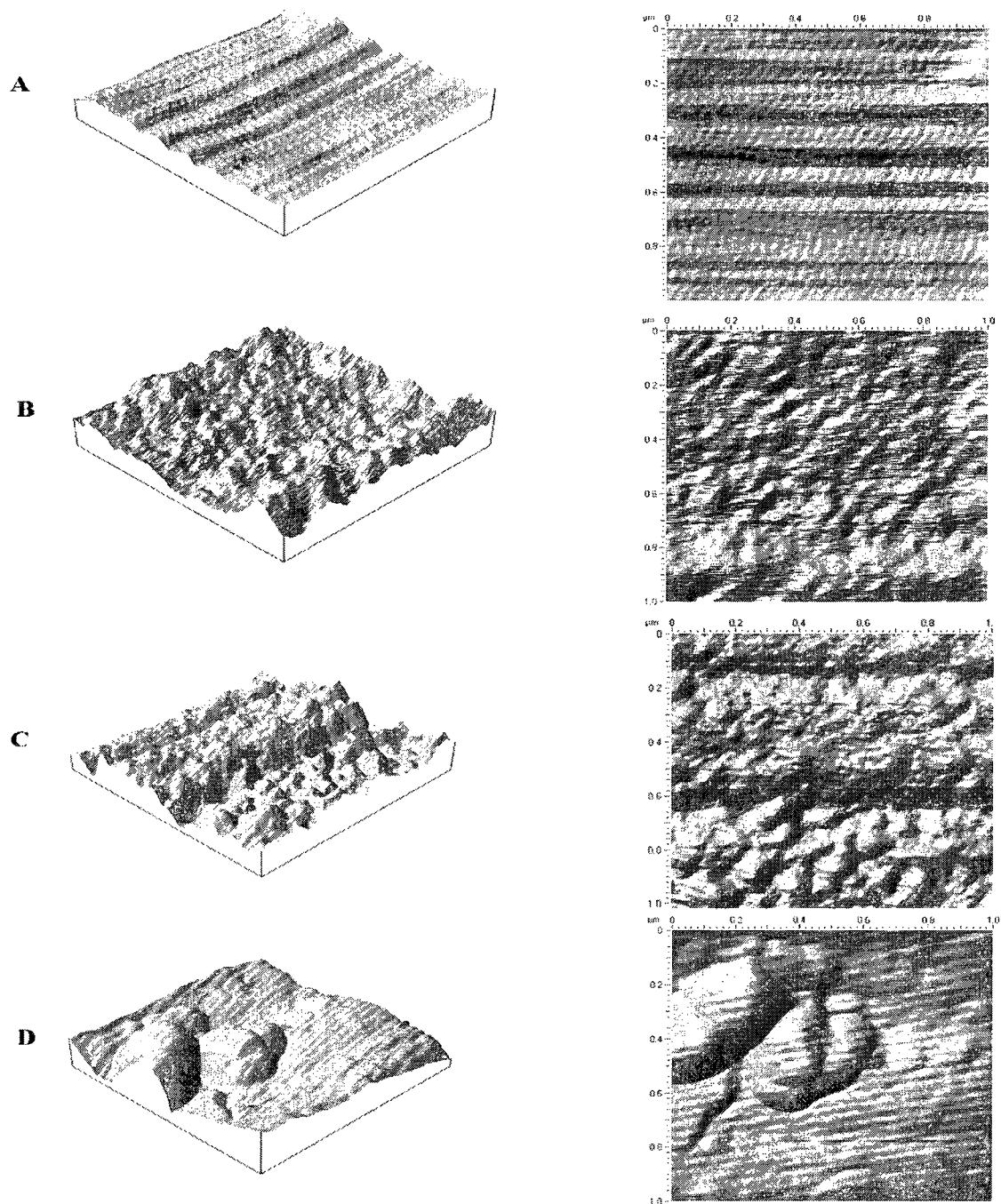
Figure 5.8:   AFM images of CMD coated PET fibres via AApp. A) PET fibre, B) PET fibre
+ AApp, C) PET fibre + AApp + PEI,   D) PET fibre + AApp + PEI + CMD
(Scan size area = 1x1 μm^2). These analyses were performed at least twice.

121
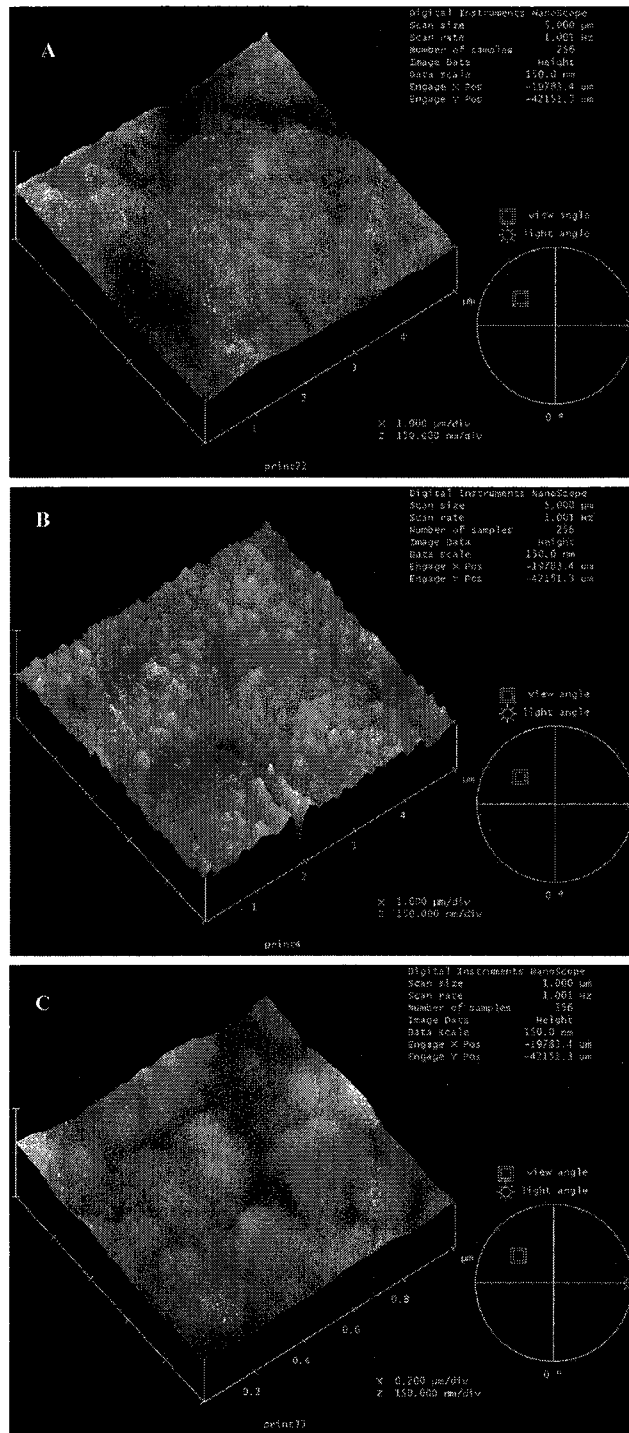
Figure 5.9: AFM images of AApp coated FEP film: A) Uncoated FEP film (Scan size area = 5x5 μm^2), B) FEP film + AApp (Scan size area = 5x5 μm^2), C) FEP film + AApp (Scan size area = 1x1 μm^2). These analyses were performed once.

5.3.2. CMD immobilization via HApp

SEM analysis showed that surfaces became smoother after the HApp coating, because the surface fine features had disappeared. The surface texture on the HApp coated PET fibre had changed, following the HApp deposition, towards decreasing the surface roughness (see Fig. 5.10). This change can be seen more clearly on the HApp-coated FEP film, on which the fine surface features have almost disappeared (Fig. 5.10). Conversely, AFM analysis did not show any difference between the HApp coated surfaces and the unncoated surfaces (Fig. 5.11). This observation suggests that the HApp coating produces a very smooth thin film on the surface, which follows the features already present. Some particles observed in the AFM images of the PET fibre shown in Figure 5.11B are probably air born dusts, electrostatically attracted to the PET fibres. The surface roughness is likely increased after the CMD coating (Fig. 5.10), while the nanometric scale features present are more clearly displayed on the FEP film, demonstrating that the CMD coating increases the roughness of the surfaces.

Taken together, the AApp increased the surface roughness at the nanometric scale, whereas HApp decreased it. CMD coating, via both AApp and Happ, generated a uniform rough coating on the surface which was particularly effective when the CMD was grafted, via AApp and PEI. Therefore these observations act as additional proof of successful performance of the different coatings employed in this study.
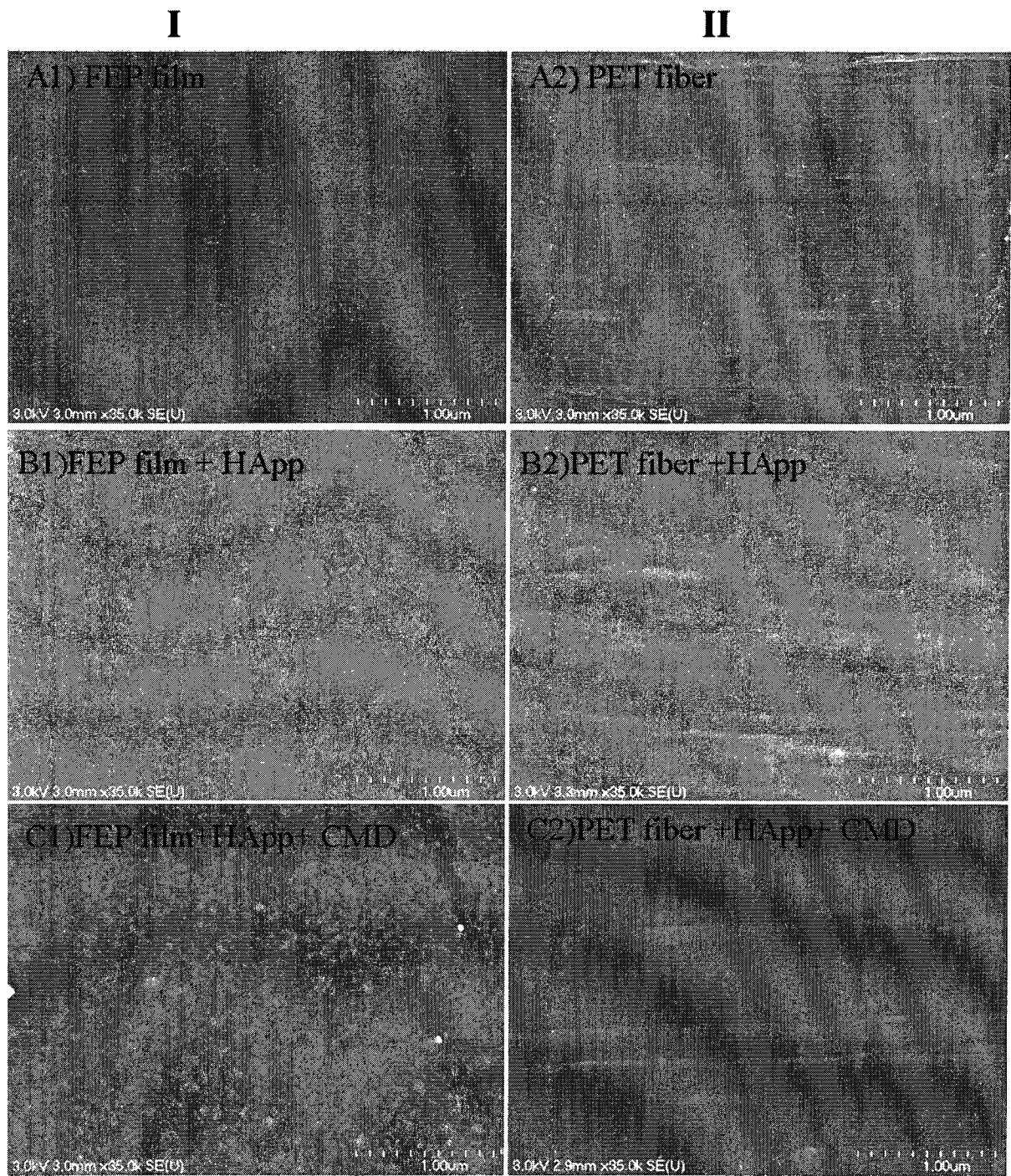
Figure 5.10: SEM images of CMD coated FEP film (left) and PET fibres (right) via HApp. These analyses were performed for 1 experiment (n=1) for each sample in different magnifications and at least 2 areas of the sample were analyzed. Magnification is at 35,000

A) PET Fiber
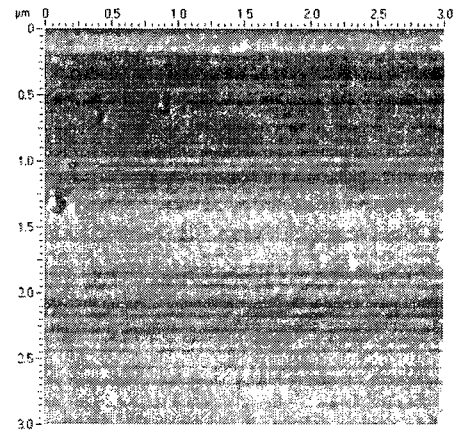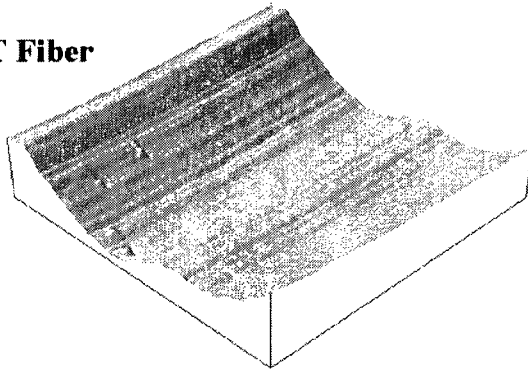
B) PET Fiber +HApp
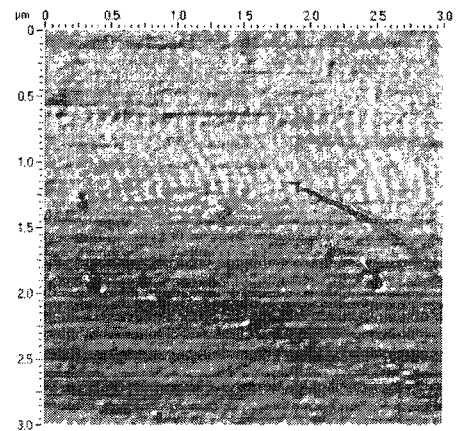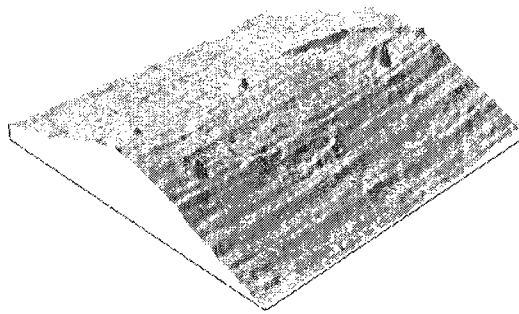
Figure 5.11: AFM images of HApp coated PET fibres. A) Uncoated clean PET, B) HApp coated PET fibre. Scan size area = 3x3 μm^2. This analysis was performed at least twice in different scan size areas.

5.4. Conclusion

The characterization of the surface chemistry and the topography shows that the multilayer fabrication steps are effective. XPS analyses revealed that, by using the RFGD method, HApp and AApp can be deposited on various substrates, such as polymer fibre, porous and non-porous polymeric film and borosilicate flat surface, with distinct rigidity and shape. Moreover, the XPS characterization of PTFE and borosilicate, which have specific elemental signals (fluorine and silicon respectively), clearly demonstrated the formation of a uniform film, thicker than 10 nm, on both the HApp and AApp surface coatings. Such coatings can offer two applications i) altering the physicochemical properties of the surface to increase both cell adhesion and growth; and ii) introducing new functional groups (i.e. amine and aldehyde) to covalently graft the desired secondary layer (e.g. CMD).

Covalent grafting of CMD, using water-soluble carbodiimide chemistry, onto the surface amine groups available on the HApp and AApp + PEI coated surfaces was successful, as demonstrated by the XPS analysis. It was also found that CMD, with a molecular weight of 70 kDa and a CMD solution concentration of 2 mg/ml, generates a more uniform and thicker film than the same molecular weight CMD at a solution concentration of 1 mg/ml, in immobilizing via both the HApp and AApp. The XPS C1s spectrum of the CMD showed that the CMD graft layer was thicker when the CMDs were grafted by means of the PEI spacer layer onto the Aapp, in comparison with the direct grafting onto the HApp surface. This layer will also play two roles i) being non-fouling towards proteins and cells, and ii) introducing COOH functional groups in order to covalently immobilize biological molecules, particularly those producing selective cell adhesion (e.g. GRGDS).

126

XPS analysis has shown the successful performance of covalent immobilization of RGD onto CMD coated surface by demonstrating an increase in the N/C atomic ratio on RGD immobilized surface, in comparison with the CMD coated surface. In addition, this technique can be applied to produce surfaces that provide an integrin-stimulated cell adhesion, or more specifically, selective cell adhesion.

The existence of thin films obtained via plasma deposition and subsequent CMD immobilization on the surfaces, were visualized by means of SEM and AFM, which produced topographic maps of the analyzed surfaces and provided qualitative results of the different coatings. The AApp plasma-deposited and CMD-coated surfaces exhibited the roughest surfaces, among all others.

Therefore, these multistep surface fabrication techniques can be applied to produce biomaterials with multifunctional surfaces that can have important applications in tissue engineering, e.g., as a scaffolding material for multicellular tissue regeneration.

Chapter 6

Results and discussion II: *In vitro* evaluation of surface modified substrates toward EC behaviour in 2D cell culture system.

6.1. Overview

The behaviours of different cell types on polymeric materials depend largely on the chemistry and topography of the surface at the cell-biomaterial interface (CURTIS and RIEHLE 2001; WONG, et al. 2004). Surface topography, as well as fibre curvature, is of particular interest in modulating the patterning of cells in 3D environments (CURTIS and RIEHLE 2001). However, on making contact with biological media, containing various proteins, protein adsorption processes occur on the surfaces of synthetic biomaterials, forming a heterogeneous biofilm in which the type of proteins and their conformations may vary depending on the underlaying surface properties (MCLEAN, et al. 2000b). One possible solution to prevent such early stage, nonspecific protein adsorption onto biomaterial surfaces, and for the goal of achieving controlled and predictable biological responses, is that a biomaterial surface can be pre-coated with a polymeric material that can exhibit predictable biological responses (HERSEL, et al. 2003). To this aim, to encourage and control directional biological responses, GRGDS peptides were immobilized via plasma polymer and CMD interlayer onto the surface of 100-μm diameter PET and ePTFE fibres (monofilaments). HUVECs were used to evaluate *in vitro* the biological responses towards each of multilayer step surface coating (i.e. plasma polymer, CMD and RGD peptide). HUVECs were seeded and grown on the fibres to examine the cell behaviour (i.e. adhesion, spreading and orientation). In

addition, flat surfaces were coated in the same way as fibres and used for detailed characterization of cell behaviour (i.e. formation of FAs and stress fibers). Phase contrast microscopy, epifluorescence microscopy and confocal microscopy were used to visualize cells seeded on the different surfaces.

In the present chapter, the results obtained from the testing of HApp- and AApp- coated substrates (i.e. Borosilicate glass, PET and ePTFE fibres) towards HUVECs are first presented and then discussed. These coatings promote cell adhesion, maintenance and stress fibre and FA formation. Secondly, the cell response to CMD coating, via both HApp and AApp on the same substrates, is presented. The results showed that, by using either HApp or AApp interlayer, CMD-coated substrates dramatically reduced cell adhesion. Thirdly, the response of HUVECs to the GRGDS-coated substrates, via plasma and CMD interlayers on the different substrates, demonstrate that covalently immobilized RGD via HApp and CMD interlayers promoted cell adhesion and spreading. More specifically, cell adhesion was enhanced as GRGDS solution concentration increased over a range of 0.1-1 mg/ml. The strong spots of vinculin (typical of FAs) and well-defined stress fibers were observed by epifluorescence microscopic visualization of cells on RGD-coated substrates. Finally the effect of surface topography such as fibre curvature and surface roughness have been discussed, suggesting that fibre curvature (with a 100-μm diameter) promots cell orientation along the fibre axis, in comparison with the flat substrates.

6.2. *In vitro* evaluation of biomaterials

Every newly fabricated biomaterial for the use in tissue engineering needs to be evaluated with respect to their biological interactions with the target cells, using cell cultures prior to

their application in tissue engineering. The testing of biomaterials towards the ECs responses can be a valuable approach, not only for cytotoxicity testing of these materials (KIRKPATRICK, et al. 1999), but also within the concept of developing new biomaterials to support tissue engineered functional tissues (KIRKPATRICK, et al. 1999). For this purpose, the investigation of the EC-biomaterial interactions is of interest in the biomaterial field. For these reasons, in this thesis, the surface modified materials have been tested towards their HUVEC response *in vitro*. For the biomaterials that will be applied as a substrate for anchorage-dependent cells in particular ECs, the *in vitro* studies include investigations of cell attachment, cell spreading, cytoskeletal reorganization and formation of FAs.

For anchorage-dependent cells (e.g. EC), cell adhesive events stimulate several intracellular signaling pathways that control cell functions. For instance, EC adhesion to ECM and spreading in an appropriate cellular shape is important for EC growth, differentiation, and survival, as shown on poly (2-hydroxyethyl methacrylate)-coated plastic (FOLKMAN and MOSCONA 1978) and FN-coated substrates (INGBER 1990).

The basic process of integrin-stimulated cell adhesion involves four different overlapping phases (Fig. 6.1): 1) contact phase: the cell makes contact with the surface and forms some ligand bindings with the surface, 2) adhesion phase: the cell plasma membrane spreads over the substrate, 3) spreading phase: actin organizes into stress fibers, and 4) FA formation: FAs are formed, resulting in the linking of the ECM to the actin filaments. These events have been mainly observed with anchorage-dependent cells seeded on either plastic plates or on ECM-grafted surfaces for cell cultures (HERSEL, et al. 2003).
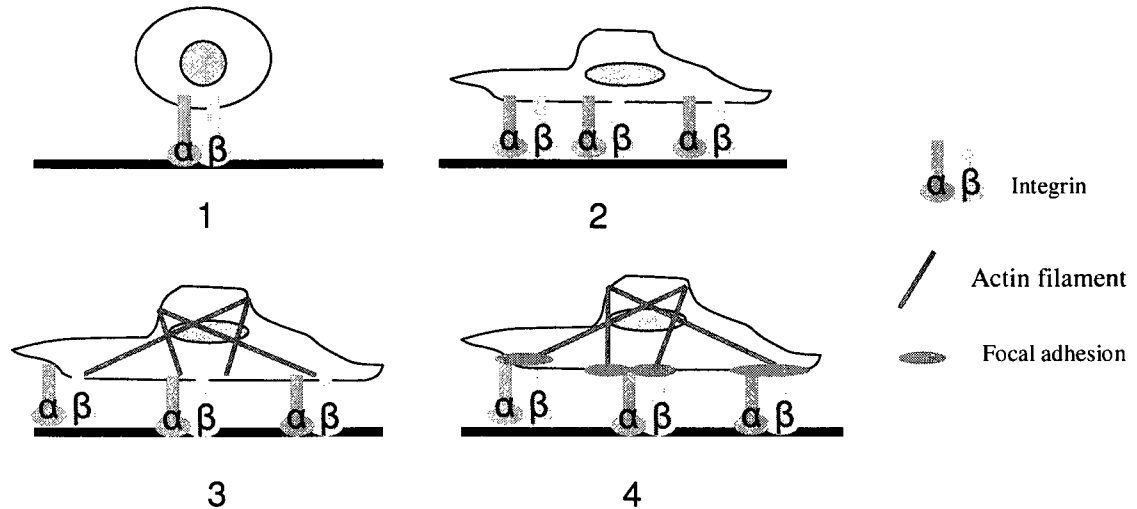
Figure 6.1: The basic process of integrin-mediated cell adhesion comprises four different overlapping events: 1) cell attachment, 2) cell spreading, 3) actin filament organization, and 4) focal adhesion formation.

6.3. The effect of surface chemistry and biochemistry on EC response

6.3.1. HApp and AApp coated surfaces

HApp (bearing amine) or AApp (bearing aldehyde groups), as a thin polymeric, interfacial layer, was deposited onto the surface of borosilicate glass surfaces, 100-μm diameter PET fibres and 200-μm ePTFE fibres by RFGD deposition (see Chapter 4, sections 4.2.5 and 4.2.6). HUVECs were seeded on surface coated materials to investigate cell behavior (i.e. adhesion, spreading and cytoskeleton organization) (see Chapter 4, sections 4.3.2-6). EC functions in terms of cell adhesion and maintenance (for a cell culture period of 3-4 days) were tested on both polymer fibres and flat surfaces coated by HApp and AApp. However, because of partial opacity of polymer fibres, actin filaments and FA formation were studied on both HApp- and AApp-coated borosilicate glass surfaces (see Chapter 4, section 4.3.6). Interestingly, it was found that both HApp and AApp coatings enhanced HUVECs adhesion,

maintenance, actin filament and FA formation which, to my knowledge, have not been investigated in such detail before.

Cell adhesion and growth

EC adhesions assay were first performed on HApp- and AApp-coated borosilicate glass surfaces because fibres were not transparent. HUVECs were seeded at a density of 1×10^4 cells/cm^2 on glass substrates. Samples were kept in culture for 4 days. Images of cells were recorded every day using phase contrast microscopy. Both HApp- and AApp-coatings supported cell adhesion by 2 hrs and reached sub-confluence by 72 hrs (see Fig. 6.2). Cell adhesion promotion and maintenance followed the pattern AApp > HApp > Glass (Fig 6.2) by day 4. Whereas, as shown in rows 3 and 5 of figure 6.2, on HApp + CMD- and AApp + PEI + CMD-coated glass surfaces, respectively, in the same cell culture period no cell adhesion was observed.
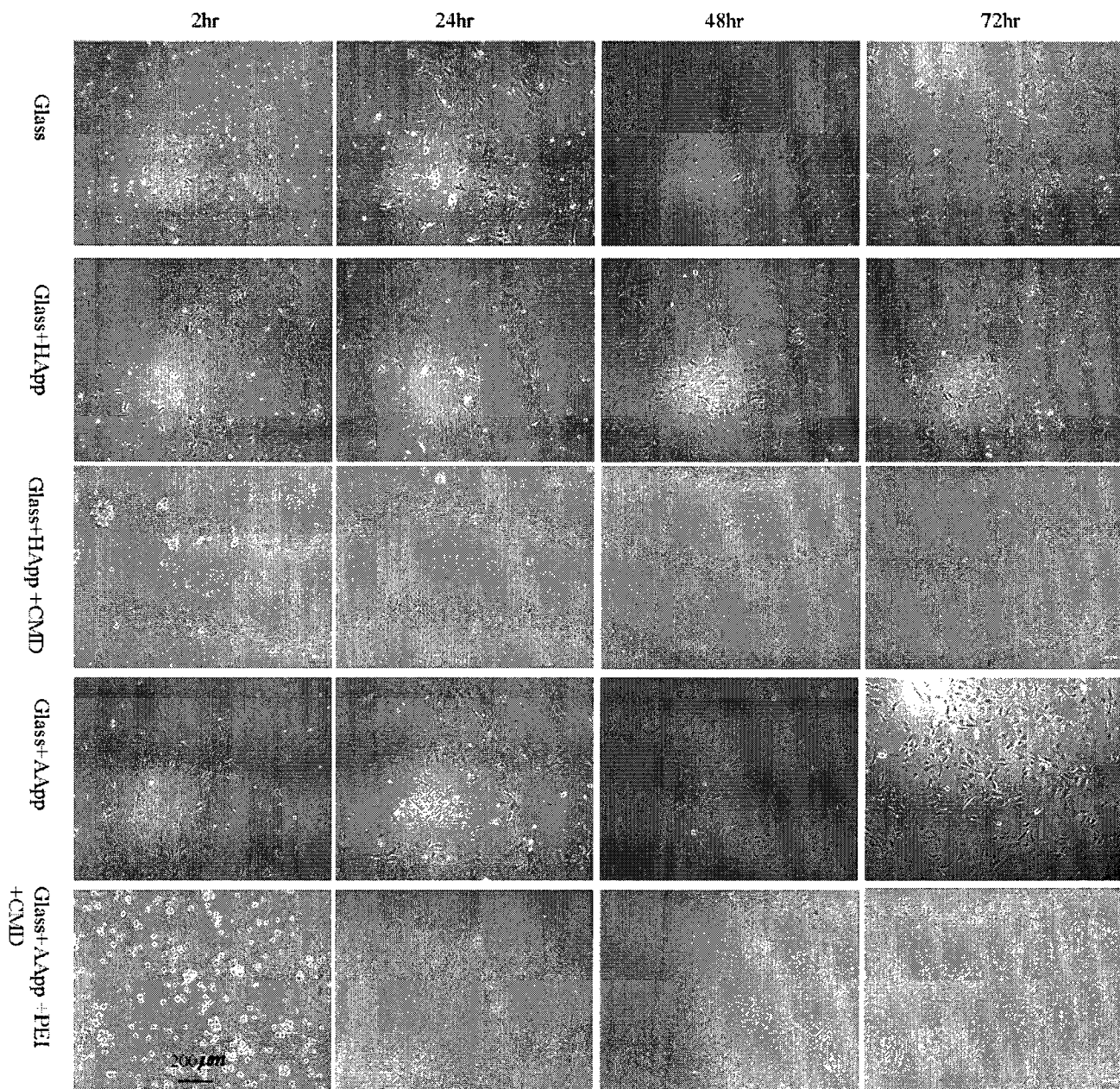
Figure 6.2: Cell adhesion on AApp-, HApp- and CMD-coated borosilicate glass surfaces (4 days following cell seeding), the pictures represent at least 2 experiments with triplicate samples.

In order to quantify the cell adhesion on HApp-, AApp- and CMD-coated borosilicate glass after a 4-day cell culture period, the numbers of cell nuclei (stained by SYTOX Green) that corresponded to the number of attached cells per mm^2 were counted (on the pictures

obtained with X4 or X10 objectives); using SigmaScan Pro5 Software. The comparison between groups were performed with ANOVA (using SigmaStat software), $P \leq 0.05$ was considered statistically significant. The values were presented as means $\pm$ standard deviations (Fig. 6.3). AApp-coated surfaces significantly promoted the cell adhesion and growth (when compared to untreated glass surface at $P \leq 0.05$). As expected, cell adhesion was significantly reduced on CMD-coated surfaces. Since the cell seeding density on the untreated and treated glass surfaces was 100 cells/ mm^2, growth of cells was evident during the 4-day culture period on specific surfaces following the pattern AApp > HApp > Glass (Fig 6.3).
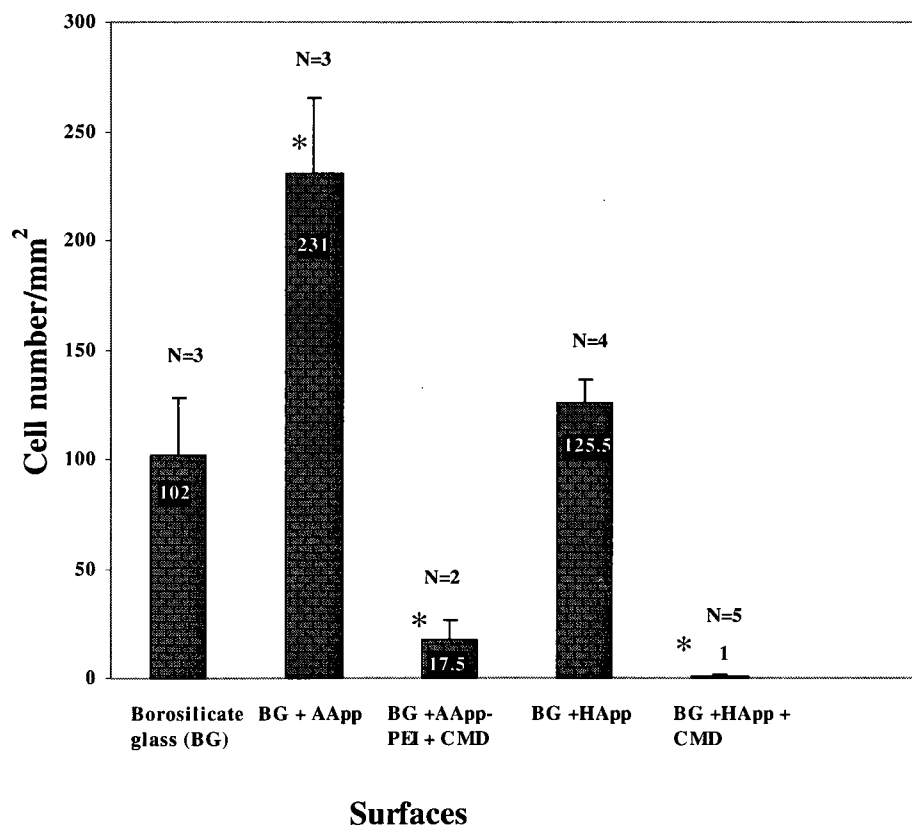
Surfaces

Figure 6.3: Cell number/mm^2 on AApp-, HApp- and CMD-coated borosilicate glass surfaces (4 days following cell seeding). Error bars represent standard deviations. N represents the number of samples (i.e. pictures obtained by using X4 or X10 objectives) from at least two separated experiments. * indicates the values significantly different from control (untreated borosilicate glass) by ANOVA at p $\leq$ 0.05.

134

In a second step, HUVECs were seeded onto PET and ePTFE fibres, according to the procedure explained in Chapter 4 (section 4.3.2). After cell seeding, the holders having the fibres were kept in the same culture plate for 4 days. Cell nuclei were stained with SYTOX Green and samples were visualized under epifluorecence microscope (Ex = 488 nm; Em = 530 nm) [website ref.6]. Adhesion of HUVECs to HApp-coated ePTFE fibres was evident in comparison with the uncoated fibres (Fig. 6.4). Similarly, more cells were observed on the two plasma-treated (i.e. HApp and AApp) PET fibres compared to the uncoated PET fibres (Fig. 6.6).

Quantitative analysis of cell adhesion was performed on ePTFE fibres with different coatings and the results expressed as relative cell adhesion values. The numbers of cell nuclei (stained by SYTOX Green), corresponding to the number of adherent cells, per fibre length were counted, following a 4 day culture period. The comparison of groups were performed by using ANOVA, $P \leq 0.05$ was considered statistically significant. The data were presented as relative cell attachment (Fig. 6.5). The relative cell adhesion was calculated by taking ratios of the average numbers of adherent cells on untreated PTFE fiber, HApp-, CMD-, and peptide-grafted fibres, to the average number of adherent cells found on untreated PTFE fibres. Similarly, the relative standard deviations (SDs) were calculated by taking the ratio of the SDs of attached cells on untreated, HApp-, CMD-, and peptide-grafted fibres, to the average number of attached cells found on untreated PTFE fibres (control). As expected, in comparison to untreated fibres, HApp- and RGD-coated fibres significantly promoted cell adhesion ($P \leq 0.05$) (Fig. 6.5).
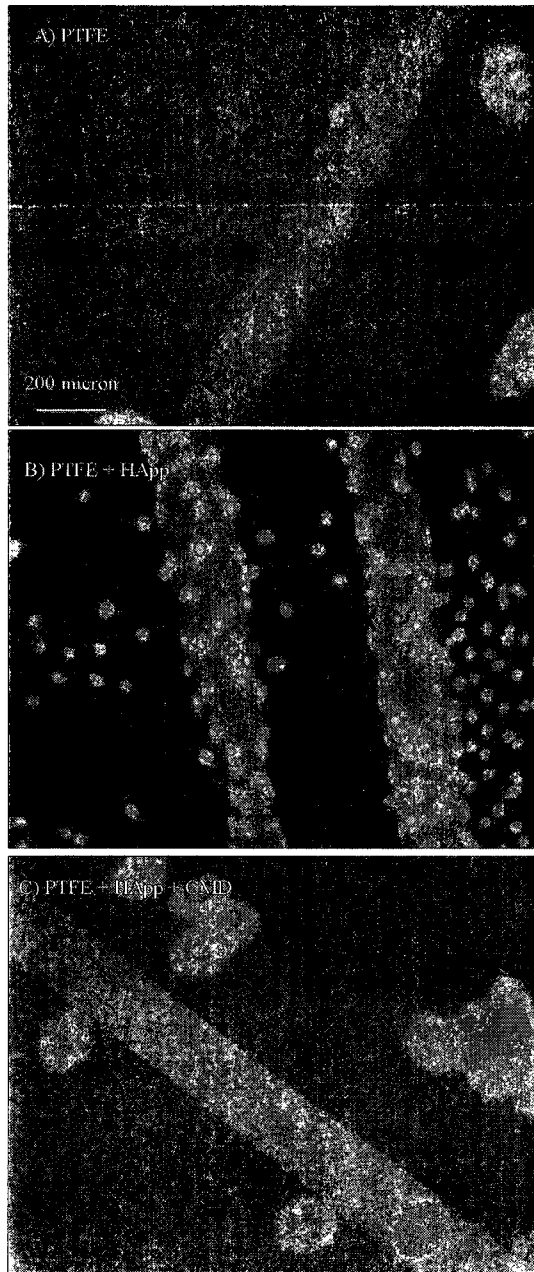
Figure 6.4: Cell adhesion on HApp- and CMD- coated ePTFE fibres (4 days following cell seeding); the pictures represent at least 2 experiments with duplicate samples. HUVECs were stained for nuclei with SYTOX Green Nucleic Acid Stain. This figure has been previously published (HADJIZADEH and VERMETTE 2007).
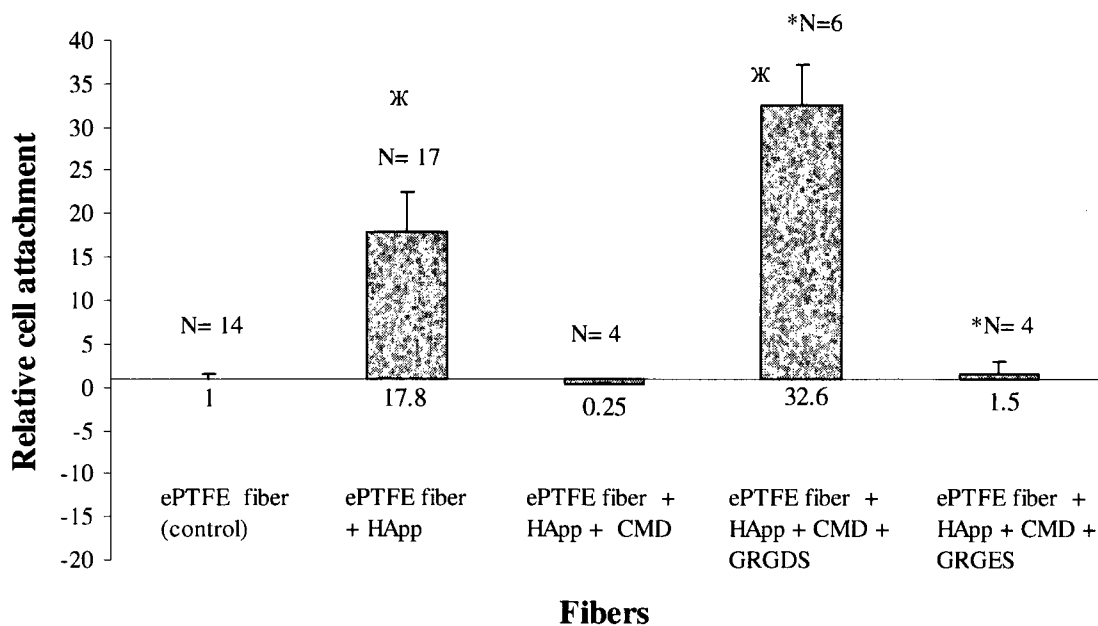
Figure 6.5: EC adhesion (4 days following cell seeding) on cleaned, untreated ePTFE fibres and surface coated ePTFE fibres. The relative cell attachment was calculated as the ratio of the average cell number on surface coated ePTFE fibres to that of uncoated ePTFE fibres. Cleaned, untreated PTFE fibres were set at 1 (control). In these experiments, CMD at 70kDa, a carboxylation degree of 1:2, and 2 mg/ml CMD solution concentration were used. The concentrations of GRGDS and GRGES in solution were both set at 0.5 mg/ml. N indicates the number of fibres from at least 2 separate experiments, except *N from one experiment. Error bars represent standard deviations. ж indicates the values significantly different from control (untreated ePTFE) by ANOVA at p $\leq$ 0.05.

As can be observed from figures 6.6A and 6.7, the adhesion of HUVECs on un-treated PET polymer fibre is low, and even on un-treated ePTFE polymer fibres almost impossible (6.4A and 6.5), this is due to their hydrophobic nature in surface. This inability towards cell adhesion makes it possible to observe the cell adhesion promotion generated due to surface modification. Therefore, the results from the cell adhesion experiments, over a 4 day cell culture period, has demonstrated that HApp and AApp treatments could be used to modify the PET and ePTFE surfaces to support the HUVEC attachment
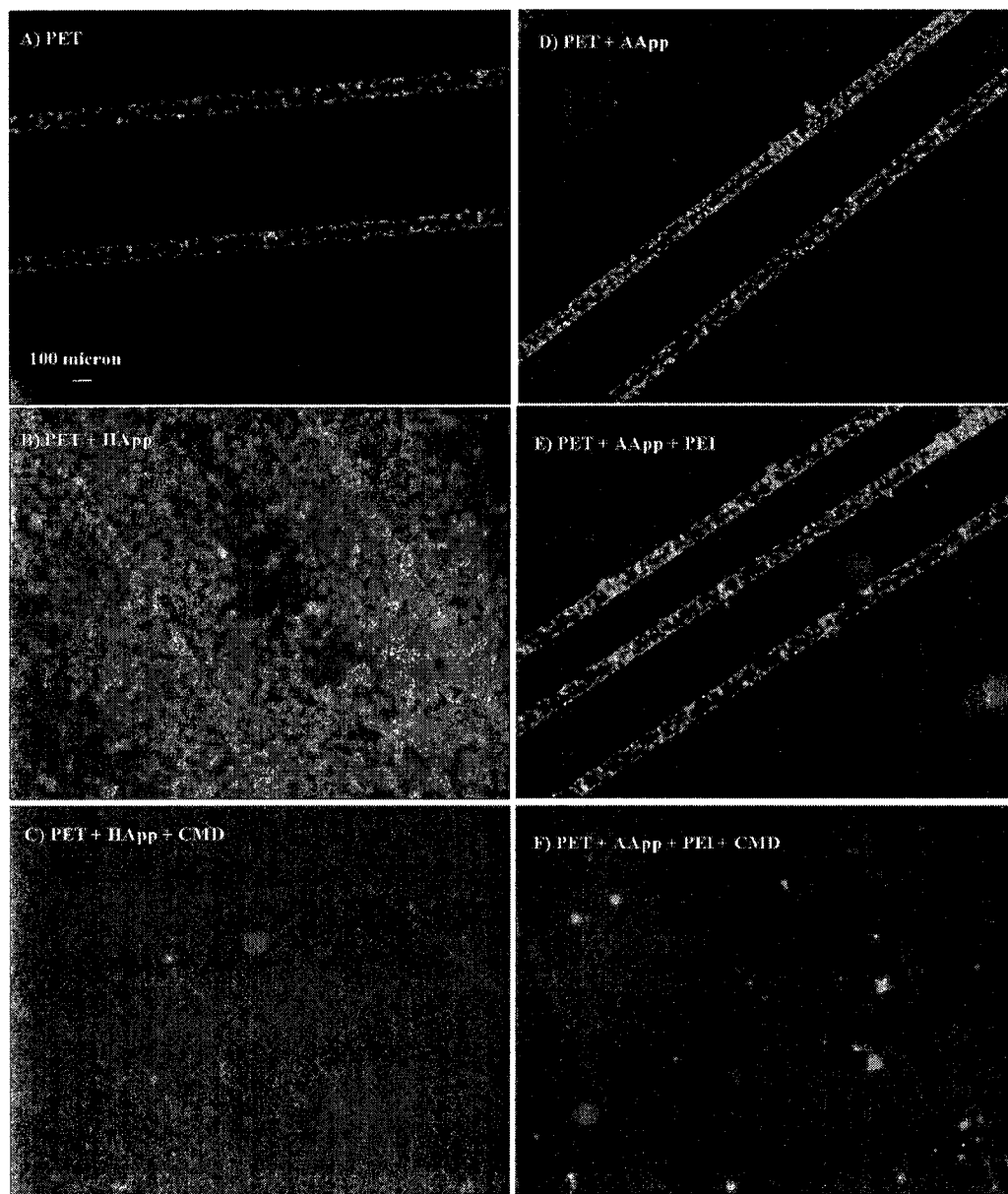
Figure 6.6: Cell adhesion on HApp- and AApp- and CMD- coated PET fibres (4 days
following cell seeding); the pictures represent at least 2 experiments with
duplicate samples. HUVECs were stained for nuclei with SYTOX Green Nucleic
Acid Stain.

Similarly, cell adhesion was evaluated on PET fibres with different coatings produced via

AApp and the results expressed as relative cell adhesion in the same way as previously

explained (in above paragraph), for PTFE fibre which was coated via HApp. The relative cell

adhesion was defined as the ratio of the cell number on surface coated PET fibres to that of uncoated PET fibres (as control). The numbers of cell nuclei, stained by SYTOX Green and corresponding to the number of adherent cells per fibre length, were counted, following a 4 days culture period. Significant differences were compared with untreated fibre at $p \le 0.05$. The AApp-PEI-CMD-coated fibres showed significantly less cells ($P \le 0.05$) adhering than untreated fibres. Cell adhesion promotions were not significant on AApp- and AApp-PEI-coated fibers (when compared to untreated PET fibres at $p \le 0.05$). This may be due to ability of PET polymer to adsorb serum-born ptoteins in culture environment, resulting in some cell uptake in early cell culture.
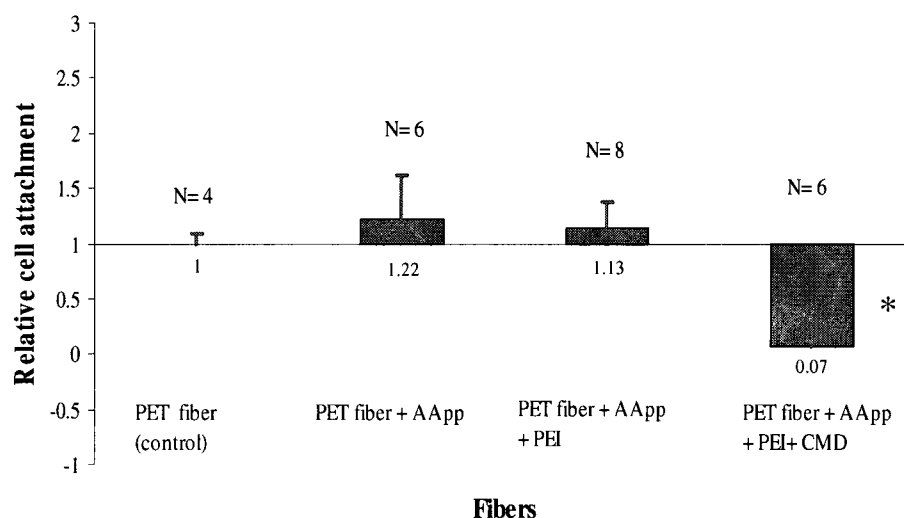
Figure 6.7: EC adhesion (4 days following cell seeding) on cleaned, untreated and treated-PET fibres, 70kDa CMD, carboxylation degree of 1:2, and 2 mg/ml CMD solution concentration were used in these experiments. The relative cell attachment was calculated as the ratio of the average cell number on surface coated PET fibres to that of uncoated PET fibre. Cleaned, untreated PET fibres were set at 1 (control). N indicates the number of fibres from at least two separated experiments. Error bars represent standard deviations. * indicates the values significantly different from control (untreated PET fibres) by ANOVA at $p \le 0.05$.

Formation of stress fibers and focal adhesion (FA)

The formation and distribution of both actin stress fibers and FAs in HUVECs in contact with plasma polymers derived from acetaldehyde and heptylamine were examined under epifluorescence microscopy. Under those conditions, the organization of cytoskeletal fibers and the presence of strong spots of vinculin (representing FA formation) were observed, characteristic of the appropriate attachments to the substrate (Fig. 6.8). Thus, these HApp- and AApp-treated substrates have the ability to support HUVECs at all of the 4 steps of strong cell adhesion (i.e. cell attachment, cell spreading, stress fiber organization, and FA formation).

Cell functions including cell adhesion and spreading are controlled by the cell cytoskeleton (a dynamic network of protein filaments) (SANBORN, et al. 2002). Since ECs are anchorage dependent cells, they adhere to the ECM proteins or a substrate at their FAs, also known as focal contacts (SANBORN, et al. 2002). FAs are specialized sites where cell cytoskeleton is linked to the ECM by means of integrin receptors (Fig. 6.9). These points are composed of integrin clusters, cytoskeletal proteins (e.g. talin, vinculin, and a-actinin) and other signaling molecules (SASTRY and BURIDGE 2000). FAs play two important roles in cellular functions: (i) to transfer cellular forces to the ECM matrix at the adhesion points, resulting in the maintaining of strong attachments to the ECM (ii) to act as signal transducer center transmitting extra- and intra-cellular signals to regulate cell functions, including growth, survival, and gene expression (SASTRY and BURIDGE 2000).The study of FAs makes it possible to provide information on cell-matrix interactions. FAs gradually form between 1 and 2 hr after cell contact with an ECM component containing surface. First focal complex forms, as a cell spreads (at periphery) or migrates (at leading edge). Then, focal complex mature into FAs when cells establish their strong attachment to substrate and tensions

140

are transferred to these adhesion points (SASTRY and BURIDGE 2000). Taken together, i.e.

the above discussion and the result obtained by examining the EC formation of FAs and stress

fibers on HApp and AApp, it can be suggested that these two plasma polymer coatings

promote initial adsorption of protein derived from biological media with subsequent strong EC

adhesion and spreading.
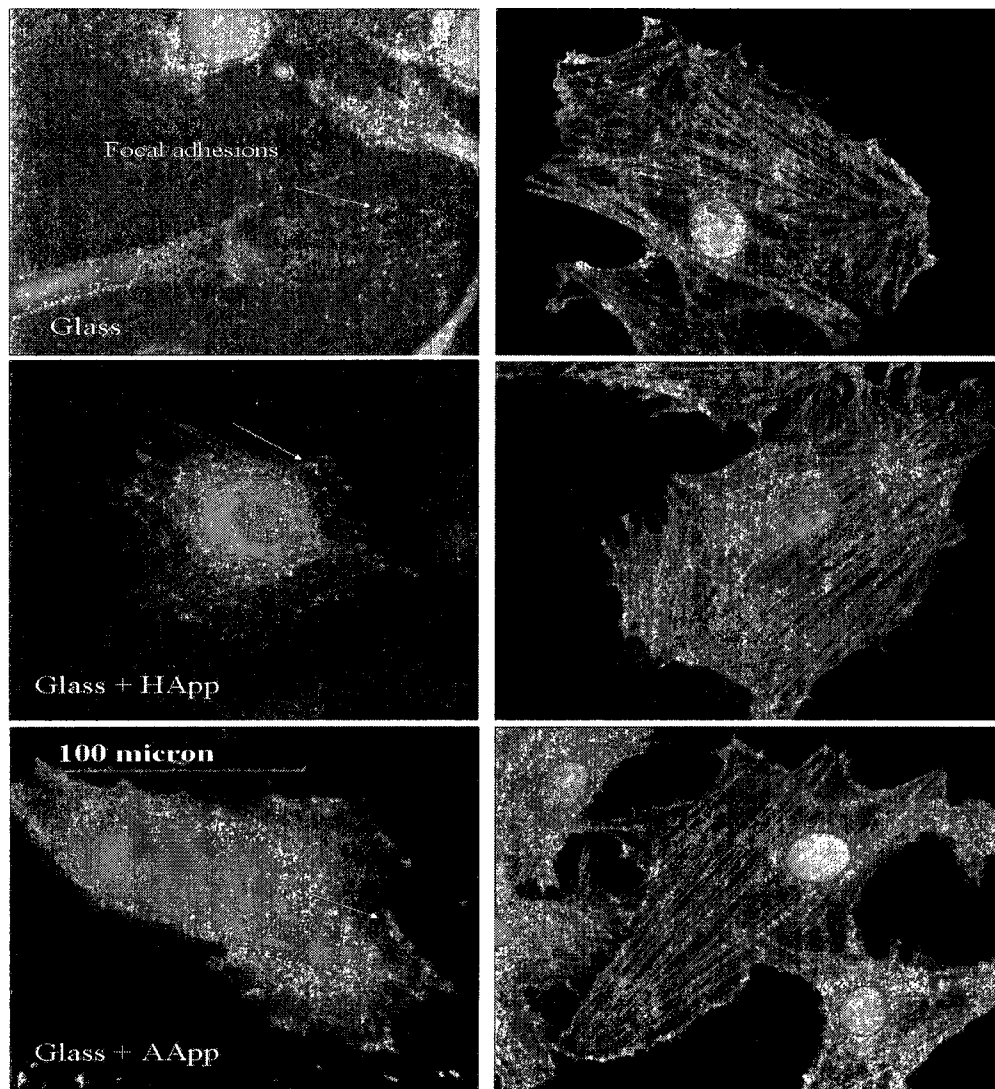
Figure 6.8: Images obtained by epifluorescence microscopy of the HUVECs stained for actin filaments with TRITC-phalloidin (red, right) and nuclei with SYTOX Green Nucleic Acid Stain (green, right); vinculin (primary antibody (Monoclonal Anti-Vinculin) and secondary antibody (Anti-Mouse IgG)) (green, left) and nuclei with Hoechst (blue, left) on borosilicate glass. The pictures represent at least 2 experiments with triplicate samples.
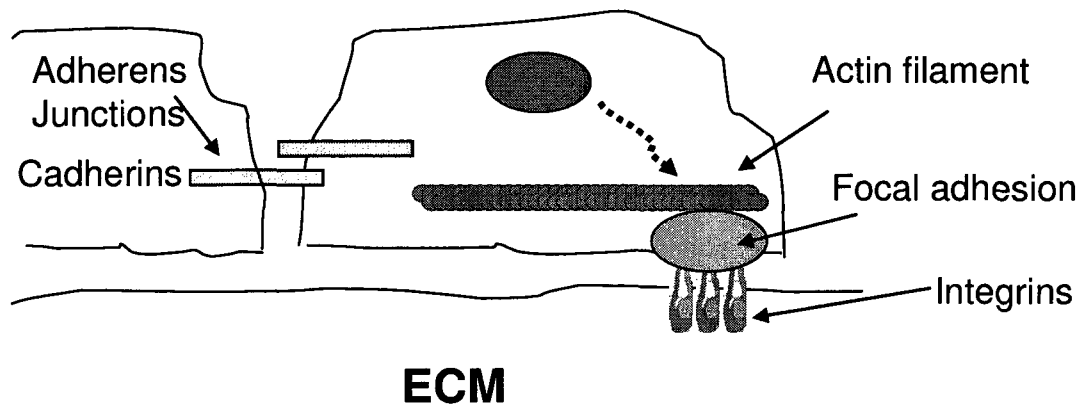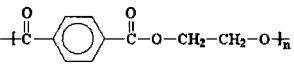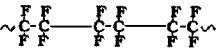
Figure 6.9: In focal adhesion points, ECM is linked to actin filaments via integrin receptors (adapted from SASTRY and BURIDGE 2000).

It has been found that many cell types tend to attach and grow on various plasma polymer deposited surfaces or on plasma-treated surfaces. Cell adhesion on plasma modified surfaces *in vitro* shows that cell-adhesive proteins can be adsorbed onto these surfaces without influential conformational changes (SIOW, et al. 2006). Studies on the cell adhesion ability of plasma-coated surfaces have focused on oxygen- and nitrogen- containing surfaces, may be due to the success of some commercial products used as tissue culture labware, such as plasma-oxidized polystyrene (PS) or nitrogen-containing Primaria tissue culture ware. However, it is still unclear whether the presence of oxygen containing groups or the total oxygen content on the substrate surface is a key element to promote cell attachment. The same confusion exists about nitrogen containing surfaces (SIOW, et al. 2006). However, some studies have shown that some typical factors, such as chemical groups e.g. amide (SIOW, et al. 2006) and carbonyl (ERTEL, et al. 1991), or even adsorption of the VN, from the serum components of the culture medium on oxygen containing surfaces, may promote cell adhesion (STEELE, et al. 1993; and 1995).

In this study, cell attachment observation, in conjunction with XPS analysis, suggests that the increase in nitrogen concentration also increased HUVEC cell adhesion. This suggestion is supported by observation that HUVEC adhesion is enhanced on HApp-coated ePTFE which dramatically increased cell adhesion (Fig. 6.4 and 6.5) when N% increased from 0% for uncoated ePTFE to a 6.5% for HApp-coated ePTFE (Table 6.1). This observation can be atributed to the presence of NH_2 groups, created by HApp or CONH groups that have been generated by post plasma oxidation. This is identical to the findings by Keselowsky et al. (2004) who investigated the effect of functional groups including NH_2 on FN adsorption and subsequent integrin mediated cell adhesion and FA formation. They showed that NH_2 surface groups mediated all of the above mentioned characteristics. The HApp coating is solid and dense; therefore the effect of interfacial steric-entropic repulsion should not be considerable. In addition, when present in buffered culture medium (pH 7.4), HApp coating should exhibit a very low density of positive surface charges (CHATELIER, et al. 1995; and 1997). Hence, protein adsorption onto the HApp layer may occur, mainly by the action of dispersion and hydrophobic forces. Therefore, it suggests that cell adhesion on HApp coated surface, in our culture study, is due to serum proteins adsorbed by dispersion and hydrophobic forces on these surfaces, and is probably due to positive surface charges produced by protonation of NH_2 groups in the buffered culture medium (pH 7.4).

Our observations also showed that in the increase in the oxygen concentration on the substrate surface can not be the sole reason to enhance adhesion of HUVECs. Borosilicate glass, having an oxygen concentration of 3.9 times greater than AApp-coated borosilicate, resulted in less cell adhesion than the AApp-coated borosilicate (Table 6.1).

Table 6.1: Chemical structures and elemental composition of surfaces and HUVECs adhesion

Surface	Elemental compositions		Chemical structure
	O%	N%	
PET	25.1	0	$\begin{array}{c}\text{O} \qquad \text{O} \\ \parallel \qquad \parallel \\ \text{+C—}\bigcirc\text{—C—O—CH}_2\text{—CH}_2\text{—O+}_n\end{array}$
ePTFE	0	0	$\sim\!\begin{array}{ccc}\text{F F} & \text{F F} & \text{F F} \\ \text{C-C} & \text{C-C} & \text{C-C} \\ \text{F F} & \text{F F} & \text{F F}\end{array}\!\sim$
Borosilicate glass (1)	63.15	0	
PET+HApp (2)	3.1	8.3	$\begin{array}{c}\text{NH}_2 \\ \mid \\ \text{CH}_3\text{(CH}_2)_3\text{CH}_2\text{CHCH}_3 \\ \textit{N}\text{-heptylamine}\end{array}$
ePTFE+HApp (3)	2	6.4	
PET+AApp (4)	19.5	0	
Borosilicate glass +AApp (5)	16.1	0	$\begin{array}{c}\text{O} \\ \parallel \\ \text{CH}_3\text{—C—H} \\ \text{Acetaldehyde}\end{array}$

Chemical bonds

NH$_2$	2,3	
COOH	PET	
OH	PET	
CONH	2,3	
CO	4, 5, PET	

HUVECs adhesion

HUVECs adhesion :	ePTFE< PET	(Fig. 6.4 and 6.5)
	PET< 2 and 4	(Fig. 6.7 and 6.11)
	ePTFE < 3	(Fig. 6.4 and 6.5)
	1< 5	(Fig. 6.2 and 6.3)

Therefore, it is possible that the type and amount of oxygen containing chemical groups manage the cell attachment. However, our observation showed that AApp coatings promoted HUVECs attachment and maintenance. These observations are supported by a few pieces of evidence reported in 2 recent publications (SIOW, et al. 2006; THISSEN, et al. 2006) in which

an aldehyde plasma supported the attachment and growth of epithelial cells to a certain extent, comparable to tissue culture PS (SIOW, et al. 2006), and that AApp coatings were able to adsorb ECM proteins, such as type I collagen (THISSEN, et al. 2006).

Thus, our findings also suggest that cell adhesion is affected by other compositions of the plasma-treated polymers or their surface structures (e.g. roughness), in addition to the presence of carbonyl or amide groups created by plasma polymer directly, or by post-plasma oxidisation indirectly.

It has been demonstrated that plasma-deposited polymeric thin films offer alternatives to enhance the performance of existing biomaterials and medical devices and for the development of new biomaterials (FAVIA, et al. 2003; SANBORN, et al. 2002). For example, in order to promote the performance of vascular prostheses, it has been suggested that these products can be seeded with the ECs of patients, isolated from their veins. However, the mateials used in vascular prostheses applications (e.g. ePTFE) are almost inert (hydrophobic surface), resulting in poor cell adhesion. Thus, some surface modifications are needed to promote ECs monolayer formation. A potential approach to this aim is to coat surfaces of substrates with materials having desired properties to promote EC adhesion and growth on the surface (KIRKPATRICK, et al. 1999). For this reason, studies have shown that plasma polymerization processes could be employed to modify substrates (e.g. PET) that support attachment and growth of cells such as ECs (HADJIZADEH, et al. 2007). There are many studies reporting application of various plasma polymerizations for biomaterial surface modifications, including PTFE (KIRKPATRICK, et al. 1999). However, to my present knowledge, there is a lack of reports investigating EC behavior on HApp and AApp plasma polymer coated surfaces. Thus, the findings of this study demonstrate the suitability of RF

HApp and AApp in inducing desirable coatings on substrates, so as to improve their ability to support the strong adhesion of ECs.

6.3.2. CMD grafted surfaces (cell resistant material)

Cell adhesion

Coating the material surface with polysaccharides is of interest in biomaterials research because of their ability to reduce surface fouling by biological molecules (particularly proteins) (MCARTHUR, et al. 2000) and cells (HADJIZADEH, et al. 2007). These coatings can prevent the adhesion of mammalian cells and also bacteria, to biomaterial surfaces (MORRA and CASSINELI 1999). Dextrans and their derivatives have been used for these purposes (LOFAS and JOHNSSON 1990; MCARTHUR, et al. 2000). Dextran has excellent ability for resisting the protein adsorption, and its multiple reactive sites can be used for the covalent grafting of biomolecules along its polymer chain (MASSIA and STARK 2001). Polysaccharides are comprised of highly hydrated hydrogel-like structure and mobile molecular chains which make them able to reject biological molecules and cells by providing steric-entropic forces. Thus, the polysaccharide molecules should be introduced in an appropriate microstructure to produce such repulsive forces more effectively (MCLEAN, et al. 2000a). For the above mentioned reasons, in this present thesis, CMD, a derivative of dextran, has been chosen as a low-fouling platform for the bioactive molecule immobilization. CMD (Fig. 2.6) is a derivative, carboxymethyl substitution, of dextran which is synthesized by the reaction of dextran with bromoacetic acid (LOFAS and JOHNSSON 1990). The effects of chemical and structural properties, generated by charge density (MCLEAN, et al. 2000b),

146

molecular weight, carboxylation degree and method of immobilization (MCLEAN, et al. 2000a), of CMD molecules, have been previously shown to play a role in the protein and cell rejection. Moreover, previously reported studies have shown that, CMD coatings, via an amine-rich polyelectrolyte interlayer (i.e. PEI), grafted onto the plasma polymer surface (i.e, AApp), generated more effective resistance towards protein adsorption and epithelial cell adhesion than the CMD coating that is directly immobilized onto the plasma polymer (i.e, HApp) (MCLEAN, et al. 2000a). In addition, a thicker CMD layer in aqueous phase solution was observed, either when the polysaccharide had a high carboxyl density (i.e. CMD 1:2) (GRIESSER, et al. 2002) or when polysaccharide was immobilized, via PEI spacer grafted onto the plasma polymer coated surface prior to polysaccharide grafting (HARTLEY, et al. 2002). Moreover, polysaccharide bearing a high density of carboxyl groups (i.e. CMD 1:2) pinned to the HApp-coated surface in many points and created a dense polysaccharide layer having loops and tails (MCARTHUR, et al. 2000).

In this thesis I use CMD coatings for two purposes: a) as a low-fouling coating and b) as a platform for biomolecule immobilization, a dense and thick coating with high density of carboxyl groups was preferable. Therefore, to achieve this aim, and based on the results obtained by others, I have tested CMDs with carboxyl substitution of 1: 2 by using two different methods of immobilization, via HApp and AApp + PEI. In addition, CMD of two different molecular weights 70 and 500 kDa, in two different CMD solution concentrations of 1 and 2 mg /ml, have been tested to determine the effect of CMD molecular weight and CMD solution concentrations on the surface coverage of the CMD coating. According to the XPS analysis the best candidate with a thicker surface coating was CMD having a molecular weight of 70 KDa and a CMD solution concentration of 2 mg/ml on AApp interlayer at the first level

and on HApp at the second level. Therefore, these two CMDs coatings were considered as optimal conditions on which the behavior of the HUVECs has been investigated.

CMD coatings on borosilicate glass surfaces, via both methods, were strongly cell resistant (Fig. 6.2 and 6.3). Two hrs after cell seeding up to 4 days of cell culture, no cell was observed neither on the CMD- coated surfaces via HApp nor on the CMD- coated surfaces, via the AApp + PEI interlayers. Similarly, CMD-coated fibres, either by means of HApp or the AApp + PEI interlayer, dramatically reduced cell attachment (Fig. 6.4, 6.5, 6.6 and 6.7). Very little difference was observed to the cell resistance efficiency of the CMDs grafted by use of two different interlayers (i.e, HApp and AApp) (Fig. 6.3, 6.5 and 6.7), and by using CMD with a carboxymethyl substitution of 1:2 and a CMD solution concentration of 2 mg/ml on different substrates surfaces (borosilicate glass, PET and PTFE fibres). This may be due to some defect caused by the manipulation process. Since HApp and PEI are cell adhesive (Fig. 6.6B and E respectively), these observations could also be interpreted as a result of incomplete CMD coverage and/or is due to the presence of a thin CMD layer on the substrates. As reported previously (MCLEAN, et al. 2000a), the CMD grafted onto the HApp and AApp layer may be seen as a "carpet pile" structure (see the schematic presentation in Fig. 6.10). The highly water soluble chains (loops and tail ends) having charged groups extend into the aqueous phase solution, spreading out away from the interface. Such a polysaccharide structure provides steric-entropic repulsive forces to reject proteins and cells from the surface. Thus, it can be concluded that the cell resistant behaviour observed on CMD-coated substrates could be mainly due to such repulsive interfacial forces (i.e. steric-entropic, hydration and electrostatic).
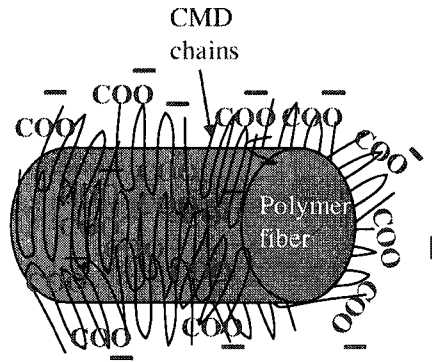
Figure 6.10: Schematic presentation of CMD chains with a "carpet pile" like structure having COO⁻ groups (red).

In conclusion, CMD immobilized by both methods results in a resistance to the adhesion of HUVECs, therefore these two strategies can be applied to providing a non-fouling surface which can serve as a platform for bimolecular immobilization to induce selective cell adhesion surfaces.

6.3.3. Biomolecule grafted surfaces (bioactive materials)

It is believed that the interaction of a cell with neighboring cells and surrounding ECM are regulated by cell adhesion receptors present on the cell membrane. Among these receptors, the integrin family plays the most important roles (HERSEL, et al. 2003). Different types of integrin receptors, composed of α and β subunits, have been shown to be present on the surface of the vascular ECs, among which $\alpha_5\beta_1$ and $\alpha_v\beta_3$ mainly mediate the EC attachment to the cell binding motifs (i.e. RGD domains) of ECM proteins (e.g. FN, VN, collagen, and fibrinogen) (PAPETTI and HERMAN 2002; HERSEL, et al. 2003). Many studies have shown that adhesion of ECs was promoted by RGD immobilization on the biomaterials surfaces (GAO, et al. 2003; KOUVROUKOGLOU, et al. 2000; MASSIA and STARK 2001). However, covalent grafting of any biomolecule, such as protein and RGD molecules, onto a

CMD coating, and its biological effectiveness towards cell behavior, have not been previously investigated.

Biomolecule immobilization via HApp and CMD interlayer

Cell adhesion

In order to ensure the performance and reproducibility of the techniques for RGD immobilization onto non-fouling CMD layer by using multilayer surface modification, this method was performed on various substrates such as flat surfaces and polymer fibres (see Chapter 4, section 4.2.2-9). Three types of bioactive molecules, such as RGD peptide, FN and gelatin, were investigated towards elucidating HUVEC behavior.

GRGDS peptide, in 3 different concentrations (0.1, 0.5 and 1 mg/ml), were immobilized via HApp and CMD interlayers onto microscope cover slips (glass) which were then seeded with HUVECs at a density of 1×10^4 cells/cm^2 (see Chapter 4 section 4.3.6) and incubated for at least 4 days. All of the surfaces supported cell adhesion except the CMD- and RGD- coated at low concentration (0.1 mg/ml) (Fig. 6.11).

In order to ensure whether the covalent immobilization of the biomolecule, via amide bond formation, onto the CMD coated surface have been successfully performed, FN were either immobilized on the same substrates, using the same strategy, or adsorbed onto uncoated microscope cover slips, considered as a control adhesion surface. Both physisorbed and covalently FN-coated surfaces showed very effective cell adhesion and reached confluence in 4 days (Fig. 6.11). Cell adhesion on those substrates demonstrated successful covalent grafting of FN onto the CMD interlayer via amide bond formation.

150

In addition to FN, gelatin was either covalently immobilized by use of the same strategy onto FEP film and PET fibre, via HApp and CMD interlayers or adsorbed onto uncoated FEP film. After cell seeding, HUVECs adhered to covalent gelatin-coated FEP film and PET fibres but not to untreated and gelatin adsorbed FEP films (Fig. 6.12). This is not surprising since FEP is hydrophobic and is almost an inert material; therefore it did not support protein or gelatin adsorption. This observation demonstrated that biomolecules can be successfully immobilized onto a CMD interlayer, via amide bond formation, which can then support cell adhesion. Moreover, mobile chains of CMD did not prevent cells from interacting with the bioactive molecules and thereby cell adhesion and maintenance on biomolecules such as RGD peptide, FN and gelatin. This observation demonstrated that the lack of cell adhesion and maintenance on the RGD (0.1 mg/ml) may be due to an insufficient number of RGD molecules present on the surface.
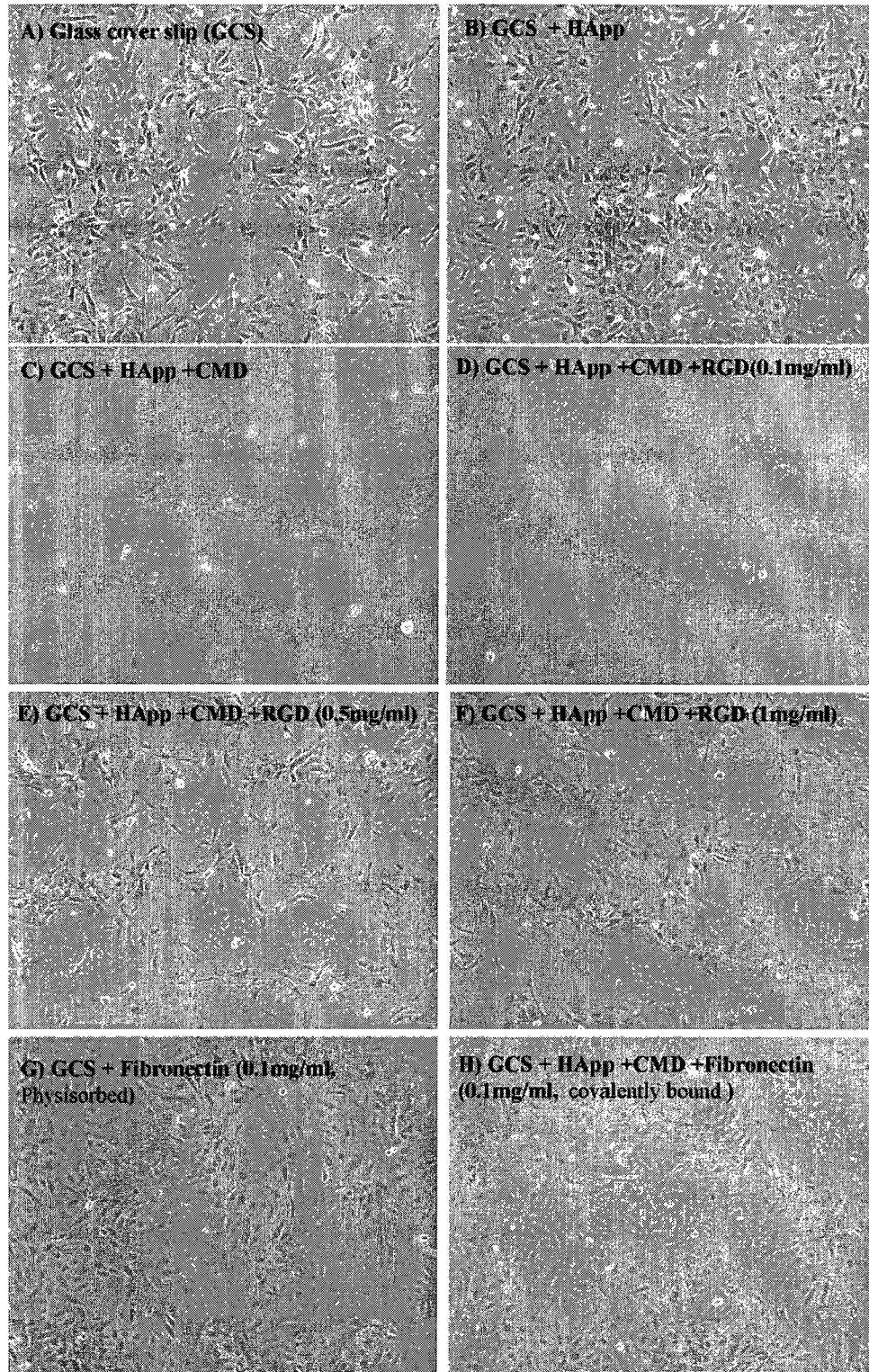
Figure 6.11: Cell adhesion and confluence (4 days following cell seeding) on glass microscope cover slip, the pictures represent one experiment with triplicate samples.
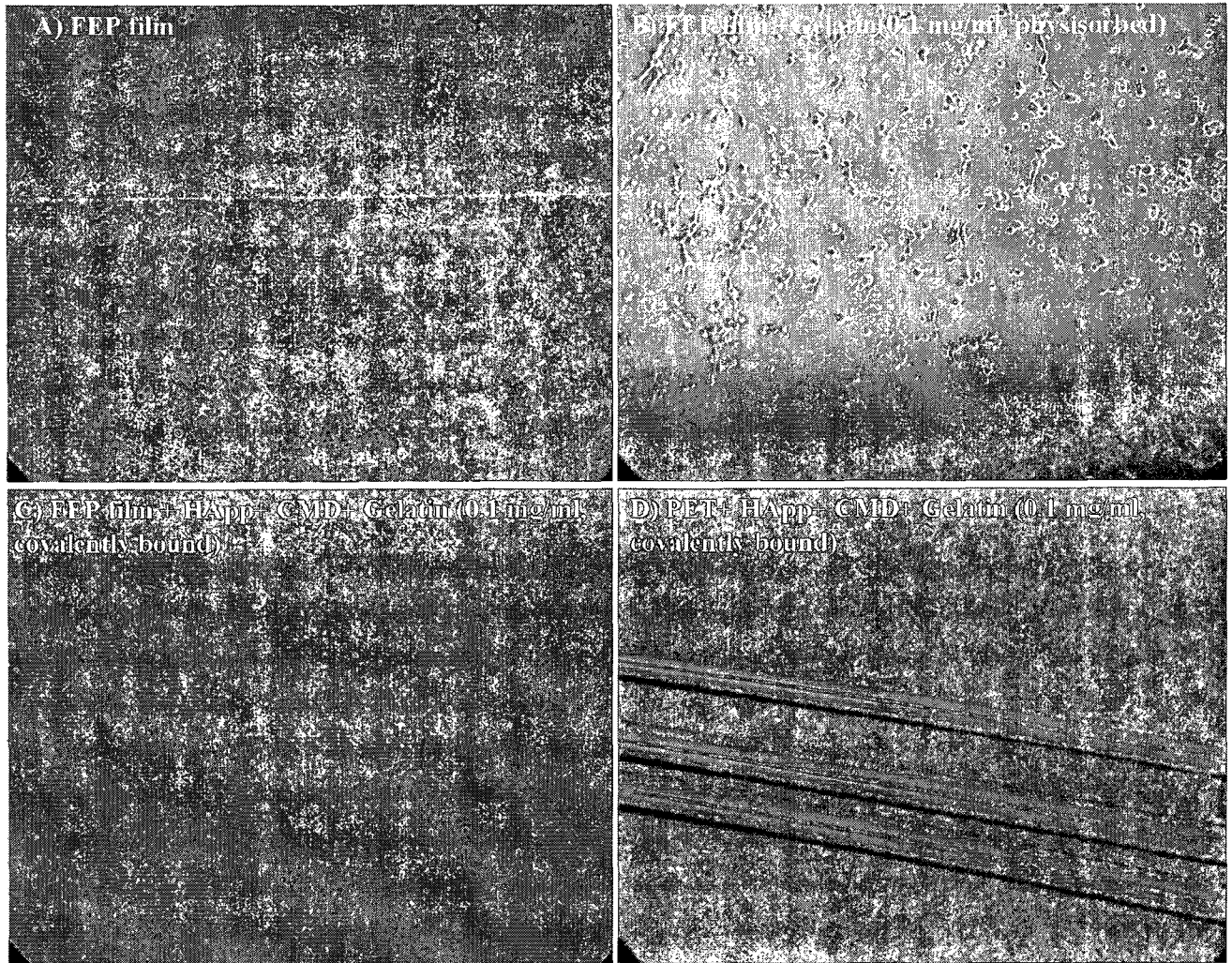
Figure 6.12: Cell adhesion on physically and covalently grafted gelatin onto FEP film and PET fibre surfaces in 2hrs after cell seeding. The pictures A, B and C represent one experiment with triplicate samples. The picture D represents at least 2 experiments with duplicate samples.

Formation of stress fibers and FA on RGD grafted surfaces

As explained earlier, stress fibers and FA formation, which take place during cell spreading or migration on substrates containing ECM components, are needed for cell functions. For this reason, the study of FAs formation is a useful approach to provide information on cell-substrate interactions. Therefore, observation of FAs and stress fibers formation by HUVECs seeded onto RGD coated surface can be a proof for both existence of

covalently grafted RGD on the non-cell adhesion CMD-coated surfaces and functionality of RGD to interact with integrins present on cell surfaces. Few studies have been reported investigating EC behaviours in terms of stress fibers and FAs formation on the surface-coupled adhesive RGD peptide (MASSIA and HUBBELL 1991b). For this aim, HUVECs were seeded on surface coated substrates including, HApp + CMD- and HApp + CMD + RGD-coated glass substrates to study the effect of these coatings on the formation of stress fibers and FAs. In figure 6.13, the red and green staining denotes stress fibers, stained with TRITC-phalloidin; and vinculin stained with a primary antibody (Monoclonal Anti-Vinculin and secondary antibody (Anti-Mouse IgG), (see Chapter 4, sections 4.3.4 and 4.3.6). Vinculin is a membrane-cytoskeletal protein present in the FA points. The sharp vinculin spots and intense actin staining observed on RGD-coated substrates when compared to the CMD-coated surfaces, on which there was no cell, demonstrate the bioactivity of RGD-coated substrates. These results suggest that the RGD peptides are strongly immobilized on the CMD graft layer. This strong ligand immobilization is needed to promote strong cell adhesion because formation of FAs only occurs if the ligands can withstand cell contractile forces (HERSEL, et al. 2003). These results and discussions have been previously published (HADJIZADEH, et al. 2007).
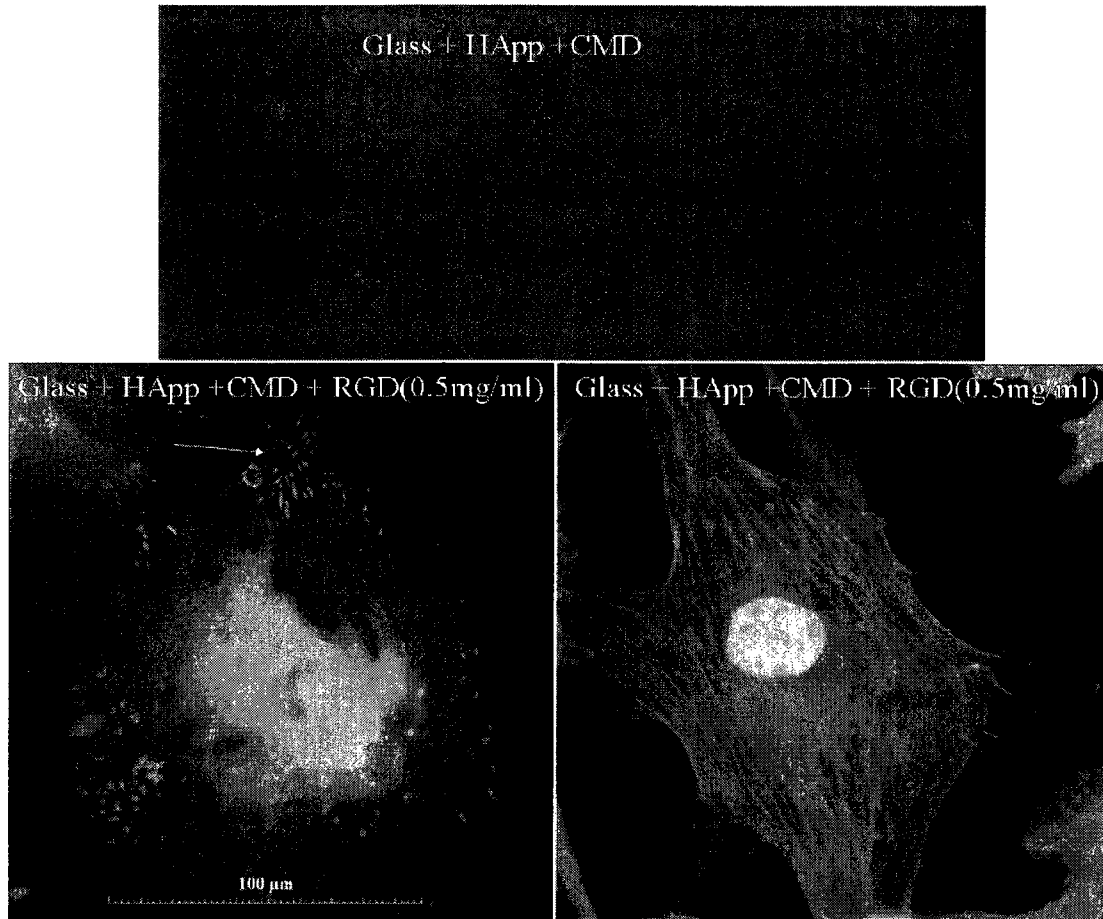
Figure 6.13: Images obtained by epifluorescence microscopy of the HUVECs stained for stress fibers (red, right) and vinculin (primary antibody (Monoclonal Anti-Vinculin) and secondary antibody (Anti-Mouse IgG)) (green, left), Original magnification was 600X. The pictures represent 2 experiments with triplicate samples. This figure has been previously published (HADJIZADEH, et al. 2007).

RGD immobilized polymer fibres

PET fibres

Many studies have investigated surface modification of flat substrates with cell-adhesive and non cell-adhesive coatings (HERSEL, et al. 2003). However, only a few studies have reported on a procedure to functionalize 3D surfaces using biological molecules that can be applied in tissue engineering. In the latter condition, this is an important requirement to direct

cell responses and tissue development by providing selective surface chemistry in a 3D environment. For this reason, I have applied the multilayer surface modification technique developed in this study to covalently graft RGD onto polymer fibres to produce bioactive polymer fibres. These bioactive fibres can be organised into a 3D network to modulate cell patterning.

In order to produce bioactive polymer fibre, PET fibres were surface coated using a multilayer step surface modification, as explained earlier (see Chapter 4 sections 4.2.2-9). Then untreated and HApp-, CMD-, GRGDS- and GREDS-coated PET fibres were seeded with HUVECs to evaluate cell adhesion and spreading (see also section 4.3.2-4). GRGDS was compared to GREDS that was considered as an inactive control coating. The result of the cell adhesion and cell spreading tests correlate with the results obtained by chemical analysis.

Cell adhesion

Cell adhesion was studied on all samples and the results expressed as relative cell adhesion percentages. The numbers of cell nuclei (stained by Hoechst), corresponding to the number of adherent cells per fibre length, were counted, four hours after cell seeding. ANOVA (using SigmaStat software) was used to compare groups, at $P \leq 0.05$. The percentage of relative cell adhesion was calculated by taking the ratios of average numbers of attached cells (obtained by ANOVA) on untreated PET, HApp-, CMD-, and peptide-grafted fibres to the average number of attached cells found on untreated PET fibres (as the control), multiplied by 100. Similarly, the relative standard deviations (SD) were calculated by taking the ratio of the SDs of attached cells (obtained by ANOVA) on untreated PET, HApp-, CMD-, and peptide-grafted fibres to the average number of attached cells found on untreated PET fibres, multiplied by 100. The

significant differences were compared with the untreated fibres at p ≤ 0.05. As shown in Fig. 6.14, cell adhesion was significantly reduced on CMD- and RGE-coated fibres, whereas the HApp- and GRGDS-coated (i.e. 0.5 and 1mg/ml) fibres significantly promoted cell adhesion. These results and discussions have been previously published (HADJIZADEH, et al. 2007).

In order to produce an effective bioactive surface, a spacer layer is often introduced onto the substrate surface before biomolecule immobilization, bioactive molecule (HERSEL, et al. 2003), preferably one with protein resistance properties (e.g. poly (ethylene oxide) (PEO), carboxy-methylated-dextrans (CMD). Such surface coatings may be useful in the production of materials resistant to non-specific cell adhesion. For this aim, CMD coatings have the advantage to act as a platform for covalent immobilization of cell-adhesive peptides or other biological signalling proteins. Such constructs enable the fabrication of systems that possess specific biological responses since the non-adhesive CMD interlayer would limit other non-specific, undesired biological responses.
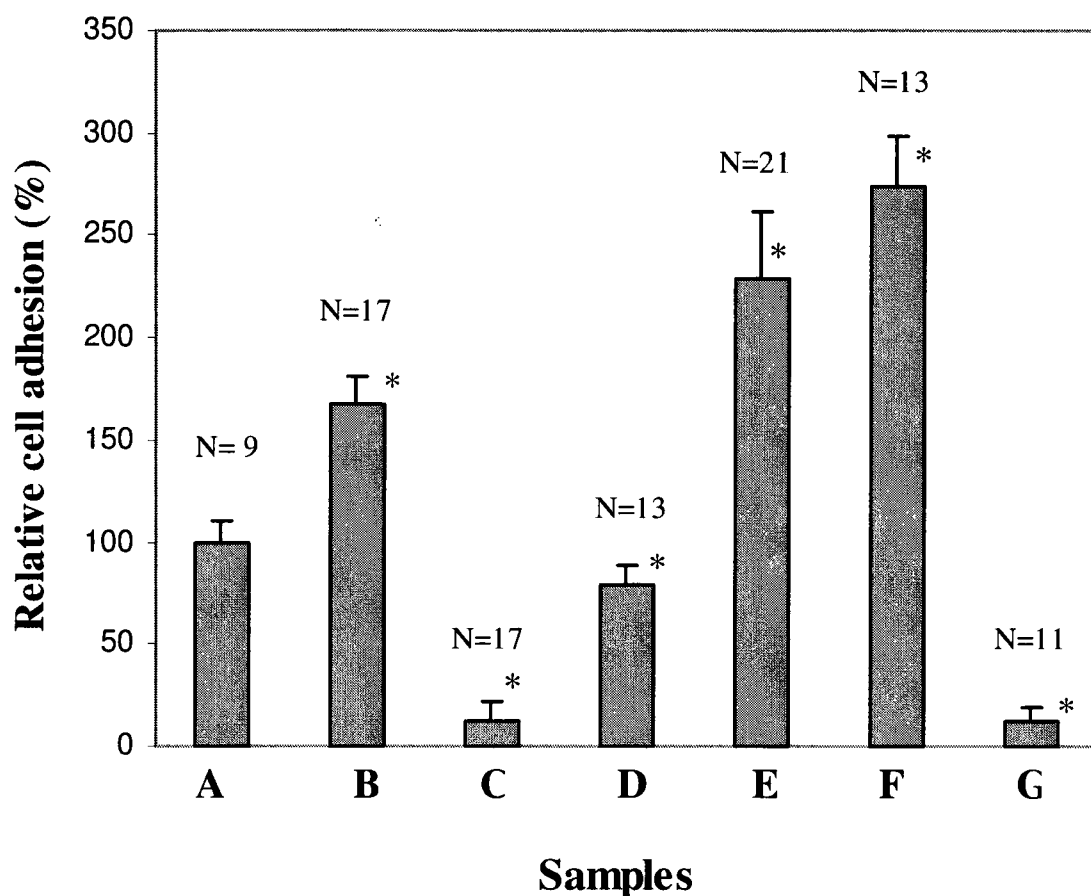
Figure 6.14: EC adhesion (4 hours following cell seeding) on clean untreated PET fibres, considered as 100% (control) (A) and the PET fibres with the different layers: PET + HApp (B), PET + HApp + CMD (C), PET + HApp + CMD + GRGDS(0.1 mg/ml) (D), PET + HApp + CMD + GRGDS (0.5 mg/ml) (E), PET + HApp + CMD + GRGDS (1 mg/ml) (F), and PET + HApp + CMD + GRGES (0.5 mg/ml) (G) interlayers. Error bars represent relative standard deviations. 70kDa CMD, carboxylation degree of 1:2, and 2 mg/ml CMD solution concentration were used in these experiments. N indicates the number of fibres which were selected from 2 to 3 different experiments. This figure has been previously published (HADJIZADEH, et al. 2007). * indicates the values significantly different from control (untreated PET fiber) by ANOVA at p ≤ 0.05.

GRGDS-coated PET fibres (or monofilaments) promoted cell adhesion significantly, when compared to CMD-coated fibres at p ≤0.05. Furthermore, cell adhesion promotion depended on the GRGDS solution concentration used during the grafting procedure (Fig. 6.14). Cell adhesion on the GRGES (inactive control, Fig. 6.14G) was significantly lower than the amounts observed on GRGDS-coated samples. These results suggest that the significant increase in EC adhesion on GRGDS-grafted PET fibres were due to the biospecific responses between cell membrane integrins and the GRGDS ligands present on the fibre surfaces. Thus, cell adhesion was effectively modulated by the covalent incorporation of small cell adhesion-peptides on the fibre surface rather than via random adsorption of serum-derived cell adhesive proteins present in culture medium. The little amount of cell adhesion observed on GRGES-immobilized surfaces (inactive control) may be due to some electrostatic forces, acting between these surfaces and proteins and cells. These results and discussions have been previously published (HADJIZADEH, et al. 2007).

The decreased cell adhesion observed on GRGDS-coated fibres (0.1 mg/ml GRGDS solution) could be due to the presence of an insufficient surface density of RGD molecules. This correlates with the low surface concentration of nitrogen found in the XPS analyses of this RGD coating (i.e. 0.1 mg/ml). Another possibility is that the GRGDS molecules are much smaller than the extended chains of the CMD layer; as a result, CMD chains could act as a "cover up" for the small GRGDS molecules present in such low density. Therefore, CMD loops and chain ends prevent cells to access the RGD molecules, by providing steric-entropic repulsion. This view is supported by another study in which reduced cell attachment was observed when the spacer moiety was too long (BEER, et al. 1992). In Beer's study, it was concluded that reduced cell attachment may be due to increased entropy of the longer flexible

spacer chains which prevent strong binding. Finally, a concentration of 0.5 mg/ml GRGDS was chosen for further experiments, because a reasonable number of adherent cells were observed in this condition. These results and discussions have been previously published (HADJIZADEH, et al. 2007).

Cell spreading

Cell spreading occurs following cell adhesion on substrate surfaces. In order to examine the effect of the fibre surface chemistry and curvature on HUVEC spreading, cells were double-stained to identify cell cytoskeleton (i.e. actin filaments) and nuclei, following 4 days of cell culture. As expected, EC spreading depends on the surface chemistry of the samples (see Fig. 6.15). Figure 6.15 shows the degree of attachment and spreading of HUVECs on surface-modified PET fibres at day 4. Although a few cells attached on the CMD-coated (Fig. 6.14C) and GRGES-coated fibres (Fig. 6.14G) at 4 hrs (cell adhesion assay); cells were absent on these surfaces by day 4 (Figs.6.13A and 6.15C, respectively). It is possible that the cells attached on these surfaces, in early culture, may detach because of their inability to establish a strong adhesion to these surfaces. In contrast, cells reached to confluence and they largely spread on GRGDS-coated fibres (Fig. 6.15B). These results suggest that GRGDS-coated fibres, with a sufficient RGD surface density, not only provide a desirable surface for EC adhesion, but cell spreading, and maintenance through an integrin stimulated cell adhesion towards GRGDS ligands present along the fibre surfaces. These results and discussions have been previously published (HADJIZADEH, et al. 2007).

Dil-acetylated LDL staining

To ensure if the GRGDS coating is stable under cell culture conditions for a longer period of time, HUVECs were seeded on the GRGDS-coated fibres (0.5 mg/ml GRGDS concentration) and kept in culture for a long period of time (i.e 10 days). At day 2, cells were stained with Dil-acetylated LDL and were daily observed with epifluorescence and confocal microscopes. All these observations showed a level of uniform cell distribution (Fig. 6.15D) and stability achieved over the fibre surface, demonstrating the stability of RGD-coating under culture condition for the above mentioned period. These results and discussions have been previously published (HADJIZADEH, et al. 2007).
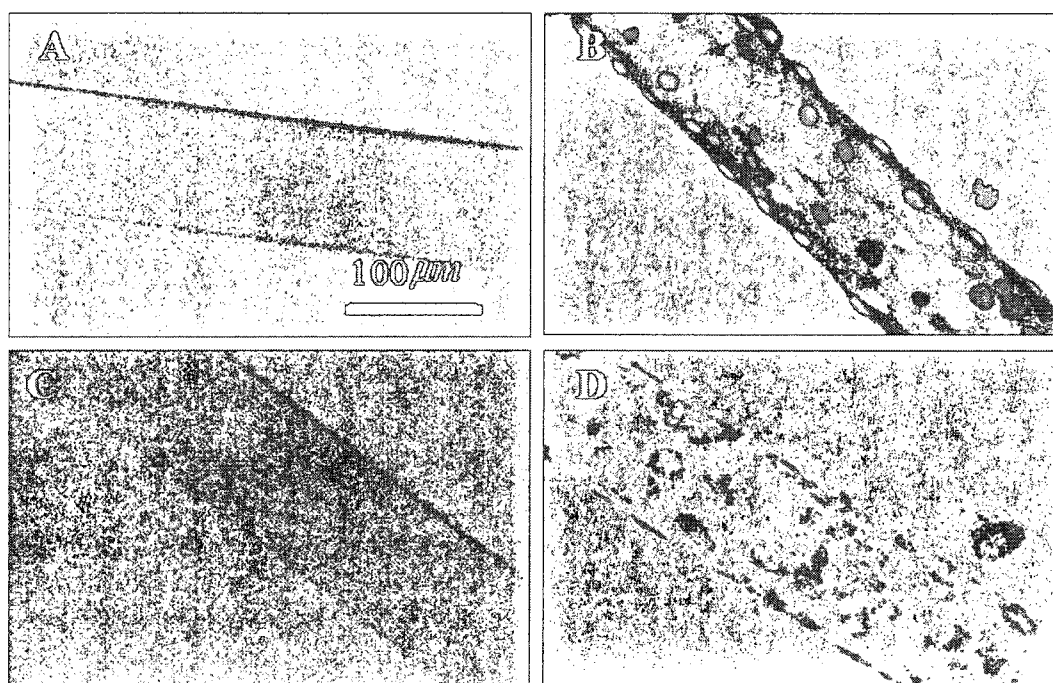
Figure 6.15: Confocal microscopic observations of HUVECs at day 4 on A) PET + HApp + CMD (70kDa, carboxylation degree of 1:2, 2 mg/ml), B) PET + HApp + CMD + GRGDS (0.5 mg/ml), C) PE + HApp + CMD + GRGES (0.5 mg/ml), and D) PET + HApp + CMD + GRGDS (0.5 mg/ml), HUVECs were stained for nuclei with SYTOX Green Nucleic Acid Stain and for actin filaments with TRITC-phalloidin in A, B, C, and with Dil-acetylated LDL in D. Original magnification was 200X. The pictures represent at least 2 experiments with duplicate samples. This figure has been previously published (HADJIZADEH, et al. 2007).

Bioactive ePTFE fibres

Cell adhesion

In another study, ePTFE fibres, of 200-μm diameter, were treated in a same manner as the PET fibres (with 100-μm diameters) with bioactive molecules on their surfaces (see Chapter 4, sections 4.2.2-9). The purpose of this exercise was to perform a comparative study, to prove the performance and reproducibility of the technique used for the biomolecule immobilization via a multilayer surface modification strategy and thereby modulation of the EC behavior on a polymer fibre with different physical and chemical properties (i.e. ePTFE) than those of the PET fibre.

The uncoated ePTFE and HApp-, CMD-, GRGDS- and the GRGES-coated ePTFE fibres were tested for HUVEC adhesion, as previously explained in Chapter 4 (see sections 4.3.2-4). As expected, no EC adhesion was observed on the CMD-modified ePTFE fibres (Fig. 6.4C) whereas the RGD-coated fibres provided the highest cell adhesion (Fig. 6.16A2). Surface grafting of GRGES (inactive control) peptides onto the CMD-coated ePTFE fibres prevented cell adhesion by comparison with those observed on GRGDS-coated fibres (Fig. 6.16B2). Moreover, these results have also been confirmed by the quantitative analysis, shown in figure 6.5, GRGDS-coated ePTFE fibres significantly promoted cell adhesion, when compared to the untreated fiber (control) at $p \leq 0.05$. However, cell adhesion was as low on the CMD-modified ePTFE fibres as on the control fibres. Conversly, on CMD- and CMD-GRGES-coated fibers, cell adhesion was significantly reduced in comparison to those observed with GRGDS and HApp (Fig. 6.5) at $p \leq 0.05$). These results are in agrement with those obtained for PET fibres with the same coatings (Fig. 6.14, 6.16A1and B1). This suggests that the technique used to

graft bioactive molecules is reproducible on polymer monofilaments (fibres), having different

physical and chemical properties.
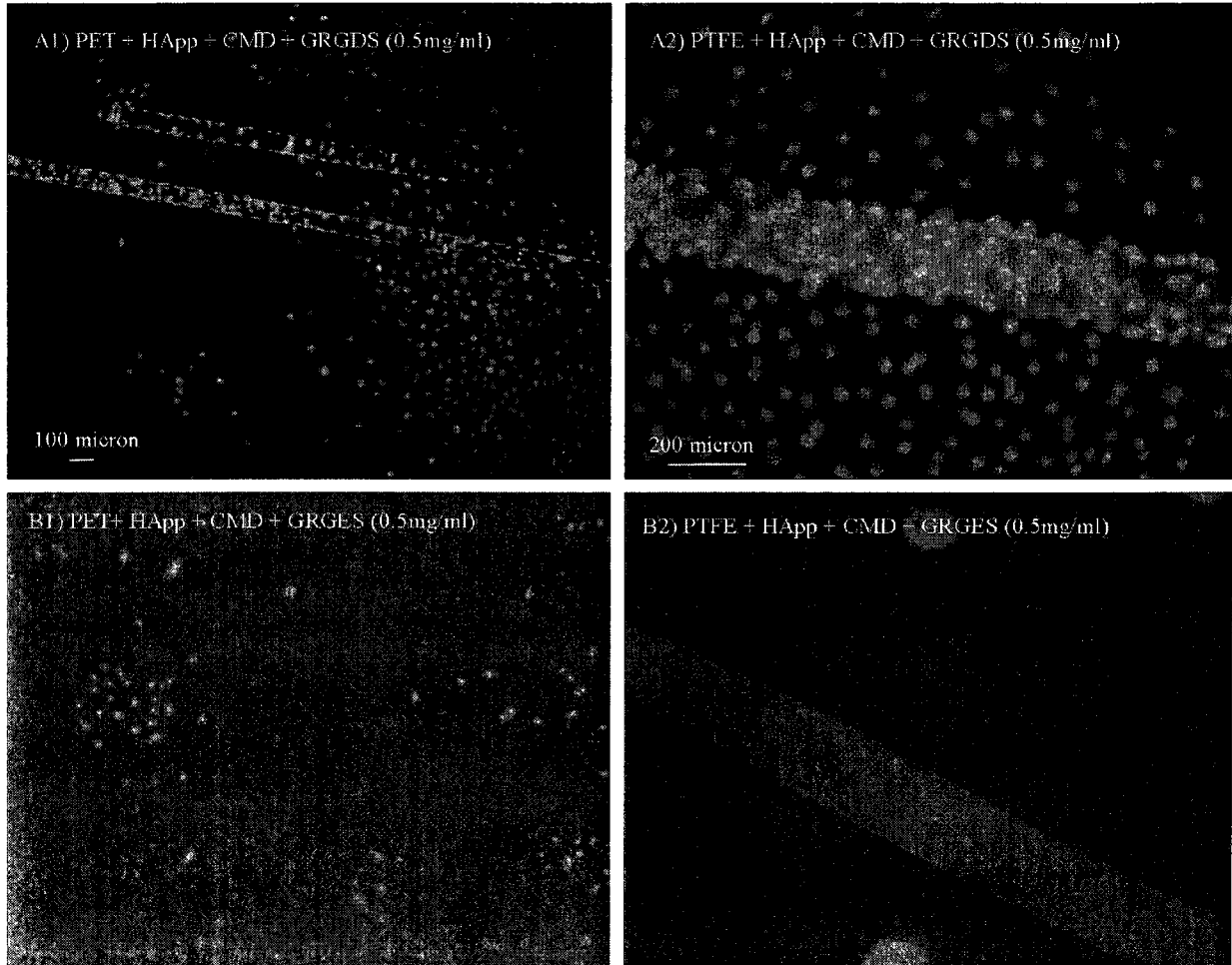
Figure 6.16: EC adhesion and distribution (4 days following cell seeding) on the PET (left)
and ePTFE (right) fibres having GRGDS and GRGES peptides.The pictures in
the right column have been previously published (HADJIZADEH and
VERMETTE 2007), Note that the cells seen in background are those which
migrated from the fibre surface to the surface of the culture plate and were grown
on that situation. However, the focus has been performed on the fibres to
specifically observe the cells attached to the fibres. The pictures A1 and B1
represent at least 2 experiments with duplicate samples. The pictures A2 and B2
represent one experiment with duplicate samples. HUVECs were stained for
nuclei with the SYTOX Green Nucleic Acid Stain.

To sum up, the RGD peptides appear to provide efficient ligand for the HUVECs to adhere to on the monofilament surfaces, as schematically presented in figure 6.17.

Polymer Monofilament   **Bioactive Polymer Monofilament**   **HUVECs adhesion**
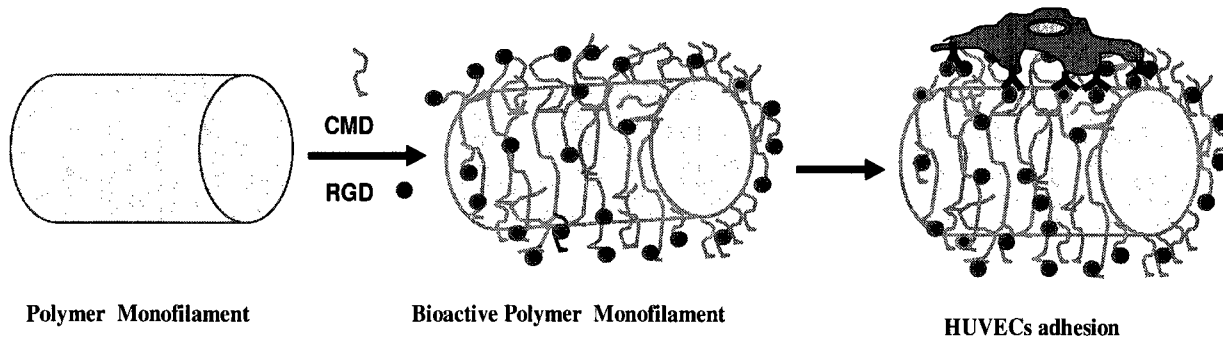
Figure 6.17: Schematic presentation of bioactive fibre fabrication and EC adhesion

RGD grafting via AApp and CMD

Cell adhesion

The aim of this study was to test the effectiveness of RGD, grafted onto CMD platforms which were immobilized; via two different interlayers, such as AApp + PEI and HApp . Such a comparative study may have an interest since the CMD grafted layers on AApp + PEI were different in surface roughness (SEM and AFM analysis) in comparison with the HApp (see Chapter 5). Furthermore, XPS high resolution spectra showed that the CMD coating, via Aapp + PEI, was more effective (or thicker) than the CMD coating via HApp. Thus, both PET fibre and borosilicate glass surfaces were coated according to the procedures described in Chapter 4 (sections 4.2.2-9). Aapp + PEI + CMD + RGD-coated fibres, in comparison with AApp + PEI + CMD-coated fibres, showed an EC attachment after some 4 hrs of culture (Fig. 6.18).
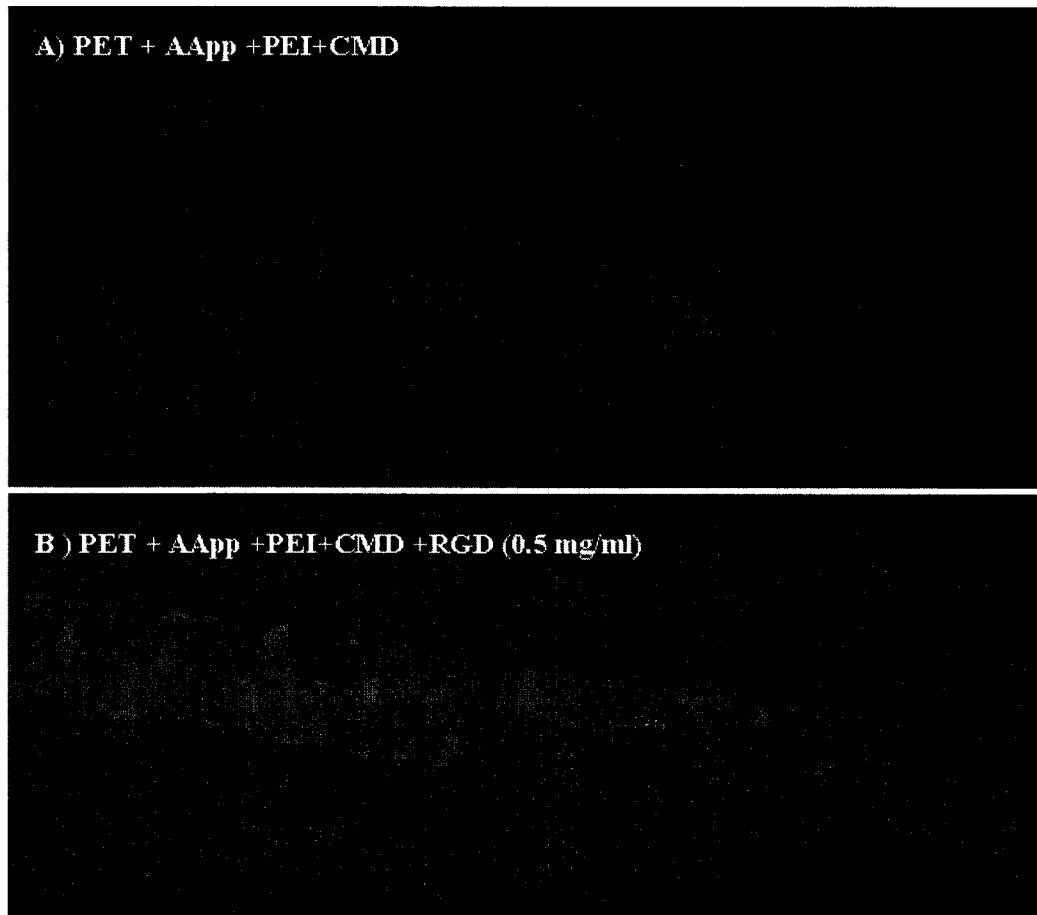
Figure 6.18: Cell adhesion on RGD- coated PET fibres via AApp + PEI + CMD, 4 hrs after HUVEC seeding. The pictures represent one experiment conducted with duplicate samples. HUVECs were stained for nuclei with Hoescht.

A quantitative analysis of the cell adhesion, following a 4 day culturing period, was performed on these coatings (Fig. 6.7). As expected, cell adhesion was significantly reduced on the CMD-coated fibres on which the CMD was grafted via the AApp–PEI (Fig. 6.7); when compared to the untreated, clean PET fibre (control) at $p \leq 0.05$. Unfortunately, data concerning the GRGDS-coated samples were not available due to a technical issue with the GRGDS peptide, while the data relating to GRGES was not included, due to lack of comparison with RGD. These preliminary results suggest that successful performance of the

biomolecule immobilization on CMD, via AApp-PEI, was achieved. However, repetition of these experiments is deemed necessary.

6.4. The effect of surface topography on EC behaviour

6.4.1. 3D cell patterning using polymer fibres

Cell patterning is an interesting concept that can have many applications over a number of domains, such as cell biology, cell-based chemical sensors, and tissue engineering. As an example, all of engineered tissues for ligaments (BASHUR, et al. 2006) and muscles (BACH, et al. 2006; LEVENBERG, et al. 2005) require cell orientation. In recent years, cell orientation by means of "contact guidance", has become an attractive research subject. In this phenomenon, a topographical feature of the substrate regulated the direction of cell spreading and migration (BASHUR, et al. 2006). Decades ago, it was observed that collagen gel aligned into parallel fibres bundles during gel contraction, which then guided the cell migration. "Contact guidance", can thus be used in tissue engineering to guide migrating cells along aligned ECM-fiber bundles for the tissue regeneration (SCHWARZ and BISCHOFS 2005). In addition to ECM fibers, a few studies have reported that different cell types can orient themselves and move along synthetic polymeric fibres having diameters ranging from 5 to 108 μm (CURTIS and RIEHLE 2001; KHANG, et al. 1999; MILLER, et al. 2002).

Furthermore, model studies on micropatterned substrates have shown that parallel microgrooves, with feature sizes of less than 100 μm, can orient numerous types of anchorage dependent cells. For example, analyses of EC behavior, on micropatterned materials with different stripe sizes (i.e. 10, 25, 50 and 100 μm), have been performed in terms of the adhesion, migration and orientation factors involved (BARBUCCI, et al. 2002). This study

showed that decreasing the stripe dimensions also modified the EC shape to that of a fusiform shape which subsequently enhanced the cell movement and orientation (BARBUCCI, et al. 2002). With the exception of a few studies, including Weiss' study (collagen gel); many studies on cell patterning have been performed on two-dimensional systems. However, transferring those results to a 3D-system, and then as 3D scaffold, is a great challenge in the tissue engineering field (BASHUR, et al. 2006). Moreover, very few studies have considered applying biological molecules in a 3D system for tissue engineering, in order to direct or guide cell responses and tissue development. In the present study, I have fabricated surface modified fibres with adhesive property (i.e. plasma polymers) (Fig. 6.4, and 6.6), non-adhesive property (i.e. CMD coating) (Fig. 6.4, and 6.6) and bioactive property (grafted with biological molecules (i.e. RGD)) (Fig. 6.15 and 6.16) to induce a directional, 3D cell patterning on these fibres, once they are dispersed in a 3D environment.

The effect of fibre curvature and surface micro and nano topography on HUVEC behaviour

Cell elongation along the fibre axis

The effect of fibre curvature and fibre surface chemistry on the EC spreading and orientation were investigated, after 10 days of EC cultures. HUVECs were stained with TRITC-phalloidin for actin filaments. As observed by confocal microscopy, the majority of actin filaments were oriented parallel to the fibre axis. Conversely, HUVECs on the flat surfaces of a TCPS exhibited randomly distributed actin filaments (Fig. 6.19). Similar actin filaments orientation was observed on un-coated and HApp- and RGD-coated PET fibres. These observations suggest that cell orientation was not related to the surface chemistry but to

the fibre curvature (100 µm) and/or the micro and nano features of fibre surface. These results and discussions have been previously published (HADJIZADEH, et al. 2007).
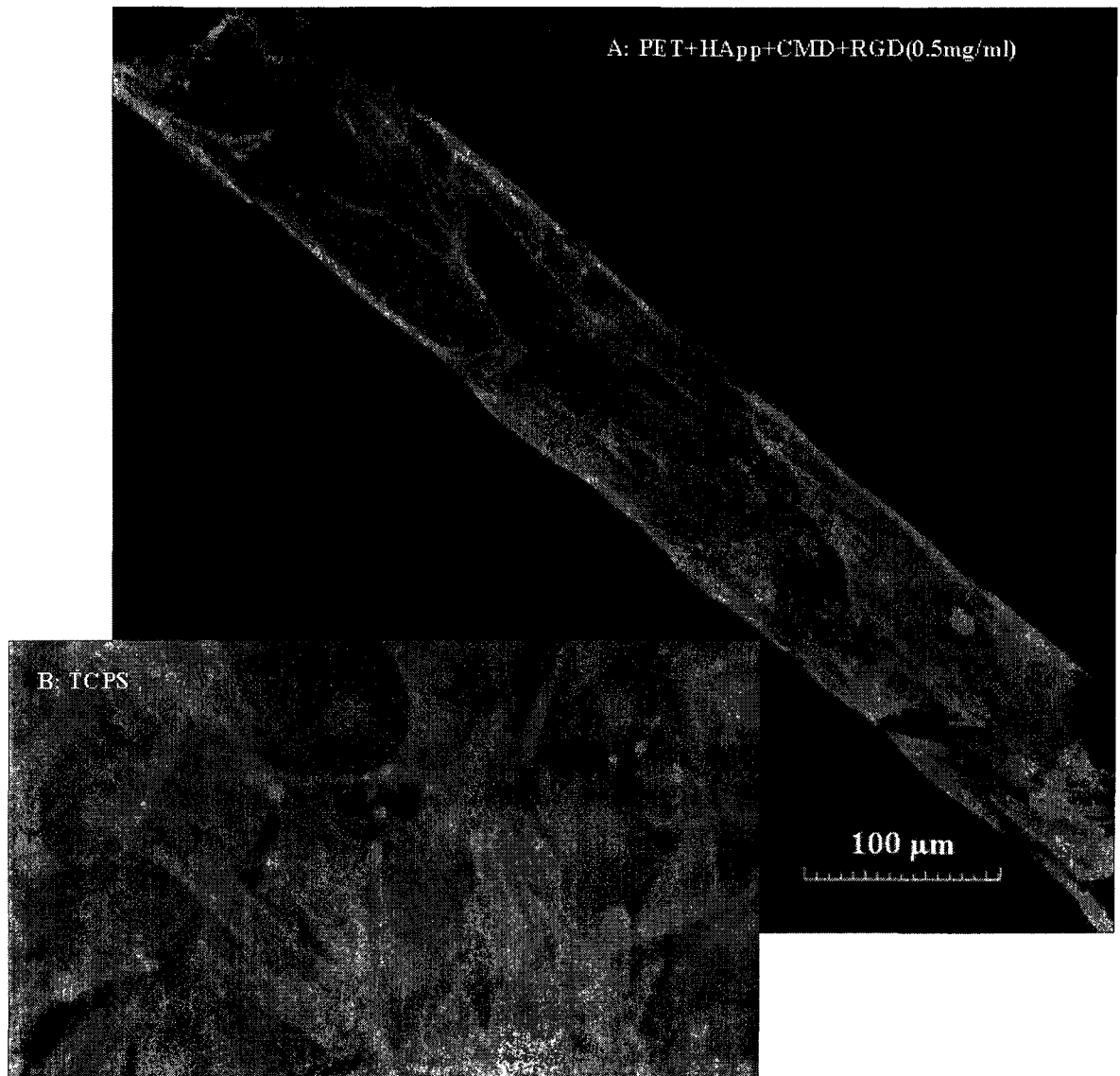
Figure 6.19: Confocal microscopic images of the EC spreading and orientation of HUVECs along a PET fibre axis (A) compared to EC spreading on a tissue culture polystyrene plate [B:TCPS] (B). The pictures represent at least 2 experiments with duplicate samples. This figure has been previously published (HADJIZADEH and VERMETTE 2007). HUVECs were stained for nuclei with Hoescht and for actin filaments with TRITC-phalloidin.

The effect of surface micro and nano features on HUVEC morphology

The PET fibre surface features and EC morphology are shown in Figure 6.20. Based on the AFM image of a PET fibre, with a large scan area (20×20 μm^2), parallel micron-scale features, formed by manufacturing techniques, are seen along the fibre (Fig. 6.20A). Furthermore, the SEM image of a PET fibre (Fig. 6.20B), at high magnification, shows the similar features on the nanometer scale. The randomly distributed "particle like" features observed in figure 6.20 B belong to the AApp coating. EC morphology on a PET fibre coated with AApp is shown in Figure 6.20 C. As this figure shows; most of the cells are oriented along the fibre.

The effect of the ePTFE fibre (with a 200μm diameter) surface features on HUVEC behavior is shown in figure 6.21. An AFM image of an ePTFE fibre in a scan area of 10×10 μm^2 is shown in figure 6.21 A1 (2D AFM image), and A2 (3D AFM image). These images show that, fibre like features with a width of about 2 μm and a height of about 600 nm, are present on the surface of this fibre. In addition to the AFM images, SEM images in low magnification (Fig. 6.21B1) and high magnification (Fig. 6.21B2) were provided, in order to identify both large size surface features (micrometric scale) and very fine features (nanometric scale) of ePTFE fibre. The two images (Fig. 6.21B1 and B2) together demonstrate the existence of oriented micro and nano features along the fibre with randomly distributed, nano scale pores. Finally, EC behavior (i.e. adhesion and spreading) is shown on both untreated ePTFE fibre (Fig. 6.21C1) and HApp-coated ePTFE fibre (Fig. 6.21C2 and C3) which demonstrate the effect of fibre surface features in conjunction with fibre surface chemistry on the EC adhesion and spreading. Based on the Figures 6.21 C1 and C2, only the surface micro and nanometer scale features are not able to promote cell adhesion, but cell adhesive surface

169

chemistry is required. Furthermore, though oriented surface features are present on the ePTFE fibre surface, cells are not oriented but their morphology resembles that of the cells on a flat surface (Fig. 6.21C3).

Therefore, cell orientation along the PET fibres can be due to the response of HUVECs to a typical fibre curvature (i.e. 100μm). Because ePTFE fibres, having oriented surface features are similar to those of PET fibres, but with the larger curvature of ≈ 200 μm, did not show cell orientation along the fibre axis (Fig. 6.21C3). This interpretation can be supported by the previously reported studies, in which cell orientation along the fibre, are influenced by the fibre curvature, and most cell types are oriented in the 5-108 μm range (CURTIS and RIEHLE 2001; KHANG, et al. 1999). However, more investigations will be needed to better understand how the fibre curvature and fibre diameter can affect the cell responses.
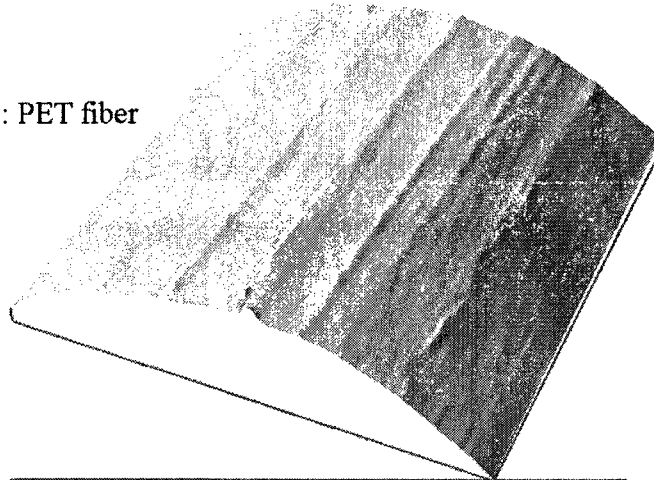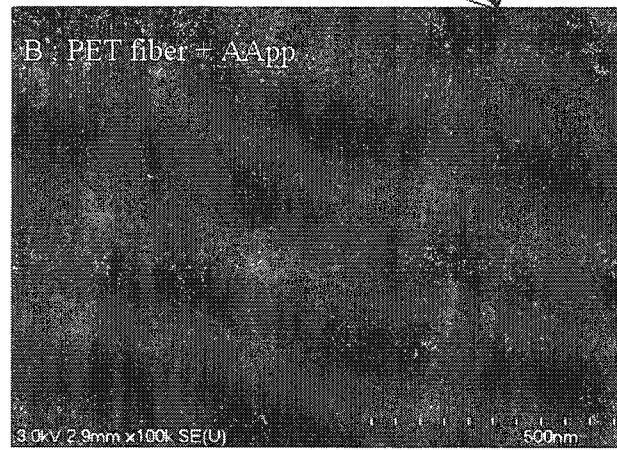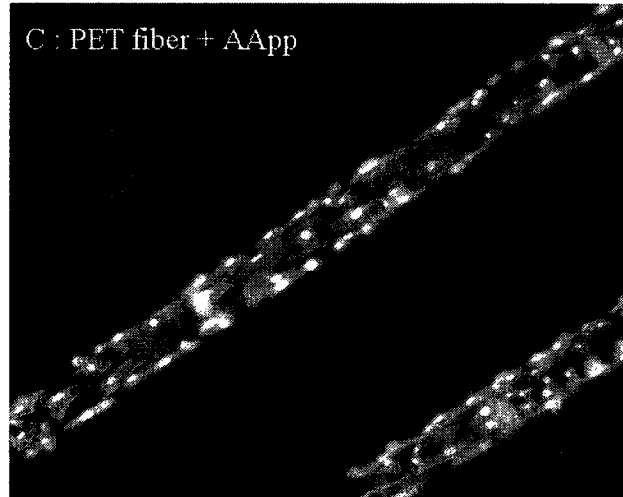
Figure 6.20: 100μm PET fibre surface and EC behavior: A) AFM image of PET fibre with scan area of 20x20 μm² B) SEM image of PET fibre + AApp, C) HUVECs morphology on a PET fibre +AApp. The pictures represent at least 2 experiments with duplicate samples. HUVECs were stained for nuclei with SYTOX Green Nucleic Acid Stain and for actin filaments with TRITC-phalloidin in C.
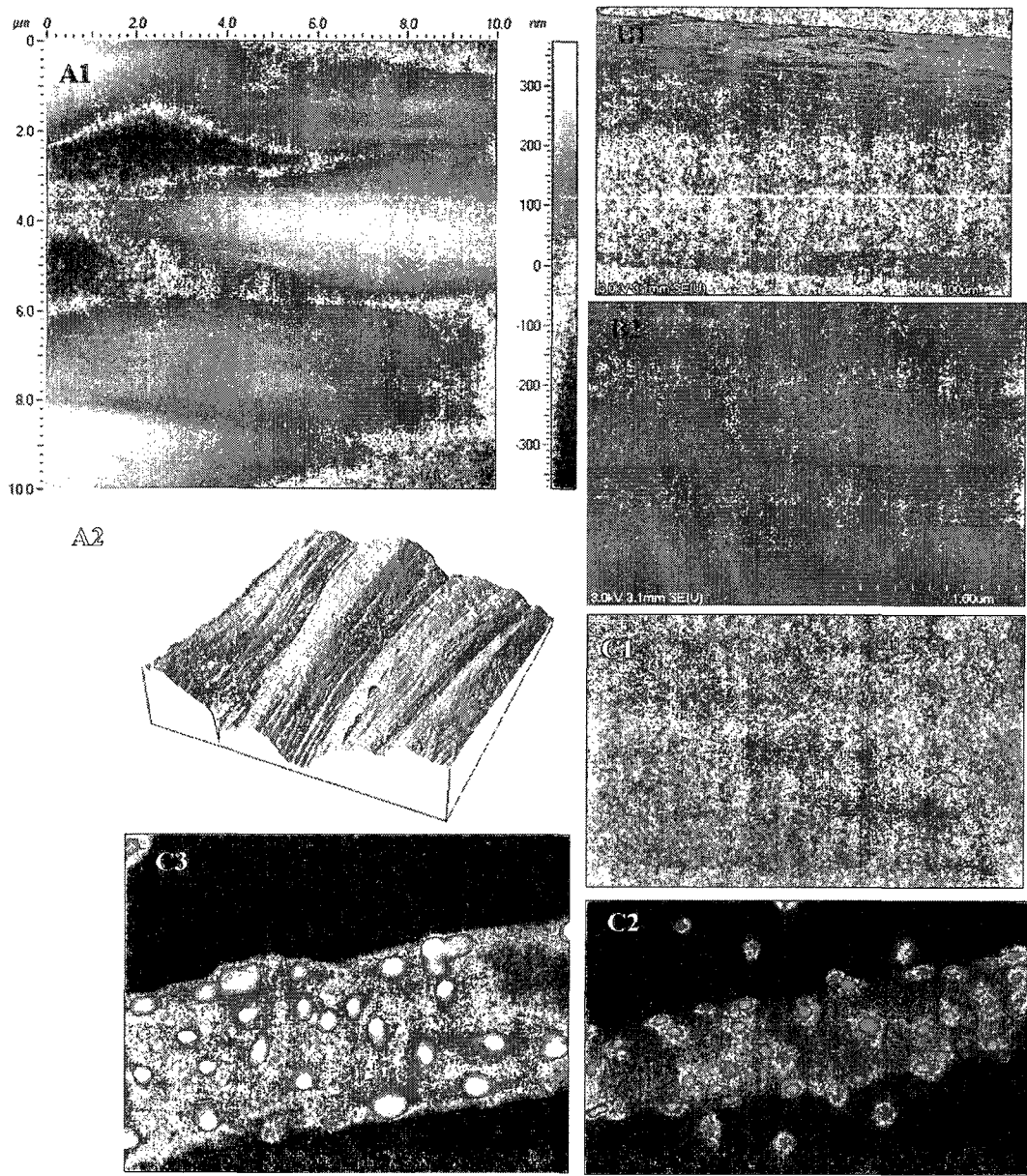
Figure 6.21: The effect of 200 μm ePTFE fibre surface features and chemistry on HUVEC response: A1 and A2) AFM image of ePTFE + HApp fibre with scan area of 10x10 μm^2, B1 and B2) SEM image of ePTFE fibre, C1) HUVEC adhesion on untreated ePTFE fibre, C2) HUVEC adhesion on HApp-coated ePTFE fibre, C3) HUVEC morphology on HApp-coated ePTFE fibre, The pictures A1 and A2 represent at least 2 experiments. The pictures B1 and B2 represent SEM images on one sample in different magnifications. The pictures C1 and C2 represent at least 2 experiments with duplicate samples. The pictures C3 represent one experiment in duplicate samples, similar cell morphology was observed on the same fibre with RGD coating. HUVECs were stained for nuclei with SYTOX Green Nucleic Acid Stain in C1-3 and for actin filaments with TRITC-phalloidin in C3.

The effect of surface micro and nano features on HUVECs adhesion

Rosso et al. (2006) have shown that the roughness of a surface generated by plasma polymerization increased the fibroblast proliferation, due to the presence of a smooth nano-structured fluorocarbon coatings deposited on PET films. In addition, it has been reported that nano-scale surface features can influence EC functions. For example, nano-structured cast poly (lactic-co-glycolic acid) (PLGA) substrates promoted endothelial and smooth muscle cell growth (MILLER, et al. 2004). Chung et al. (2003b) showed that even graft layers, such as PEG-RGD, increased the surface roughness of biomaterial surfaces (i.e. polyurethane coated with PEG-RGD) at nanometric scale and could enhance the adhesion and growth of the HUVECs. Moreover, in a very recent study, the size and proliferation rate of fibroblasts decreased when cultured on needle-like nanoposts, while blade-like nano-grates enhanced the elongation of the same cells (CHOI, et al. 2007).

Based on those previous studies, I have hypothesized that the increased cell adhesion and growth on the AApp, in comparison with that of the HApp (Fig. 6.2), may be attributed to the nanometric surface roughness, as previously shown in Chapter 5 (Fig. 5.7 and 5.8). Furthermore, non-coated ePTFE fibre, having micrometric and nanometric surface roughness values (Figs.6.21A1 6.21A2, 6.21B1 and 6.21B2) exhibited very poor cell adhesion, whereas the same fibre coated with HApp promotes cell adhesion (Fig. 6.21C1 and 6.18C2).

Taken together, it can be concluded that, topographical parameters become effective once surface chemistry promotes cell adhesion. Therefore, controlled cell growth in tissue engineering can be achieved using polymer fibres having diameters in the micrometer range, having those identified chemical and topographical characteristics which can applied to the design of new substrates.

6.5. Conclusions

In the present chapter, surface modified substrates, including polymer fibres, which were earlier developed and characterized in Chapters 4 and 5 respectively, are validated with respect their biological functionality, using HUVEC. The EC behaviours in terms of the cell adhesion, spreading, and orientation, were investigated as a function of the fibre surface properties. As expected, the cell adhesion was reduced on CMD-coated fibres, whereas aldehyde-, amine- and GRGDS-coated fibres all promoted cell adhesion and spreading. Low-fouling CMD surface coatings, in conjunction with topograpghical characteristics of the polymer fibres could be an approach that may allow a specific control of the directional cellular interactions at the tissue-biomaterial interface. Moreover, reduced cell adhesion on the GRGES-coated fibres (inactive peptide control) suggests that the high EC adhesion on the polymer fibres bearing surface-grafted GRGDS were due to the integrin stimulated cell adhesion towards the RGD ligands present on the surfaces. Cell adhesion increased as a function of GRGDS solution concentration (over a range of 0.1-1 mg/ml). Cells on RGD-coated substrates formed strong spots of vinculin (typical of Fas) and well-defined stress fibers. In addition, in comparison with flat surfaces, fibre curvature (100µm) promoted cell orientation along the fibre axis, and this event occurred more effectively in the longer-term cell culture. In addition, it was also observed that the surface chemistry is dominant in modifying the HUVEC cell behavior. Topographical parameters become effective when specific surface chemistry promotes cell adhesion. Moreover, the findings of this study point to the suitability, of RF n-heptylamine and acetaldehyde plasma polymerization, to induce desirable coatings to form on the presented substrates, as well as to improve their ability to support strong adhesion of HUVECs. In addition, the cell responses on PET fibres were in

agreement with those on ePTFE fibres and flat substrates. Therefore, the multilayer surface modification technique is reproducible and performs adequately.

This multilayer surface modification technique have the following advantages: 1) HApp or AApp enhanced cell adhesion by altering physicochemical properties of the substrate surface; and allows the inducement of new functional groups (i.e. amine or aldehyde) to covalently graft a second desired layer (e.g. CMD), 2) CMD layer provides a non-fouling surface towards proteins and cells, and also allows the introduction of COOH functional groups, in order to covalently immobilize bioactive molecules (e.g. RGD) and producing predictable cell adhesive surfaces. 3) Covalently grafted-RGD on the surface carboxylic groups correlates with an integrin stimulated cell adhesion.

In conclusion, surface-modified polymer fibres bearing cell adhesive and non-adhesive coatings can be applied to produce biomaterials (e.g. 3D-scaffold) with multifunctional surfaces with the capability of 3D cell patterning. These materials may have an important impact in current and future tissue engineering applications and regenerative medicine.

175

Chapter 7

Results and discussion III: *In vitro* evaluation of surface modified PET fibres towards microvessel formation in 3D cell culture system

7.1. Overview

Preserving the viability of thick and complex tissue masses, such as muscle, within the tissue construct both *in vitro and* in *vivo* is a challenging issue in the tissue engineering field. Thus, developing an *in vitro* pre-vascularized tissue construct could be one of the more promising solutions. Furthermore, physicochemical properties of the scaffolding material and the method of cell seeding can regulate angiogenesis in the *in vitro* constructs. To this aim, in this chapter, the development of an *in vitro* vascularized 3D tissue construct, using the physicochemical properties of multilayer surface modified PET polymer fibres, and three different methods of cell seeding by HUVECs, have been studied. The capability of enhancing angiogenesis in contact with fibres and the induction and guidance of microvessel formation within a 3D scaffold, were investigated. The preparation, characterization and evaluation of surface modified polymer fibres, towards HUVECs, have been currently published (HADJIZADEH, et al. 2007) and explained further in Chapters 5 and 6 of this thesis. Briefly, biological molecules (e.g. RGD peptides and gelatin) have been immobilized onto the surface of 100-μm dia. PET monofilaments, treated via HApp and CMD interlayers. Three *in vitro* cell culture systems have been used to investigate the microvessel formation. The first system attempted to combine simultaneously HUVECs and fibres in the fibrin gel. In the second

176

system, the HUVECs and fibres, having various coatings, were sandwiched between two layers of fibrin gel. In the third arrangement, cell adhesive fibres were precoated with HUVECs and then embedded in the fibrin gel. The 3D constructs (culture systems) were examined under phase contrast microscopy, epifluorescence microscopy and confocal microscopy, periodically, and finally through the tissue sections which were prepared for histological observations. Angiogenesis did not occur in the first model whereas in the second and third systems, angiogenesis appeared along the fibres axis. The presence of fibroblasts over fibrin gel promoted the formation and stabilization of the microvessels. Though cell adhesive coatings accelerated tube-like structure formation, may be by enhancing EC attachment, no major differences were observed between fibres having different coatings on the induction of angiogenesis. Furthermore, the architecture of polymer fibres in conjunction with cell attachment to fibrin (as an ECM component) may be largely involved in modeling a 3D EC pattern which promoted the formation of directional microvessels along the fibres axis. With increased incubation times the microvessel number increased and a network was formed in which microvessels connected to each other, from one fibre to another. A fibre spacing ranging from 200 to 600 µm, was optimal to form a network. This approach uses the phenomena of contact guidance to modulate 3D patterning of EC by enhancing HUVECs migration, proliferation and orientation and ECM components (covalently grafted onto the fibre) to support EC attachment and growth on and along the fibre. These factors enhance the induction of directional angiogenesis *in vitro*. Therefore, these results demonstrate that, by using fibre-shape polymeric material which was surface coated with a cell adhesive material preferably with an ECM component such as RGD peptide or gelatin, guidance and interconnection of microvessel was possible. This approach can be applied in tissue

engineering such as *in vitro* prevascularised tissue construct fabrication and in therapeutic angiogenesis.

7.2. First system: system containing polymer fibres and HUVECs both dispersed in fibrin gels

In this system (see Chapter 4, first system), randomly dispersed fibres (i.e. not on the holder) were embedded in a fibrin gel mixed with HUVECs. PET monofilaments coated with i) HApp + CMD, ii) HApp + CMD + RGD, and iii) HApp + CMD + gelatin, were tested in this system. First fibres and HUVECs were mixed with fibrinogen solution and then thrombin was added to form fibrin gel in the plates. Angiogenesis was not observed after 10 days of culture. From days 3 to 10, cell adhesion was only observed on gelatin and RGD coated fibres (Fig. 7.1). Moreover, no cell adhesion was observed on CMD coated fibres. It should be noted that, no fibroblast cell were used in this system.
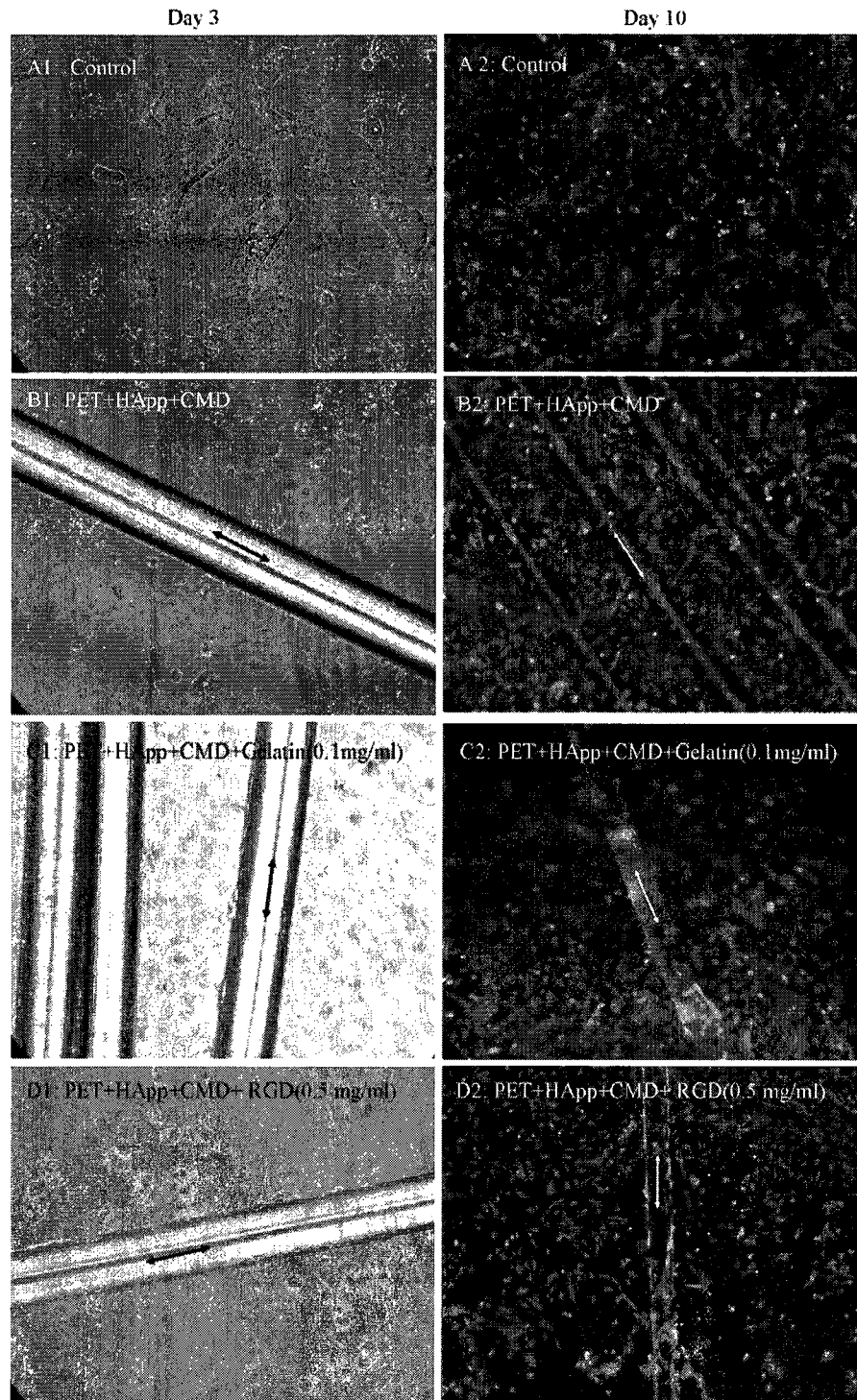
Figure 7.1: First system: surface coated PET fibres and HUVECs randomly embedded in fibrin gel. No EC organization to make well-formed tube-like structures were observed in control samples (without fibres, A1 and A2) or in samples containing fibre (B1-D2). The pictures represent one experiment with triplicate samples. Fibre diameter: 100μm. The double head arrows indicate the fibres. HUVECs were stained with calcein-AM (left column)

7.3. Second system: system with HUVECs sandwiched between two fibrin gels containing cell-free fibres

Previous studies with HUVECs sandwiched at high density between two layers of fibrin have been shown to induce rapidly microvessels at the fibrin interface (BACH, et al. 1998). Based on this culture system, HUVECs and the holder holding fibres were introduced at the fibrin interface in order to investigate the physicochemical properties of surface coated fibres to enhance and orient the formation of microvessels. Non-coated PET fibres and HApp- and RGD-coated PET fibres as well as cell-non-adhesive fibres (i.e. CMD- and RGE-coated fibres) induced similar response of microvessel formation by days 2-5 of culture. EC strands were observed between the two layers of fibrin gel largely over the interface. Much of these strands presented tube-like structures that were directed along the fibres (Fig. 7.2). These directional tube-like structures were observed for all tested fibres. In addition they presented branches and connections between microvessels resulting in a complex EC network. Figure 7.2, as an example, shows these observations for uncoated PET and HApp-, CMD- and RGD-coated PET fibres.
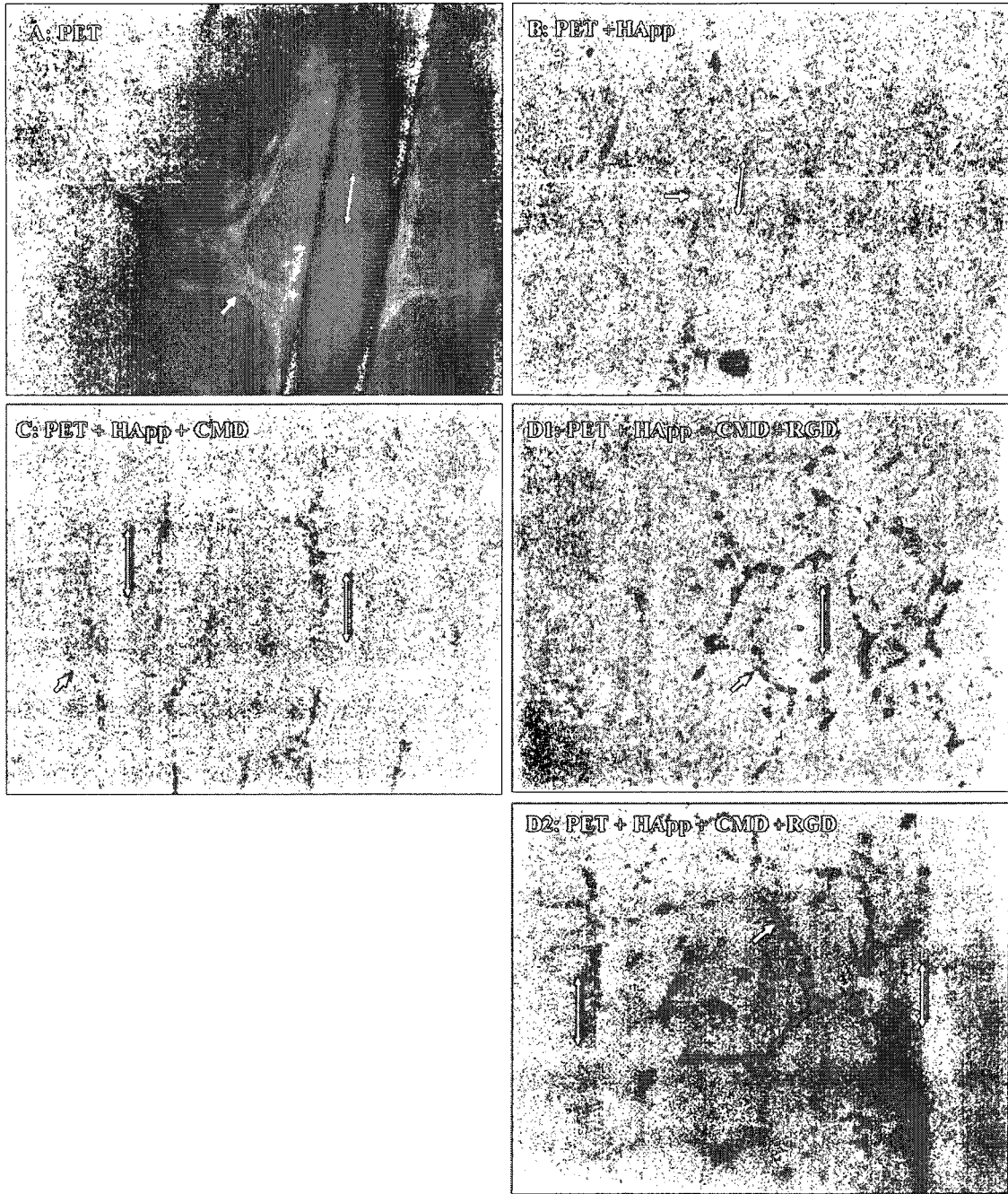
Figure 7.2: Observation by epifluorescence microscopy of the second system (after 2-5 days of culture) in which HUVECs and cell-free fibres were sandwiched at the interface of 2 fibrin gels, In A cells stained with calcein AM. In B and C HUVECs stained with Dil-acetylated LDL. In D1 and D2, microvessels around the fibre were stained for actin filaments, using TRITC-phalloidin, and counterstained with Sytox Green to highlight the position of the nuclei. The double head arrows indicate the fibres and single head arrows the microvessels. The pictures represent 3 experiments with triplicate samples. Fibre diameter: 100μm.

Furthermore, it has been previously reported that the presence of fibroblasts facilitated angiogenesis in fibrin gel in which ECs were seeded on beads (NEHLS and DRENCKHAHN 1995). In our system the presence of a monolayer of fibroblasts on the top of the 2nd layer of fibrin gel facilitated the endothelial progression (Fig. 7.3). These observations have not been reported previously in this system neither with fibres nor with fibroblasts cells (BACH, et al. 1998).

Qualitatively, the formation of directional tube-like structures was not observed in controls (i.e. in the absence of fibres) (Fig. 7.3 A1 and A2). This suggests that, physical shape of fibres may induce directional microvessel formation around the fibres in this system. This interpretation, particularly in the case of non-cell adhesive fibres (i.e. CMD-coated fibres) is supported by accumulation of HUVECs along the fibre at the time of cell seeding (Fig. 7.4). This high density of cells may lead to cell aggregation inducing cell strands and tube formation along the fibre and network formation between the fibres. This event is based on the fact that positioning the holder bearing fibre onto the under-layer fibrin gel; a fine deformation may be generated around the fibre by gravity. At the time of cell seeding, HUVECs may be rolled over down on the fibres and subsequently gathered at the fibre-gel border (see the schematic presentation in Fig. 7.5). In the case of cell adhesive coated fibres, similar events of gathering cells were present; in addition cell attachment was further facilitated the maintenance of more cells on the fibres and around them by the adhesiveness of the fibre surfaces. Therefore polymer fibres, typically those with a cell adhesive coating, enhanced directional tub-like structure formation and interconnected networks in the second system.
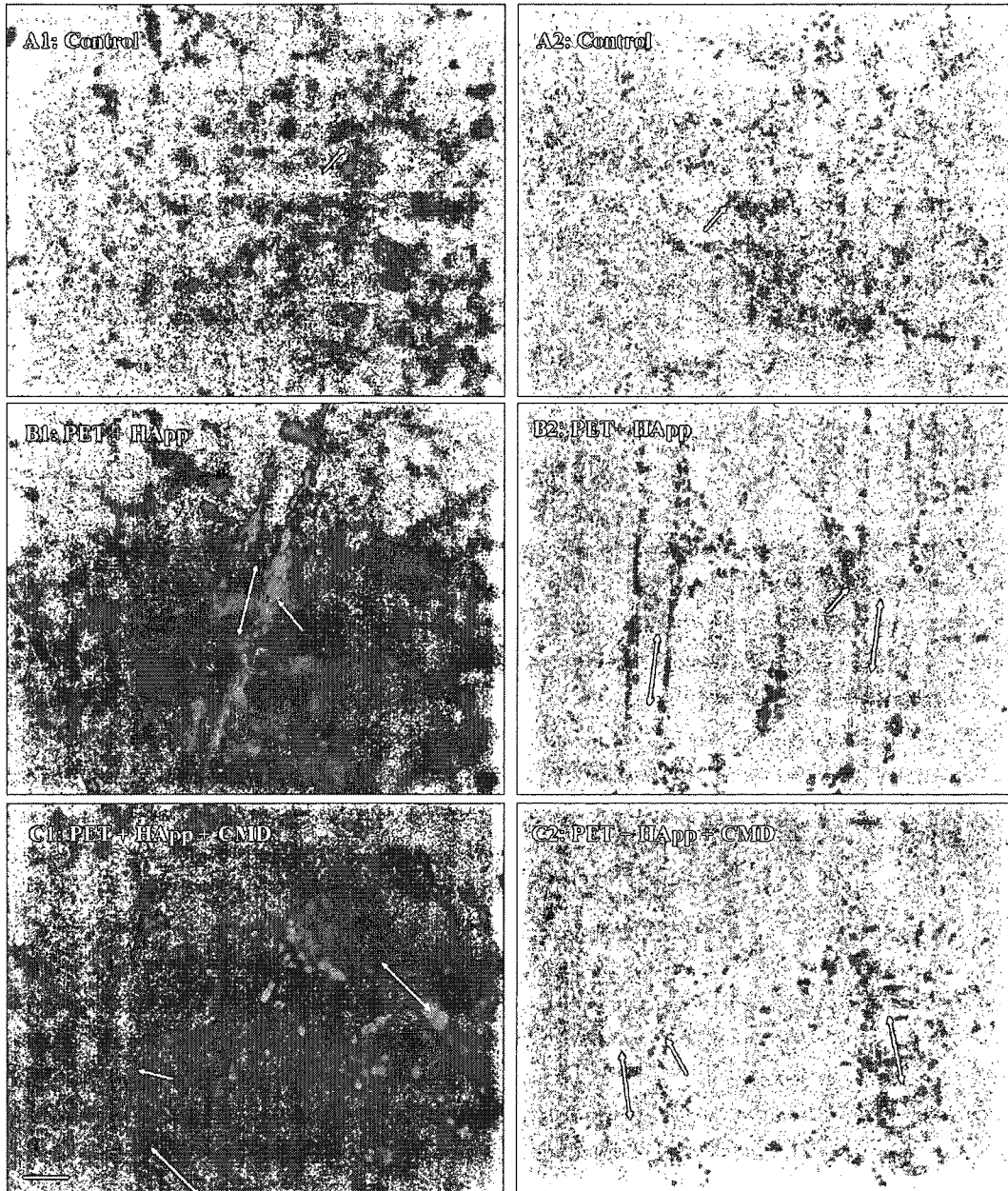
Figure 7.3: The effect of fibroblast monolayer on top of the fibrin gel and as well as the physical effect of fibre on micro vessel formation in the second system: In A1, B1 and C1 cells stained with calcein AM did not showed well formed tube-like structures in the absence of fibroblasts, after 5 days of culture. Conversely, in the presence of fibroblasts, HUVECs stained with DiI-acetylated LDL formed a microvessel network as shown in A2, B2 and C2. In A1 and A2 in the absence of polymer fibres (i.e. controls) no directional EC strands can be observed but in B1, B2, C1 and C2 in the presence of polymer fibre the directional cell strands are observed. The pictures represent 2 experiments with triplicate samples. Scale bar: 100µm. The double head arrows indicate the fibres and single head arrows the cell strands.
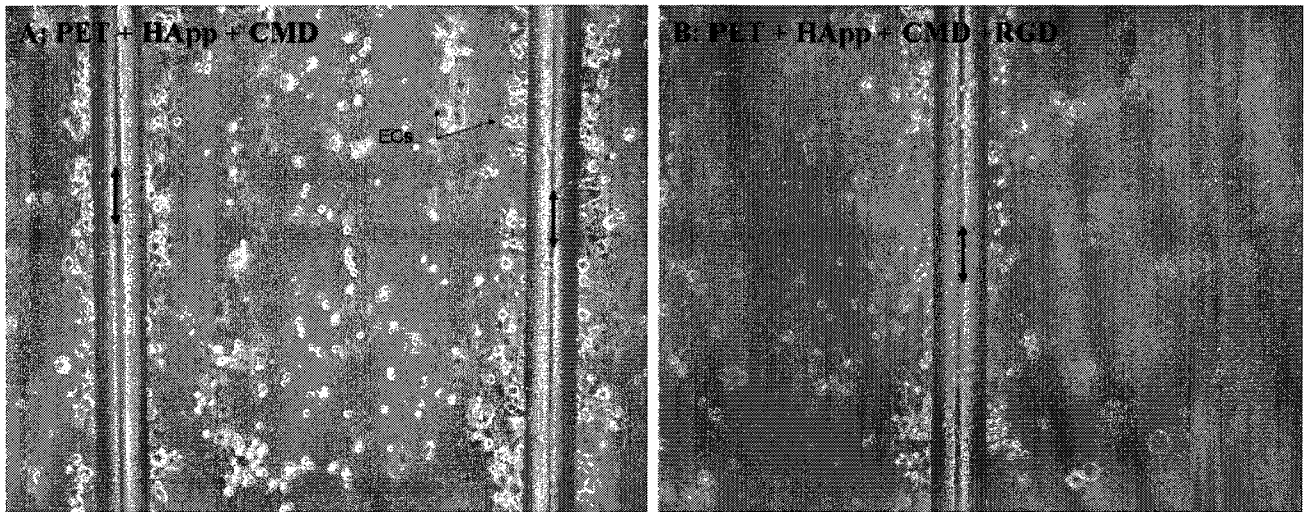
Figure7.4:   HUVEC accumulation along the fibre at the time of cell seeding in second system, the double head arrows indicate the fibres and single head arrows the HUVECs.
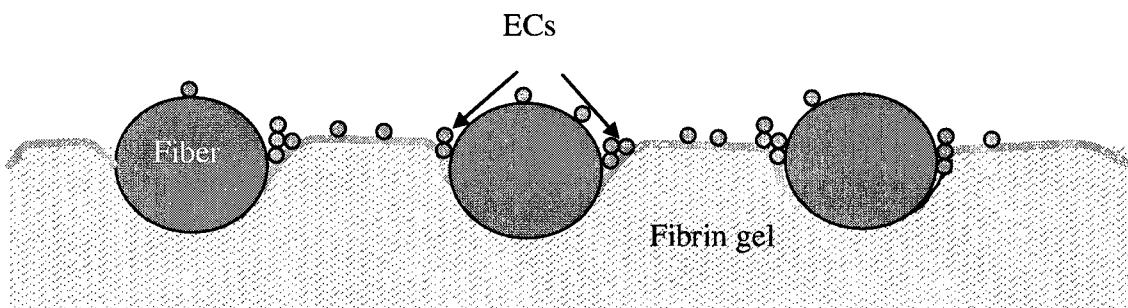
Figure 7.5:   A schematic presentation of the hypothetical position of PET fibres on the surface of underlying fibrin gel (1st layer) in the second system and HUVEC distribution around fibres at the time of cell seeding

7.4. Third system: system with cell-precoated fibres embedded in fibrin

Within 2–3 days of cultures, elongated EC strands were formed along the fibres which appeared on both side of the fibres as viewed under microscopy focusing at different depths in the fibres. Sprouting was also observed from these cell strands (Figure 7.6). After an 8-10 day

culture period, fully formed tube-like structures were generated, reaching lengths ranging between 0.1 to 1mm (Fig. 7.7). When left in the culture for up to 20 days, the capillary network continued to remodel itself, developing a network both along and between the neighboring fibres (Fig. 7.8). Phase-contrast microscopy images revealed the presence of lumens within tube-like structures (Fig. 7.8A, B, D and E1). As additional evidence of lumen formation, histological sections of the specimens also showed the presence of lumens having multi-cellular architecture (Fig. 7.9). In figure 7.9, specific staining for vWf confirms the existence of endothelial lining (brown) and counter-staining by hematoxylin shows the nucleus (blue). These observations were in the presence of fibroblast cells. Conversely, in the absence of fibroblasts, the HUVECs on fibres remained dispersed in the fibrin and did not exhibit any well-formed tube-like structures (Fig. 7.10).
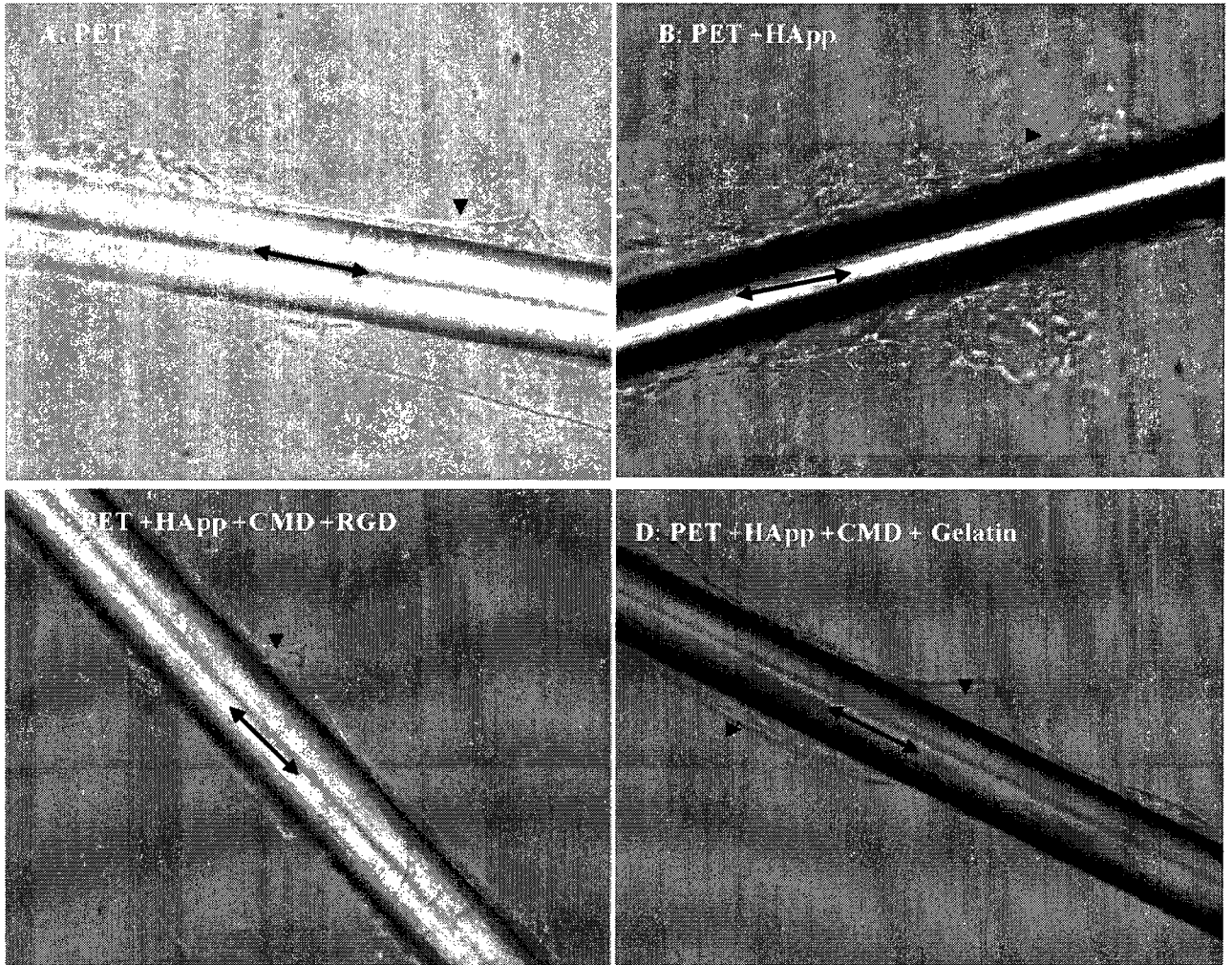
Figure 7.6: Third system: *In vitro* cell strands and sprout formation along the cell-coated polymer fibres embedded in fibrin gel. By day 2-3 HUVECs formed cell strands and sprouts as observed by phase contrast on PET (A), PET + HApp (B), PET + HApp + CMD + RGD peptide (C) and PET + HApp + CMD + gelatin (D). Fibre diameter: $100\mu m$. The pictures represent at least 3 experiments with triplicate samples. The double head arrows indicate the fibres and arrow heads the microvessel-like structures.
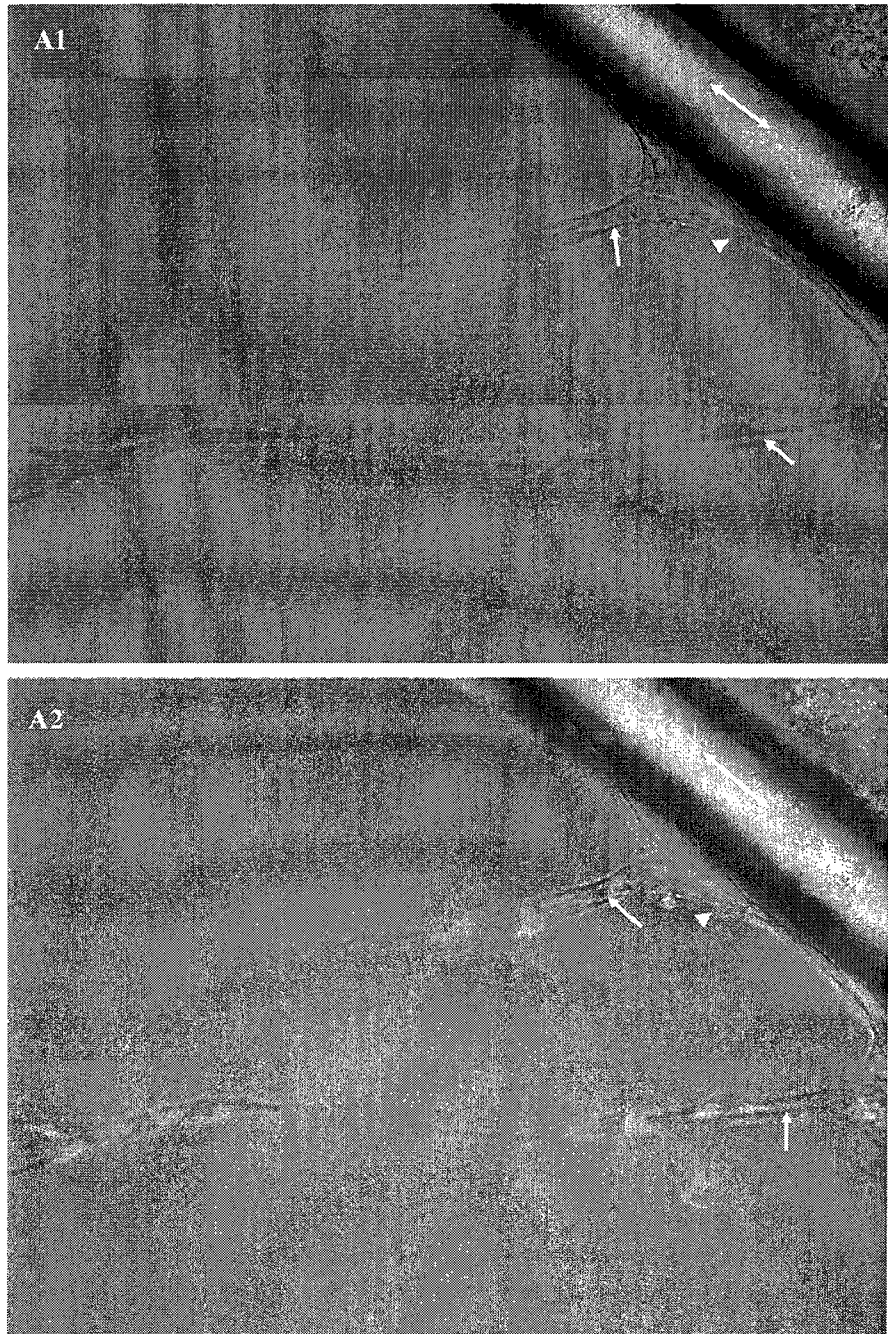
Figure 7.7: Third system (by day 8-10): Initially formed directional microvessel (indicated by arrow head) along the fibre, branching, elongation and lumen formation (narrow arrows), as observed by phase contrast (A1) and after Dil-acetylated LDL uptake (A2), fibre type: covalently gelatin grafted fibre (i.e. PET fibre + HApp + CMD + gelatin). The pictures represent one experiment with triplicate samples. Fibre diameter: 100μm.
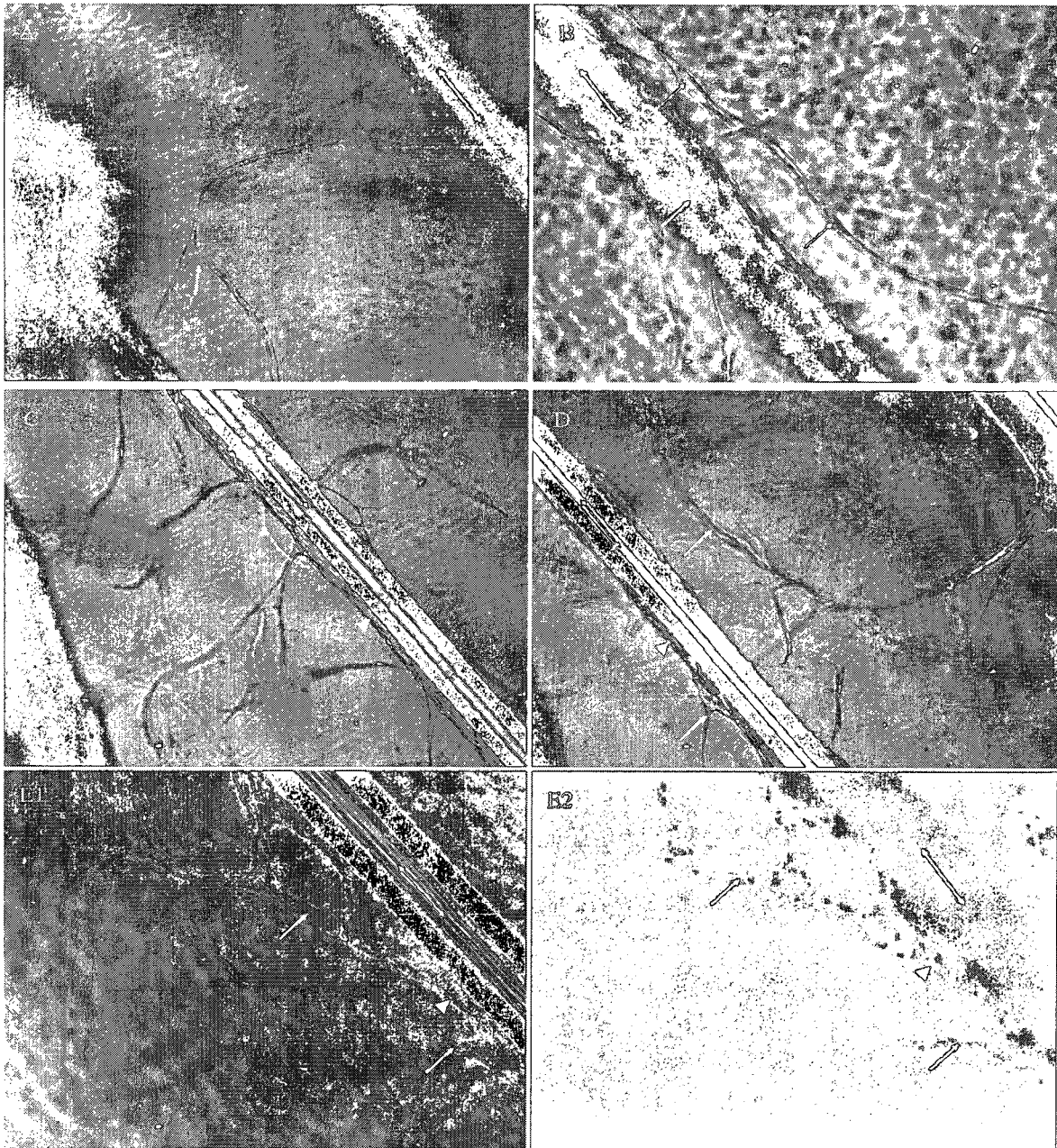
Figure 7.8: Third system: Phase contrast observation demonstrates the progression of microvessel reorganization and network formation (day 14-22). Tube-like structures have extended in fibrin and connections were established between the different microvessels, as observed by phase contrast (A-E1) and after DiI-acetylated LDL uptake (E2). Note, the presence of a lumen within the microvessel (A, B, D and E1), the fibre types are covalently gelatin grafted fibres (i.e. PET fibre + HApp + CMD + gelatin). The pictures represent at least 2 experiments with triplicate samples. Fibre diameter: 100µm. The double head arrows indicate the fibres, the arrow head the initially formed directional microvessel and single head arrows the microvessels.

Counter-stained with
hematoxylin (Blue nuclei)

Specific stained for
von Willebrand factor (VWF)
(Brown endothelial lining)
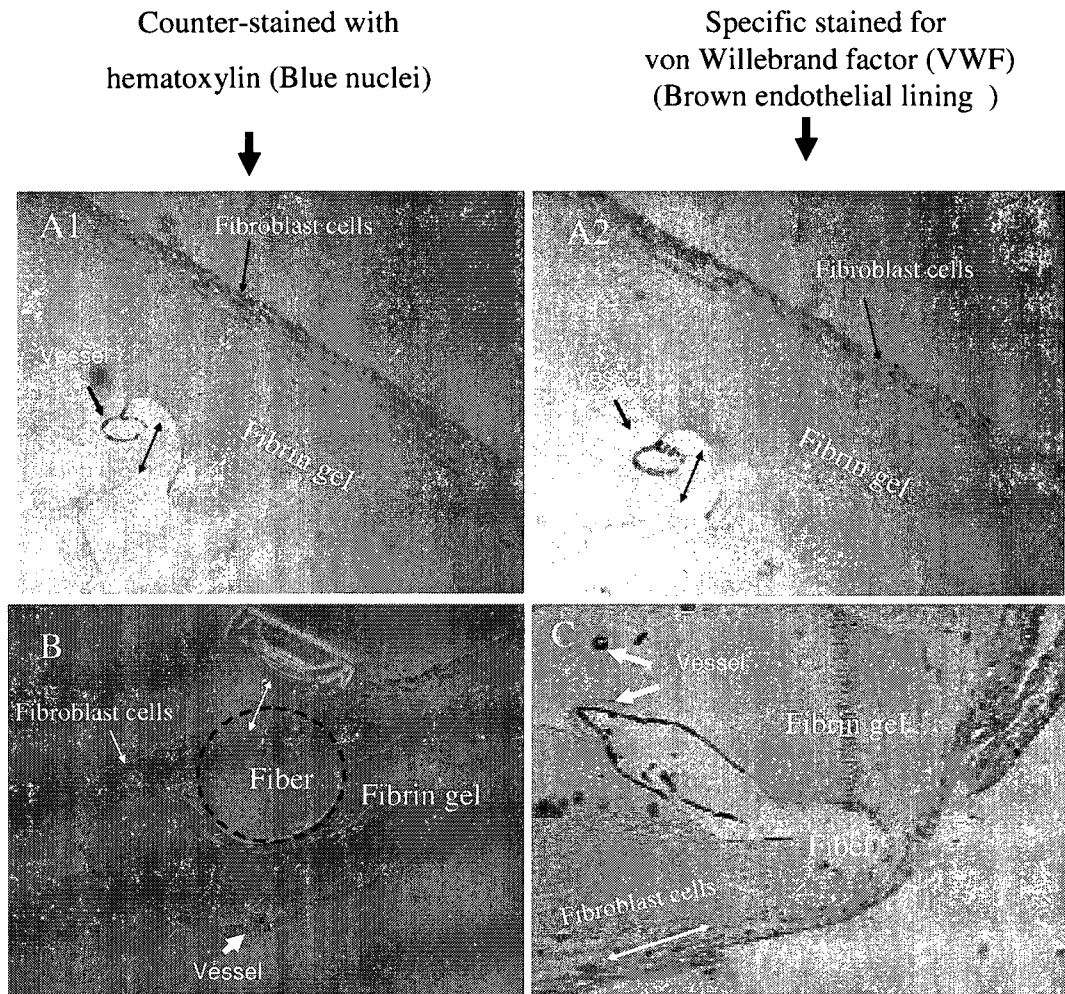
Figure 7.9: Histology and immunohistochemistry demonstrating tube-like structure with lumen near the polymer fibres in the third system: Sections counterstained with hematoxylin (A1 and B in blue color) demonstrates cellular region near the fibre. Immunohistochemistry with Factor VIII antibody on histological sections identified HUVECs from fibroblasts and underlined the HUVECs forming a lumen close to the fibre as observed in A2 and C (in brown color) Fibre type: gelatin- grafted fibre (i.e. PET fibre + HApp + CMD + gelatin). The pictures represent sections from at least 3 different experiments with triplicate samples. Fibre diameter: 100µm.
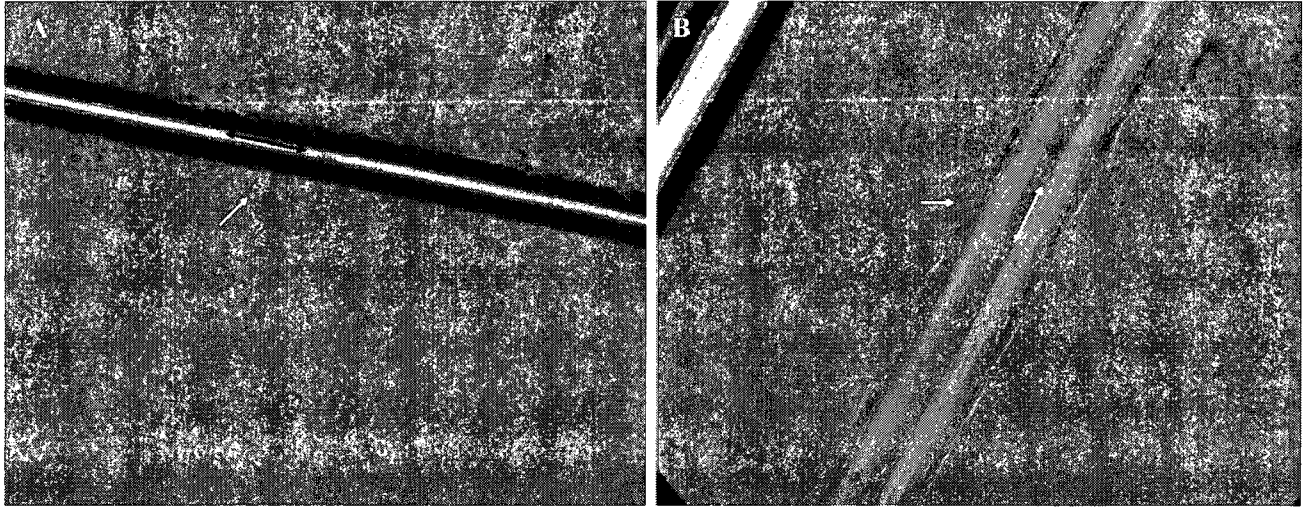
Figure 7.10: In the third system HUVECs in the absence of a fibroblast monolayer remained close to the fibers without any tube-like structures formation. RGD- coated (A) and gelatin-coated (B) fibre, the pictures represent at least 2 experiments with triplicate samples. Fibre diameter: 100μm. The double head arrows indicate the fibres and single head arrows the HUVECs.

The incubation time period seems to be important in the development of microvascular network within a fibrin-based construct. The effect of incubation time period was indirectly quantified by determining the average vessel number per unit length of fibre, according to the procedure explained in Chapter 4 (section 4.4.4 and 4.4.5). Microvessel formation was significantly increased after 10-15-day culture period compared to the shortest time periods ($p \leq 0.05$) (Fig. 7.11). The results suggest that by increasing over time of culture period did not significantly enhance the number of microvessels.
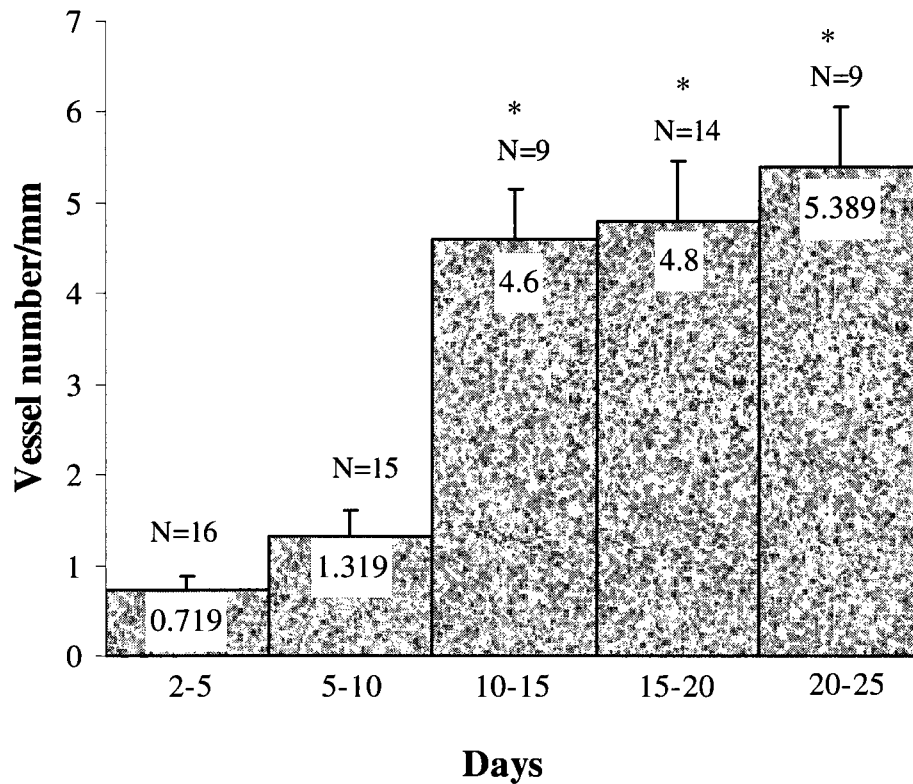
Figure 7.11: The number of microvessels as a function of incubation time periods. Fibre type: gelatin-grafted fibres (i.e. PET fibre + HApp + CMD + gelatin). The number of vessels has been counted on both sides of the fibres. Short sprouts have also been taken into account. N represents the number of fibres used for image analysis from at least one experiment. * indicates values significantly different from the early culture period (2-5 days) by ANOVA at p ≤ 0.05. Error bars represent the standard error of the mean (SEM).

7.4.1. Effect of fibre surface chemistry on angiogenesis stimulation

Despite ultimate knowledge of the roles of cell-matrix interactions in angiogenesis, the successful control of this process by implementation of ECM in artificial scaffolds has still to be achieved (POMPE, et al. 2004). The incorporation of specific ECM molecules with angiogenic properties in biomaterials may enhance angiogenesis and subsequently tissue ingrowth (BATTISTA, et al. 2005; FOURNIER and DOILLON 1992; FOURNIER and DOILLON 1996; WU, et al. 2007). ECM molecules can be simply mixed with scaffolding

material, immobilized onto the surface of these materials, or composed the scaffold. Such designs have been reviewed early in Chapter 3 (section 3.4.1).

Although, the adhesion of ECs using ECM and derivatives (e.g. RGD peptides) have been achieved on biomaterials (e.g. synthetic polymeric materials), induction of angiogenesis by this approach has rarely been reported (FOURNIER and DOILLON 1996; KIDD, et al. 2002; UNGER, et al. 2005b). In this thesis, the aim was to create a desirable surface for cells mimicking a close to natural cell environment thought that by covalently coating polymer fibre surfaces, using biomolecules. Moreover, as a result of these, the possibility of developing directional microvessel formation within a 3D environment would be provided. By using biological molecules (i.e. RGD or gelatin), it was expected to have a more efficient EC organisation in the nearby of a fibre which could have been a controllable and predictable biological response. Surprisingly, all surface-modified fibres, with cell-adhesive coatings, (i.e. PET coated by HApp, RGD and gelatin), showed similar behaviours towards microvessel formation. Even these phenomena observed, in lower level, on uncoated PET fibres (Fig. 7.12).
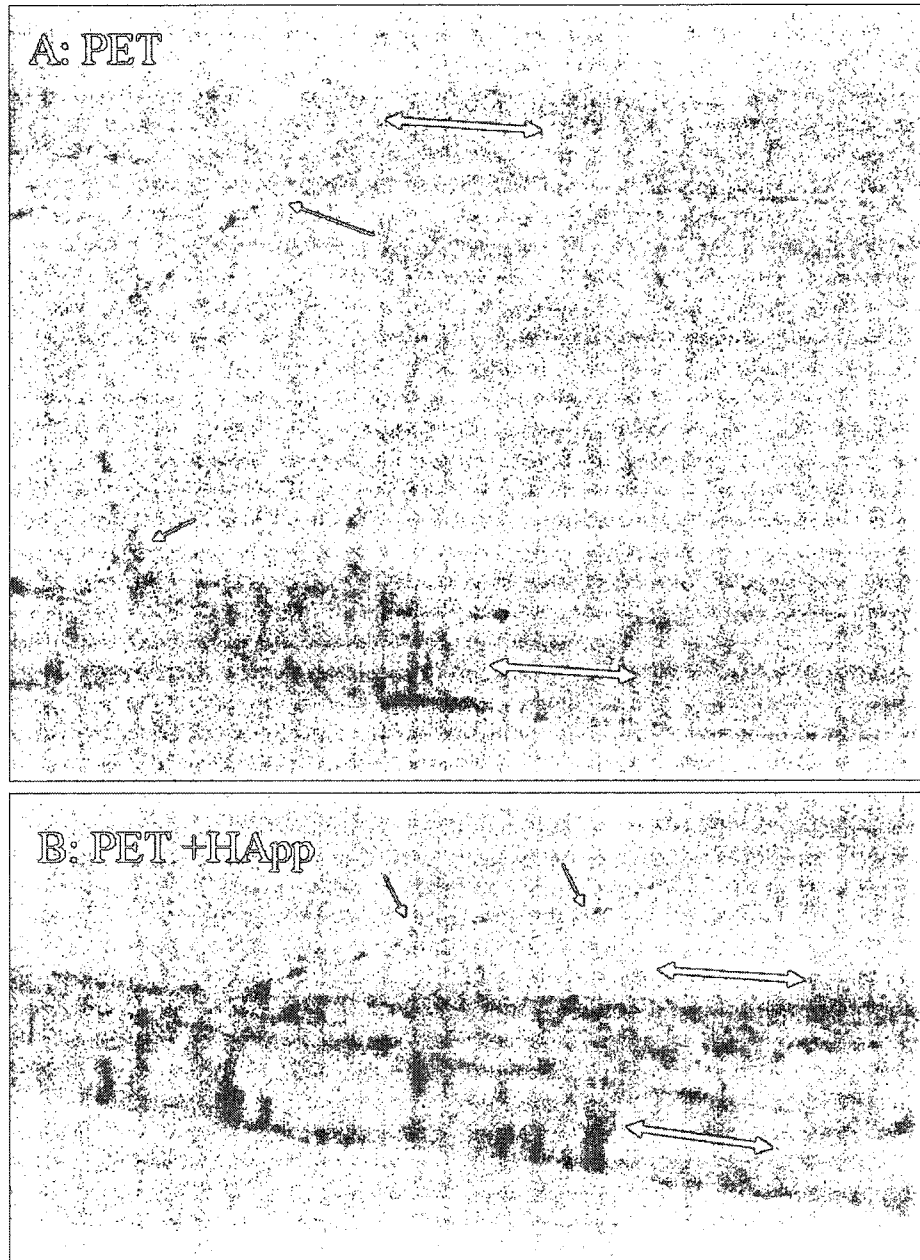
Figure 7.12: Microvessel formations on un-coated PET (A) and on PET + HApp (B) fibre in the third system (after 12 days of cell culture), the pictures represent one experiment with triplicate samples. Fibre diameter: 100μm. The double head arrows indicate the fibres and single head arrows the microvessels. HUVECs were stained with Dil-acetylated LDL.

The effect of gelatin-coated fibres on angiogenesis

Gelatin hydrogels have been used for sustained release of growth factors in tissue engineered devices in order to promote tissue regeneration and vascularization (DOI, et al. 2007; YOUNG, et al. 2005). Gelatin-coated substrates have been used to enhance EC adhesion and proliferation (CHOONG, et al. 2006). However, there are very few reports about angiogenesis occurring on gelatin coated surfaces (UNGER, et al. 2005b). Our results demonstrate that, covalent immobilization of gelatin via a hydrogel like interlayer (i.e. CMD) onto PET polymer fibres enhanced HUVEC adhesion, confluence in 2D cell culture system, and microvessel formation in 3D fibrin gel system (Fig. 7.7-7.9). Therefore, this approach can be applied on polymeric scaffolding material to enhance vacularization of tissue engineering constructs.

The effect of RGD-coated fibres on angiogenesis

Additional to the formation of sprouting and tube-like structures (Fig. 7.6), RGD-coated fibres exhibited "zigzag-shape" structures around the fibre after 2 days of culture (Fig. 7.13). These structures may correspond to short-length microvessels and branches rather than elongated and separate microvessels as observed on gelatin- and HApp-coated fibres (Figs.7.7 and 7.12 respectively). In some of the observations, even "zigzag-shape" structures were maintained with no branch and short-length microvessel formation for a period of 3-11 days (Fig. 7.14). Theses particular forms of microvessels structures as observed on RGD-coated fibres are schematically shown in Figure 7.15.
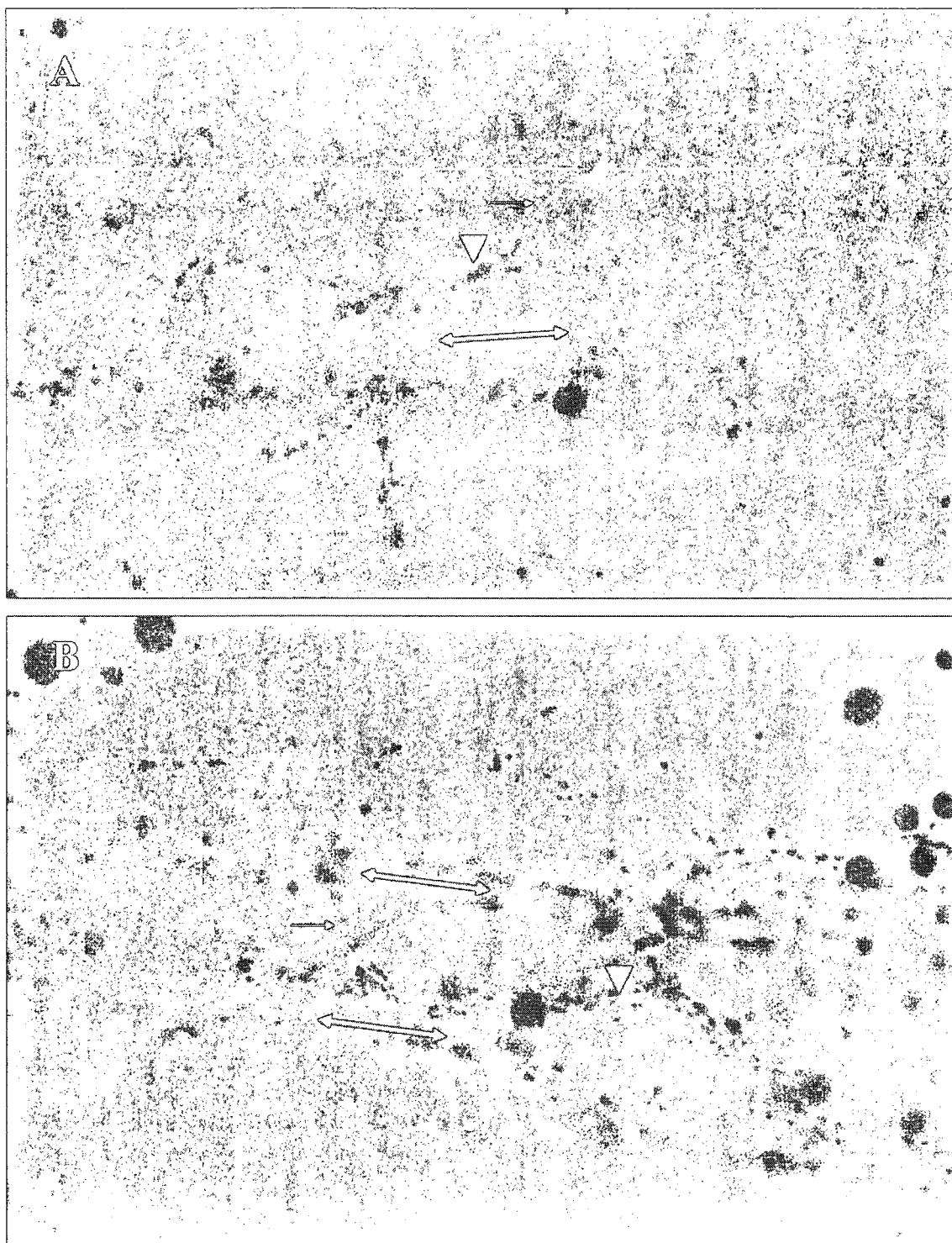
Figure 7.13: "Zigzag-shape" microvessels with short branches on RGD- coated fibres at days 4 (A) and 8 (B) in the third system, the double head arrows show the fibres, the arrow head the zigzag-shape microvessel and the narrow ones the branches. The pictures represent 2 experiments with triplicate samples. Fibre diameter: 100μm. HUVECs were stained with Dil-acetylated LDL.

Figure 7.14: "Zigzag-shape" microvessels without branch (indicated by arrow heads) along RGD-coated fibre, observed at days 2 (A1) and 9-11 (A2-A3) in the third system, the pictures represent at least 2 experiments with triplicate samples. Fibre diameter: 100μm. The double- head arrows indicate the fibres.

The formation of zigzag-shape microvessel suggests that previously attached cells may detach from the fibres in some areas, giving raise to short-length microvessels and branching. Whereas the cells remaining attached to the fibres may be activated to sprout and also to form subsequent branches.

The effects of tripeptide RGD on tissue regeneration *in vivo* and *in vitro* have been extensively reported. For example, RGD-containing peptides have been shown to accelerate the healing response and to improve the quality of the regenerated tissue in bone (KARDESTUNCER, et al. 2006; RAMMELT, et al. 2006), in cardiovascular (TWEDEN, et al. 1995), in diabetic (STEED, et al. 1995; WETHERS, et al. 1994), and in brain tissue repairs (CUI, et al. 2006). Nevertheless, there is little evidence of the effect of RGD peptide to trigger directly angiogenesis (CUI, et al. 2006) and there are many reports suggesting that soluble RGDs peptides inhibited angiogenesis (BUERKLE, et al. 2002; HAUBNER and WESTER 2004; KIM, et al. 2006; MEEROVITCH, et al. 2003; SHEU, et al. 1997; WESTLIN 2001).
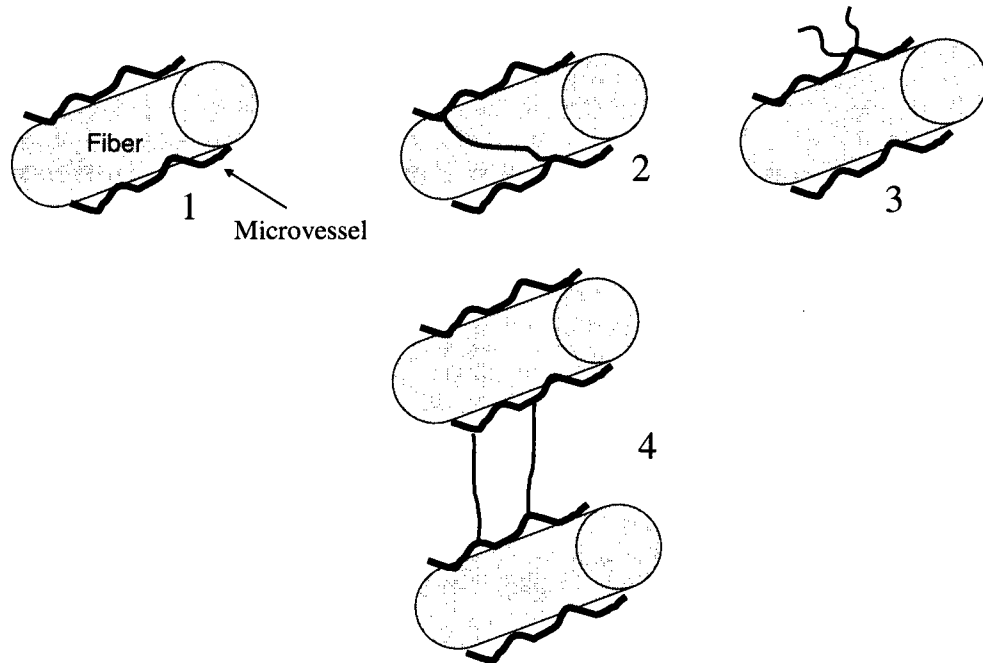
Figure 7.15: Typical microvessel forms observed on RGD coated fibres: "zigzag-shape" microvessels along the fibres (1), with a branch connecting microvessels of the same fibre (2), with branches issued from a microvessel towards fibrin gel (3), and with branches that connect two neighboring fibres (4).

Indeed, linear and cyclic RGD peptides have been used in cancer therapy by which $\alpha_v \beta_3$ integrins were targeted (ZHANG, et al. 2007). In fact, the RGD sequence mediates ECs attachment to the ECM by specific cell membrane receptors i.e., $\alpha_5\beta_1$ and $\alpha_v\beta_3$ integrins. It has been demonstrated that RGD-containing peptides are able to detach ECs from plastic or ECM-coated substrate by competing with the binding of RGD-containing ECM compounds to integrins. As mentioned earlier, during angiogenesis ECs interact with RGD-containing ECM compounds i.e., FN, laminin, collagen, vWf and VN (SHEU, et al. 1997). These interactions play prominent roles in EC function i.e., adhesion and migration. Since EC adhesion and migration are two important factors in angiogenesis, thus the RGD sequence modulates the interactions between sprouting ECs and the ECM molecules during microvessel development

(SHEU, et al. 1997). In conclution, soluble RGD inhibits tumor angiogenesis by targeting $\alpha_v\beta_3$ integrins inhibiting adhesion and migration of ECs via ECM molecules (SHEU, et al. 1997). In contrast, RGD-coated implants accelerated wound healing (STEED, et al. 1995). Though there are few studies reporting this effect *in vivo*, to our knowledge there is no *in vitro* study reporting the effect of RGD on angiogenesis. In thesis, it has been demonstrated that at least in a 3D *in vitro* system that covalently immobilized RGD peptide can induce angiogenesis as shown in Figure 7.13-14.

7.4.2. Physical effect of fibre on angiogenesis induction

Cellular functions such as cell shape, migration, and orientation can be controlled by the phenomenon called contact guidance or "topographic guidance" (LO, et al. 2000; CURTIS and RIEHLE 2001). Many studies have reported the guiding of cells by topographical features, for example cell orientation along micro-grooves (FLEMMING, et al. 1999) as well as fibres (HADJIZADEH, et al. 2007). In addition, some studies have reported that cell (i.e. fibroblast) movement can be guided by solely physical interactions at the cell-substrate interface (LO, et al. 2000). In fact, fibroblasts followed a rigidity gradient (with Young's modulus values varying from 140 to 300 kdyne/cm) when cultured on collagen-coated polyacrylamide sheets. Moreover, it has been also reported that fibroblasts exhibited different shapes and motility rates when cultured on collagen-coated polyacrylamide with different rigidities (LO, et al. 2000). The 3D network formation by ECs is regulated by mechanical properties of adhesion matrix. For example, ECs formed dense, thin networks in the flexible gel (YAMAMURA, et al. 2007) and the softer and more malleable substrate (i.e. ECM matrix) exhibited an increase in the formation of tube-like structures (INGBER and FOLKMAN 1989). In

addition, it has been suggested that the *in vitro* capillary sprouting are regulated by the relative magnitudes of forces generated by ECs and matrix rigidity (SIEMINSKI et al. 2004). Accordingly, it can be hypothesized that the ECs situated at the interface between the rigid fibres and the soft fibrin gel in the culture system responded to two distinct substrate rigidities or deformabilities, in this study. Subsequently, activated ECs may be mobilized toward a preferred direction or destination along the fibre long axis. Such phenomenon has been previously reported, at least, for fibroblasts (SHEETZ, et al. 1998).

7.4.3. Effect of fibre-fibre distance on angiogenesis

The distance between two distinct fibres seems also to play role in the development of microvascular network within a fibrin-based construct. Although the design of our fibre holder is limited to investigate certain distances in a random manner (i.e. between ca.0.1 and 2mm), it was possible to figure out some effect of fibre spacing. The quantitative analysis of this effect was performed according to the procedure explained in Chapter 4 (section 4.4.4 and 4.4.5). Microvessel formation was particularly observed between two fibres distanced of 200-600 which is higher than those found below 200μm or above 1mm (Fig. 7.16) However, the majority of connections were in the vicinity of 200-300 microns (Figure 7.17 B1 and B2). Below distances of 200μm juxtaposed microvessels were frequently observed along the respective fibres (Figures 7.17 A) and, in some instances, communicated to each other.

200
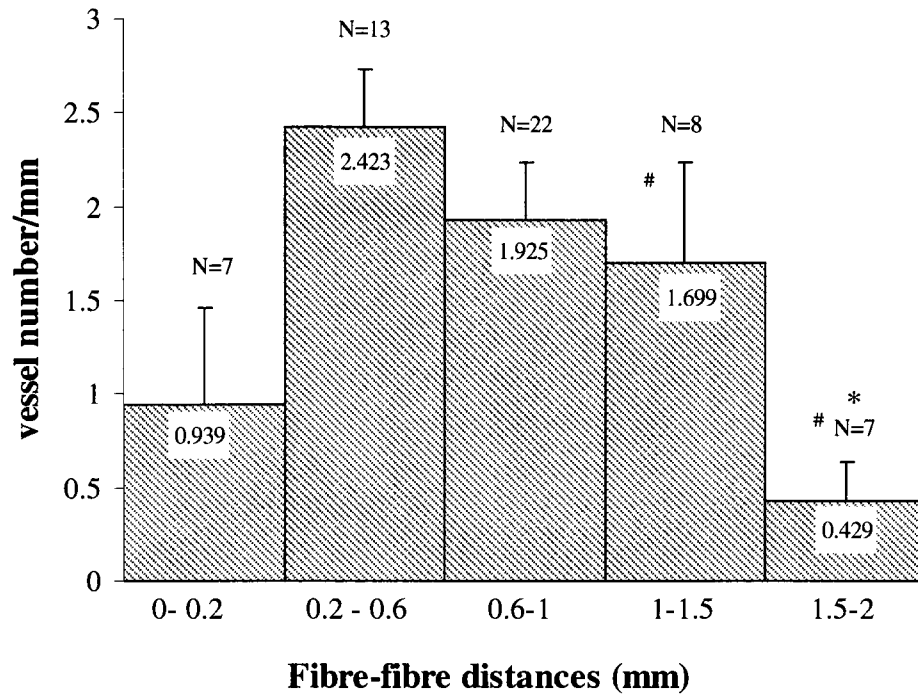
Figure 7.16: Number of microvessels relative to the range of distances between fibres, this quantification has been performed on specimens in cultures for a 14-21 day period. Covalently gelatin-grafted fibres (i.e. PET fibre + HApp + CMD + gelatin) were considered. The number of vessels has only been counted in face to face sides of the fibres. Short length sprouts have also been taken into account. Error bars represent standard errors of the mean (SEM), N is the number of fibres from 2 separated experiments, #N from one experiment. * indicates the values significantly different from the lowest distance (0.2-0.6 mm) by ANOVA at $p \leq 0.05$.
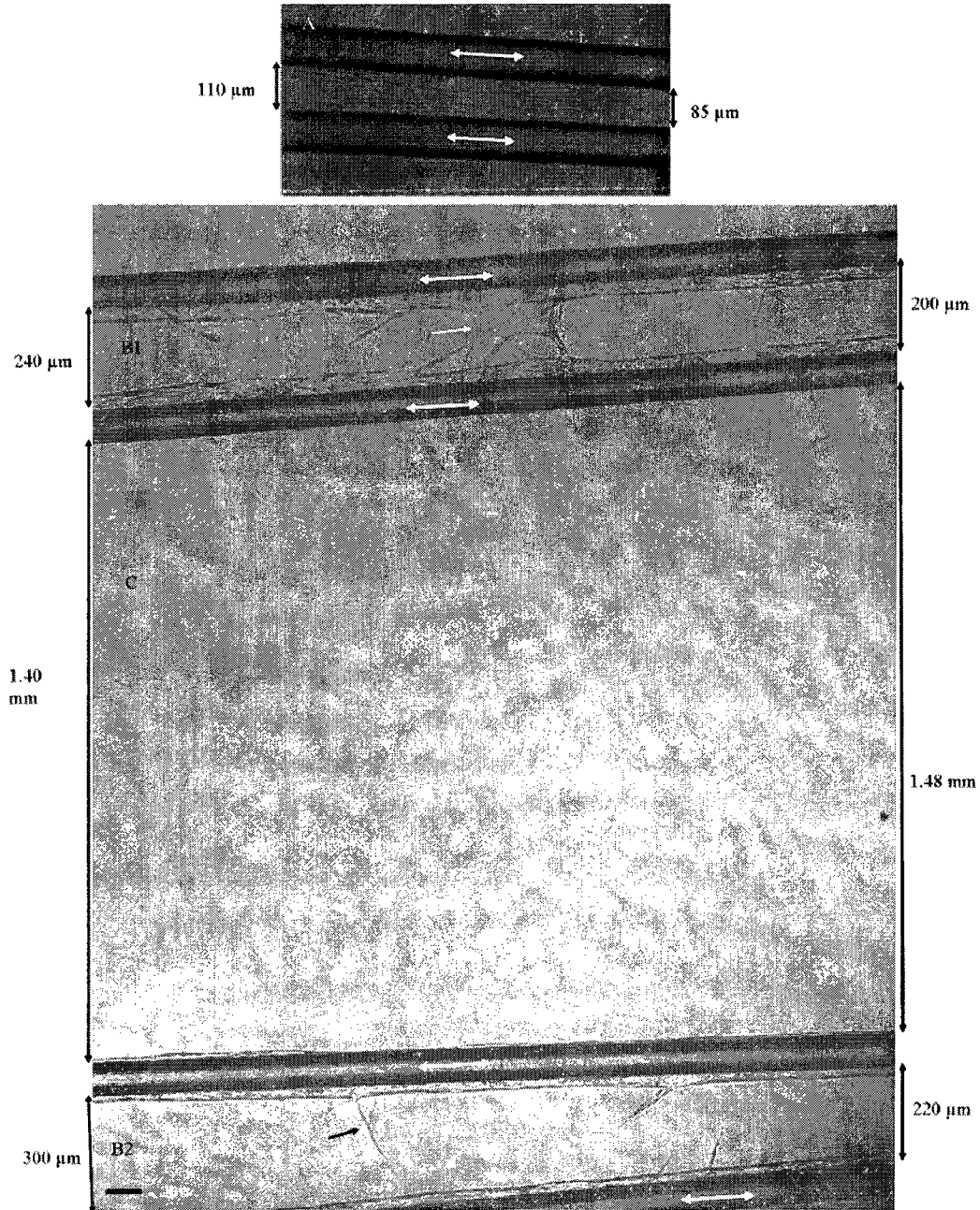
Figure 7.17: An example of the effect of fibre-fibre distances on microvessel formation. In A, fibres were distanced in space about 100μm. Two microvesssels with lumens that follow along the neiboring fibres and even connect to each other, In B1 and B2, the distance is below 300μm and vascular connection is observed, particularly close to a 200μm distance. In C, the distance is higher than 1mm which results in no vascular connection. The double-head arrows show the fibre and single- heads the microvessels. The pictures represent one experiment with three different fibres coatings, untreated, HApp- and gelatin-coated PET fibers, with triplicate samples (having similar results). Scale bar: 100μm

7.5. Conclusion

The two main goals of this study were (i) to investigate the feasibility of producing a pre-vascularized fibrin-based tissue construct *in vitro*, and (ii) to influence the guidance of vessels in a pre-determined direction using 100μm diameter polymer fibres. Using fibres, the whole angiogenic process can take place *in vitro* ranging from "sprouting" of HUVECs from cell pre-coated fibres (mimicking a pre-existing vessel) to tubes and through connections between branches as schematically presented in Figure 7.18. These two goals have been largely achieved by the use of surface modified polymer fibres on which covalently immobilized gelatin and RGD peptides facilitate and modulate the directional vessel formation within the 3D gel environment. Two 3D culture systems have been developed to investigate microvessel formation along the fibres, in optimal condition such as the presence of a fibroblast monolayer over fibrin gel. Moreover, the physical effect of fibres in conjunction with the surface chemistry of fibres enhanced microvessel formation *in vitro,* and allowed an interconnected microvessel network. Therefore, these specifically modified polymer fibres have interesting features towards tissue engineering such as the development of an *in vitro* prevascularized composite construct consisting of a biocompatible matrix (e.g. fibrin) and polymer fibres. Furthermore, production of directional vascularization within the construct may be subsequently employed to orient new tissue for replacement or substitution.
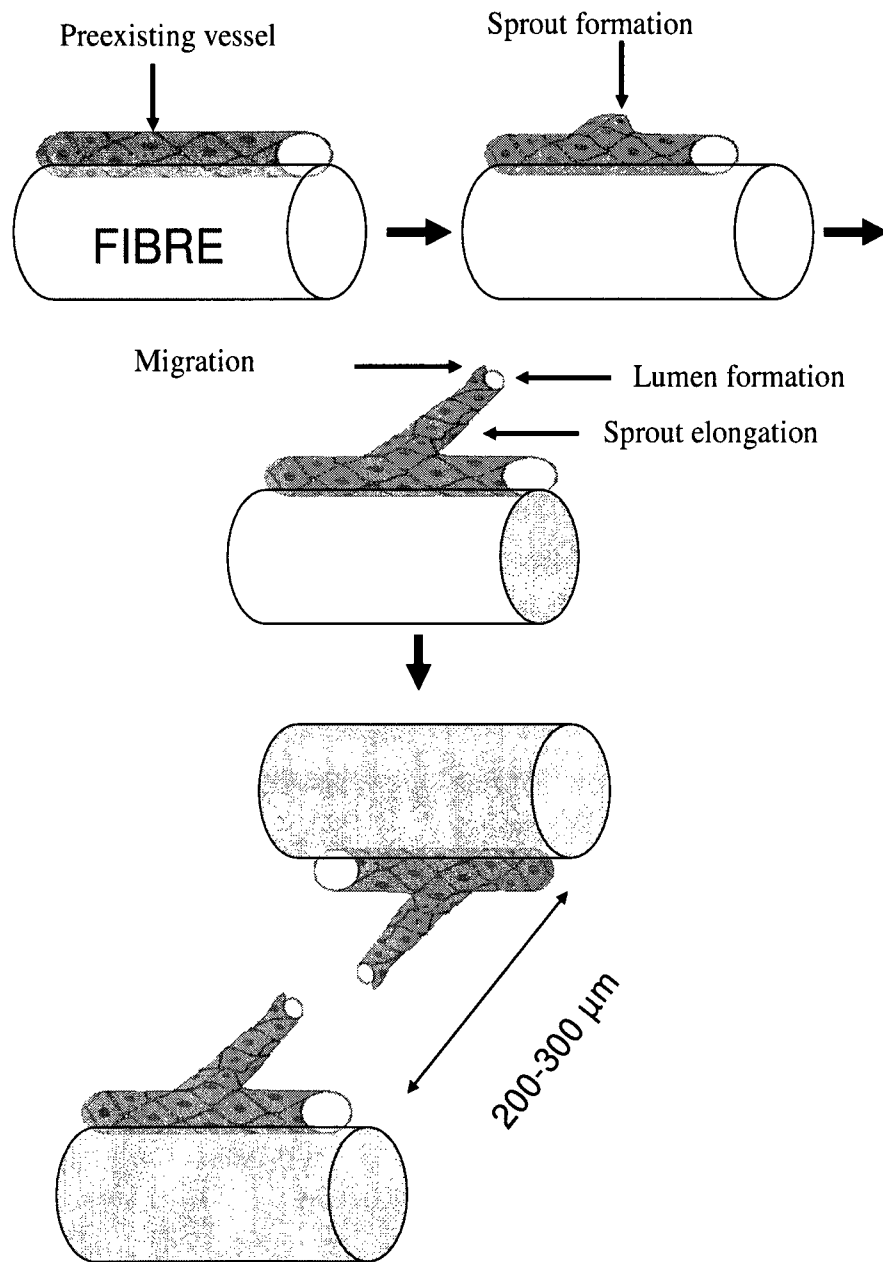
Figure 7.18: Schematic presentation of the microvessel network formed progressively in the fibrin-based constructs with fibres *in vitro*. By 14-22 days, connections between microvessels have been established. Presentation adapted from [website ref. 7].

Chapter 8

Preliminary study: Designing of a large-scale 3D composite scaffold involving bioactive polymer fibres, porous hollow membrane sheet and fibrin gel

8.1. Overview

The overall objective of this study is to design a 3D large-scale scaffold that will create a desirable directional condition firstly for blood microvessel formation and secondly to allow formation of tissue mass within a bioreactor. This aim can be achieved by designing of a 3D composite scaffold involving bioactive polymer fibre, porous hollow membrane sheet (PHMSH) and fibrin gel. The fabrication, characterization and evaluation of bioactive polymer fibres as well as the *in vitro* 3D tissue construct models have been explained in previous chapters of this thesis. In this chapter, first the design of a 3D scaffold is studied. Then, the preliminary results obtained in the design, fabrication and morphology analysis of a PHMSH as well as its behavior towards EC and fibroblast adhesion is presented. Finally, the future experimentation including characterization of the PHMSH and testing in a bioreactor, to complete this study, is briefly explained.

8.2. 3D scaffold designing

Based on previously developed the two *in vitro* 3D angiogenesis model (see Chapter 4 and 7 of this thesis) in which HUVECs form a directional angiogenic network when they were present on the surface modified polymer fibres between 2 layers of fibrin gel or embedded in it, we (Davod Mohebbi Kalhori and I) have proposed a sandwich-shape 3D composite scaffold for this study. In this scaffold the two above mentioned systems in conjunction with a PHMSH will generate a new approach to produce a large scale vascularised tissue mass. The reasons, for choosing the components of this proposed scaffold, are presented in Figure 8.1 (i.e. chart).

One of the issues in tissue engineering is the limitation in size of any tissue grown *in vitro*, even using a bioreactor. This is due to the lack of a capillary network for nutrient supply and waste product removal within the construct. To overcome this problem, fabrication of a capillary bed to supply engineered tissue as it grows in a bioreactor is essential. However, the technical construction of a capillary-like architecture is complex and chalenging. For this reason we have proposed to design a PHMSH.

In our design the bioactive polymer fibres (developed in this thesis), a PHMSH and a hydrogel will be combined to create suitable conditions for microvessel formation inside the 3D scaffold within a bioreactor to investigate microvessel and subsquent tissue formation under well-controlled physiological conditions. In this 3D scaffold, gel, as a soft matrix is expected to provide a desirable environment for microvessel formation in the extra-capillary space of the PHMSH during the bioreactor culture which should allow continuous nutrient supply from the perfused circulating medium. Cells are expected to orient onto the bioactive polymer fibres in the extra-capillary spaces. Nutrients and oxygen in the circulating medium

will diffuse through the PHMSH walls to nourish the cells. This scaffold design is a novel concept in tissue engineering. This is because, not only cells will be guided along a defined growth directions in a 3D environment, but also these scaffolds will allow nutrient supply and waste product removal within a large-scale 3D environment. This design can be unique approach for the generation of large-scale living tissues. This sandwich-shape 3D scaffold can be in flat or rolled format which their architecture is shown in figure 8.2.

Why this structure?

Because:

Micro-vessel	Directional	Large scale
↓ needs	↓ needs	↓ needs
Soft matrix	Directional stimulator	System for fluid flow and mass transport
↓	↓	↓
Gel	Bioactive polymer fiber	Porous hollow membrane

↓

Effective structure and easy way for fabrication of a composite scaffold?

↓

A sandwich shaped architecture
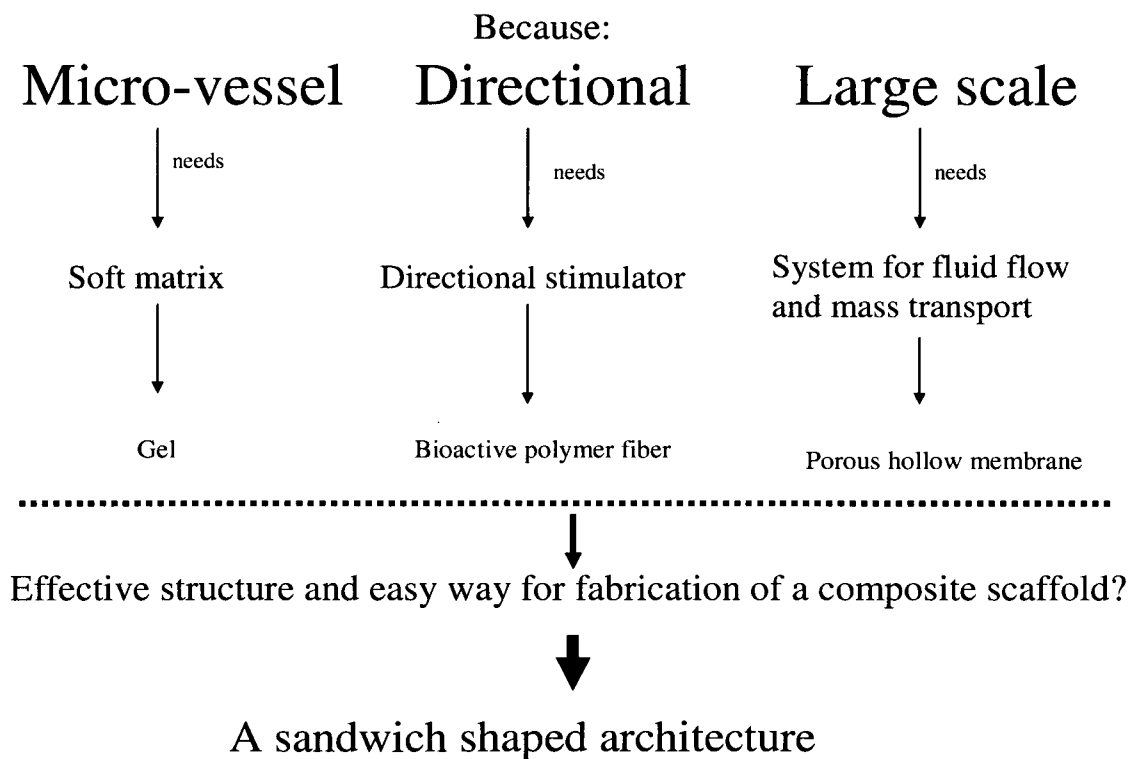
Figure 8.1: The chart represents the components and the purposes of our proposed 3D large-scale scaffold

207
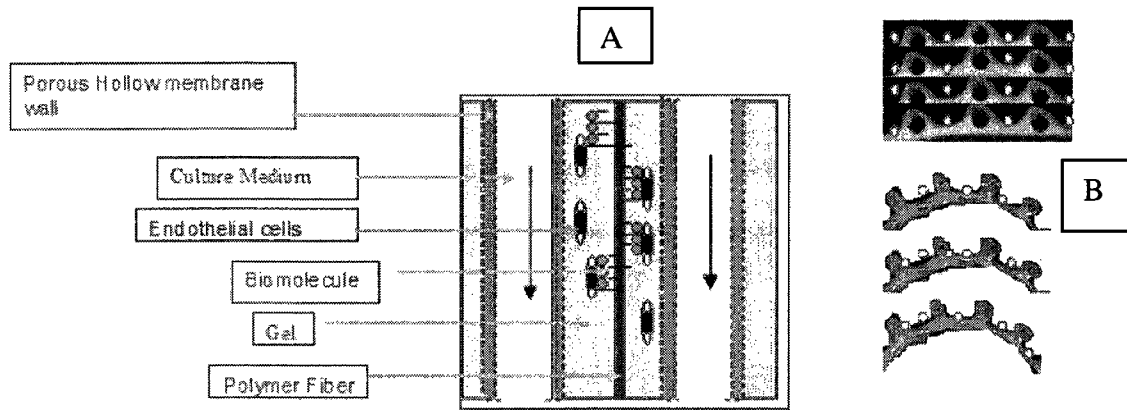
Figure 8.2: Components of 3D scaffold in longitudinal sectional view (A) and in cross sectional view (B)

8.3. Materials and methods

Bioactive polymer fibre, one of the components of this composite 3D scaffold, have been already fabricated and evaluated towards EC behavior in 2D cell culture system which has been published (HADJIZADEH, et al. 2007) and explained in this thesis as well. Moreover their effect in 3D cell culture system towards angiogenesis has been investigated (see Chapter 4 and 7 of this thesis). The PHMSH, the second component of this scaffold has been previously produced which is briefly explained below.

8.3.1. PHMSH fabrication

The material to be used should be sterilizable, biocompatible, biodegradable, and able to supply nutrients through porous tubing, mechanically strong, flexible and processable into desired 3D porous structure.

Based on desired properties (i.e. biodegradability and permeability, elasticity, mechanical strength, processing techniques and commercially availability), the selected polymers were

Poly (DL-lactide) (PDLLA) and Poly (ε-caprolactone) (PCL) blends, PDLA–co-PCL copolymer and PCL. PDLLA is a glassy polymer that is rapidly degraded due to its amorphous structure. However, PCL is rubbery. Simple blending between these two polymers results in a biodegradable material having a range of physical properties. Preparation of blends by solution is advatageous in comparion to the melting of mixed polymers, because melting at high temperature can cause degradation of aliphatic polyesters and transesterification between them. The considered dimensions and distances of the tubes in PHMSH are based on a primarily Computational Fluid Dynamics (CFD) study by the software of Fluent (data from Davod Mohebbi kalhori) and on acceptable distance to nourish cells (<500µm) as previously reported (EISELT, et al. 1998). Our design therefore considers tubes with an internal diameter below 1 mm, a wall thickness < 1 mm, and distances between tubes < 1 mm. In addition, this design should be available in several lengths to adapt according to their further applications. According to the above mentioned dimensions a mold has been designed and fabricated. Pieces and assembly are presented in Figure 8.3.
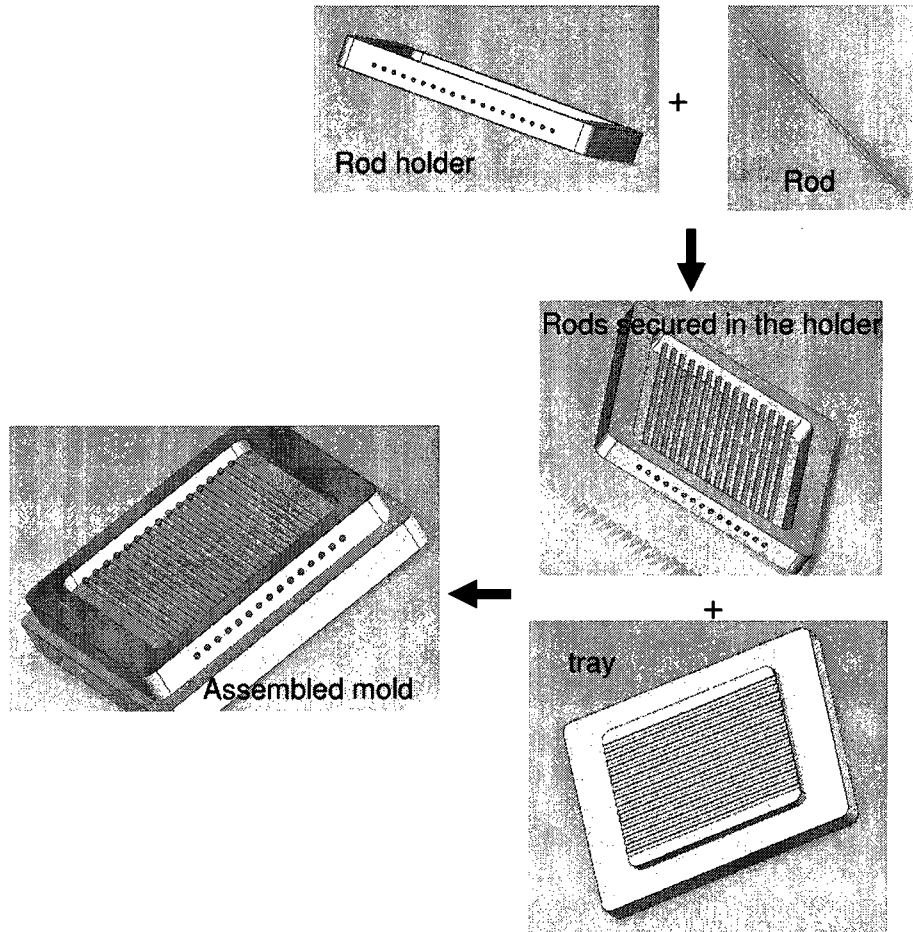
Figure 8.3: Pieces and assembly of mold designed for PHMSH fabrication (polymer solution casting). The pictures have been provided using the SolidWork software (drawn by Marc G. Couture).

The phase separation techniques from a polymer solution were considered to shape the PHMSH in the homemade mold and around rods. The phase separation techniques have been widely employed to fabricate porous architecture such as polymer membranes and scaffold for tissue engineering applications (DAY, et al. 2004; KIM, et al. 2004). Phase separation of polymer solutions can be induced by several methods such as air-casting of the polymer solution, immersion precipitation and thermally induced phase separation. The two first methods have been selected for design studied in this thesis. In the dry phase inversion

method, porous membranes were made by evaporating the solvent from a solution of PDLLA and PCL in acetone or methylene chloride. This technique (schematically) is shown in Figure 8.4.
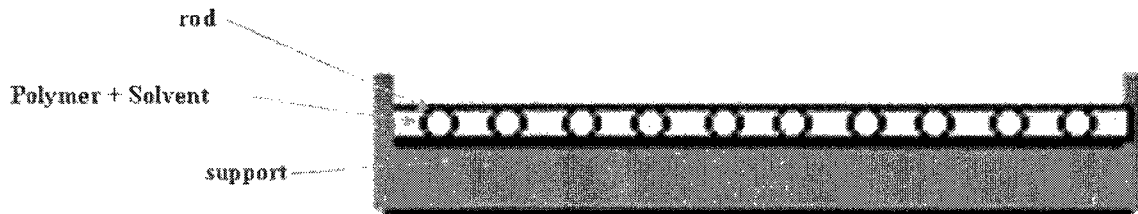
Schematic depiction of the air drying

Figure 8.4: Schematic representation of the system used in dry phase inversion method

The second method used was immersion precipitation. In this method, the polymer solution was cast as a thin film on our homemade mold, which was subsequently immersed in a non-solvent bath (i.e. water). Phase separation and gelation in solution were responsible for the pore generation and for the fixation of the porous morphology. In the preparation of porous PDLLA and PCL structures by the immersion precipitation method, 1,4-dioxane, chloroform, or acetone can be used as the solvent while water, methanol, or ethanol can be used as the non-solvent in a ternary casting solution. This technique is shown in Figure 8.5.
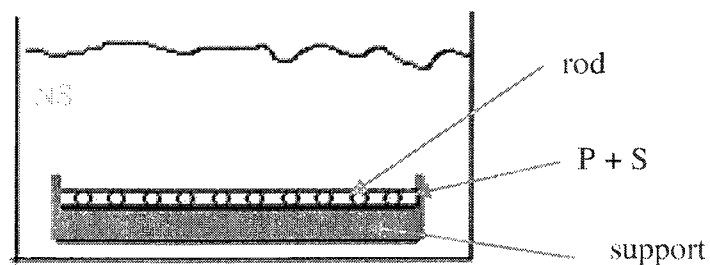
Figure 8.5: Schematic depiction of the immersion precipitation process: P, polymer; S, solvent; NS, nonsolvent

8.4. Preliminary results

Characterization

The SEM and optical microscopy images of PHMSH resulted in the air-drying method by using PCL or PCL + PDLA (4% w/v in chloroform) is shown in Figure 8.6. A flexible sheet containing tubes can be produced by this method which can be rolled without any fracture or breaking. According to SEM analysis this sheet contains small pore size around 1 μm.

SEM   Optical microscopy
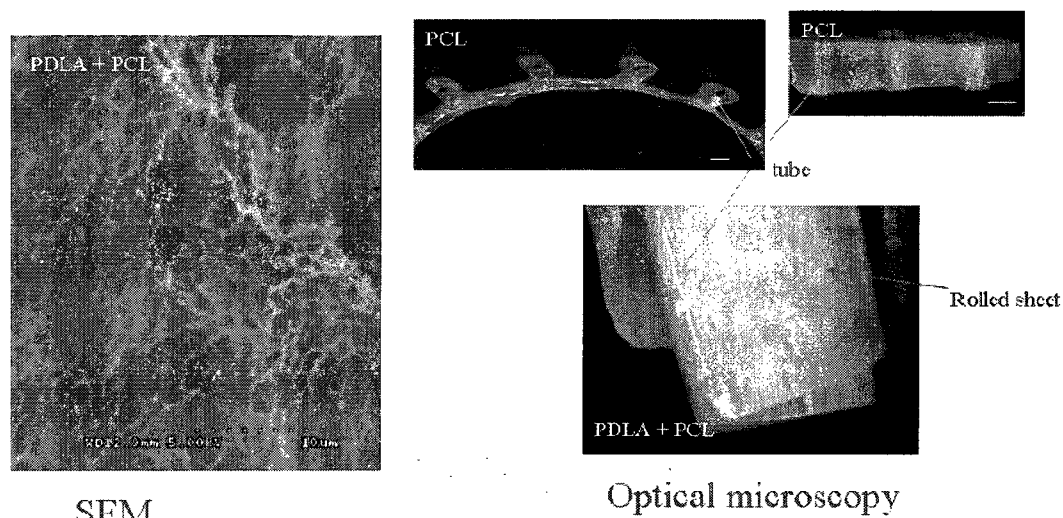
Figure 8.6: Microscopic pictures of PHMSH made by PCL and PCL + PDLA resulted from air-drying method

The SEM and optical microscopy images of PHMSH resulted in immersion precipitation process by using PCL (4% w/v in chloroform) and using water as non-solvent is shown in figure 8.7. This PHMSH has foam-like appearance and it is flexible which can be bended or rolled without being damaged. According to SEM analysis, this sheet had a well porous structure. This sheet contains hollow fibre- like tubes (Fig. 8.7A) with open pores which can

be seen on cross section (Fig. 8.7A) inside the tube (Fig. 8.7B) and on the back side of the

sheet (Fig. 8.7C).
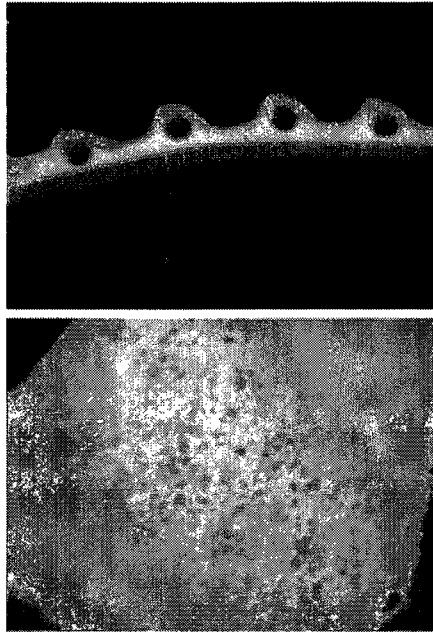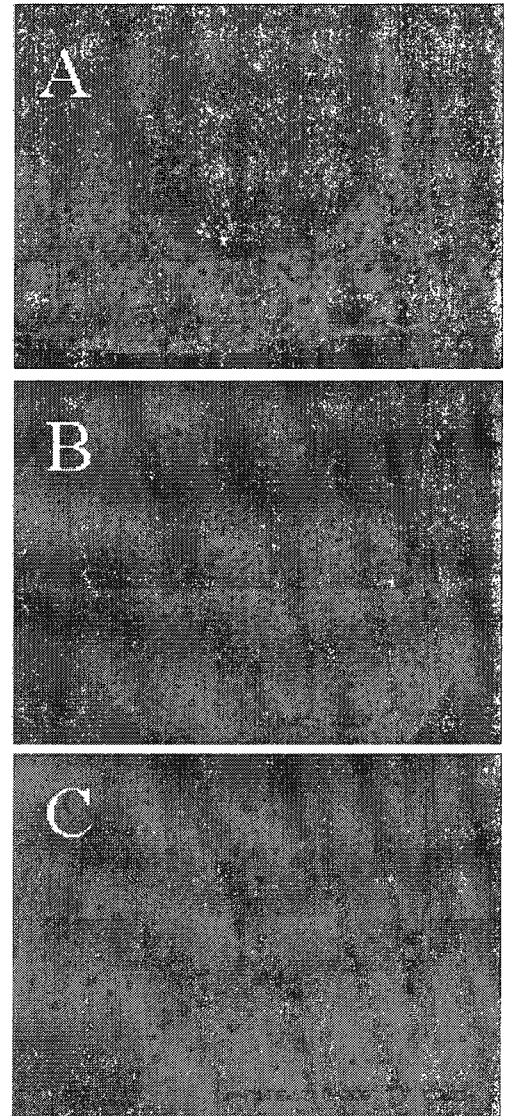
Figure 8.7: SEM and optical microscopic pictures of PCL membrane obtained by immersion precipitation method

Cell culture in static system

To investigate the cell response towards our PHMSH, HUVECs and fibroblast were seeded onto it in static cell culture system. None of the two cells types were attached to the sheets, but when the same membrane was coated with HApp the both cell types were considerably attached on it (Fig. 8.8).

Moreover by adapting to our third system of angiogenesis, developed in this thesis (see Chapter 7) a co-culture cell seeding by using 50% HUVECs and 50% fibroblast cells (with a cell density of 10^6 cells/ml were performed on RGD coated PET fibres, as developed in my thesis and previously published (HADJIZADEH, et al. 2007). These fibres were then embedded in fibrin gel. In an 11 day culture period a layer of fibroblasts were formed (Fig. 8.9 gray color) containing microvessel-like structures, formed by HUVECs (Fig. 8.9 red color, stained by Dil-acetylated LDL). All these preliminary observations demonstrate that our composite scaffold (i.e. comprising PHMSH, polymer fibre and fibrin gel) can be further applied to investigate multicellular tissue fabrication in a bioreactor system.
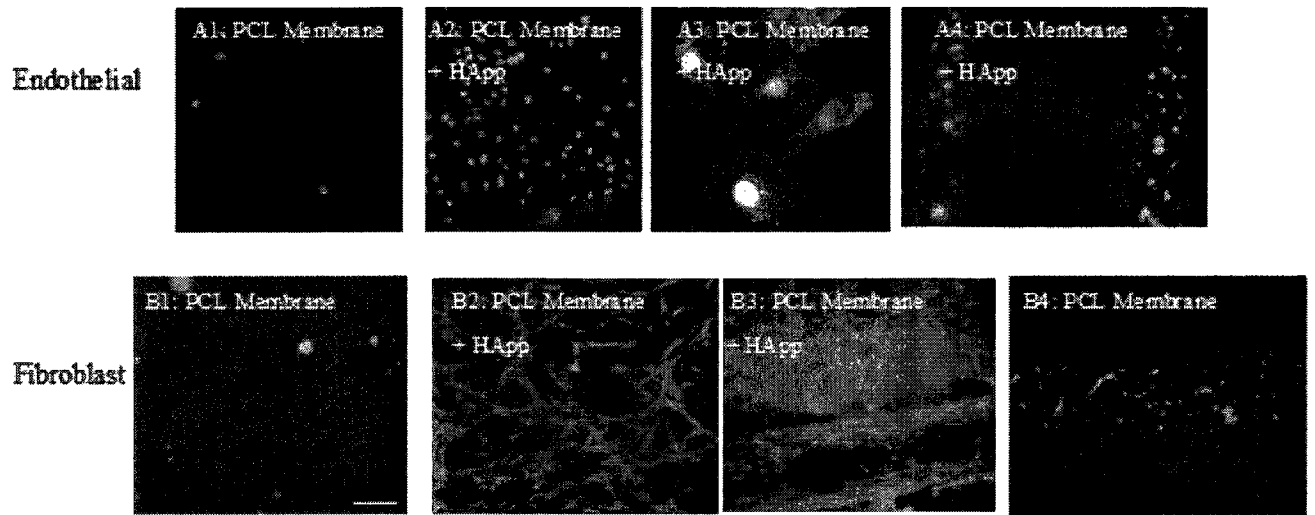
Figure 8.8: Endothelial and fibroblast adhesion on PCL PHMSH: Observation by epifluorescence microscopy of PCL PHMSH seeded by EC (A1-4) and fibroblast (B1-4). In A1-4, B1 and B4 cells stained with Sytox Green to highlight the position of the nuclei. In A3 cells stained using TRITC–phalloidin, and counterstained with Sytox Green. In B2 and B3 cells stained with calcein AM. In A4 and B4 cells were injected inside the tubes of PHMSH but in the others cells were seeded on the PHMSH. The pictures A1-3 and B1-2 have been previously published (HADJIZADEH and VERMETTE 2007).
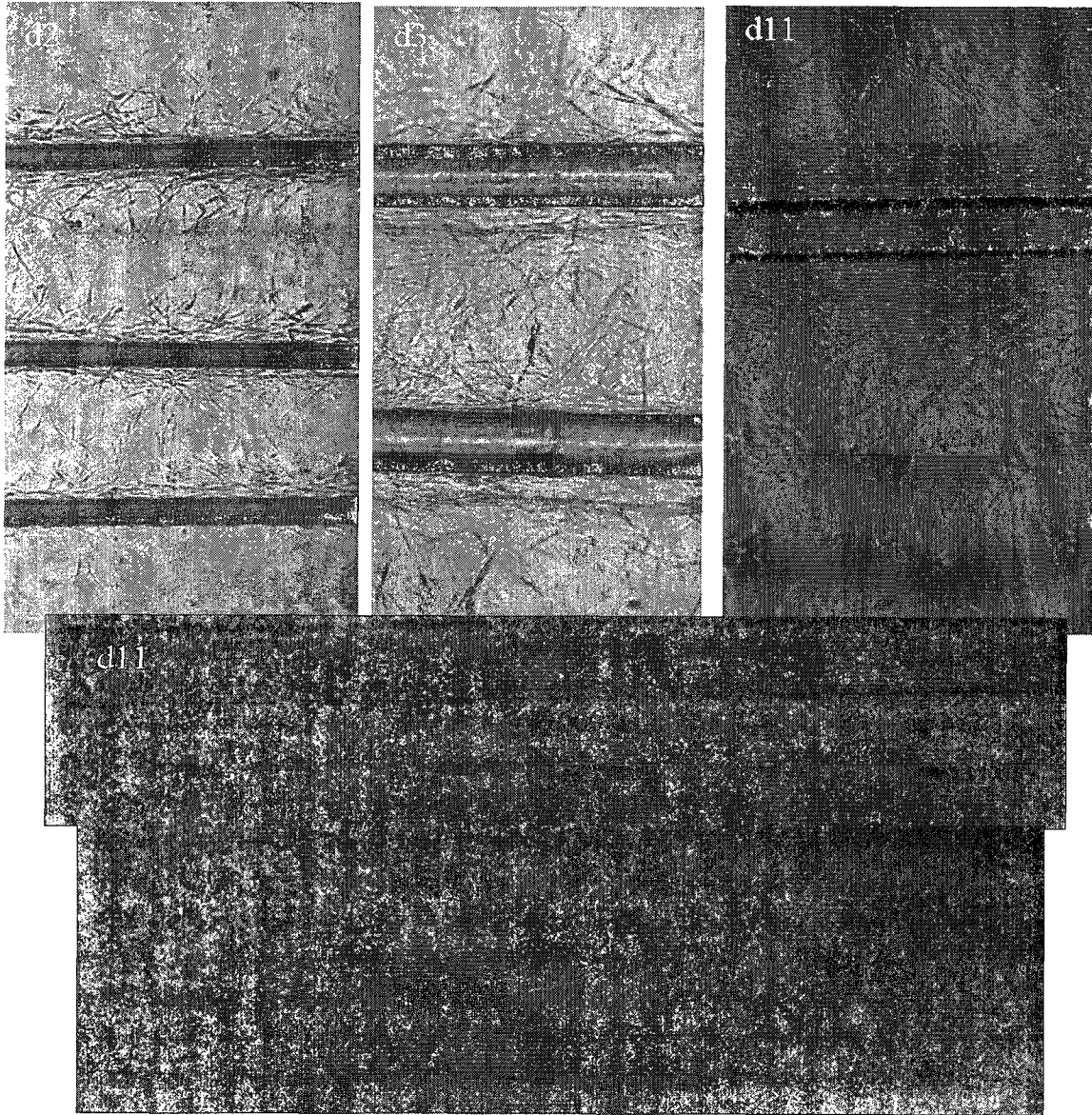
Figure 8.9: EC and fibroblasts (50:50 %, co-culture) were seeded on RGD-coated polymer fibres then embedded in fibrin gel (performing the third system). Phase contrast microscopy images show fibroblasts around the RGD-coated PET fibres after 2 (d2), 3 (d3) and 11 days (d11) and after Dil-acetylated LDL uptake at day 11 of culture (d11, red color). Fibre diameter: 100µm.

8.5. Future experimentations

PHMSH characterization

Determination of porosity, mechanical properties and degradation will be performed in future experiments.

Cell culture test in bioreactor

Finally, the 3D scaffold will be tested in bioreactor culture. A chamber has been previously designed (data from Davod Mohebbi Kalhori and myself) and made for bioreactor cell culture testing of the PHMSH and then the above mentioned 3D composite flat shape scaffold.
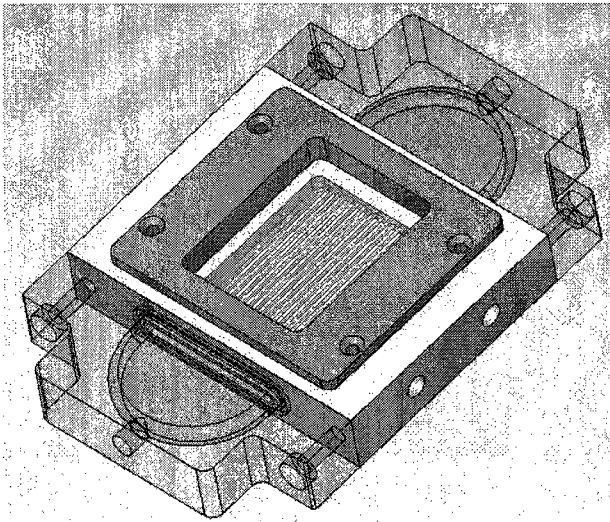
Figure 8.10: Chamber for cell and tissue culture in bioreactor (data from Davod Mohebbi Kalhori and myself)

8.6. Conclusion

The findings in previous chapters of this thesis were used for designing and fabrication of a large scale, sandwich-shape 3D composite scaffold. The preliminary results obtained by SEM analysis and cell culture testing demonstrated the successful design, fabrication and evaluation of the PHMSH which is the main part of the composite scaffold. In this scaffold, our *in vitro* 3D angiogenesis models in conjunction with the PHMSH will generate a new approach to produce a large scale vascularised mass-like tissue.

Chapter 9

Conclusion and perspectives

9.1. Conclusion

In order to enhance vascularization in engineered tissue constructs, several approaches are currently under investigation. Biomaterials in the form of scaffolds are currently the subject of intensive research on this matter. These include; enhancing the capability of scaffolds to induce vascularization with the incorporation of ECM compounds and, angiogenic growth factors, as well as modifying the architecture and biomechanics of scaffolds. However, in order to induce prompt vascularization, needed to supply oxygen for the cells within a scaffold on its implantation in the host, a tissue construct or scaffold should be able to be vascularized in vitro, prior to implantation. Therefore, in this research project, fibrous scaffolding materials have been fabricated and then *in vitro* angiogenesis models have been developed to guide vascularization within a 3D environment. Such developments create a desirable directional condition for blood microvessel formation. Therefore, the aim of this study was to investigate the possibility of producing surface modified polymeric fibres, with the capability of both directional EC patterning and of inducing angiogenesis in a 3D cell culture system. This is the goal for developing an *in vitro*, prevascularized 3D scaffold, made of a fibre network. The fibres were surface coated with an ECM component, RGD peptide or gelatin. Then, by the use of these fibers, exhibiting the phenomenon of contact guidance to modulate the 3D patterning of EC, the directional angiogenesis *in vitro* was created. These approaches have been achieved through following three specific objectives in this study:

1) Surface modification and characterization of flat and fibrous materials, with both cell resistant and cell adhesive compounds, to produce controlled biological responses.

2) *In vitro* evaluation of surface modified substrates towards the EC behavior in a 2D cell culture system.

3) *In vitro* evaluation of surface modified polymer fibres towards a more complex EC behavior (i.e. angiogenesis) in a 3D cell culture system.

These studies and their results for each step have been summarized in the paragraphs below.

Surface modification and characterization of materials, more specifically polymeric fibre surfaces, with cell adhesive, cell non-adhesive and bioactive compounds

Surface chemistry; physics and topography can all control the behaviours of different cell types on polymeric materials at the cell-biomaterial interface. To achieve controlled and predictable biological responses, the surface of polymer fibres were pre-coated with a layer of the desired biomolecule, using a multilayer surface coating strategy, that exhibited predictable biological responses. This surface modification consists of the following steps and aims:

1) HApp or AApp was deposited onto the surfaces as a thin polymeric interfacial layer having amine or aldehyde groups, respectively, by RFGD deposition. These coatings offer two advantages; i) introduction of new functional groups (i.e. the amine or aldehyde) for the covalent grafting of a desired second layer (e.g. CMD), and ii) altering physicochemical properties of the surface to increase the cell adhesion.

2) CMD has been covalently immobilized onto the amine functional groups, present on the substrate surfaces via water-soluble carbodiimide chemistry

(EDC/NHS). Prior to the CMD grafting, the acetaldehyde coated surfaces were amine functionalised by on-the grafting of PEI layers. Here, the CMD layer plays two roles; i) prevent surface fouling towards proteins and cells, and ii) introducing -COOH functional groups in order to covalently immobilize bio-active molecules.

3) Finally, biological molecules, such as the RGD peptides, have been covalently immobilized onto the surface carboxylic acid groups (COOH), present on the surfaces, again, by use of water-soluble carbodiimide chemistry (EDC/NHS). This coating enables the surface to exhibit an integrin stimulated, cell adhesion.

The characterization of surface chemistry and topography, using XPS, AFM and SEM respectively, shows that the multilayer production steps were effective. XPS analyses revealed that HApp and AApp, using the RFGD method, can be deposited on different substrates with distinct rigidity and shape. Substrates include: - polymer fibre, porous and non porous polymeric films and non polymeric, flat surfaces. Moreover, XPS characterization of PTFE and borosilicate, which have specific elemental signals (fluorine and silicon respectively) clearly demonstrate the formation of uniform films, thicker than 10 nm, in both HApp and AApp surface coatings.

CMD was successfully grafted covalently onto the surface amine groups, being available on the HApp and AApp + PEI coated surfaces, as demonstrated by the XPS analysis. It has also been found that CMD, with a molecular weight of 70kDa, and a CMD solution concentration of 2 mg/ml, generate more uniform and thicker films, in comparion to that of CMD, with the same molecular weight, at a solution concentration of 1 mg/ml, in immobilizing, both on the HApp and the on AApp + PEI. The XPS C1s spectrum of CMD

221

indicates that the CMD bound on the AApp-coated surface, via a PEI spacer layer, creates a thicker and more effective layer than the same CMD, when directly attached to the HApp surface.

According to the XPS analysis, covalent immobilization of RGD onto the CMD coated surface was deemed to be successful, as the N/C atomic ratio increased on the RGD immobilized surface, in comparison to the CMD coated surface. In addition, by increasing the concentration of the RGD solutions, from 0.1 to 1 mg/ml, the N/C atomic ratio also increased, thus demonstrating an increase in the density of the covalently grafted RGD on the surface. This technique can be applied to produce surfaces with the capability of integrin-stimulated cell adhesion.

The existence of thin films obtained by plasma deposition, and subsequent surface CMD immobilization, as determined by SEM and AFM, produced topographic maps of the analyzed surfaces and provided qualitative information on the different coatings. The AApp plasma-deposited and CMD-coated surfaces were more rough, in comparison to the other surface modifications.

Therefore, in conclusion, these multistep surface fabrication techniques can be applied to produce biomaterials with multifunctional surfaces that can have important applications in tissue engineering, especially as scaffolding materials for tissue generation.

In vitro evaluation of surface modified polymer fibres towards EC behavior in a 2D cell culture system.

Control over cell behavior such as the adhesion, spreading, proliferation and orientation, by modifying the surface properties of biomaterial (e.g. scaffold), plays an important role in the formation of living tissues. The presence of micro-curvature and bio-signals on a surface allows the control of cell-substrate interaction to create patterns of oriented cells.

The biological properties of surface modified polymer fibres (PET and ePTFE) were validated towards the behaviour of HUVECs in a 2D *in vitro* system. For this purpose, HUVECs were used to investigate cell responses (i.e. adhesion, spreading, and orientation) as a function of the fibre surface properties. As expected, the cell adhesion was reduced on CMD-coated fibres, whereas aldehyde-, amine-, gelatin- and GRGDS-coated fibres promoted cell adhesion and spreading. Conversely, cell adhesion on the GRGES-coated fibres (in-active peptide control) was significantly lower than that observed on GRGDS-coated fibres. These observations suggest that the EC adhesion promotion on RGD-coated polymer fibres can be attributed to the biospecific responses of cell surface integrins towards RGD ligands present on the surfaces. On these fibres, cell adhesion increased by increasing the GRGDS solution concentration from 0.1 to 1.0 mg/ml. The formation of well-defined stress fibers and strong vinculin spots (typical of FAs) on RGD-coated substrates, demonstrated a strong cell adhesion on this coating. In addition, the cells showed a more oriented morphology along the fibre axis in comparison to flat surface substrates, and this became increasingly evident in long-term cell cultures. In addition, it was observed that in comparison to the surface features (i.e. roughness) surface chemistry was the dominant parameter in inducing HUVEC adhesion and spreading. More importantly, this study points out the suitability of RF heptylamine and acetaldehyde plasma polymerization, in inducing desirable coatings on substrates, with the subsequent

ability to support the attachment and spreading of HUVECs. In order to ensure the performance and reproducibility of this multilayer surface modification technique, and to further characterize the cell response to the coatings generated by this technique, flat substrates were surface coated and cell culture tested, in the same manner as PET and PTFE polymer fibres. All results obtained were in agreement with each other, thus demonstrating reproducibility of these multilayer steps, surface modifications.

In vitro evaluation of the surface modified polymer fibres towards complex EC behavior (i.e. angiogenesis) in a 3D cell culture system

The two main goals of this study were; (i) to investigate the possibility of producing pre-vascularized *in vitro* 3D tissue constructs, and (ii) to influence the guidance of vessels in a pre-determined direction, using 100μm diameter polymer fibres, being distanced one from the other. Using fibres, an angiogenic process can take place *in vitro*, ranging from tube formation by HUVECs to the connections made between branches. These behaviors have been achieved in particular by the use of surface modified polymer fibres on which gelatin and RGD peptides were covalently immobilized, via HApp and CMD interlayers, to encourage and modulate directional vessel formation within the 3D environment of the construct. Among the three different *in vitro* fibrin-based systems, used to investigate angiogenesis along the fibres, only two systems worked well. In addition, the presence of fibroblasts over fibrin gel promoted the formation of the microvessels. The physical effect of fibres, in conjunction with the surface chemistry of the fibres, influenced in *vitro* microvessel formation, as observed in both systems. The prolongation of the culture period allowed the formation of a network in which microvessels, connected to each other, from one fibre to another, following efficient fibre

spacing, ranging from 200 to 600 μm. Therefore, these specifically modified polymer fibres, have interesting features towards tissue engineering. These include (i) the development of an *in vitro* prevascularized system composed of a biocompatible matrix (e.g. fibrin) and polymer fibres, and (ii) the production of a directionally vascularized tissue construct, which can subsequently be employed to produce directional orientation of tissues.

In conclusion, I have developed a new approach that can be applied in therapeutic angiogenesis and prevascularised tissue engineered construct fabrication. In addition, this strategy can also be a suitable *in vitro* system to evaluate the angiogenic ability of ECM components, (investigated for RGD and gelatin in this thesis). Moreover, each of the multilayer surface modification steps (i.e. plasma polymerization, non fouling material coating and biomolecule immobilization), can be applied for various purposes in tissue engineering.

Furthermore, the research findings, as mentioned in the three above sections, were used to design and fabricate a large scale, sandwich-shape, 3D composite scaffold. This scaffold design has been based on our two *in vitro* 3D angiogenesis models, in which HUVECs form a directional angiogenic network, when they are present on the surface modified polymer fibres between 2 layers of fibrin gel or when HUVECs are pre-coated onto the fibres bearing cell-adhesive coating and embedded in the fibrin gel. The preliminary study shows that, in this scaffold, the two above mentioned systems in conjunction with a PHMSH will generate a new approach to produce a large scale, vascularised mass-like tissue.

It should be noted that, in this study, the idea of using polymer fibre (100-μm diameter), for both EC patterning and inducing angiogenesis, is quite original. Moreover, polymer fibre surface modifications, using multilayer surface coatings, including cell adhesive plasma polymers (i.e. HApp and AApp), non cell adhesive material (i.e. CMD), and bioactive

molecules (i.e. RGD), have not previously been reported by others. In addition, the physicochemical characterization of these fibre surface coatings, as well as their influence on EC behaviours (i.e. cell adhesion, spreading and patterning) in 2D cell culture system and toward the angiogenesis in the two above mentioned 3D cell culture systems (i.e. using hydrogel), have not been reported elsewhere. The 3D large scale scaffold design, the PHMSH design and fabrication and the bioreactor chamber design and construction, all are truly new approaches achieved in this study (by the contribution of Davod mohebbi kalhori).

9.2. Perspective study

RGD-grafted polymer fibres in induction and guidance of angiogenesis *in vitro* and *in vivo:* The effect of peptide surface density

In this study, RGD peptides will be immobilized on surface functionalized polymer fibres in the same way as explained earlier in this thesis, in using various RGD solution concentrations in order to produce distinct, RGD surface densities. The different densities of the RGD present on the surface will be determined by the use of tagged molecules (e.g. fluorinated tag molecules) and XPS analysis. The RGD-coated fibres will then be tested in a 3D cell culture system (by performing the models developed in this thesis, i.e. the second and third systems, as explained earlier) and also in *in vivo* models. The latter will have to be developed further.

Chapter 10

Appendix

10.1. Analytical techniques used for surface characterization

The base of the techniques employed for the characterization of surface modified materials, in this thesis, is briefly explained in the following paragraphs.

10.1.1. X-Ray Photoelectron Spectroscopy (XPS)

XPS operates based on photoemission of core-level electrons in an atom. Energetic X-rays with energy (hv) strike an atom and liberate core-level electrons, with adequate kinetic energy (E_K) to escape from the material surface. Figure 10.1 schematically shows the photoemission process within an atom. These electrons will pass through the vacuum chamber to the energy spectrum analyzer, for which the E_K will be measured. The binding energy (E_B) is determined according to the energy balance, as presented in figure 10.2, and the data are typically collected as survey spectra spanning the E_B range of about 10 to 1000 electron volts (eV). Then high-resolution spectra can be collected in a region of interest to look at carefully for the fine structure of typical core-level peaks (e.g. carbon 1s, oxygen 1s, *etc.*). Typical C1s and O1s E_B values for the chemical groups present in polymers can be found in typical tables in the references (RATNER and CASTER 1997).
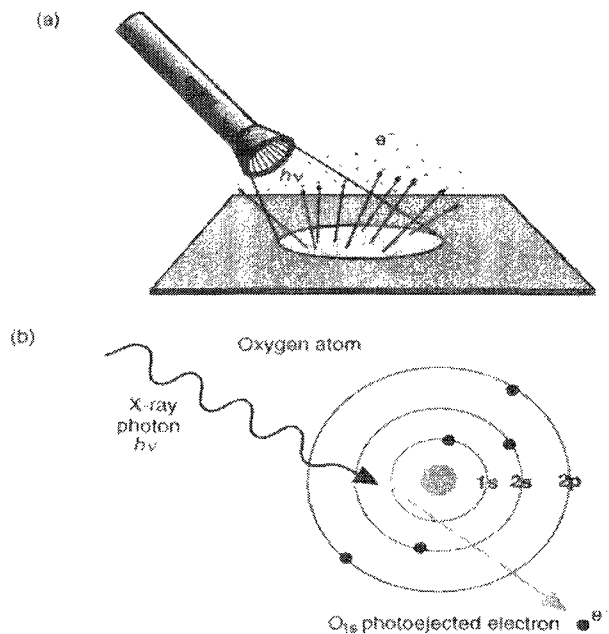
Figure 10.1: (a) A surface striked by a high energy photon source will emit electrons. If the light source is in the X-ray energy range, this is the XPS experiment. (b) The X-ray photon transfers its energy to a core-level electron and generates a photoelectron (reproduced from RATNER and CASTER 1997).

$$h\nu = E_B + E_{Kin}$$

Figure 10.2: Energy balance for the process described by (Einstein in 1905). Where E_B is the binding energy of the electron in the atom (a function of the atom type and its environment), $h\nu$ is the energy of the X-ray source, and E_{kin} represents the kinetic energy of the ejected electron from the atom which is measured in the XPS spectrometer (RATNER and CASTER 1997).

10.1.2. Scanning Electron Microscopy (SEM)

SEM uses electrons to create an image. In SEM analysis the sample (coated with a very thin electrically conductive layer (e.g. gold or platinum) by a sputter coater) is placed inside

229

the microscope's vacuum column. Once the electron beam strikes the sample, the electrons and

X-rays are ejected from the sample, as shown in Figure.10.3 [website ref.8].

Incident Beam

X-rays

primary backscattered electrons

Auger electrons

secondary electrons
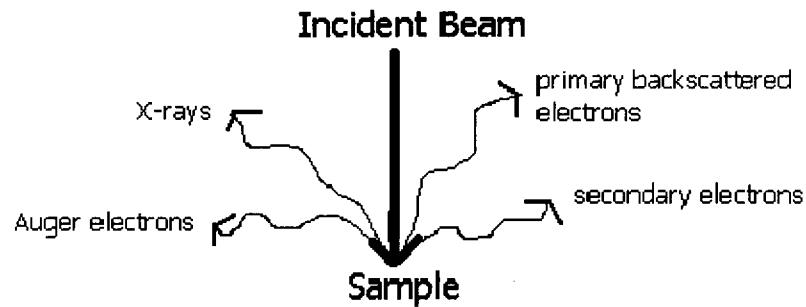
Sample

Figure 10.3: Ejection of secondary electrons, backscattered electrons, Auger electrons and X-rays from the sample when electron beam hits the sample in SEM analysis [reproduced from website ref. 8].

Among them secondary electrons are used for surface morphological analysis which are collected by a detector and transformed into a signal that is sent to a screen to appear as a 3D image [website ref.8]. Secondary electrons refer to those electrons of the test specimen that are pushed out of the atom by electron beam, and exit the surface of the sample [Website ref.9].

Secondary
Electrons

Electron
Beam

Electrons

Nucleus
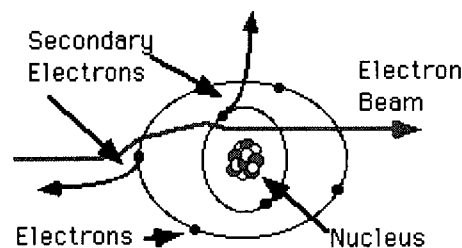
Field Emission Gun Scanning Electron Microscope (FEGSEM)

Cold cathode field emission microscopy is a new generation of SEM for which the resolution and beam density (brightness) is higher than that of a conventional SEM. Moreover, the tip life is longer than Thermal Tungsten wire SEMs (conventional SEM) [website ref. 10].

230

10.1.3. Atomic force microscopy (AFM)

Surface texture measurements

The full characterization of the surface texture becomes easy and precise by direct visualization of a surface. AFM has been developed for this purpose, especially in those cases that the surface feature sizes are of nanometric scale [Website ref.11]. Topographical imaging of a surface with atomic-level resolution on rigid materials can be performed by AFM. In surface analysis by AFM, laser light, is reflected from a microfabricated cantilever, of typical spring constant (0.1-1 Nm^{-1}). The deflection of the cantilever is recorded by a photodetector. The cantilever has a tip that comes very close to the surface and scans the surface in both the x and y directions. A feedback system keeps a constant force on the sample by means of a fixed laser beam on the photodiode. At the same time, piezoelectric translators adjust the z-axis of the sample to complete the processes (LEGGETT 1997).
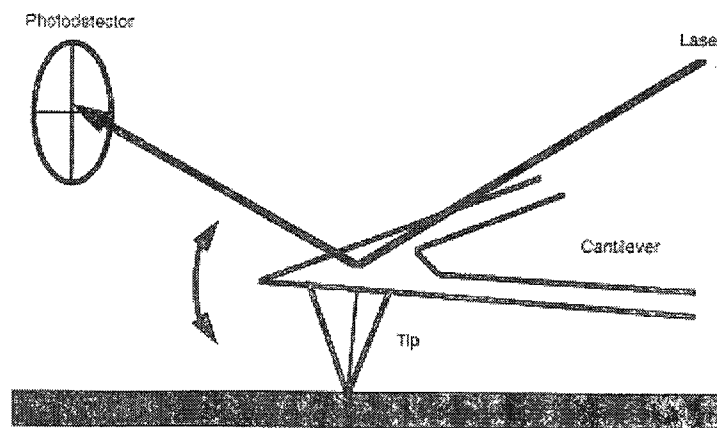
Figure 10.4: Schematic representation of the operation of the AFM (reproduced from LEGGETT 1997).

10.2. Mechanisms of reactions in carbodiimide coupling using EDC/NHS

The formation of amide bonds between carboxylic acids (COOH) and amines (NH_2) can be catalyzed by carbodiimide, forming an O-urea derivative. This derivative is prone to the nucleophillic attacks by nucleophilies (basic, electron-rich reagents that tend to attack the nucleus of carbon) resuling in forming amide bonds. 1-Ethyl – 3-(3- dimethylaminopropyl)– carbodiimide (EDAC) is a water–soluble derivative of carbodiimide, widely used for this purpose [Website ref.12].

EDC
1-Ethyl-3-(3-dimethylaminopropyl)
Carbodiimide. Hydrochloride
MW 191.7
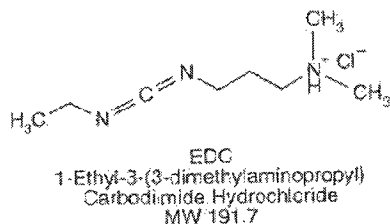
N- hydroxysuccinimide (NHS) has been used to accelerate the carbodiimide coupling in the presence of EDC. In this reaction, the carboxylic group and NHS condense and produce an active ester (as an intermediate), which subsequently produces the final amide bond by reacting with the amine group. Figure 10.6 shows the mechanism of the carbodiimide coupling reaction provided by EDC and promoted by NHS (HERMANSON 1996).

N- Hydroxysuccinimide (NHS)

232
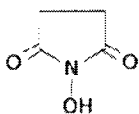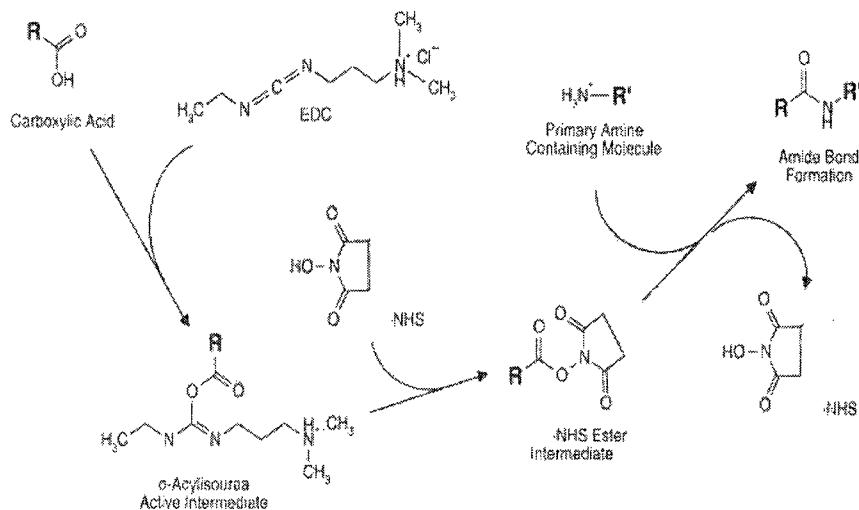
Figure 10.5:   The mechanism of the carbodiimide coupling reaction provided by EDC and promoted by NHS (reproduced from HERMANSON 1996).

10.3. Materials

10.3.1. CMD characterization

The degree of carboxylation was assessed using 1H NMR. The NMR spectra of the two CMDs, 70 kDa and 500 kDa MW, are shown in Figure 10.7. The experimentally determined ratios were ca. 1 carboxyl groups per 2 sugar units.

Nuclear magnetic resonance (NMR)

High-resolution NMR spectroscopy is able to quantitatively identify nuclei and their environments in a polymer molecule. Proton NMR (1HNMR) is commonly used for the characterization of polymers. The proton ([1]Hydrogen nucleus) is the most sensitive (apart from tritium) nucleus and is known to produce strong signals [Website ref. 13].
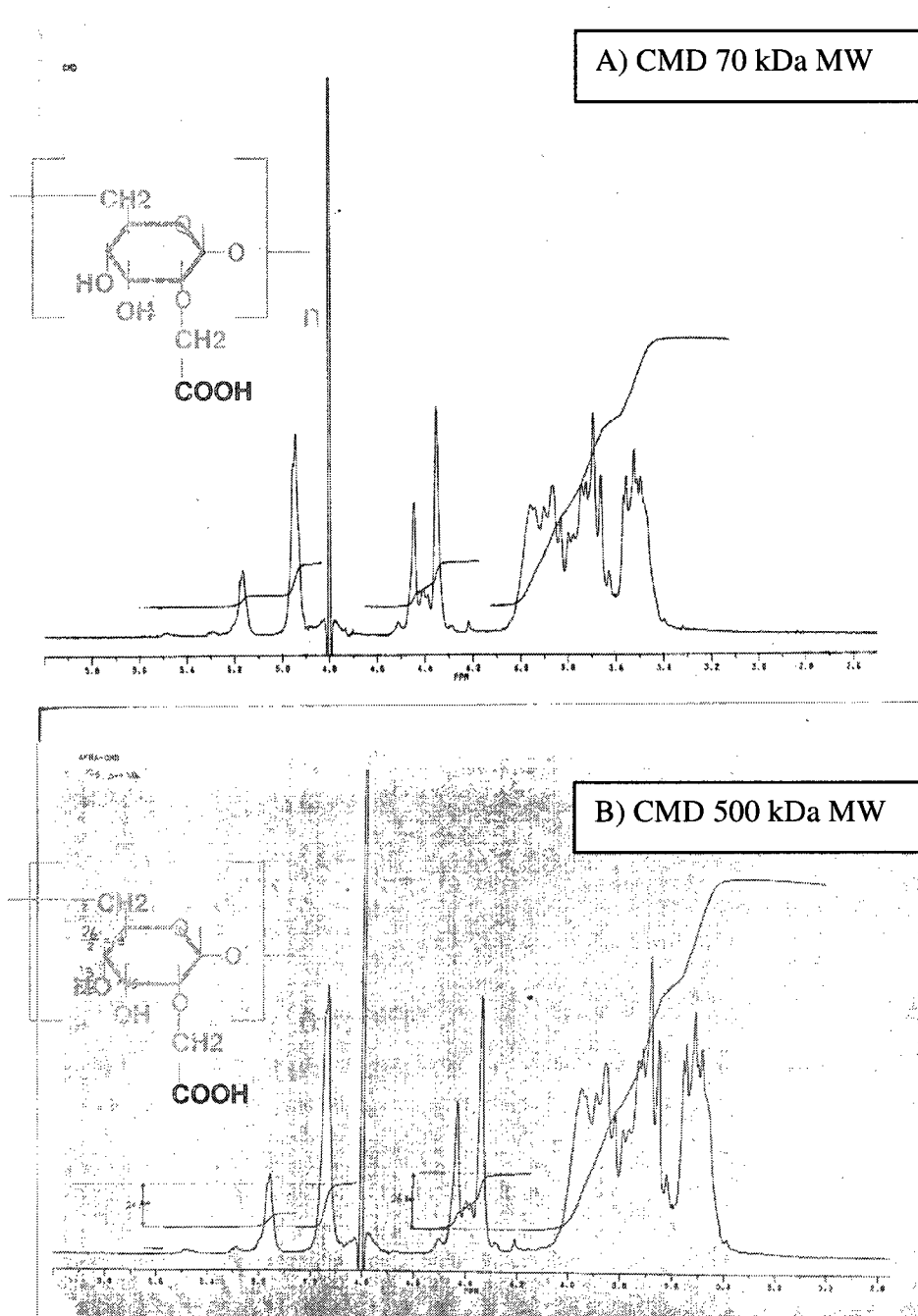
Figure 10.6: The ^{1}H NMR spectra of two synthesized CMDs, 70 kDa and 500 kDa MW which were used in this study.

Fibre holder design
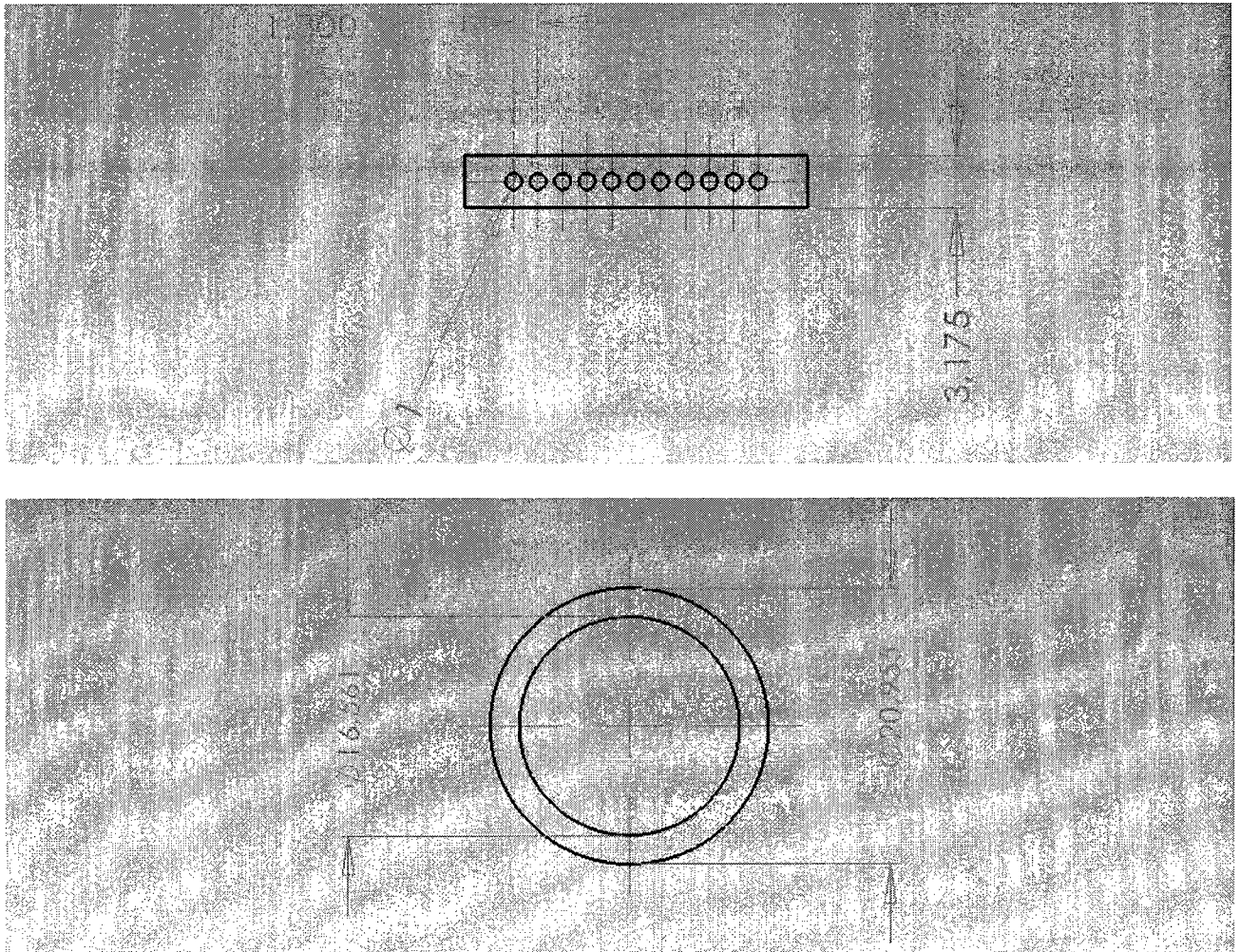
Figure 10.7: Dimensions of the circular fibre holder, provided by SolidWork software (drawn
by Marc G. Couture)

References

ALCANTAR, N. A., E. S. AYDIL and J. N. ISRAELACHVILI (2000). "Polyethylene glycol-coated biocompatible surfaces", *J Biomed Mater Res*, vol. 51, p. 343-351.

ANDERSSON, A. S., et al. (2003). "Nanoscale features influence epithelial cell morphology and cytokine production", *Biomaterials*, vol. 24, p. 3427-3436.

ARIMA, Y. and H. IWATA (2007). "Effect of wettability and surface functional groups on protein adsorption and cell adhesion using well-defined mixed self-assembled monolayers ", *Biomateriasl*, vol. 28, n° 20, p. 3074-3082.

ASAHARA, T. and J. M. ISNER (2002). "Endothelial progenitor cells for vascular regeneration", *J Hematother Stem Cell Res*, vol. 11, p. 171-178.

ATALA, A. (2004). "Tissue engineering and regenerative medicine: concepts for clinical application", Rejuvenation *Res*, vol.7, p. 15-31.

BACH, A. D., et al. (2006). "A new approach to tissue engineering of vascularized skeletal muscle", *J Cell Mol Med*, vol. 10, p. 716-726.

BACH, T. L., et al. (1998). "VE-Cadherin mediates endothelial cell capillary tube formation in fibrin and collagen gels", *Exp Cell Res*, vol. 238, p. 324-334.

BADYLAK, S. F. (2007). "The extracellular matrix as a biologic scaffold material", *Biomaterials*, vol. *28*, n° 25, p. 3587-3593.

BARBUCCI, R., et al. (2002). "Micropatterned surfaces for the control of endothelial cell behaviour", *Biomol Eng*, vol. 19, p. 161-170.

BARBUCCI, R., et al. (2005). "Role of the Hyal-Cu (II) complex on bovine aortic and lymphatic endothelial cells behavior on microstructured surfaces", *Biomacromolecules*, vol. 6, p. 212-219.

BARBUCCI, R., et al. (2003). "Micro and nano-structured surfaces", *J Mater Sci Mater Med*, vol. 14, p. 721-725.

BARRETT, D. A., et al. (2001). "Resistance to nonspecific protein adsorption by poly(vinyl alcohol) thin films adsorbed to a poly(styrene) support matrix studied using surface plasmon resonance", *Anal Chem*, vol. 73, p. 5232-5239.

BASHUR, C. A., L. A. DAHLGREN and A. S. GOLDSTEIN (2006). "Effect of fibre diameter and orientation on fibroblast morphology and proliferation on electrospun poly (D, L-lactic-co-glycolic acid) meshes", *Biomaterials*, vol. 27, p. 5681-5688.

236

BATTISTA, S., et al. (2005). "The effect of matrix composition of 3D constructs on embryonic stem cell differentiation", *Biomaterials*, vol. 26, p. 6194-6207.

BEER, J. H., K. T. SPRINGER and B. S. COLLER (1992). "Immobilized Arg-Gly-Asp (RGD) peptides of varying lengths as structural probes of the platelet glycoprotein IIb/IIIa receptor", *Blood*, vol. 79, p. 117-128.

BENMAKROHA, Y., S. ZHANG, and P. ROLFE (1995). "Haemocompatibility of invasive sensors", *Medical and Biological Engineering and Computing*, vol. 33, p. 811-821.

BERNA, M., et al. (2006). "Novel monodisperse PEG-dendrons as new tools for targeted drug delivery: synthesis, characterization and cellular uptake", *Biomacromolecules*, vol. 7, p. 146-153.

BESSELINK, G. A., T. BEUGELING and A. BANJES (1993). "N-hydroxysuccinimide-activated glycine-sepharose hydrolysis of activated groups and coupling of amino-compounds", *Appl Biochem Biotechnol*, vol. 43, p. 227-246.

BILODEAU, K., et al. (2005). "Design of a perfusion bioreactor specific to the regeneration of vascular tissues under mechanical stresses", Artif *Organs*, vol. 29, p. 906-912.

BILTRESSE, S., M. ATTOLINI and J. MARCHAND-BRYNAERT (2005). "Cell adhesive PET membranes by surface grafting of RGD peptidomimetics", *Biomaterials*, vol. 26, p. 4576-4587.

BLOMBACK, B. and M. OKADA (1982). "Fibrin gel structure and clotting time", *Thromb Res*, vol. 25, p. 51-70.

BONGRAZIO, M., et al. (2006). "Shear stress modulates the expression of thrombospondin-1 and CD36 in endothelial cells *in vitro* and during shear stress-induced angiogenesis *in vivo*", *Int J Immunopathol Pharmacol*, vol. 19, p. 35-48.

BORGES, J., et al. (2004). "Angiogenesis investigations in tissue engineering. The cylinder model on the chorioallantois membrane", *Chirurg*, vol. 75, p. 284-290.

BORSELLI, C., et al. (2007). "Induction of directional sprouting angiogenesis by matrix gradients", *J Biomed Mater Res A*, vol. 80, p. 297-305.

BROWN, M. P. and R. R. POOL (1983). "Experimental and clinical investigations of the use of carbon fibre sutures in equine tendon repair", *J Am Vet Med Assoc*, vol. 182, p. 956-966.

BUERKLE, M. A., et al. (2002). "Inhibition of the alpha-nu integrins with a cyclic RGD peptide impairs angiogenesis, growth and metastasis of solid tumours *in vivo*", *Br J Cancer*, vol. 86, p. 788-795.

CAI, W., et al. (2006). "How molecular imaging is speeding up antiangiogenic drug development", *Mol Cancer Ther*, vol. 5, n° 11, p. 2624-2633,

237

CALKINS, C. M., et al. (2007). "Late abscess formation following indirect hernia repair utilizing silk suture", *Pediatr Surg Int,* vol. 23, n° 4, p. 349-52.

CAMPBELL, D. (2000). *Polymer characterization: physical techniques,* 2 editions, CRC, 108-154 p.

CARMELIET, P. (2000). "Mechanisms of angiogenesis and arteriogenesis", *Nat Med,* vol. 6, p. 389-395.

CARMELIET, P. (1999). "Basic concepts of (Myocardial) angiogenesis: role of vascular endothelial growth factor and angiopoietin", *Curr Interv Cardiol Rep,* vol. 1, p. 322-335.

CARMELIET, P. and D. COLLEN (2000). "Molecular basis of angiogenesis. Role of VEGF and VE-cadherin", *Ann N Y Acad Sci,* vol. 902, p. 249-62, discussion p. 262-264.

CATANESE, J., et al. (1999). "Mechanical properties of medical grade expanded polytetrafluoroethylene: the effects of internodal distance, density, and displacement rate", *J Biomed Mater Res,* vol. 48, p. 187-192.

CHANG, C. W., et al. (2007). "Non-ionic amphiphilic biodegradable PEG-PLGA-PEG copolymer enhances gene delivery efficiency in rat skeletal muscle", *J Control Release,* vol. 118, p. 245-253.

CHATELIER, R. C., et al. (1997). "Determination of the Intrinsic Acid-Base Dissociation Constant and Site Density of Ionizable Surface Groups by Capillary Rise Measurements", *Langmuir,* vol. 13, p. 3043.

CHATELIER, R. C., et al. (1995). "Theory of contact angles and the free energy of formation of ionizable surfaces: application to heptylamine radio-frequency plasma-deposited films", *Langmuir,* vol. 11, p. 4122.

CHEN, J., F. HUANG and C. QI (2004). "Vascularization in transplantation of bio-derived bone compounded with marrow stromal stem cells in repair of goat tibial shaft defect", *Zhongguo Xiu Fu Chong Jian Wai Ke Za Zhi,* vol. 18, p. 309-313.

CHINN, J. A., et al. (1998). "Blood and tissue compatibility of modified polyester: thrombosis, inflammation, and healing", *J Biomed Mater Res,* vol. 39, p. 130-140.

CHOI, C. H., et al. (2007). "Cell interaction with three-dimensional sharp-tip nanotopography", *Biomaterials,* vol. 28, p. 1672-1679.

CHOONG, C. S., D. W. HUTMACHER and J. T. TRIFFITT (2006). "Co-culture of bone marrow fibroblasts and endothelial cells on modified polycaprolactone substrates for enhanced potentials in bone tissue engineering", *Tissue Eng,* vol. 12, p. 2521-2531.

CHOU, A. M., et al. (2006). "Tissue engineering of a periodontal ligament-alveolar bone graft construct", *Int J Oral Maxillofac Implants,* vol. 21, p. 526-534.

CHUNG, H. J., et al. (2006). "Heparin immobilized porous PLGA microspheres for angiogenic growth factor delivery", *Pharm Res*, vol. 23, p. 1835-1841.

CHUNG, S., et al. (2003a). "Vascularized acellular dermal matrix island flaps for the repair of abdominal muscle defects", *Plast Reconstr Surg*, vol. 111, p. 225-232.

CHUNG, T. W., et al. (2003b). "Enhancement of the growth of human endothelial cells by surface roughness at nanometer scale", *Biomaterials*, vol. 24, p. 4655-4661.

CLEAVER, O. and D. A. MELTON (2003). "Endothelial signaling during development", *Nat Med*, vol. 9, p. 661-668.

COLLINSON, D. J. and R. DONNELLY (2004). "Therapeutic angiogenesis in peripheral arterial disease: can biotechnology produce an effective collateral circulation?", Eur *J Vasc Endovasc Surg*, vol. 28, p. 9-23.

CONWAY, E. M., D. COLLEN and P. CARMELIET (2001). "Molecular mechanisms of blood vessel growth", *Cardiovasc Res*, vol. 49, p. 507-521.

CRONIN, K. J., et al. (2006). "The role of biological extracellular matrix scaffolds in vascularized three-dimensional tissue growth *in vivo*", *J Biomed Mater Res B Appl Biomater*, vol. 82b, n° 1, p. 122-128.

CUI, F. Z., et al. (2006). "Hyaluronic acid hydrogel immobilized with RGD peptides for brain tissue engineering", *J Mater Sci Mater Med*, vol. 17, p. 1393-1401.

CUKIERMAN, E., R. PANKOV and K. M. YAMADA (2002). "Cell interactions with three-dimensional matrices", *Curr Opin Cell Biol*, vol. 14, p. 633-639.

CULLEN, J. P. et al. (2002). "Pulsatile flow-induced angiogenesis: role of G (i) subunits", *Arterioscler Thromb Vasc Biol*, vol. 22, p. 1610-1616.

CUMMINGS, C. L., et al. (2004). "Properties of engineered vascular constructs made from collagen, fibrin, and collagen-fibrin mixtures", *Biomaterials*, vol. 25, p. 3699-3706.

CURTIS, A. and M. RIEHLE (2001). "Tissue engineering: the biophysical background", *Phys Med Biol*, vol. 46, p. R47-65.

CURTIS, A. and C. WILKINSON (1997). "Topographical control of cells", *Biomaterials*, vol. 18, p. 1573-1583.

DAY, R. M., et al. (2004). "*In vivo* characterisation of a novel bioresorbable poly (lactide-co-glycolide) tubular foam scaffold for tissue engineering applications", *J Mater Sci Mater Med*, vol. 15, p. 729-734.

DOI, K., et al. (2007). "Enhanced angiogenesis by gelatin hydrogels incorporating basic fibroblast growth factor in rabbit model of hind limb ischemia", *Heart Vessels*, vol. 22, p. 104-108.

DRURY, J. L. and D. J. MOONY (2003). "Hydrogels for tissue engineering: scaffold design variables and applications", *Biomaterials,* vol. 24, p. 4337-4351.

DUNEHOO, A. L., et al. (2006). "Cell adhesion molecules for targeted drug delivery", *J Pharm Sci,* vol. 95, p. 1856-1872.

DUNN, G. A. and T. EBENDAL (1978). "Contact guidance on oriented collagen gels", *Exp Cell Res,* vol. 111, p. 475-479.

DUNN, G. A. and A. F. BROWN (1986). "Alignment of fibroblasts on grooved surfaces described by a simple geometric transformation", *J Cell Sci,* vol. 83, p. 313-340.

DZIUBLA, T. D. and A. M. LOWMAN (2004). "Vascularization of PEG-grafted macroporous hydrogel sponges: a three-dimensional *in vitro* angiogenesis model using human microvascular endothelial cells", *J Biomed Mater Res A,* vol. 68, p. 603-614.

DZIUBLA, THOMAS D. *Macroporoushydrogels as vascularizable soft tissue – implant interfaces: materials characterization, in vitro evaluation, computer simulations, and applications in implantable drug delivery devices,* Thesis (Doctoral), Drexel University, 2003, [on line]
[http://dspace.library.drexel.edu/bitstream/1860/36/1/dziubla_thesis.pdf] (Accessed March 2007)

EISELT, P., et al. (1998). "Development of technologies aiding large-tissue engineering", *Biotechnol Prog,* vol. 14, p. 134-140.

ELCIN, A. E., Y. M. ELCIN (2006). "Localized angiogenesis induced by human vascular endothelial growth factor-activated PLGA sponge", *Tissue Eng,* vol. 12, p. 959-968.

ENGEL, J. (1991). "Domains in proteins and proteoglycans of the extracellular matrix with functions in assembly and cellular activities", *Int J Biol Macromol,* vol. 13, p. 147-151.

ENNETT, A. B., D. KAIGLER and D. J. MOONEY (2006). "Temporally regulated delivery of VEGF *in vitro* and *in vivo*", *J Biomed Mater Res A,* vol. 79, p. 176-184.

ENTCHEVA, E. and H. BIEN (2005). "Acoustic micromachining of three-dimensional surfaces for biological applications", *Lab Chip,* vol. 5, p. 179-183.

ERTEL, S. I., et al. (1991). "Endothelial cell growth on oxygen-containing films deposited by radio-frequency plasmas: the role of surface carbonyl groups", *J Biomater Sci Polym Ed,* vol. 3, p. 163-183.

EVANS, P. D., G. A. PRITCHARD and D. H. JENKINS (1987). "Carbon fibre used in the late reconstruction of rupture of the extensor mechanism of the knee", *Injury,* vol. 18, p. 57-60.

FAVIA, P., et al. (2003). "Novel plasma processes for biomaterials: micro-scale patterning of biomedical polymers", *Surface and Coatings Technology,* vol. 169-170, p. 707-711.

240

FLAMME, I., T. FROLICH and W. RISAU (1997). "Molecular mechanisms of vasculogenesis and embryonic angiogenesis", *J Cell Physiol,* vol. 173, p. 206-210.

FLEMMING, R. G., et al. (1999). "Effects of synthetic micro- and nano-structured surfaces on cell behavior", *Biomaterials,* vol. 20, p. 573-588.

FOLKMAN, J. and C. HAUDENSCHILD (1980). "Angiogenesis *in vitro*", *Nature,* vol. 288, p. 551-556.

FOLKMAN, J. and P. A. D'AMORE (1996). "Blood vessel formation: what is its molecular basis?", *Cell,* vol. 87, p. 1153-1155.

FOLKMAN, J. and C. HAUDENSCHILD (1980). "Angiogenesis by capillary endothelial cells in culture", *Trans Ophthalmol Soc U K,* vol. 100, p. 346-353.

FOLKMAN, J. and A. MOSCONA (1978). "Role of cell shape in growth control", *Nature,* vol. 273, p. 345-349.

FOURNIER, N. and C. J. DOILLON (1996). "Biological molecule-impregnated polyester: an *in vivo* angiogenesis study", *Biomaterials,* vol. 17, p. 1659-1665.

FOURNIER, N. and C. J. DOILLON (1992). "*In vitro* angiogenesis in fibrin matrices containing FN or hyaluronic acid", *Cell Biol Int Rep,* vol. 16, p. 1251-1263.

FRIEDL, P. and E. B. BROCKER (2000). "The biology of cell locomotion within three-dimensional extracellular matrix", *Cell Mol Life Sci,* vol. 57, p. 41-64.

FUCHS, J. R., B. A. NASSERI and J. P. VACANTI (2001). "Tissue engineering: a 21st century solution to surgical reconstruction", *Ann Thorac Surg,* vol. 72, p. 577-591.

GAFNI, Y. et al. (2006). "Design of a filamentous polymeric scaffold for *in vivo* guided angiogenesis", *Tissue Eng,* vol.12, n° 11, p. 3021-3024.

GAO, C. Y., et al. (2003). "Surface immobilization of bioactive molecules on polyurethane for promotion of cytocompatibility to human endothelial cells", Macromol *Biosci,* vol. 3, p. 157-162.

GEIGER, B., et al. (2001). "Transmembrane crosstalk between the extracellular matrix--cytoskeleton crosstalk", *Nat Rev Mol Cell Biol,* vol. 2, p. 793-805.

GENGENBACH, T. R., R. C. CHATELIER and H. J. GRIESSER (1996). "Characterization of the ageing of plasma-deposited polymer films: global analysis of X-ray photoelectron spectroscopy data", *Surface and interface analysis,* vol. 24, p. 271-281.

GENGENBACH, T. R., et al. (1994). "A multitechnique study of the spontaneous oxidation of N-hexane plasma polymers", J *Polym Sci A,* vol. 32, p. 1399-1414.

GENTLEMAN, E., et al. (2007). "Operating curves to characterize the contraction of fibroblast-seeded collagen gel/collagen fibre composite biomaterials: effect of fibre mass", *Plast Reconstr Surg*, vol. 119, p. 508-516.

GODDARD, J. M. and J. H. HOTCHKISS (2007). "Polymer surface modification for the attachment of bioactive compounds", *Progress in Polymer Science*, vol. 32, n°7, p. 698-725.

GOMES, M. E. and R. L. REIS (2004). "Tissue engineering: key elements and some trends", *Macromol Biosci*, vol. 4, p. 737-742.

GOSSELIN, C., et al. (1996). "ePTFE coating with fibrin glue, FGF-1, and heparin: effect on retention of seeded endothelial cells", *J Surg Res*, vol. 60, p. 327-332.

GRAF, M., R. GALERA GARCIA and H. WATZIG (2005). "Protein adsorption in fused-silica and polyacrylamide-coated capillaries", *Electrophoresis*, vol. 26, p. 2409-2417.

GRIESSER, H. J., et al. (2002). "Interfacial properties and protein resistance of nano-scale polysaccharide coatings", *Smart Mater Struct*, vol. 11, p. 652-661.

GRIFFITH, C. K., et al. (2005). "Diffusion limits of an *in vitro* thick prevascularized tissue", *Tissue Eng*, vol. 11, p. 257-266.

GUPTA, B., et al. (2002). "Plasma-induced graft polymerization of acrylic acid onto poly (ethylene terephthalate) films: characterization and human smooth muscle cell growth on grafted films", *Biomaterials*, vol. 23, p. 863-871.

HADJIZADEH, A., C. J. DOILLON and P. VERMETTE (2007). "Bioactive Polymer Fibres to Direct Endothelial Cell Growth in a Three-Dimensional Environment", *Biomacromolecules*, vol. 8, p. 864-873.

HADJIZADEH, A. and P. VERMETTE (2007). "Bioactive compositions and their use in cell patterning", Can. Pat. Appl. (2007), 65pp. CODEN: CPXXEB CA 2591459 A1 20071213 CAN 148:62182 AN 2007:1439347

HANKER, J. S. and B. L. GIAMMARA (1988). "Biomaterials and biomedical devices", *Science*, vol. 242, p. 885-892.

HARTLEY, P. G., et al. (2002). "Physicochemical properties of polysaccharide coatings based on grafted multiplayer assemblies", *Langmuir*, vol. 18, p. 2483-2494.

HARTLEY, P. G., et al. (2000). "A Surface masking technique for the determination of plasma polymer film thickness by AFM", *Plasmas and Polymers*, vol. 5, p. 47.

HAUBNER, R. and H. J. WESTER (2004). "Radiolabeled tracers for imaging of tumor angiogenesis and evaluation of anti-angiogenic therapies", *Curr Pharm Des*, vol. 10, p. 1439-1455.

HAYEN, W., et al. (1999). "Hyaluronan stimulates tumor cell migration by modulating the fibrin fibre architecture", *J Cell Sci*, vol. 112, Pt 13, p. 2241-2251.

HELM, C. L., A. ZISCH and M. A. SWARTZ (2007). "Engineered blood and lymphatic capillaries in 3D VEGF-fibrin-collagen matrices with interstitial flow", *Biotechnol Bioeng*, vol. 96, p. 167-176.

HERMANSON, G. T. (1996). *Bioconjugate Techniques*, New York, Academic Press.

HERN, D. L. and J. A. HUBBELL (1998). "Incorporation of adhesion peptides into nonadhesive hydrogels useful for tissue resurfacing", *J Biomed Mater Res*, vol. 39, p. 266-276.

HERSEL, U., C. DAHMEN and H. KESSLER (2003). "RGD modified polymers: biomaterials for stimulated cell adhesion and beyond", *Biomaterials*, vol. 24, p. 4385-4415.

HO, M. H., et al. (2005). "Preparation and characterization of RGD-immobilized chitosan scaffolds", *Biomaterials*, vol. 26, p. 3197-3206.

HODDE, J. (2006). "Extracellular matrix as a bioactive material for soft tissue reconstruction", *ANZ J Surg*, vol. 76, p. 1096-1100.

HODDE, J. (2002). "Naturally occurring scaffolds for soft tissue repair and regeneration", vol. 8, n° 2, p. 295-308.

HODIVALA-DILKE, K. M., A. R. REYNOLDS and L. E. REYNOLDS (2003). "Integrins in angiogenesis: multitalented molecules in a balancing act", *Cell Tissue Res*, vol. 314, p. 131-144.

HOLLAND, J. et al. (1996). "Culture of human vascular endothelial cells on an RGD-containing synthetic peptide attached to a starch-coated polystyrene surface: comparison with fibronectin-coated tissue grade polystyrene", *Biomaterials*, vol. 17, p. 2147-2156.

HOLT, D. B., R. C. EBERHART and M. D. PRAGER (1994). "Endothelial cell binding to Dacron modified with polyethylene oxide and peptide", *ASAIO J*, vol. 40, p. M858-63.

HORBETT, T. A. (1981). "Adsorption of proteins from plasma to a series of hydrophilic-hydrophobic copolymers. II. Compositional analysis with the prelabeled protein technique", *J Biomed Mater Res*, vol. 15, p. 673-695.

HOSSEINKHANI, H., et al. (2006). "Enhanced angiogenesis through controlled release of basic fibroblast growth factor from peptide amphiphile for tissue regeneration", *Biomaterials*, vol. 27, p. 5836-5844.

HUANG, Y. C., et al. (2005). "Combined angiogenic and osteogenic factor delivery enhances bone marrow stromal cell-driven bone regeneration", *J Bone Miner Res*, vol. 20, p. 848-857.

HUANG, NING- PING. *Biochemical interactions of surface-bound PEG copolymers*, Thesis (Doctoral), Suiss federal institute of technology, Zürich, 2002, [on line] [http://e-collection.ethbib.ethz.ch/ecol-pool/diss/fulltext/eth14589.pdf] (Accessed March 2007)

HUBBELL, J. A., et al. (1991). "Endothelial cell-selective materials for tissue engineering in the vascular graft via a new receptor", Bio/Technology, vol. 9, p. 568–572.

HUBBELL, J. A. (1995). "Biomaterials in Tissue Engineering", *Biotechnology*, vol. 13, p. 565-576.

HUMPERT, P. M., et al. (2005). "Adult vascular progenitor cells and tissue regeneration in metabolic syndrome", *Vasa*, vol. 34, n° 2, p. 73-80.

HUTMACHER, D. W. (2001). "Scaffold design and fabrication technologies for engineering tissues--state of the art and future perspectives", *J Biomater Sci Polym Ed*, vol. 12, p. 107-124.

HURTADO, A. (2006). "Poly (D,L-lactic acid) macroporous guidance scaffolds seeded with Schwann cells genetically modified to secrete a bi-functional neurotrophin implanted in the completely transected adult rat thoracic spinal cord", *Biomaterials*, vol. 27, p. 430-442.

HYNES, R. O. (1999). "Cell adhesion: old and new questions", *Trends Cell Biol*, vol. 9, p. M33-7.

IBRAHIM, S., et al. (2007). "A surface-tethered model to assess size-specific effects of hyaluronan (HA) on endothelial cells", *Biomaterials*, vol. 28, p. 825-835.

IGARASHI, S., J. TANAKA and H. KOBAYASHI (2007). "Micro-patterned nanofibrous biomaterials", *J Nanosci Nanotechnol*, vol. 7, p. 814-817.

ILAN, N. and J. A. MADRI (2003). "PECAM-1: old friend, new partners", *Curr Opin Cell Biol*, vol. 15, p. 515-524.

INGBER, D. E. (1990). "Fibronectin controls capillary endothelial cell growth by modulating cell shape", *Proc Natl Acad Sci U S A*, vol. 87, p. 3579-3583.

INGBER, D. E. and J. FOLKMAN (1989). "Mechanochemical switching between growth and differentiation during fibroblast growth factor-stimulated angiogenesis *in vitro*: role of extracellular matrix", *J Cell Biol*, vol. 109, p. 317-330.

INGBER, D. E., et al. (1995). "Cell shape, cytoskeletal mechanics, and cell cycle control in angiogenesis", *J Biomech*, vol. 28, p. 1471-1484.

IRVINE, D. J., A. M. MAYES and L. G. GRIFFITH (2001). "Nanoscale clustering of RGD peptides at surfaces using Comb polymers. 1. Synthesis and characterization of Comb thin films", *Biomacromolecules*, vol. 2, p. 85-94.

ISHIKAVA, M. and T. ASAHARA (2004). "Endothelial progenitor cell culture for vascular regeneration", *Stem Cells Dev*, vol. 13, p. 344-349.

ITO, Y., M. KAJIHARA and Y. IMANISHI (1991). "Materials for enhancing cell adhesion by immobilization of cell-adhesive peptide", *J Biomed Mater Res*, vol. 25, p. 1325-1337.

JAFFE, E. A. (1980). "Culture of human endothelial cells", *Transplant Proc*, vol. 12, p. 49-53.

JAIN, R. K. (2003). "Molecular regulation of vessel maturation", *Nat Med*, vol. 9, p. 685-693.

JANG, J. H., C. B. RIVES and L. D. SHEA (2005). "Plasmid delivery *in vivo* from porous tissue-engineering scaffolds: transgene expression and cellular transfection", *Mol Ther*, vol. 12, p. 475-483.

JOCKENHOEVEL, S., et al. (2001). "Fibrin gel -- advantages of a new scaffold in cardiovascular tissue engineering", *Eur J Cardiothorac Surg*, vol. 19, p. 424-430.

JOHANSSON, B. L., et al. (2002). "Characterization of air plasma-treated polymer surfaces by ESCA and contact angle measurements for optimization of surface stability and cell growth", *J Appl Polym Sci*, vol. 86, p. 2618-2625.

JUNG, S. Y., et al. (2003). "The Vroman effect: a molecular level description of fibrinogen displacement", *J Am Chem Soc*, vol. 125, p. 12782-12786.

KAEHLER, J., et al. (1989). "Precoating substrate and surface configuration determine adherence and spreading of seeded endothelial cells on polytetrafluoroethylene grafts", *J Vasc Surg*, vol. 9, p. 535-541.

KAIGLER, D., et al. (2006). "VEGF scaffolds enhance angiogenesis and bone regeneration in irradiated osseous defects", *J Bone Miner Res*, vol. 21, p. 735-744.

KANTLEHNER, M., et al. (2000). "Surface coating with cyclic RGD peptides stimulates osteoblast adhesion and proliferation as well as bone formation", *Chembiochem*, vol. 1, p. 107-114.

KARAGEORGIOU, V. and D. KAPLAN (2005). "Porosity of 3D biomaterial scaffolds and osteogenesis", *Biomaterials*, vol. 26, p. 5474-5491.

KARDESTUNCER, T., et al. (2006). "RGD-tethered silk substrate stimulates the differentiation of human tendon cells", *Clin Orthop Relat Res*, vol. 448, p. 234-239.

KEDEM, A., et al. (2005). "Vascular endothelial growth factor-releasing scaffolds enhance vascularization and engraftment of hepatocytes transplanted on liver lobes", *Tissue Eng* vol. 11, p. 715-722.

KESELOWSKY, B. G., D. M. COLLARD and A. J. GARCIA (2005). "Integrin binding specificity regulates biomaterial surface chemistry effects on cell differentiation", *Proc Natl Acad Sci U S A*, vol. 102, p. 5953-5957.

KESELOWSKY, B. G., D. M. COLLARD and A. J. GARCIA (2004). "Surface chemistry modulates focal adhesion composition and signaling through changes in integrin binding", *Biomaterials*, vol. 25, p. 5947-5954.

KESELOWSKY, B. G., D. M. COLLARD and A. J. GARCIA (2003). "Surface chemistry modulates fibronectin conformation and directs integrin binding and specificity to control cell adhesion", *J Biomed Mater Res A*, vol. 66, p. 247-259.

KESHAW, H., A. FORBES and R. M. Day (2005). "Release of angiogenic growth factors from cells encapsulated in alginate beads with bioactive glass", *Biomaterials*, vol. 26, p. 4171-4179.

KHADEMHOSSEINI, A., et al. (2006). "Microscale technologies for tissue engineering and biology", *Proc Natl Acad Sci U S A*, vol. 103, p. 2480-2487.

KHANG, G., et al. (1999). "Interaction of fibroblast cells onto fibres with different diameter", *Korea Polymer J*, vol. 7, p. 102-107.

KIAN KWAN OO, K., et al. (2007). "Tissue engineered prefabricated vascularized flaps", *Head Neck*, vol. 29, p. 458-464.

KIDD, K. R., R. B. NAGLE and S. K. WILLIAMS (2002). "Angiogenesis and neovascularization associated with extracellular matrix-modified porous implants", *J Biomed Mater Res*, vol. 59, p. 366-377.

KIM, H. D., et al. (2004). "Effect of PEG-PLLA diblock copolymer on macroporous PLLA scaffolds by thermally induced phase separation", *Biomaterials*, vol. 25, p. 2319-2329.

KIM, W. J., et al. (2006). "Anti-angiogenic inhibition of tumor growth by systemic delivery of PEI-g-PEG-RGD/pCMV-sFlt-1 complexes in tumor-bearing mice", *J Control Release*, vol. 114, p. 381-388.

KIRKPATRICK, C. J., et al. (1999). "Endothelial cell cultures as a tool in biomaterial research", *J Mater Sci Mater Med*, vol. 10, p. 589-594.

KIRKPATRICK, C. J., et al. (2003). "Experimental approaches to study vascularization in tissue engineering and biomaterial applications", *J Mater Sci Mater Med*, vol. 14, p. 677-681.

KOCH, S., et al. (2006). "Enhancing angiogenesis in collagen matrices by covalent incorporation of VEGF", *J Mater Sci Mater Med*, vol. 17, p. 735-741.

KOIKE, N., et al. (2004). "Tissue engineering: creation of long-lasting blood vessels", *Nature* vol. 428, p. 138-139.

KONSTANTINOVIC, M. L., et al. (2007). "Tensile strength and host response towards different polypropylene implant materials used for augmentation of fascial repair in a rat model", *Int Urogynecol J Pelvic Floor Dysfunct*, vol. 18, $n°6$, p. 619-626.

KOUVROUKOGLOU, S., et al. (2000). "Endothelial cell migration on surfaces modified with immobilized adhesive peptides", *Biomaterials*, vol. 21, p. 1725-1733.

KRISHNAN, A., C. A. SIEDLECKI, and E. A. VOGLER (2004). "Mixology of protein solutions and the Vroman effect", *Langmuir*, vol. 20, p. 5071-5078.

KURANE, A., D. T. SIMIONESCU and N. R. VYAVAHARE (2007). "*In vivo* cellular repopulation of tubular elastin scaffolds mediated by basic fibroblast growth factor", *Biomaterials*, vol. 28, p. 2830-2838.

LAI, P. H., et al. (2006). "Acellular biological tissues containing inherent glycosaminoglycans for loading basic fibroblast growth factor promote angiogenesis and tissue regeneration", *Tissue Eng*, vol. 12, p. 2499-2508.

LAMALICE, L., F. LE BOEUF and J. HUOT (2007). "Endothelial cell migration during angiogenesis", *Circ Res*, vol. 100, p. 782-794.

LARSEN, C. C., et al. (2006). "The effect of RGD fluorosurfactant polymer modification of ePTFE on endothelial cell adhesion, growth, and function", Biomaterials, vol. 27, p. 4846-4855.

LASCHKE, M. W., et al. (2006). "Angiogenesis in tissue engineering: breathing life into constructed tissue substitutes", *Tissue Eng*, vol. 12, p. 2093-2104.

LASSO, J. M., et al. (2007). "Improving flap survival by transplantation of a VEGF-secreting endothelised scaffold during distal pedicle flap creation", *J Plast Reconstr Aesthet Surg*, vol. 60, p. 279-286.

LATEEF, S. S., et al. (2002). "GRGDSP peptide-bound silicone membranes withstand mechanical flexing *in vitro* and display enhanced fibroblast adhesion", *Biomaterials*, vol. 23, p. 3159-3168.

LAUFFENBURGER, D. A. and A. F. HORWITZ (1996). "Cell migration: a physically integrated molecular process", *Cell*, vol. 84, p. 359-369.

LAVIK, E. and R. LANGER (2004). "Tissue engineering: current state and perspectives", *Appl Microbiol Biotechnol*, vol. 65, p. 1-8.

LEE, J. H., et al. (1998). "Interaction of different types of cells on polymer surfaces with wettability gradient", *J Colloid Interface Sci*, vol. 205, p. 323-330.

LEE, J. H., et al. (1997). "Interaction of cells on chargeable functional group gradient surfaces", *Biomaterials*, vol. 18, p. 351-358.

LEGGETT, G. (1997). "Scanning tunnelling microscopy and atomic force microscopy", *Surface Analysis -the principal techniques*, VICKERMAN, J. C. (ed.), New York, John Wiley & Sons Published, p 393-451.

LETOURNEUR, D., et al. (1993). "Antiproliferative capacity of synthetic dextrans on smooth muscle cell growth: the model of derivatized dextrans as heparin-like polymers", *J Biomater Sci Polym Ed*, vol. 4, p. 431-444.

LEVENBERG, S., et al. (2005). "Engineering vascularized skeletal muscle tissue", *Nat Biotechnol*, vol. 23, p. 879-884.

LI, J., Y. P. ZHANG and R. S. KIRSNER (2003). "Angiogenesis in wound repair: angiogenic growth factors and the extracellular matrix", *Microsc Res Tech*, vol. 60, p. 107-114.

LI, J. M., et al. (1992). "Precoating expanded polytetrafluoroethylene grafts alters production of endothelial cell-derived thrombomodulators", *J Vasc Surg*, vol. 15, p. 1010-1017.

LI, Y., et al. (2001). "Thermal compression and characterization of three-dimensional nonwoven PET matrices as tissue engineering scaffolds", *Biomaterials*, vol. 22, p. 609-618.

LIN, H., et al. (2006). "The effect of collagen-targeting platelet-derived growth factor on cellularization and vascularization of collagen scaffolds", *Biomaterials*, vol. 27, p. 5708-5714.

LIN, H. B., et al. (1992) "Endothelial cell adhesion on polyurethanes containing covalently attached RGD-peptides", *Biomaterials*, vol. 13, p. 905-914.

LIN, H. B., et al. (1993) "Surface properties of RGD-peptide grafted polyurethane block copolymers: variable take-off angle and cold-stage ESCA studies", *J Biomater Sci Polym Ed*, vol. 4, p. 183-198.

LIN, H. B., et al. (1994) "Synthesis, surface, and cell-adhesion properties of polyurethanes containing covalently grafted RGD-peptides", *J Biomed Mater Res*, vol. 28, p. 329-342.

LIN, H. B., et al. (1992) "Synthesis of a novel polyurethane co-polymer containing covalently attached RGD peptide", *J Biomater Sci Polym Ed*, vol. 3, p. 217-227.

LIU, Y., et al. (2006). "Layer-by-layer assembly of biomacromolecules on poly (ethylene terephthalate) films and fibre fabrics to promote endothelial cell growth", *J Biomed Mater Res A*, vol. 81A, p. 692-704.

LIU, Y., et al. (2005). "3D femtosecond laser patterning of collagen for directed cell attachment", *Biomaterials*, vol. 26, p. 4597-4605.

LO, C. M., et al. (2000). "Cell movement is guided by the rigidity of the substrate", *Biophys J*, vol. 79, p. 144-152.

LOFAS, S. and B. JOHNSSON (1990). "A novel hydrogel matrix on gold surfaces in surface-plasmon resonance sensors for fast and efficient covalent immobilization of ligands", *Journal of the Chemical Society-Chemical Communications*, vol. 21, p. 1526-1528.

LOKMIC, Z., et al. (2007). "An arteriovenous loop in a protected space generates a permanent, highly vascular, tissue-engineered construct", *FASEB J*, vol. 21, p. 511-522.

LU, X., et al. (2006). "Integrins in drug targeting-RGD templates in toxins", *Curr Pharm Des*, vol. 12, p. 2749-2769.

LUSCINSKAS, F. W. and J. LAWLER (1994). "Integrins as dynamic regulators of vascular function", *FASEB J*, vol. 8, p. 929-938.

MADEDDU, P. (2005). "Therapeutic angiogenesis and vasculogenesis for tissue regeneration", *Exp Physiol*, vol. 90, p. 315-326.

MAGNANI, A., A. PRIAMO and D. PASQUI (2003). "Cell behaviour on chemically microstructured surfaces", *Materials Science and Engineering*, vol. 23, n° 3, p. 315-328.

MAHESHWARI, G., et al. (2000). "Cell adhesion and motility depend on nanoscale RGD clustering", J *Cell Sci*, vol. 113, Pt 10, p. 1677-1686.

MAMMEN, M., S. K. CHOI and G. M. WHITESIDES (1998). "Polyvalent interactions in biological systems: implications for design and use of multivalent ligands and inhibitors", *Chem Int Ed*, vol. 37, p. 2755-2794.

MANN, B. K., et al. (1999). "Modification of surfaces with cell adhesion peptides alters extracellular matrix deposition" *Biomaterials*, vol. 20, p. 2281-2286.

MARCHAND-BRYNAERT, J., et al. (1999). "Biological evaluation of RGD peptidomimetics, designed for the covalent derivatization of cell culture substrata, as potential promotors of cellular adhesion", *Biomaterials*, vol. 20, p. 1773-1782.

MARKOWICZ, M., et al. (2006). "Human bone marrow mesenchymal stem cells seeded on modified collagen improved dermal regeneration *in vivo*", *Cell Transplant*, vol. 15, p. 723-732.

MARTIN, Y., D. BOUTIN and P. VERMETTE (2007). "Study of the effect of process parameters for n-heptylamine plasma", *Thin Solid Films*, vol. 515, p. 6844–6852.

MASSIA, S. P. and J. A. HUBBELL (1991a). "Human endothelial cell interactions with surface-coupled adhesion peptides on a nonadhesive glass substrate and two polymeric biomaterials", *J Biomed Mater Res*, vol. 25, p. 223-242.

MASSIA, S. P. and J. A. HUBBELL (1991b). "An RGD spacing of 440 nm is sufficient for integrin alpha V beta 3-mediated fibroblast spreading and 140 nm for focal contact and stress fibre formation", *J Cell Biol*, vol. 114, p. 1089-1100.

MASSIA, S. P. and J. STARK (2001). "Immobilized RGD peptides on surface-grafted dextran promote biospecific cell attachment", *J Biomed Mater Res*, vol, 56, p. 390-399.

MATSUDA, T. and Y. NAKAYAMA (1996). "Surface microarchitectural design in biomedical applications: *in vitro* transmural endothelialization on microporous segmented

polyurethane films fabricated using an excimer laser", *J Biomed Mater Res*, vol. 31, p. 235-242.

MATTHEW, H. W. T. (2001). "Medical and pharmaceutical application of polymers", *polymeric biomaterials*, DUMITRIU, S. (ed.), Marcel Dekker, Inc., p. 545.

MCARTHUR, S. L., et al. (2000). "Effect of polysaccharide structure on protein adsorption", *Colloid Surf B*, vol. 17, p. 37-48.

MCCLOSKEY, K. E., M. E. GILORY and R. M. NEREM (2005). "Use of embryonic stem cell-derived endothelial cells as a cell source to generate vessel structures *in vitro*", *Tissue Eng*, vol. 11, p. 497-505.

MCLEAN, K. M., et al. (2000a). "Method of immobilization of carboxymethyl-dextran affects resistance to tissue and cell colonization", *Colloids Surf B Biointerfaces*, vol. 18, p. 221-234.

MCLEAN, K. M., et al. (2000b). "Hybrid biomaterials: Surface-MALDI mass spectrometry analysis of covalent binding versus physisorption of proteins", *Colloids Surf B Biointerfaces*, vol. 17, p. 23-35.

MEDDAHI-PELLE, A., et al. (2004). "Vascular biomaterials: from biomedical engineering to tissue engineering", *Med Sci (Paris)*, vol. 20, p. 679-684.

MEEROVITCH, K., et al. (2003). "A novel RGD antagonist that targets both alphavbeta3 and alpha5beta1 induces apoptosis of angiogenic endothelial cells on type I collagen", *Vascul Pharmacol*, vol. 40, p. 77-89.

MENDEZ-VILAS, A., J. M. BRUQUE and M. L. GONZALEZ-MARTIN (2006). "Sensitivity of surface roughness parameters to changes in the density of scanning points in multi-scale AFM studies. Application to a biomaterial surface", *Ultramicroscopy*, vol. 107, n° 8, p. 617-625.

MERTSCHING, H., et al. (2005). "Engineering of a vascularized scaffold for artificial tissue and organ generation", *Biomaterials*, vol. 26, p. 6610-6617.

MILLER, D. C., et al. (2002). "An *in vitro* study of nano-fibre polymers for guided vascular regeneration", *Res Soc Symp Proc*, vol. 711, p. 201-204.

MILLER, D. C., et al. (2004). "Endothelial and vascular smooth muscle cell function on poly (lactic-co-glycolic acid) with nano-structured surface features", *Biomaterials*, vol. 25, p. 53-61.

MIRONOV, V., et al. (2003). "Organ printing: computer-aided jet-based 3D tissue engineering", *Trends Biotechnol*, vol. 21, p. 157-161.

MIYATA, T., et al. (1991). "Delayed exposure to pulsatile shear stress improves retention of human saphenous vein endothelial cells on seeded ePTFE grafts", *J Surg Res,* vol. 50, p. 485-493.

MOROSOFF, N. (1990). "An introduction to plasma polymerization", *Plasma deposition, treatment, and etching of polymers,* AGOSTINO, R. D. (ed.), NewYork, Academic Press, p. 1-84.

MORPURGO, M., E. A. BAYER and M. WILCHEK (1999). "N-hydroxysuccinimide carbonates and carbamates are useful reactive reagents for coupling ligands to lysines on proteins", *J Biochem Biophys Methods,* vol. 38, p. 17-28.

MORRA, M. and C. CASSINELI (1999). "Non-fouling properties of polysaccharide-coated surfaces", *J Biomater Sci Polym Ed,* vol. 10, p. 1107-1124.

MURAYAMA, T. and T. ASAHARA (2002). "Bone marrow-derived endothelial progenitor cells for vascular regeneration", *Curr Opin Mol Ther,* vol. 4, p. 395-402.

MUSCHLER, G. F., C. NAKAMOTO and L. G. GRIFFITH (2004). "Engineering principles of clinical cell-based tissue engineering", *J Bone Joint Surg Am,* vol. 86-A, p. 1541-1558.

NAKATSU, M. N., et al. (2003). "Angiogenic sprouting and capillary lumen formation modeled by human umbilical vein endothelial cells (HUVEC) in fibrin gels: the role of fibroblasts and Angiopoietin-1", *Microvasc Res,* vol. 66, p. 102-112.

NEFF, J. A., P. A. TRESCO and K. D. CALDWELL (1999). "Surface modification for controlled studies of cell-ligand interactions", *Biomaterials,* vol. 20, p. 2377-2393.

NEHLS, V. and D. DRENCKHAHN (1995a). "A microcarrier-based cocultivation system for the investigation of factors and cells involved in angiogenesis in three-dimensional fibrin matrices *in vitro"*, *Histochem Cell Biol,* vol. 104, p. 459-466.

NEHLS, V. and D. DRENCKHAHN (1995b). "A novel, microcarrier-based *in vitro* assay for rapid and reliable quantification of three-dimensional cell migration and angiogenesis", *Microvasc Res,* vol. 50, p. 311-322.

NEHLS, V., E. SCHUCHARDT and D. DRENCKHAHN (1994). "The effect of fibroblasts, vascular smooth muscle cells, and pericytes on sprout formation of endothelial cells in a fibrin gel angiogenesis system", *Microvasc Res,* vol. 48, p. 349-363.

NEUMANN, T., S. D. HAUSCHKA and J. E. SANDERS (2003). "Tissue engineering of skeletal muscle using polymer fibre arrays", *Tissue Eng,* vol. 9, p. 995-1003.

NILLESEN, S. T., et al. (2007). "Increased angiogenesis and blood vessel maturation in acellular collagen-heparin scaffolds containing both FGF2 and VEGF", *Biomaterials,* vol. 28, p. 1123-1131.

NOMI, M., et al. (2002). "Principals of neovascularization for tissue engineering", *Mol Aspects Med,* vol. 23, p. 463-483.

NOVINSKA, M. S., et al. (2006). "The alleles of PECAM-1", *Gene,* vol. 376, p. 95-101.

OLIVIERI, M. P. and K. S. TWEDEN (1999). "Human serum albumin and fibrinogen interactions with an adsorbed RGD-containing peptide", *J Biomed Mater Res,* vol. 46, p. 355-359.

PALMAZ, J. C., A. BENSON and E. A. SPRAGUE (1999). "Influence of surface topography on endothelialization of intravascular metallic material", *J Vasc Interv Radiol,* vol. 10, p. 439-444.

PAPENBURG, B. J., et al. (2007). "One-step fabrication of porous micropatterned scaffolds to control cell behavior", *Biomaterials,* vol. 28, p. 1998-2009.

PAPETTI, M. and I. M. HERMAN (2002). "Mechanisms of normal and tumor-derived angiogenesis", *Am J Physiol Cell Physiol,* vol. 282, p. C947-70.

PASCHE, S., et al. (2005). "Relationship between interfacial forces measured by colloid-probe atomic force microscopy and protein resistance of poly (ethylene glycol)-grafted poly (L-lysine) adlayers on niobia surfaces", *Langmuir,* vol. 21, p. 6508-6520.

PASQUI, D., et al. (2005). "Hyaluronan and sulphated hyaluronan micropatterns: effect of chemical and topographic cues on lymphatic endothelial cell alignment and proliferation" *Lymphology,* vol. 38, p. 50-65.

PATEL, N., et al. (1998). "Spatially controlled cell engineering on biodegradable polymer surfaces", *FASEB J,* vol. 12, p. 1447-1454.

PELHAM, R. J. and Y. WANG (1997). "Cell locomotion and focal adhesions are regulated by substrate flexibility", *Proc Natl Acad Sci U S A,* vol. 94, p. 13661-13665.

PELHAM, R. J. and Y. L. WANG (1998). "Cell locomotion and focal adhesions are regulated by the mechanical properties of the substrate", *Biol Bull,* vol. 194, p. 348-9, discussion p. 349-50.

PINNEY, E., et al. (2000). "Human three-dimensional fibroblast cultures express angiogenic activity", *J Cell Physiol,* vol. 183, p. 74-82.

PLOW, E. F., et al. (2000). "Ligand binding to integrins", *J Biol Chem,* vol. 275, p. 21785-21788.

POMPE, T., M. MARKOWSKI and C. WERNER (2004). "Modulated fibronectin anchorage at polymer substrates controls angiogenesis", *Tissue Eng,* vol. 10, p. 841-848.

PORTE-DURRIEU, M. C., et al. (1999). "Development of RGD peptides grafted onto silica surfaces: XPS characterization and human endothelial cell interactions", *J Biomed Mater Res,* vol. 46, p. 368-375.

RADOMSKI, J. S., et al. (1989). "Effects of *in vitro* aging on human endothelial cell adherence to Dacron vascular graft material", *J surg Resh,* vol. 47, p. 173-177.

RAI, B., et al. (2007). "Combination of platelet-rich plasma with polycaprolactone-tricalcium phosphate scaffolds for segmental bone defect repair", *J Biomed Mater Res A,* vol. 81A, n°4, p. 888-899.

RAMMELT, S., et al. (2006). "Coating of titanium implants with collagen, RGD peptide and chondroitin sulfate", *Biomaterials,* vol. 27, p. 5561-5571.

RATCLIFFE, A. (2000). "Tissue engineering of vascular grafts", *Matrix Biol, vol.* 19, p. 353-357.

RATNER, B. and D. CASTER (1997). "Electron spectroscopy for chemical analysis", *Surface Analysis -the principal techniques,* VICKERMAN, J. C. (ed.), New York, John Wiley & Sons Published, p. 43-84.

RINGEISEN, B. R., et al. (2006). "Jet-based methods to print living cells", *Biotechnol J,* vol. 1, p. 930-948.

RISAU, W. (1997). "Mechanisms of angiogenesis", *Nature,* vol. 386, p. 671-674.

ROSSO, F., et al. (2005). "Smart materials as scaffolds for tissue engineering", *J Cell Physiol,* vol. 203, p. 465-470.

ROSSO, F., et al. (2006). "Adhesion and proliferation of fibroblasts on RF plasma-deposited nanostructured fluorocarbon coatings: evidence of FAK activation", *J Cell Physiol* vol. 207, p. 636-643.

ROYCE, S. M., M. ASKARI and K. G. MARRA (2004). "Incorporation of polymer microspheres within fibrin scaffolds for the controlled delivery of FGF-1", *J Biomater Sci Polym Ed,* vol. 15, p. 1327-1336.

RUCKER, M., et al. (2006). "Angiogenic and inflammatory response to biodegradable scaffolds in dorsal skinfold chambers of mice", *Biomaterials,* vol. 27, p. 5027-5038.

SAHOTA, P. S., et al. (2004). "Approaches to improve angiogenesis in tissue-engineered skin", *Wound Repair Regen,* vol. 12, p. 635-642.

SANBORN, S. L., et al. (2002). "Endothelial cell formation of focal adhesions on hydrophilic plasma polymers", *Biomaterials,* vol. 23, p. 1-8.

SANTOS, M. I., et al. (2007). "Response of micro- and macrovascular endothelial cells to starch-based fibre meshes for bone tissue engineering", *Biomaterials,* vol. 28, p. 240-248.

SASTRY, S. K. and K. BURRIDGE (2000). "Focal adhesions: a nexus for intracellular signaling and cytoskeletal dynamics", *Exp Cell Res,* vol. 261, p. 25-36.

SAXENA, A. K., G. H. WILLITAL and J. P. VACANTI (2001). "Vascularized three-dimensional skeletal muscle tissue-engineering", *Biomed Mater Eng*, vol. 11, p. 275-281.

SCHACHT, E. (2004). "Biomaterials", *Verh K Acad Geneeskd Belg*, vol. 66, p. 242-245.

SCHAEFERLING, M., et al. (2002). "Application of self-assembly techniques in the design of biocompatible protein microarray surfaces", *Electrophoresis*, vol. 23, p. 3097-3105.

SCHECHNER, J. S., et al. (2003). "Engraftment of a vascularized human skin equivalent", *FASEB J*, vol. 17, p. 2250-2256.

SCHNELL, E., et al. (2007). "Guidance of glial cell migration and axonal growth on electrospun nanofibres of poly-epsilon-caprolactone and a collagen/poly-epsilon-caprolactone blend", *Biomaterials*, vol. 28, n° 19, p. 3012-3025.

SCHWARZ, U. S. and I. B. BISCHOFS (2005). "Physical determinants of cell organization in soft media", *Med Eng Phys*, vol. 27, p. 763-772.

SEEGER, J. M. and N. KLINGMAN (1985). "Improved endothelial cell seeding with cultured cells and fibronectin-coated grafts", *J Surg Res*, vol. 38, p. 641-647.

SENESI, G. S., et al. (2007). "Surface characterization of plasma deposited nano-structured fluorocarbon coatings for promoting *in vitro* cell growth", *Surface Science*, vol. 601, p. 1019-1025.

SERINI, G., D. VALDEMBRI and F. BUSSOLINO (2006). "Integrins and angiogenesis: a sticky business", *Exp Cell Res*, vol. 312, p. 651-658.

SHEETZ, M. P., et al. (1999). "Cell migration as a five-step cycle", *Biochem Soc Symp*, vol. 65, p. 233-243.

SHEETZ, M. P., D. P. FELSENFELD and C. G. GALBRAITH (1998). "Cell migration: regulation of force on extracellular-matrix-integrin complexes", *Trends Cell Biol*, vol. 8, p. 51-54.

SHEU, J. R., et al. (1997). "Inhibition of angiogenesis *in vitro* and *in vivo*: comparison of the relative activities of triflavin, an Arg-Gly-Asp-containing peptide and anti-alpha (v) beta3 integrin monoclonal antibody", *Biochim Biophys Acta*, vol. 1336, p. 445-454.

SHIMAMURA, N., et al. (2006). "Comparison of silicon-coated nylon suture to plain nylon suture in the rat middle cerebral artery occlusion model", *J Neurosci Methods*, vol. 156, p. 161-165.

SHISHATSKAYA, E. I., et al. (2004). "Tissue response to the implantation of biodegradable polyhydroxyalkanoate sutures", *J Mater Sci Mater Med*, vol. 15, p. 719-728.

SHIU, Y. T., et al. (2004). "Rho mediates the shear-enhancement of endothelial cell migration and traction force generation", *Biophys J*, vol. 86, p. 2558-2565.

SHIU, Y. T., et al. (2005). "The role of mechanical stresses in angiogenesis", *Crit Rev Biomed Eng*, vol. 33, p. 431-510.

SIEMINSKI, A. L., R. P. HEBBEL and K. J. GOOCH (2004). "The relative magnitudes of endothelial force generation and matrix stiffness modulate capillary morphogenesis *in vitro*", *Exp Cell Res*, vol. 297, p. 574-584.

SINGH, S. P., et al. (2007). "Cyclic mechanical strain increases production of regulators of bone healing in cultured murine osteoblasts", *J Am Coll Surg*, vol. 204, p. 426-434.

SIOW, K. S., et al. (2006). "Plasma methods for the generation of chemically reactive surfaces for biomolecule immobilization and cell colonization - A Review", *Plasma Processes and Polymers*, vol. 3, p. 392-418.

SIROIS, E., et al. (1998). "Endothelial cells exposed to erythrocytes under shear stress: an *in vitro* study", *Biomaterials*, vol. 19, p. 1925-1934.

SIROIS, E., M. F. COTE and C. J. DOILLON (1993). "Growth factors and biological supports for endothelial cell lining: *in vitro* study", *Int J Artif Organs*, vol. 16, p. 609-619.

STEED, D. L., et al. (1995). "Promotion and acceleration of diabetic ulcer healing by arginine-glycine-aspartic acid (RGD) peptide matrix. RGD Study Group", *Diabetes Care*, vol. 18, p. 39-46.

STEELE, J. G., et al. (1995). "Adsorption of fibronectin and vitronectin onto Primaria and tissue culture polystyrene and relationship to the mechanism of initial attachment of human vein endothelial cells and BHK-21 fibroblasts", *Biomaterials*, vol. 16, p. 1057-1067.

STEELE, J. G., et al. (1993). "Polystyrene chemistry affects vitronectin activity: an explanation for cell attachment to tissue culture polystyrene but not to unmodified polystyrene", *J Biomed Mater Res*, vol. 27, p. 927-940.

STEFFENS, G. C., et al. (2004). "Modulation of angiogenic potential of collagen matrices by covalent incorporation of heparin and loading with vascular endothelial growth factor", *Tissue Eng*, vol. 10, p. 1502-1509.

SUURONEN, E. J., et al. (2006a). "Promotion of angiogenesis in tissue engineering: developing multicellular matrices with multiple capacities", *Int J Artif Organs*, vol. 29, p. 1148-1157.

SUURONEN, E. J., et al. (2006b). "Tissue-engineered injectable collagen-based matrices for improved cell delivery and vascularization of ischemic tissue using CD133+ progenitors expanded from the peripheral blood", *Circulation*, vol. 114, p. I138-44.

TAN, J. and W. M. SALTZMAN (2002). "Topographical control of human neutrophil motility on micropatterned materials with various surface chemistry", *Biomaterials*, vol. 23, p. 3215-3225.

THEMISTOCLEOUS, G. S., et al. (2004). "Three-dimensional type I collagen cell culture systems for the study of bone pathophysiology", *In Vivo,* vol. 18, p. 687-696.

THIERRY, B., et al. (1999). "Chemical assays end-groups displayed on the surface of poly (ethylene terephthalate) (PET) films and membranes by radiolabeling", *Polymers for Advanced Technologies,* vol. 7, p. 589-598.

THISSEN, H., et al. (2006). "Two-dimensional patterning of thin coatings for the control of tissue outgrowth", *Biomaterials,* vol. 27, p. 35-43.

THOMSON, G. J., et al. (1991). "Adult human endothelial cell seeding using expanded polytetrafluoroethylene vascular grafts: a comparison of four substrates", *Surgery,* vol. 109, p. 20-27.

TRANQUI, L. and P. TRACQUI (2000). "Mechanical signalling and angiogenesis. The integration of cell-extracellular matrix couplings", *C R Acad Sci III,* vol. 323, p. 31-47.

TREMBLAY, P. L., et al. (2005). "Inosculation of tissue-engineered capillaries with the host's vasculature in a reconstructed skin transplanted on mice", *Am J Transplant,* vol. 5, p. 1002-1010.

TWEDEN, K. S., et al. (1995). "Accelerated healing of cardiovascular textiles promoted by an RGD peptide", *J Heart Valve Dis 4 Suppl,* vol. 1, p. S90-7.

UCUZIAN, A. A. and H. P. GREISLER (2007). *"In vitro* models of angiogenesis", *World J Surg,* vol. 31, p. 654-663.

UENO, T., et al. (2006). "Angiogenic cell therapy for hepatic fibrosis", *Med Mol Morphol,* vol. 39, p. 16-21.

UNGER, R. E., et al. (2005a). "Growth of human cells on polyethersulfone (PES) hollow fibre membranes", *Biomaterials,* vol. 26, p. 1877-1884.

UNGER, R. E., et al. (2005b). "Vascularization and gene regulation of human endothelial cells growing on porous polyethersulfone (PES) hollow fibre membranes", *Biomaterials,* vol. 26, p. 3461-3469.

UNGER, R. E., et al. (2004). "Endothelialization of a non-woven silk fibroin net for use in tissue engineering: growth and gene regulation of human endothelial cells", *Biomaterials,* vol. 25, p. 5137-5146.

VAILHE, B., D. VITTET and J. J. FEIGE (2001). *"In vitro* models of vasculogenesis and angiogenesis", *Lab Invest,* vol. 81, p. 439-452.

VALAPPIL, S. P., et al. (2006). "Biomedical applications of polyhydroxyalkanoates: an overview of animal testing and *in vivo* responses", *Expert Rev Med Devices,* vol. 3, p. 853-868.

VAN DER FLIER, A. and A. SONNENBERG (2001). "Function and interactions of integrins", *Cell Tissue Res,* vol. 305, p. 285-298.

VAN WACHEM, P. B., et al. (1985). "Interaction of cultured human endothelial cells with polymeric surfaces of different wettabilities", *Biomaterials,* vol. 6, p. 403-408.

VATS, A., et al. (2003). "Scaffolds and biomaterials for tissue engineering: a review of clinical applications", *Clin Otolaryngol Allied Sci,* vol. 28, p. 165-172.

VERNON, R. B., et al. (2005). "Microgrooved fibrillar collagen membranes as scaffolds for cell support and alignment", *Biomaterials,* vol. 26, p. 3131-3140.

VERNON, R. B. and E. H. SAGE (1999). "A novel, quantitative model for study of endothelial cell migration and sprout formation within three-dimensional collagen matrices", *Microvasc Res,* vol. 57, p. 118-133.

VOGEL, V. and G. BANEYX (2003). "The tissue engineeting puzzle: a molecular perspective", *Annu Rev Biomed Eng,* vol. 5, p. 441-463.

VROMAN, L., A. L. ADAMS and M. KLINGS (1971). "Interactions among human blood proteins at interfaces", *Fed Proc,* vol. 30, p. 1494-1502.

WANG, J., Y. JIN and Z. GUO (2003). "Expression of basic fibroblast growth factor and fibronectin in tissue engineering skin allograft during healing process", *Hua Xi Kou Qiang Yi Xue Za Zhi,* vol. 21, p. 41-43.

WARY, K. K. (2005). "Recognizing scientific excellence in the biology of cell adhesion", *Cell Commun Signal,* vol. 3, p. 7.

WEBB, K., V. HLADY and P. A. TRESCO (1998). "Relative importance of surface wettability and charged functional groups on NIH 3T3 fibroblast attachment, spreading, and cytoskeletal organization", *J Biomed Mater Res,* vol. 41, p. 422-430.

WEISS, P. and B. GARBER (1952). "Shape and movement of mesenchyme cells as functions of the physical structure of the medium: Contributions to a quantitative morphology", *Proc Natl Acad Sci U S A,* vol. 38, p. 264-280.

WEN, C. H., M. J. CHUANG and G. H. HSIUE (2006). "Asymmetric surface modification of poly (ethylene terephthalate) film by CF4 plasma immersion", *Appl Surf Sci,* vol. 252, p. 3799-3805.

WESTLIN, W. F. (2001). "Integrins as targets of angiogenesis inhibition", *Cancer J 7 Suppl,* vol. 3, p. S139-43.

WETHERS, D. L., et al. (1994). "Accelerated healing of chronic sickle-cell leg ulcers treated with RGD peptide matrix. RGD Study Group", *Blood,* vol. 84, p. 1775-1779.

257

WILLIAMS, S. F., et al. (1999). "PHA applications: addressing the price performance issue: I. Tissue engineering", *Int J Biol Macromol*, vol. 25, p. 111-121.

WILLIAMS, S. K., et al. (2006). "Covalent modification of porous implants using extracellular matrix proteins to accelerate neovascularization", *J Biomed Mater Res A*, vol. 78, p. 59-65.

WINTERMANTEL, E., et al. (1991). "Angiopolarity: a new design parameter for cell transplantation devices and its application to degradable systems", *ASAIO Trans*, vol. 37, p. M334-6.

WONG, J. Y., et al. (1997). "Direct measurement of a tethered ligand-receptor interaction potential", *Science*, vol. 275, p. 820-822.

WONG, J. Y., J. B. LEACH and X. Q. BROWN (2004). "Balance of chemistry, topography, and mechanics at the cell-biomaterial interface: Issues and challenges for assessing the role of substrate mechanics on cell response", *Surf Sci*, vol. 570, p. 119-133.

WOZNIAK, M. A., et al. (2004). "Focal adhesion regulation of cell behavior", *Biochim Biophys Acta*, vol. 1692, p. 103-119.

WU, X., et al. (2007). "Preparation and assessment of glutaraldehyde-crosslinked collagen-chitosan hydrogels for adipose tissue engineering", *J Biomed Mater Res A*, vol. 81, p. 59-65.

WU, X., et al. (2004). "Tissue-engineered microvessels on three-dimensional biodegradable scaffolds using human endothelial progenitor cells", *Am J Physiol Heart Circ Physiol*, vol. 287, p. H480-H487.

XIE, Y., et al. (2002). "Nanoscale modifications of PET polymer surfaces via oxygen-plasma discharge yield minimal changes in attachment and growth of mammalian epithelial and mesenchymal cells *in vitro*", *J Biomed Mater Res*, vol. 61, p. 234-245.

XIONG, J. P., et al. (2001). "Crystal structure of the extracellular segment of integrin alpha Vbeta3", *Science*, vol. 294, p. 339-345.

XIONG, J. P., et al. (2002). "Crystal structure of the extracellular segment of integrin alphaV beta3 in complex with an Arg-Gly-Asp ligand", *Science*, vol. 296, p. 151-155.

YAMAMURA, N., et al. (2007). "Effects of the mechanical properties of collagen gel on the *in vitro* formation of microvessel networks by endothelial cells", *Tissue Eng*, vol. 13, n° 7. p. 1443-1453.

YANCOPOULOS, G. D., et al. (2000). "Vascular-specific growth factors and blood vessel formation", *Nature*, vol. 407, p. 242-248.

YAO, C., et al. (2004). "Modification of collagen matrices for enhancing angiogenesis", *Cells Tissues Organs*, vol. 178, p. 189-196.

YAO, C., et al. (2006). "The impact of proteinase-induced matrix degradation on the release of VEGF from heparinized collagen matrices", *Biomaterials,* vol. 27, p. 1608-1616.

YARLAGADDA, P. K., M. CHANDRASEKHARAN and J. Y. SHYAN (2005). "Recent advances and current developments in tissue scaffolding", *Biomed Mater Eng,* vol. 15, p. 159-177.

YEUNG, T., et al. (2005). "Effects of substrate stiffness on cell morphology, cytoskeletal structure, and adhesion", *Cell Motil Cytoskeleton,* vol. 60, p. 24-34.

YI, C., et al. (2006). "Transplantation of endothelial progenitor cells transferred by vascular endothelial growth factor gene for vascular regeneration of ischemic flaps", *J Surg Res,* vol. 135, p. 100-106.

YIM, E. K., I. C. LIAO and K. W. LEONG (2006). "Tissue compatibility of interfacial polyelectrolyte complexation fibrous scaffold: evaluation of blood compatibility and biocompatibility", *Tissue Eng,* vol. 13, n°2, p. 423-433.

YOUNG, S., et al. (2005). "Gelatin as a delivery vehicle for the controlled release of bioactive molecules", *J Control Release,* vol. 109, p. 256-274.

YU, T. T. and M. S. SHOICHET (2005). "Guided cell adhesion and outgrowth in peptide-modified channels for neural tissue engineering", *Biomaterials,* vol. 26, p. 1507-1514.

ZANTOP, T., et al. (2006). "Extracellular matrix scaffolds are repopulated by bone marrow-derived cells in a mouse model of achilles tendon reconstruction", *J Orthop Res,* vol. 24, p. 1299-1309.

ZHANG, C., et al. (2007). "Specific targeting of tumor angiogenesis by RGD-conjugated ultrasmall superparamagnetic iron oxide particles using a clinical 1.5-T magnetic resonance scanner", *Cancer Res,* vol. 67, p. 1555-1562.

ZHANG, M., T. DESAI and M. FERRARI (1998). "Proteins and cells on PEG immobilized silicon surfaces", *Biomaterials,* vol. 19, p. 953-960.

ZHAO, Q., et al. (2003). "Research in synthesis of bioactive peptide RGD and the method for its grafting on PET surface", *Sheng Wu Yi Xue Gong Cheng Xue Za Zhi,* vol. 20, p. 384-387.

ZHOU, Y., et al. (2007). "Combined marrow stromal cell-sheet techniques and high-strength biodegradable composite scaffolds for engineered functional bone grafts", *Biomaterials,* vol. 28, p. 814-824.

Website references

1. Plasma surface treatment
   [http://www.anatechusa.com/plasma_surface_treatment/default.html] (Accessed June 2007)

2. Blood vessels
   [http://www.ivy-rose.co.uk/Topics/Blood_Vessels.htm] (Accessed September 2004)

3. Blood vessel structure
   [http://www-ermm.cbcu.cam.ac.uk/0300663Xh.htm] (Accessed June 2007)

4. What is Angiogenesis?
   [http://www.unizh.ch/onkwww/angio2.html] (Accessed September 2003)

5. Organic analysis techniques: XPS, TOF-SIMS, FTIR, Raman, GC/MS, Evans analytical group/Evan texas,
   [http://www.mrc.utexas.edu/seminars/Evans-Organic.pdf] (Accessed September 2006)

6. Spectra -SYTOX Green/DNA
   [http://probes.invitrogen.com/servlets/spectra?fileid=7020dna] (Accessed June 2007)

7. Basic mechanisms of capillary development
   [classes.aces.uiuc.edu/.../Capilary/Angilect.htm] (Accessed May 2006)

8. Scanning electron microscope
   [http://www.purdue.edu/REM/rs/sem.html] (Accessed June 2007)

9. SEM
   [http://mse.iastate.edu/microscopy/second2.html] (Accessed June 2007)

10. Hitachi S-4700 SEM
    [http://www.charfac.umn.edu/InstDesc/S4700SEMdesc.html] (Accessed June 2007)

11. Application Note- Nano-Surface Texture/Roughness
    [http://www.lotoriel.de/site/site_down/pn_roughness_deen.pdf] (Accessed June 2007)

12. Activation and Coupling
    [http://www.vuw.ac.nz/staff/paul_teesdale-spittle/peptide-synthesis/pep-syn-files/activation-coupling.htm] (Accessed September 2004)

13. Hydrogen (Proton, Deuterium and Tritium) NMR
    [http://chem.ch.huji.ac.il/nmr/techniques/1d/row1/h.html] (Accessed September 2004)